Transmission distribuée dans le canal multi-antennaire à interférences

Ka Ming Ho

DISSERTATION

In Partial Fulfillment of the Requirements
for the Degree of Doctor of Philosophy
from TELECOM ParisTech

Specialization: Communication and Electronics

Zuleita Ka Ming Ho

Distributed Transceiver Design for the Multi-Antenna Interference Channel

Defense scheduled on the 20th Dec, 2010 before a committee composed of:

Reviewers	Prof. Wolfgang Utschick, Technische Universitat Muenchen,
	Dr. Samson Lasaulce, CNRS, France,
Examiners	Dr. Maxime Guillaud, University of Vienna,
	Prof. Dirk Slock , EURECOM
Thesis Supervisor	Prof. David Gesbert, EURECOM

THESE

présentée pour obtenir le grade de

Docteur de TELECOM ParisTech

Spécialité: Communication et Electronique

Zuleita Ka Ming Ho

Distributed Transceiver Design for the Multi-Antennas Interference Channel

Soutenance de thèse prévue le 20 Decembre 2010 devant le jury composé de :

Rapporteurs	Prof. Wolfgang Utschick, Technische Universitat Muenchen,
	Dr. Samson Lasaulce, CNRS, France,
Examinateurs	Dr. Maxime Guillaud, University of Vienna,
	Prof. Dirk Slock , EURECOM
Directeur de thèse	Prof. David Gesbert, EURECOM

Abstract

0.1 Introduction

Dans cette thèse, notre objectif est d'optimiser les stratégies de transmission et de réception dans un réseau où il y a peu ou pas de gestion centrale des ressources du tout, et où les nœuds ont une connaissance limitée du canal avec seulement un lien restreint entre eux. En particulier, les émetteurs ont la plupart du temps des informations locales seulement sur le canal, et nous considérons qu'il n'y a pas de partage des données à transmettre aux utilisateurs, ce qui empêche la transmission conjointe en système virtuel MIMO.

L'utilisation commune des ressources du système (par exemple en transmettant en même temps et dans la même bande de fréquence) conduit à la génération d'interférence au niveau des différents récepteurs, ce qui rend la gestion des interférences essentielle. En considérant l'optimisation du précodeur dans le cadre de la théorie des jeux, des stratégies extrêmes, égoiste ou altruiste, peuvent être définies. Un émetteur égoiste agit en prenant compte de son propre intérêt et recherche la maximisation de son propre rapport signal sur bruit plus interférence (SINR) sans considération des interférences générées aux autres récepteurs. Un émetteur altruiste, par contre, utilise toutes ses ressources afin d'annuler les interférences qu'il crée aux autres récepteurs. Il est intuitif qu'aucune de ces deux stratégies extrêmes n'est optimale pour maximiser le débit total du réseau. Un travail récent [31] sur le design du vecteur de précodage dans un canal d'interférence MISO (MISO-IC) sans décodage des interférences au récepteur (SUD) a mis en évidence qu'il est possible, en balançant les approches égoiste et altruiste, d'atteindre un point d'opération se situant sur la frontière Pareto optimale de la région de débit, qui est la frontière limitant la région des débits atteignables par l'utilisation de précodage linéaire. En gardant à l'esprit ce résultat, nous étudions l'optimisation distribuée des vecteurs de précodage pour le MISO-IC-SUD dans le chapitre 3. Nous développons un algorithme qui est initialisé à l'équilibre de Nash (point d'opération égoiste) et se déplace à chaque itération vers la solution du zéro-forcing (point d'opération altruiste) à pas fixe. L'algorithme s'arrête si un des émetteurs observe une baisse de son débit, imitant ainsi le procédé de négociation. L'algorithme proposé atteint un point d'opération proche de la frontière Pareto optimale, et chaque utilisateur obtient un débit supérieur à celui qu'il aurait eu à l'équilibre de Nash. Nous démontrons ainsi que les joueurs (les paires émetteur-récepteur) peuvent atteindre des débits supérieurs dans le MISO-IC-SUD en coopérant et en balançant égoisme et altruisme.

Le problème du design des vecteurs de précodage pour le MISO-IC-SUD est étendu au cas du MIMO-IC-SUD au chapitre 4. En supposant une connaissance locale, nous modélisons ce problème en un jeu bayésien prenant en compte le fait que le canal ne soit pas complètement connu, et où les joueurs maximisent l'espérance de leur fonction d'utilité à partir des statistiques du canal. Nous trouvons le point d'équilibre de ce jeu

bayésien et étudions la maximisation de la somme des débits dans un MIMO-IC-SUD. Nous observons que la maximisation du débit total peut aussi être interprétée dans ce scénario comme un équilibre entre les approches égoistes et altruistes. Avec cette analyse, un algorithme dans lequel les vecteurs de transmission et de réception sont obtenus par une optimisation alternée aux émetteurs et aux récepteurs est développée. L'algorithme converge vers une solution qui aligne les interférences lorsque le SNR devient large, ce qui implique que le débit total augmente indéfiniment avec le SNR (avec une pente égale aux nombre de degrés de liberté). Dans le régime à faible SNR, notre approche fonctionne mieux que les algorithmes conventionnels visant à aligner les interférences, ce qui est une conséquence de l'équilibre entre égoisme et altruisme. En particulier, l'algorithme proposé atteint des performances presque optimales dans des réseaux asymétriques pour lesquels certains récepteurs sont soumis à du bruit de fond incontrôlé.

Dans le chapitre 5, nous considérons enfin des récepteurs ayant la capacité de décoder les interférences (IDC) dans un MISO-IC. Ce degré de liberté additionnel permet aux récepteurs de décoder les interférences et de les soustraire au signal reçu, ce qui permet ainsi d'obtenir une communication sans interférence. En revanche, les choix des récepteurs dépendent des vecteurs de précodage aux émetteurs. Pour chaque choix de vecteur de précodage, nous obtenons un nouveau SISO-IC avec une nouvelle région de capacité correspondante. Ainsi, nous devons choisir pour chaque réalisation d'un canal MISO le vecteur de précodage et la puissance de transmission de manière à atteindre un débit maximal après avoir considéré toutes les possibilités pour les actions des récepteurs (décodage des interférences ou traitement des interférences comme du bruit). Il y a trois paramètres influant le design: la structure du récepteur, le vecteur de précodage, et la puissance de transmission. Ces trois paramètres sont interdépendants et l'obtention du triplet optimal est un problème qui a été démontré comme étant NP-complet [39]. Quoi qu'il en soit, nous avons simplifié cette analyse en reformulant la région des débits atteignables d'un MISO-IC-IDC comme l'union des régions pour les différentes structures. Ensuite nous avons caractérisé les limites de ces régions de débit atteignable et obtenu ainsi la frontière Pareto optimale du problème initial. Les vecteurs de précodage Pareto optimaux sont obtenus par une combinaison linéaire de deux vecteurs du canal avec des poids dépendant seulement de deux scalaires réels entre zéro et un. Nous utilisons ensuite cette caractérisation de la frontière Pareto optimale pour obtenir une caractérisation du point où le débit total maximum est atteint. Cet ensemble de solutions potentielles est un sous-ensemble strict de la frontière Pareto optimale, ce qui réduit ainsi considérablement l'espace de recherche du problème NP-complet initial.

0.2 MISO-IC sans Décodage de l'interf'erence

Dans un MISO-IC avec N paires d'émetteurs et récepteurs, nous proposons une heuristique intuitivement motivée, que nous appelons solution de négociation distribuée (distributed bargaining solution (DBS)) et la comparons à l'équilibre non-coopératif de Nash ainsi qu'à la solution altruiste, tous deux introduits ci-dessus. La difficulté réside en ce que les points de coopération optimaux (situés sur la frontière de Pareto) peuvent être exprimés comme une combinaison linéaire des vecteurs de précodage ZF et MRT où les coefficients de pondération nécéssite la connaissance centralisée et complète des canaux. Pour rendre l'algorithme plus distribué, nous introduisons l'idée d'un lien de feedback limité de chaque utilisateur vers la station de base *qui le sert*. Le deuxième aspect nouveau est l'idée d'une négociation itérative où les émetteurs modifient légèrement et simultanément leurs

vecteurs de précodage de manière à ce que les débits de toutes les parties concernées soient améliorés. Les utilisateurs doivent observer leurs débits et indiquer à leur station de base si la négociation a été réussie ou pas (en utilisant un seul bit de feedback). Dans le cadre proposé, une baisse de débit chez l'un des utilisateurs résultera en cet utilisateur cessant de coopérer.

0.2.1 L'algorithme DBS

Nous proposons un algorithme itératif qui s'approche de la frontière Pareto en modifiant progressivement la direction des vecteurs de précodage à chaque itération afin que *chaque* paire émetteur-récepteur obtienne un débit plus haut.

Soit $\mathbf{w}_i(j)$ le vecteur de beamforming de l'émetteur i à l'itération j. Intuitivement, il est raisonnable d'initialiser les vecteurs $\mathbf{w}_i(0)$ à la solution MRT $\mathbf{w}_i^{MRT}$ parce que les joueurs commencent dans un cadre non-coopératif. Cependant ils peuvent également tous initialiser leurs vecteurs de beamforming dans un cadre altruiste (voir ci-dessous).

Le vecteur de beamforming est mis à jour à l'itération j de la façon suivante:

$$\mathbf{w}_i(j) = \mathbf{w}_i(j-1) + \delta_w(j) \tag{1}$$

$$\mathbf{w}_i(j) \to \frac{\mathbf{w}_i(j)}{\|\mathbf{w}_i(j)\|} \tag{2}$$

où $\delta_w(j)$ est un vecteur calculé à partir de l'information locale sur le canal. A l'itération j, chaque récepteur calcule son débit utilisant son information locale,

$$r_i^{(j)} = \log_2\left(1 + \frac{|\mathbf{h}_{ii}^H \mathbf{w}_i(j)|^2}{I_i(j)}\right) \tag{3}$$

où $\mathbf{h}_{kl}$ représente le canal complexe Gaussian à évanouissement entre Tx l et Rx k, $I_i(j)$ est l'interférence mesurée ajoutée à la puissance du bruit au récepteur i à l'itération j,

$$I_i(j) = \sum_{k \neq i}^{N} |\mathbf{h}_{ik}^H \mathbf{w}_k(j)|^2 + \sigma^2. \tag{4}$$

Donc, Rx i rend compte au Tx i d'un seul bit pour informer la station de base de son degré de satisfaction: un 1 correspond à une demande d'augmenter le débit de données, un 0 à une demande de le diminuer.

Nous proposons la stratégie d'initialisation suivante qui s'adapte au SNR du système en supposant que les SINRs correspondant à l'utilisation de ZF and MRT soient connus:

$$\mathbf{w}_i(0) = \begin{cases} \mathbf{w}_i^{ZF} & \text{if } R^{ZF} > R^{MRT}; \\ \mathbf{w}_i^{MRT} & \text{otherwise.} \end{cases} \tag{5}$$

où $R^{ZF} = \sum_{i=1}^{N} \log_2\left(1 + \gamma_i\left(\mathbf{w}_1^{ZF}, \ldots, \mathbf{w}_N^{ZF}\right)\right)$ et
$R^{MRT} = \sum_{i=1}^{N} \log_2\left(1 + \gamma_i\left(\mathbf{w}_1^{MRT}, \ldots, \mathbf{w}_N^{MRT}\right)\right)$. Il est intéressant de noter que les différents mechanimes de mise à jour dans (3.16) résulteraient en des trajectoires de débits différentes et que la somme des débits une fois l'algorithme converge sera différente. Ici nous montrons deux exemples simples de $\delta_{w_i(j)}$ qui obtiennent de meilleurs résultats que les solutions non-cooperative et altruiste. Ces algorithmes fournissent tous deux une trajectoire liant le point d'opération MRT à celui de ZF dans la région de débits. Si $R^{ZF} > R^{MRT}$, $\delta_{w_i(j)} = \mathbf{w}_i^{MRT}$, dénoté ZFI, sinon $\delta_{w_i(j)} = \mathbf{w}_i^{ZF}$, dénoté OBI.

Une condition d'arrêt est implémentée pour que la trajectoire du vecteur de transmission s'arrête aussi prêt de la frontière Pareto que possible. La condition d'arrêt reflète la stratégie de partage et plusieurs options sont possibles. Une condition d'arrêt raisonnable et intuitive consiste en ce que chaque émetteur arrête de coopérer et met fin à l'algorithme dès que son débit diminue. L'utilisateur i, $1 \leq i \leq N$ arrête donc de coopérer si

$$\frac{|\mathbf{h}_{ii}^H \mathbf{w}_i(j)|^2}{I_i(j)} > \frac{|\mathbf{h}_{ii}^H \mathbf{w}_i(j+1)|^2}{I_i(j+1)} \tag{6}$$

où $I_i(j)$ est la puissance de l'interférence plus bruit mesurée dans (3.19).

0.2.2 Résultats et Discussion

Dans cette section, nous illustrons la dynamique (trajectoires dans la région de débit) et la somme des débits obtenue par DBS.

Dans la figure 3.1, la région de débit réalisable pour une instance particulière des canaux est tracée pour le canal MISO-IC-SUD à deux utilisateurs. La solution ZF et la solution MRT sont marquées par un cercle et un triangle respectivement, à l'intérieur de la région. Le SNR du système est égal à 15dB. Pour cette instance du canal, ni ZF ni MRT n'atteignent la frontière Pareto. La trajectoire de DBS à chaque itération commence à la solution MRT. La ligne continue correspond à la trajectoire avec condition d'arrêt qui garantit que la négociation cesse dès que le débit de l'un des émetteurs baisse. La ligne pointillée est la trajectoire sans condition d'arrêt. Comme le montre la figure, la trajectoire finit par atteindre la solution ZF mais sans aucune garantie des débits des émetteurs. A noter que le vecteur de beamforming est orienté vers le vecteur zéro-forceur mais s'arrête avant de l'atteindre ce qui résulte en une somme des débits plus grande et un point de fonctionnement plus proche de la frontière Pareto. La somme des débits obtenue est supérieure à celles obtenues par les solutions ZF et MRT. Pour cette réalisation des canaux, l'algorithme DBS atteint presque la frontière Pareto au bout de 3 itérations seulement ce qui signifie que seulement 3 bits de feedback sont suffisants pour améliorer la performance de façon significative.

Dans un canal à interférence où les émetteurs sont en concurrence pour l'utilisation de la bande de fréquence en l'absence d'une structure du réseau qui s'occupe de la gestion de l'interférence, un algorithme distribué est essentiel pour l'amélioration de la performance du système. Nous avous proposé deux solutions de négociations distribuées simples qui essaient de trouver un équilibre entre la solution égoiste (MRT) et la solution altruiste (ZF). Dans la section qui suit, nous étudions l'équilibrage entre égoisme et altruisme dans le contexte d'un canal MIMO-IC-SUD.

0.3 MIMO-IC sans décodage d'interférence

Dans cette section, nous proposons un algorithme distribué pour la maximisation de la somme des débits sur un canal MIMO-IC asymétrique. L'équilibrage entre l'altruisme et l'égoisme pour le joueur i peut être réalisé par un compromis entre le précodeur qui adopte une direction proche de celles des vecteurs propres dominants de l'équilibre égoiste $\mathbf{E}_i = \mathbf{H}_{ii}\mathbf{w}_i\mathbf{w}_i^H\mathbf{H}_{ii}^H$ et celle des matrices d'équilibre altruiste $\{-\mathbf{A}_{ji}\}$ $(j \neq i)$ où $\mathbf{A}_{ji} = \mathbf{H}_{ji}\mathbf{w}_i\mathbf{w}_i^H\mathbf{H}_{ji}^H$. Ce qui est intéressant, comme il sera démontré dans les sections suivantes, c'est que le précodage qui maximise la somme des débits pour le MIMO-IC fait exactement ceci. Nous revenons donc brièvement sur les approches de maximisation des débits telles

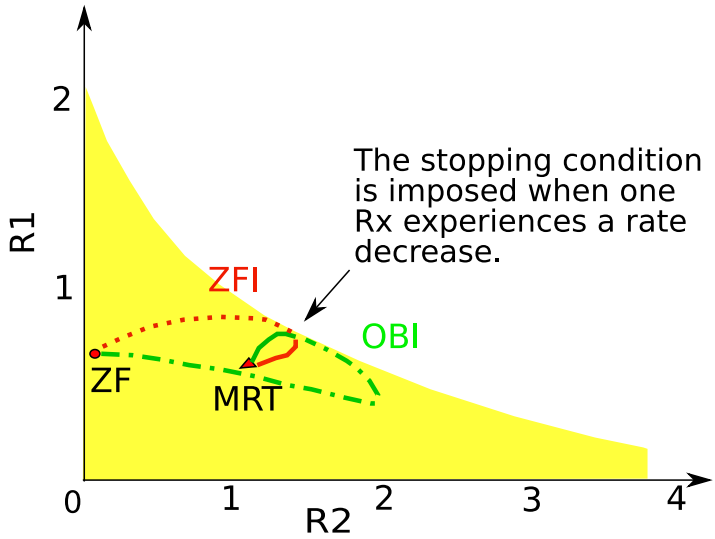

Figure 1: La trajectoire de DBS dans la région de débit pour un MISO-IC-SUD à 2 utilisateurs opérant à un SNR de 15dB. Les trajectoires de ZFI et OBI, qui commencent au point MRT (marqué par un triangle), sont en lignes continues, en rouge et en vert respectivement; en l'absence d'une condition d'arrêt, les trajectoires se terminent au point ZF (marqué par un cercle) et sont representées par des lignes pointillées. Comme le montre la figure, les algorithmes s'arrêtent prêt de la frontière Pareto.

que [61]. Soit $\bar{R} = \sum_{i=1}^{N_c} R_i$ la somme des débits où $R_i = \log_2\left(1 + \frac{|\mathbf{v}_i^H \mathbf{H}_{ii}\mathbf{w}_i|^2 P}{\sum_{j\neq i}^{N_c} |\mathbf{v}_i^H \mathbf{H}_{ij}\mathbf{w}_j|^2 P + \sigma_i^2}\right)$.

Lemma 1. *Le vecteur de transmission qui maximise la somme des débits $\bar{R}$ est le vecteur propre d'une matrice donnée par une combinaison linéaire de $\mathbf{E}_i$ et $\mathbf{A}_{ji}$:*

$$\left(\mathbf{E}_i + \sum_{j\neq i}^{N_c} \lambda_{ji}^{opt} \mathbf{A}_{ji}\right) \mathbf{w}_i = \mu_{max}\mathbf{w}_i \tag{7}$$

où

$$\lambda_{ji}^{opt} = -\frac{|\mathbf{v}_j^H \mathbf{H}_{jj}\mathbf{w}_j|^2 P}{\sum_{k=1}^{N_c} |\mathbf{v}_j^H \mathbf{H}_{jk}\mathbf{w}_k|^2 P + \sigma_j^2} \frac{\sum_{k=1}^{N_c} |\mathbf{v}_i^H \mathbf{H}_{ik}\mathbf{w}_k|^2 P + \sigma_i^2}{\sum_{k\neq j}^{N_c} |\mathbf{v}_j^H \mathbf{H}_{jk}\mathbf{w}_k|^2 P + \sigma_j^2} \tag{8}$$

et μ_{max} est défini plus tard dans la thèse.

On peut montrer que les paramètres d'équilibrage $\{\lambda_{ji}^{opt}\}$ sont en fait les 'prix' échangés au cours de l'algorithme itératif proposé par [61]. Ces paramètres jouent un rôle clé, cependant leur calcul est fonction de la connaissance *globale* du canal et nécessite des échanges supplémentaires de messages (les prix). Pour éviter ceci, nous obtenons ci-dessous une technique sous-optimale d'équilibrage d'egoisme-altruisme qui nécessite la connaissance des statistiques des canaux uniquement, tout en démontrant la même pente de la courbe de performance en fonction du SNR qui si le connaissance du canal était parfaite.

0.3.1 Un algorithme pratique distribué pour le design du beamforming: *DBA*

Nous proposons l'agorithme distribué suivant (*DBA*) où les vecteurs en émission et en réception sont calculés de façon itérative:

$$\mathbf{w}_i = V^{max}\left(\mathbf{E}_i + \sum_{j\neq i}^{N_c} \lambda_{ji}\mathbf{A}_{ji}\right) \tag{9}$$

$$\mathbf{v}_i = \frac{\mathbf{C}_{Ri}^{-1}\mathbf{H}_{ii}\mathbf{w}_i}{\left\|\mathbf{C}_{Ri}^{-1}\mathbf{H}_{ii}\mathbf{w}_i\right\|} \tag{10}$$

où λ_{ji} dépend des statistiques du canal seulement. A ce stade, il est intéressant de comparer avec des stratégies proposés précedemment basées sur l'alignement des interférences telles que celles dans [49]. Dans ces stratégies, $\mathbf{w}_i$ ne dépend pas de $\mathbf{H}_{ii}$. A noter cependant que $\mathbf{w}_i$ est corrélé au gain du canal direct $\mathbf{H}_{ii}$ à travers la matrice égoiste $\mathbf{E}_i$ dans *DBA*. Cette corrélation est utile en termes de la somme des débits puisqu'elle permet de pondérer entre les contributions des matrices egoiste et altruiste d'une manière qui dépend des liens.

Les paramètres d'équilibrage entre égoisme et altruisme λ_{ji} sont obtenus de manière heuristique qui dépend des statistiques des canaux. (4.18) indique que

$$\lambda_{ji}^{opt} = -\frac{S_j}{S_j + I_j + \sigma_j^2}\frac{S_i + I_i + \sigma_i^2}{I_j + \sigma_j^2} \tag{11}$$

où $S_j = |\mathbf{v}_j^H\mathbf{H}_{jj}\mathbf{w}_j|^2P$ et $I_j = \sum_{k\neq j}^{N_c}|\mathbf{v}_j^H\mathbf{H}_{jk}\mathbf{w}_k|^2P$.

L'étude des principes derrière la maximisation de la somme des débits, nous conjecturons qu'à la convergence de l'algorithme, l'interférence résiduelle coordinée sera de l'ordre du bruit et de la puissance de l'interférence provenant de l'extérieur du groupe de cellules coopérant (out-of-cluster interference), c'est à dire $I_j = O(\sigma_j^2)$. Nous proposons donc la charactérisation suivante :

$$\lambda_{ji} = -\frac{1+\gamma_i^{-1}}{1+\gamma_j^{-1}}\gamma_j. \tag{12}$$

Pour les détails de la dérivation, se référer à la thèse. Les résultats ci-dessus suggèrent que Tx i doit être plus altruiste envers le lien j quand le SNR de ce lien est haut ou quand le SNR du lien i est relativement bas. Ceci est conforme à l'intuition derrière la maximisation des débits sur les canaux gaussiens parallèles.

0.3.2 Résultats de Simulations

Dans cette section, nous étudions la somme des débits de *DBA* et la comparons à celle obtenue par des méthodes voisines, à nommer la méthode *Max-SINR* [20], la méthode de minimisation alternée (*Alt-Min*) pour l'alignement des interférences [49] et la méthode de maximisation de la somme des débits (*SR-Max*) [61]. The *SR-Max* qui est par construction optimale mais plus complexe et nécessite plus d'échange ou de feedback d'information de prix entre les émetteurs. Pour garantir une comparaison équitable, tous les algorithmes sont initialisés à la même solution et ont la même condition d'arrêt. Nous considérons que l'algorithme a convergé si les sommes des débits obtenues pour deux itérations successives

Figure 2: Somme des débits pour des canaux asymétriques. Le gain du lien direct de la paire 1 d'émetteur-récepteur est 30dB plus faible que les autres liens.

diffèrent de moins de 0.001. Dénotons le rapport signal à interférence du lien i par $SIR_i = \frac{\alpha_{ii}}{\sum_{j\neq i}^{N_c} \alpha_{ij}}$. Le SIR est supposé égal à 1 pour tous les liens, à moins que le contraire ne soit indiqué. Dénotons la différence en SNR entre 2 liens pour les canaux asymétriques par ΔSNR.

Dans un système asymétrique, les différents liens sont soumis à des niveaux inégaux de bruit et d'interférence. Une autre source d'asymétrie peut être la différence entre les atténuations sur différents liens (affaiblissement de propagation et ombrage).

Dans la Fig. 4.6, 3 liens coopèrent dans le système. Chaque émetteur et récepteur a 2 antennes et un seul flux de données est transmis par récepteur. Le bruit au niveau de chaque récepteur est le même. Le système est asymétrique: le gain du canal direct H_{11} du lien of link 1 est plus faible de 30dB que les autres liens dans le réseau. Ce scenario représente un environnement réaliste où l'utilisateur souffre d'un ombrage fort. *DBA* atteint une somme des débits proche de celle obtenue par *SR-Max* et bien meilleure que les autres stratégies d'alignement de l'interférence, *Max-SINR* et *Alt-Min*.

A noter que l'algorithme proposé peut aussi être utilisé dans des réseaux avec un nombre arbitraire de joueurs et de nombres d'antennes.

0.3.3 Conclusion

Nous modélisons le problème d'optimisation du beamforming distribué sur le canal MIMO d'interférence en utilisant le cadre des jeux bayésiens qui permettent aux joueurs d'avoir une connaissance incomplète de l'information sur le jeu, dans ce cas l'information sur l'état du canal. Selon les motifs/objectifs des joueurs, nous proposons deux jeux: un jeu bayésien egoiste (chaque joueur veut maximiser son propre débit) et un jeu bayésien altruiste (chaque joueur veut minimiser l'interférence générée vers les autres joueurs). Nous avons prouvé l'existence d'équilibres pour ces types de jeux et la stratégie de meilleure réponse des joueurs est obtenue. Inspiré des équilibres, une technique de beamforming qui essaient d'équilibrer le comportement egoiste et le comportement altruiste afin de maximiser la somme des débits est proposée. Un tel algorithme de beamforming présente la même pente que la performance optimale en fonction du SNR démontrée par des méthodes récentes iteratives basées sur l'alignement des interférences. L'algorithme de beamforming proposé a une performance quasi-optimale en termes de somme des débits [61] sans le coût supplémentaire en feedback et a une performance supérieure aux méthodes d'alignement d'interférence pour des réseaux asymétriques.

0.4 MISO-IC avec possibilité de Décodage de l'interférence

Dans cette section, nous considérons des récepteurs qui peuvent décoder l'interférence (IDC), c'est à dire que le signal interférant peut être décodé et soustrait du signal reçu. Nous supposons un système simple constitué de deux paires d'émetteur-récepteur où chaque émetteur a N antennes de transmission alors que chaque récepteur a une seule antenne de réception seulement. Nous étudions donc un canal à interférence à deux util-

isateurs MISO (MISO-IC). Nous supposons que les émetteurs utilisent des codebooks dont la connaissance est commune et donc que le récepteur peut, si la qualité du canal le permet, décoder l'interférence et la soustraire du signal reçu. Nous supposons également que l'interférence est décodée avec succès si le débit du signal d'interférence est plus petit que la capacité de Shannon du canal d'interférence.

Dans le cas du MISO-IC-SUD, il a été démontré que les précodeurs optimaux de transmission sont de rang 1 et donc que le beamforming permet d'atteindre la frontière de Pareto. Cependant, il n'a pas encore été démontré que cette conclusion tient toujours pour un MISO-IC-IDC. Nous établissons ceci dans ce qui suit en commençant par une matrice de covariance générale. Soit $\mathbf{S}_i$ la matrice de covariance de transmission de Tx i et soit $\mathbf{h}_{\bar{i}i}$ le canal entre l'émetteur i et le récepteur $\bar{i}$, où $i \in \{1,2\}, \bar{i} \neq i$, $\mathbf{h}_{\bar{i}i} \in \mathbb{C}^{N\times 1}$. Les gains des canaux sont supposés i.i.d complexes gaussiens de moyenne égale à zéro et de variance égale à 1. Le signal reçu au niveau du récepteur i est donc

$$y_i = \mathbf{h}_{ii}^H \mathbf{S}_i^{1/2} \mathbf{x}_i + \mathbf{h}_{i\bar{i}}^H \mathbf{S}_{\bar{i}}^{1/2} \mathbf{x}_{\bar{i}} + n_i. \tag{13}$$

Le bruit n_i est une variable aléatoire complexe gaussienne de moyenne égale à zéro et de variance égale à 1. $\mathbf{x}_i$ représente le symbole transmis par lémetteur i et a une puissance égale à 1. Les matrices de covariance de transmission qui satisfont les contraintes de puissance $tr(\mathbf{S}_i) \leq P_{max}$ sont

$$\mathcal{S} = \left\{ \mathbf{S} \in \mathbb{C}^{N\times N} : \mathbf{S} \geq 0, tr(\mathbf{S}) \leq P_{max} \right\}, \; i = \{1,2\}. \tag{14}$$

0.4.1 Région de Débit Réalisable

Nous considérons les 4 structures de décodage suivantes: (N,N), (N,D), (D,N) and (D,D) [10], où "N" veut dire que le récepteur traite l'interférence comme du bruit (noise) et "D" veut dire que le récepteur décode l'interférence et la soustrait du signal reçu. Donc, (D,N) veut dire que le récepteur 1 décode et soustrait l'interférence alors que le récepteur 2 traite l'interférence comme du bruit. Dans [10], ces 4 structures de décodage sont proposées et il est démontré que les points de débits correspondants sont réalisables pour un SISO-IC. Nous étendons ce concept au MISO-IC et définissons les quantités suivantes:

$$\begin{aligned} C_i(\mathbf{S}_i) &\triangleq \log_2(1 + \mathbf{h}_{ii}^H \mathbf{S}_i \mathbf{h}_{ii}), \\ D_i(\mathbf{S}_i, \mathbf{S}_j) &\triangleq \log_2 \left(1 + \frac{\mathbf{h}_{ii}^H \mathbf{S}_i \mathbf{h}_{ii}}{\mathbf{h}_{ij}^H \mathbf{S}_j \mathbf{h}_{ij} + 1} \right), \\ T_i(\mathbf{S}_i, \mathbf{S}_j) &\triangleq \log_2 \left(1 + \frac{\mathbf{h}_{ji}^H \mathbf{S}_i \mathbf{h}_{ji}}{\mathbf{h}_{jj}^H \mathbf{S}_j \mathbf{h}_{jj} + 1} \right). \end{aligned} \tag{15}$$

C_i est le *débit utilisateur unique (single user rate)*, le plus haut débit que l'utilisateur i peut obtenir en l'absence d'interférence. D_i est le débit que correspond au décodage du signal désiré en traitant l'interférence comme du bruit et T_i est le débit que correspond à décoder l'interférence d'abord en traitant le signal désiré comme du bruit.

Dénotons la région des débits réalisable avec décodage de l'interférence aux deux récepteurs par la ̊egion Decode-Decode (DD). Cette dernière est égale à:

$$\mathcal{R}^{dd} = \bigcup_{\mathbf{S}_1, \mathbf{S}_2 \in \mathcal{S}} \left\{ (R_1, R_2) \leq \left(\min\left\{ C_1(\mathbf{S}_1), T_1(\mathbf{S}_1, \mathbf{S}_2) \right\}, \min\left\{ C_2(\mathbf{S}_2), T_2(\mathbf{S}_1, \mathbf{S}_2) \right\} \right) \right\}. \tag{16}$$

D'autre part, si les deux récepteurs décident de traiter l'interférence comme du bruit, nous obtenons la région NN,

$$\mathcal{R}^{nn} = \bigcup_{\mathbf{S}_1,\mathbf{S}_2\in\mathcal{S}} \Big\{ (R_1,R_2) \leq \big(D_1(\mathbf{S}_1,\mathbf{S}_2), D_2(\mathbf{S}_1,\mathbf{S}_2)\big) \Big\}. \tag{17}$$

Si le récepteur 1 décode l'interférence mais le récepteur 2 traite l'interférence comme du bruit, l'émetteur 2 doit transmettre à un débit qui garantit que l'interférence peut être décodée au récepteur 1. La région correspondante, dénotée par la région DN est donnée par

$$\mathcal{R}^{dn} = \bigcup_{\mathbf{S}_1,\mathbf{S}_2\in\mathcal{S}} \left\{ (R_1,R_2) \leq \left(C_1(\mathbf{S}_1), \min\left\{ D_2(\mathbf{S}_1,\mathbf{S}_2), T_2(\mathbf{S}_1,\mathbf{S}_2) \right\} \right) \right\}. \tag{18}$$

De même, la région ND est égale à

$$\mathcal{R}^{nd} = \bigcup_{\mathbf{S}_1,\mathbf{S}_2\in\mathcal{S}} \left\{ (R_1,R_2) \leq \left(\min\left\{ D_1(\mathbf{S}_1,\mathbf{S}_2), T_1(\mathbf{S}_1,\mathbf{S}_2) \right\}, C_2(\mathbf{S}_1) \right) \right\}. \tag{19}$$

Finalement, une région réalisable pour le MISO-IC avec capacité de décodage de l'interférence est donc l'union des régions ci-dessus:

$$\mathcal{R} = \mathcal{R}^{nn} \cup \mathcal{R}^{dd} \cup \mathcal{R}^{dn} \cup \mathcal{R}^{nd}. \tag{20}$$

Nous nous concentrons maintenant sur l'étude de la frontière Pareto de la région des débits. Afin d'obtenir des solutions qui atteignent cette frontière, nous commençons par identifier un ensemble de dimension plus petite que $\mathcal{S}\times\mathcal{S}$ mais qui est garanti de contenir les solutions Pareto optimales. Par conséquence, cet ensemble offre une réduction de complexité significative comparée à une recherche exhaustive dans l'ensemble $\mathcal{S}\times\mathcal{S}$ en entier.

Definition 1. *L'ensemble de solutions potentielles de $\mathcal{B}(\mathcal{R}^{xy})$, $x,y\in\{n,d\}$, est l'ensemble de matrices de covariance de transmission qui contient les matrices de covariance de transmission qui atteignent la frontière Pareto de $\mathcal{R}^{xy}$. Si $(\mathbf{S}_1,\mathbf{S}_2)$ sont Pareto optimaux, alors $(\mathbf{S}_1,\mathbf{S}_2)\in\Omega^{xy}$. De même, l'ensemble de solutions potentielles $\mathcal{B}(\mathcal{R})$ est Ω qui contient toutes les paires de $(\mathbf{S}_1,\mathbf{S}_2)$ qui sont Pareto optimales dans la région $\mathcal{R}$.*

Theorem 1. *Les frontières Pareto des régions NN, DN et DD sont atteintes par des matrices de rang 1. Il résulte que la frontière Pareto de MISO-IC-IDC est obtenue par des matrices de covariances de transmission de rang 1, c'est à dire par un beamforming en transmission.*

Dans Le théorème 11, nous avons établi que la frontière Pareto peut être atteinte en utlisant des vecteurs de beamforming en transmission. Afin de faciliter les discussions suivantes, nous définissons les vecteurs de tranmission beamforming $\mathbf{w}_i$ et la puissance de transmission P_i, pour $i=1,2$,

$$\mathbf{S}_i = \mathbf{w}_i\mathbf{w}_i^H P_i \tag{21}$$

avec $\|\mathbf{w}_i\|^2 = 1$.

Avec la structure de décodage $\mathbf{R}^{nd}$, le récepteur 1 traite l'interférence comme du bruit et le récepteur 2 décode et soustrait le signal d'interférence du signal reçu avant de décoder le signal désiré.

$$\mathcal{W}_i = \left\{ \mathbf{w}_i : \mathbf{w}_i = \sqrt{\lambda_i}\frac{\Pi_{ji}\mathbf{h}_{ii}}{\|\Pi_{ji}\mathbf{h}_{ii}\|} + \sqrt{1-\lambda_i}\frac{\Pi_{ji}^{\perp}\mathbf{h}_{ii}}{\|\Pi_{ji}^{\perp}\mathbf{h}_{ii}\|} \; ; \; 0 \le \lambda_i \le 1 \right\}, \quad i,j = 1,2, i \neq j. \tag{23}$$

Theorem 2. *La frontière Pareto $\mathcal{B}(\mathcal{R}^{nd})$ est réalisable avec l'ensemble de solutions potentielles Ω^{nd}*

$$\Omega^{nd} = \{\mathcal{W}_1, \mathcal{W}_2, P_1 = P_{max}, 0 \le P_2 \le P_{max}\} \tag{22}$$

où $\mathcal{W}_1, \mathcal{W}_2$ défini en (5.21)*, sont les ensembles des vecteurs beamforming composés de combinaisons linéaires des vecteurs correspondants à deux canaux; pour atteindre la frontière Pareto, lémetteur 1 transmet à pleine puissance P_{max} alors que lémetteur 2 transmet à une puissance $P_2 \le P_{max}$.*

Theorem 3. *L'ensemble de solutions potentielles à la maximisation de la somme des débits $\bar{R}^{nd}$ dénoté par $\tilde{\Omega}^{nd}$, donc $\boldsymbol{\omega}^* \subset \tilde{\Omega}^{nd} \subset \Omega^{nd}$, est donné par*

$$\tilde{\Omega}^{nd} = \left\{ \tilde{\mathcal{W}}_1, \tilde{\mathcal{W}}_2, P_{max}, P_{max} \right\} \tag{24}$$

où Ω^{nd} est l'ensemble de solutions potentielles à la frontière Pareto $\mathcal{B}(\mathcal{R}^{nd})$ dans (5.20)*. En particulier, $\tilde{\mathcal{W}}_1$ est l'ensemble suivant de cardinalit'e égale à trois :*

$$\tilde{\mathcal{W}}_1 = \left\{ \frac{\mathbf{h}_{11}}{||\mathbf{h}_{11}||}, \frac{\mathbf{h}_{21}}{||\mathbf{h}_{21}||}, \mathbf{w}_1(\lambda_1^{(b)}) \right\} \tag{25}$$

with $\lambda_1^{(b)} = \frac{c_1||\Pi_{21}^{\perp}\mathbf{h}_{11}||^2}{c_2||\mathbf{h}_{21}||^2 - 2\sqrt{c_1c_2}|\mathbf{h}_{21}^H\mathbf{h}_{11}| + c_1||\mathbf{h}_{11}||^2}$. L'ensemble de solutions potentielles $\tilde{\mathcal{W}}_2$ est l'ensemble des vecteurs beamforming charactérisés par un paramètre λ_2 qui appartient à une région plus restreinte que $\mathcal{W}_2$:

$$\tilde{\mathcal{W}}_2 = \left\{ \mathbf{w}_2 \in \mathcal{S} : \mathbf{w}_2 = \sqrt{\lambda_2}\frac{\Pi_{12}\mathbf{h}_{22}}{\|\Pi_{12}\mathbf{h}_{22}\|} + \sqrt{1-\lambda_2}\frac{\Pi_{12}^{\perp}\mathbf{h}_{22}}{\|\Pi_{12}^{\perp}\mathbf{h}_{22}\|} \; ; \; \lambda_2^{(b)} \le \lambda_2 \le \lambda_2^{\mathrm{MRT}} \right\} \tag{26}$$

où $\lambda_2^{\mathrm{MRT}} = \frac{|\mathbf{h}_{12}^H\mathbf{h}_{22}|}{||\mathbf{h}_{12}||||\mathbf{h}_{22}||}$ est un paramètre qui spécifie la solution de beamforming vers le canal $\mathbf{h}_{22}$ et $\mathbf{w}_2(\lambda_2^{(b)}) = \frac{\tilde{b}}{\sqrt{\tilde{a}+\tilde{b}}}\mathbf{v}_a + \frac{e^{j\phi_{\tilde{a}}}}{\sqrt{\tilde{a}+\tilde{b}}}\mathbf{v}_b$ pour des vecteurs $\mathbf{v}_a, \mathbf{v}_b$ définis ci-après et des scalaires positifs $\tilde{a}, \tilde{b}$. Les vecteurs $\mathbf{v}_a, \mathbf{v}_b$ sont, respectivement, les vecteurs propres les plus et moins dominants de la matrice $\mathbf{S} = \mathbf{h}_{22}\mathbf{h}_{22}^H - \frac{g_{21}}{g_{11}}\mathbf{h}_{12}\mathbf{h}_{12}^H$.

0.4.2 La charactérisation du point qui maximise la somme des débits dans la région DD

Dans cette section, nous calculons l'ensemble de solutions potentielles qui permettent d'atteindre la somme des débits maximale dans la région DD.

Theorem 4. *L'ensemble de solutions potentielles pour la maximisation de la somme des débits dans $\mathbf{R}^{dd}$ est*

$$\tilde{\Omega}^{dd} = \left\{ \mathcal{V}_1^{dd}, \mathcal{V}_2^{dd}, P_{max}, P_{max} \right\} \tag{27}$$

où pour l'utisateur i, $i = 1, 2$, les vecteurs de beamforming qui maximisent la somme des débits sont soit une combinaison linéaire de deux vecteurs orthogonaux soit maximisent la puissance du signal désiré soit un vecteur spécifique:

$$\mathcal{V}_i^{dd} = \left\{ \tilde{\mathcal{V}}_i, \frac{\mathbf{h}_{ii}}{\|\mathbf{h}_{ii}\|}, \mathbf{w}_i(\lambda_i^A) \right\} \tag{28}$$

$$\tilde{\mathcal{V}}_i = \left\{ \mathbf{w}_i : \sqrt{\lambda_i} \frac{\Pi_{ii}\mathbf{h}_{ji}}{\|\Pi_{ii}\mathbf{h}_{ji}\|} + \sqrt{1-\lambda_i} \frac{\Pi_{ii}^{\perp}\mathbf{h}_{ji}}{\|\Pi_{ii}^{\perp}\mathbf{h}_{ji}\|}, \lambda_i^A \leq \lambda_i \leq \lambda_i^{\text{MRT}} \right\} \tag{29}$$

où $\lambda_i^{\text{MRT}} = \frac{|\mathbf{h}_{ii}^H \mathbf{h}_{ji}|^2}{\|\mathbf{h}_{ii}\|^2 \|\mathbf{h}_{ji}\|^2}$ *et* $\lambda_i^A = \frac{\|\Pi_{ii}^{\perp}\mathbf{h}_{ji}\|}{\|\mathbf{h}_{ji}\|^2 + (1+g_{jj})\|\mathbf{h}_{ii}\|^2 - 2|\mathbf{h}_{ii}^H \mathbf{h}_{ji}|\sqrt{1+g_{jj}}}$.

Pour résumer, nous obtenons l'ensemble de solutions potentielles pour le point de somme des débits maximaux dans les régions ND et DD, dans les théorèmes 14 et 15 respectivement. Nous pouvous échanger les rôles des émetteurs 1 et 2 dans le théorème 14 afin d'obtenir tous les points dans la région DN, $\tilde{\Omega}^{dn}$. Pour la région NN, l'ensemble de solutions potentielles est identique à celui de la frontière Pareto, Ω^{nn}. Le point maximisant la somme des débits pour le MISO-IC-IDC appartient à l'ensemble $\tilde{\Omega}$, donné par:

$$\tilde{\Omega} = \tilde{\Omega}^{nd} \bigcup \tilde{\Omega}^{dn} \bigcup \tilde{\Omega}^{dd} \bigcup \Omega^{nn}. \tag{30}$$

0.4.3 Une stratégie de transmission simple

Dans cette section, nous proposons une stratégie de transmission très simple avec un nombre limité de choix de vecteurs de précodage. Bien que la performance sera sous-optimale, des choix sont proposés ci-dessous qui devraient maximiser la somme des débits dans certaines conditions du canal et résulte en une somme des débits presque maximale dans d'autres cas.

Cette stratégie de transmission est inspirée par la paramétrisation de chaque structure de décodage. Nous proposons de choisir seulement 2 vecteurs de beamforming dans chaque ensemble de solutions potentielles. Étant donnée l'information sur l'état des canaux, nous comparons la performance correspondant à ces 8 options de vecteurs de beamforming et choisissons les vecteurs et la structure de décodage correspondante qui atteint la somme des débits la plus grande.

- Région NN : $\left(\frac{\Pi_{21}^{\perp}\mathbf{h}_{11}}{\|\Pi_{21}^{\perp}\mathbf{h}_{11}\|}, \frac{\Pi_{12}^{\perp}\mathbf{h}_{22}}{\|\Pi_{12}^{\perp}\mathbf{h}_{22}\|}\right)$ et $\left(\frac{\mathbf{h}_{11}}{\|\mathbf{h}_{11}\|}, \frac{\mathbf{h}_{22}}{\|\mathbf{h}_{22}\|}\right)$.
- Région ND : $\left(\frac{\mathbf{h}_{21}}{\|\mathbf{h}_{21}\|}, \frac{\mathbf{h}_{22}}{\|\mathbf{h}_{22}\|}\right)$ et $\left(\frac{\mathbf{h}_{11}}{\|\mathbf{h}_{11}\|}, \frac{\mathbf{h}_{22}}{\|\mathbf{h}_{22}\|}\right)$.
- Région DN : $\left(\frac{\mathbf{h}_{11}}{\|\mathbf{h}_{11}\|}, \frac{\mathbf{h}_{12}}{\|\mathbf{h}_{12}\|}\right)$ et $\left(\frac{\mathbf{h}_{11}}{\|\mathbf{h}_{11}\|}, \frac{\mathbf{h}_{22}}{\|\mathbf{h}_{22}\|}\right)$.
- Région DD : $\left(\frac{\mathbf{h}_{21}}{\|\mathbf{h}_{21}\|}, \frac{\mathbf{h}_{12}}{\|\mathbf{h}_{12}\|}\right)$ et $\left(\frac{\mathbf{h}_{11}}{\|\mathbf{h}_{11}\|}, \frac{\mathbf{h}_{22}}{\|\mathbf{h}_{22}\|}\right)$.
- TDMA : une stratégie de partage en temps entre les points à un utilisateur, pour lesquels $\mathbf{w}_i = \frac{\mathbf{h}_{ii}}{\|\mathbf{h}_{ii}\|}$.

Il a été démontré que pour un SISO-IC la stratégie DD est optimale en termes de somme des débits maximale quand les deux canaux interférents sont puissants et les stratégies DN ou ND sont optimales quand un canal d'interférence est puissant alors que l'autre

est faible comparé au canal du signal désiré. La solution de beamforming qui maximise l'interférence et celle qui maximise la puissance du signal désiré sont choisies dans les régions DN, ND et DD dans l'algorithme proposé afin de vérifier l'analogie entre SISO-IC et MISO-IC.

0.4.4 Résultats de Simulation

Dans cette section, nous fournissons des résultats de simulations liées à la parametrisation proposée. En variant les vecteurs de beamforming et l'allocation de puissance de transmission selon cette dernière, nous pouvons tracer la région des débits réalisable par chaque structure de décodage pour une certaine réalisation des canaux dans la Section 5.9.1. Les points correspondant à la somme de débits maximale et à la solution MRT pour chaque méthode de décodage sont également marqués dans la région de débits réalisables correspondante. Dans la Section 5.9.2, nous calculons la fréquence empirique des stratégies MRT dans $\mathbf{R}^{nd}$ et $\mathbf{R}^{dd}$ moyennée sur 500 réalisations des canaux. Dans la section 5.9.3, nous permettons aux canaux d'être corrélés et observons que la structure de décodage qui maximise la somme des débits change avec la puissance du canal d'interférence, ce qui est conforme aux résultats obtenus dans le cas du SISO-IC.

0.4.5 Région de débits réalisables et Point de somme maximale des débits

Dans la Fig. 5.7, nous montrons les régions de débits réalisables avec les structures de décodage $\mathbf{R}^{nd}$, $\mathbf{R}^{dn}$, $\mathbf{R}^{dd}$ et $\mathbf{R}^{nn}$ dans les Fig. 5.7a, 5.7b, 5.7c et 5.7d respectivement. Nous fixons le nombre d'antennes de transmission à $N = 3$ et le SNR à 0dB. Nous laissons λ_1 et λ_2 prendre 20 valeurs différentes entre 0 et 1, inclus. Pour chaque paire de (λ_1, λ_2), les vecteurs de beamforming $\mathbf{w}_1, \mathbf{w}_2$ correspondant sont obtenus et les débits résultants pour des puissances de transmission P_1, P_2 sont calculés. Selon l'ensemble de solutions potentielles pour chaque structure de décodage, les puissances de transmission optimales peuvent être strictement inférieures ou strictement égales à la puissance de transmission maximale P_{max}. Par exemple, dans $\mathbf{R}^{nn}$, la puissance maximale est toujours utilisée: $P_1 = P_2 = P_{max}$, alors que pour $\mathbf{R}^{nd}$, $P_1 = P_{max}$ and $0 \leq P_2 \leq P_{max}$ et pour $\mathbf{R}^{dd}$, $0 \leq P_1, P_2 \leq P_{max}$. Dans les simulations, nous laissons les puissances de transmission prendre 10 valeurs diffeérentes entre 0 et P_{max}, inclus. Les points de débits marqués sont obtenus grâce à la parametrisation de la frontière Pareto proposée et l'astérisque rouge correspond au point de somme maximale des débits en utilisant la parametrisation correspondante alors que les carrés rouges correspondent aux stratégies MRT: $\left(\mathbf{w}_1 = \frac{\mathbf{h}_{21}}{\|\mathbf{h}_{21}\|}, \mathbf{w}_2 = \frac{\mathbf{h}_{22}}{\|\mathbf{h}_{22}\|}\right)$ dans $\mathbf{R}^{nd}$; $\left(\mathbf{w}_1 = \frac{\mathbf{h}_{11}}{\|\mathbf{h}_{11}\|}, \mathbf{w}_2 = \frac{\mathbf{h}_{12}}{\|\mathbf{h}_{12}\|}\right)$ dans $\mathbf{R}^{dn}$ et $\left(\mathbf{w}_1 = \frac{\mathbf{h}_{11}}{\|\mathbf{h}_{11}\|}, \mathbf{w}_2 = \frac{\mathbf{h}_{22}}{\|\mathbf{h}_{22}\|}\right)$ dans $\mathbf{R}^{dd}$ et $\mathbf{R}^{nn}$.

0.4.5.1 Canaux Corrélés et Structures de décodage optimales de maximisation de la somme des débits

Dans cette section, nous supposons un canal symétrique [3] dans lequel les canaux directs, $\mathbf{h}_{ii}$, sont des canaux vectoriels i.i.d complexes gaussiens. Le canal interférent $\mathbf{h}_{ji}$ a un angle de projection θ_i sur le canal direct $\mathbf{h}_{ii}$:

$$|\mathbf{h}_{ji}^H \mathbf{h}_{ii}| = \|\mathbf{h}_{ii}\| \|\mathbf{h}_{ji}\| \cos(\theta_i). \tag{31}$$

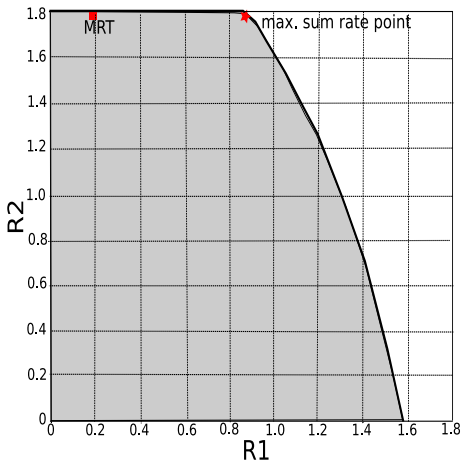

(a) Région des débits réalisable par $\mathbf{R}^{nd}$: la paramétrisation proposée atteint la frontière Pareto et le point de somme des débits maximale.

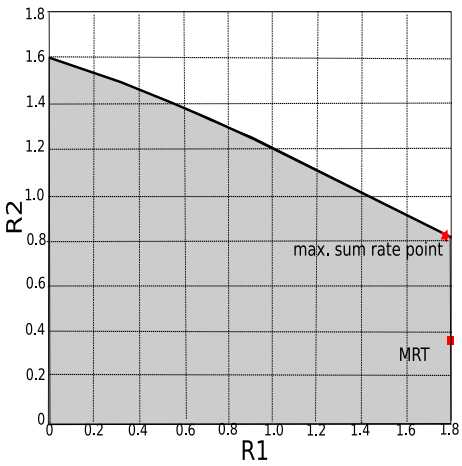

(b) Région des débits réalisable par $\mathbf{R}^{dn}$: la paramétrisation proposée atteint la frontière Pareto et le point de somme des débits maximale.

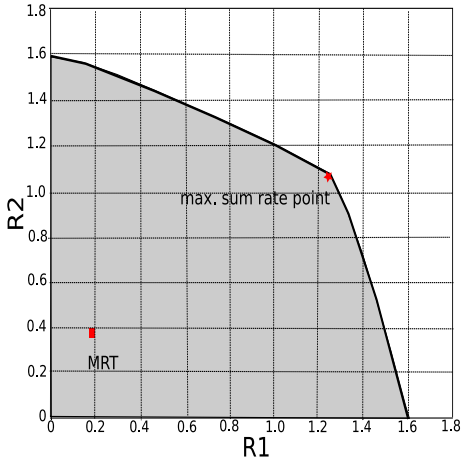

(c) Région des débits réalisable par $\mathbf{R}^{dd}$: la paramétrisation proposée atteint la frontière Pareto et le point de somme des débits maximale.

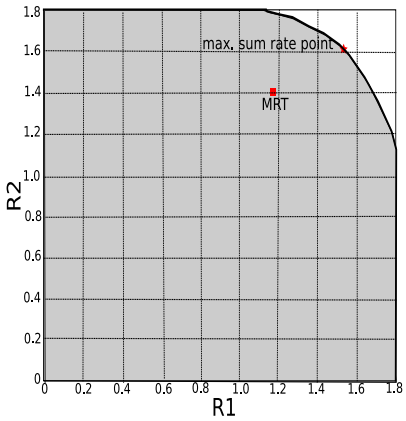

(d) Région des débits réalisable par $\mathbf{R}^{nn}$: la paramétrisation proposée atteint la frontière Pareto et le point de somme des débits maximale.

Figure 3: Régions des débits réalisables par les différentes structures de décodage.

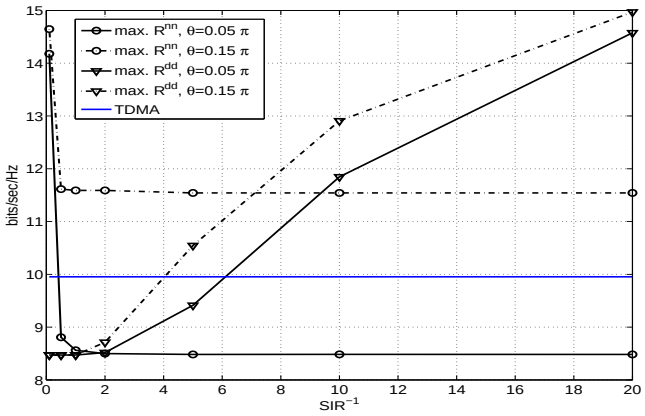

Figure 4: La somme des débits moyenne pour les différentes structures de décodage comparées à une transmission TDMA dans un canal symétrique en fonction de la puissance du canal d'interférence.

En plus, nous définissons le rapport signal à interférence SIR comme

$$\mathrm{SIR} = \frac{\|\mathbf{h}_{ii}\|^2}{\|\mathbf{h}_{ji}\|^2}. \tag{32}$$

Dans la Figure 5.11, nous comparons la somme des débits obtenue par $\mathbf{R}^{nn}$, $\mathbf{R}^{dd}$ et TDMA. Quand la puissance du canal interférent augmente, il y a une transition de $\mathbf{R}^{nn}$ à TDMA à $\mathbf{R}^{dd}$: traiter l'interférence comme du bruit est optimal en termes de somme des débits quand le SIR est faible alors que le décodage de l'interférence devient optimal dans le régime de haute interférence, en passant par le partage en temps. Quand l'angle entre l'interférence et le canal direct augmente jusqu'à $\theta = 0.15\pi$, c'est à dire à peu près 27 degrés, il y a une transition directe entre traiter l'interférence comme du bruit et le décodage de l'interférence. Donc, quand le canal direct et le canal interférent sont *plus séparés*, le partage dans le temps n'est pas optimal en termes de somme des débits et les deux autres structures de décodage ont une performance supérieure.

Dans la Fig. 5.12, nous comparons la somme maximale des débits pour les différentes structures de décodage avec celle correspondant à une transmission TDMA en fonction du SNR. Quand le lien interférent est aussi puissant que le lien direct, SIR= 1, traiter l'interférence comme du bruit est optimal en termes de somme des débits à n'importe quel SNR. Quand la puissance du canal interférent augmente $\mathrm{SIR}^{-1} = 5, 10, 20$, il est optimal pour les deux récepteurs de décoder l'interférence d'abord à un SNR faible alors qu'un récepteur traitant l'interférence comme du bruit alors que l'autre décode l'interférence est optimal en termes de la somme des débits pour un SNR haut.

0.4.5.2 Performance de l'algorithme sous-optimal

Dans la Fig. 5.13, nous avons tracé la somme des débits maximale réalisée pour différentes structures de décodage et nous la comparons avec le simple algorithme proposé pour un SIR décroissant. On observe que quand l'interférence est faible, il est optimal en terme de maximisation de la somme des débits de traiter l'interférence comme du bruit et quand

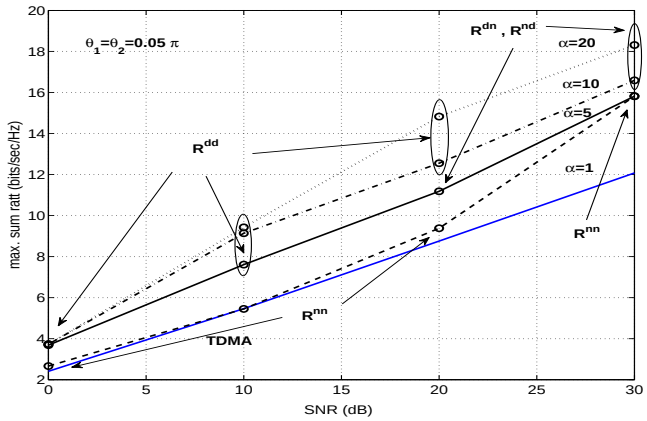

Figure 5: Somme moyenne des débits pour différentes structures de décodage comparées à TDMA dans un canal symétrique en fonction du SNR.

l'interférence devient plus forte, la somme des débits peut être augmentée en permettant à l'un des récepteurs de décoder l'interférence. Dans le régime d'interférence forte, les deux récepteurs doivent décoder l'interférence pour pouvoir atteindre la somme des débits maximale. Selon les coéfficients de canaux, TDMA peut parfois avoir une performance supérieure à $\mathbf{R}^{nn}$ et $\mathbf{R}^{dd}$ dans le régime d'interférence moyenne. Noter que le calcul du point de maximisation de la somme des débits est NP-difficile. Cependant, on observe que le simple algorithme proposé a une performance satisfaisante avec seulement 5 choix de vecteurs de beamforming.

0.4.6 Conclusion

La capacité de décodage de l'interférence apporte plus de liberté aux niveaux des récepteurs: ces derniers peuvent soit décoder l'interférence soit la traiter comme du bruit. Cependant, il n'est pas trivial de décider au niveau des émetteurs quand il faut éviter de générer de l'interférence et quand il faut au contraire l'amplifier. Pour répondre à cette question, nous formulons la région de débit réalisable pour un canal MISO-IC-SUD à deux utilisateurs. Nous fournissons une analyse approfondie de la région de débit réalisable, comme l'union de différentes structures de décodage. La frontière Pareto est ensuite characterisée en fonction de l'allocation de puissance et des vecteurs de beamforming. En application directe de la characterisation de la frontière de Pareto, nous caractérisons les points qui peuvent maximiser la somme des débits. L'ensemble de solutions potentielles à la maximisation de la somme des débits est un strict sous-ensemble de l'ensemble de solutions potentielles à la frontière Pareto. Avec la caractérisation de la somme des débits maximale, nous trouvons les conditions d'optimalité de MRT qui décrivent les conditions dans lesquelles les simples stratégies MRT sont optimales en termes de somme des débitsl. [1] Nous concluons en montrant des résultats de simulations qui permettent d'avoir une idée de la réponse à la question " *Quand est-il optimal d'être egoiste?*". Dans les canaux symétriques, il y a une transition dans la structure de décodage optimale allant de traiter l'interférence comme du bruit, à une stratégie TDMA, au décodage de l'interférence au niveau des deux recépteurs

[1] Se réferer à la thèse pour plus de détails.

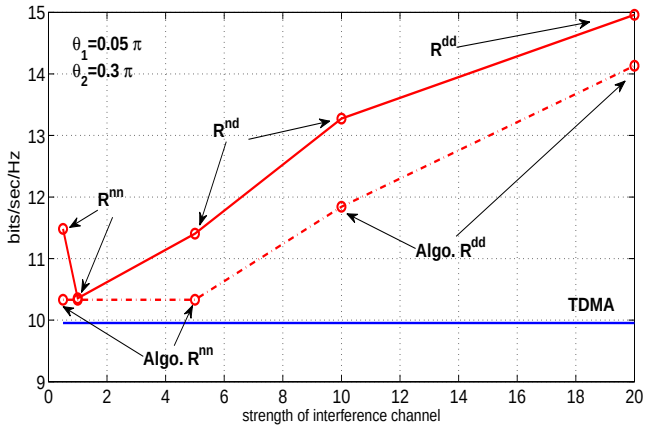

Figure 6: Structures de décodage optimales en fonction de la puissance du canal interférent.

à mesure que l'interférence augmente.

0.5 Conclusions et Travaux futurs

Au cours de cette thèse, nous avons abordé le problème de conception des vecteurs de beamforming de manière distribuée dans les canaux gaussiens vectoriels sans et avec décodage de l'interférence (SUD et IDC, respectivement). Nous résumons les contributions ci-dessous.

- Dans la section 3, nous proposons un algorithme à complexité réduite pour la conception de beamforming distribué sur le MISO-IC-SUD qui permet aux utilisateurs de coopérer et d'opérer à un point de fonctionnement proche de la frontière Pareto. Les vecteurs de beamforming proposés équilibrent entre les solutions MRT (egoiste) et ZF (altruiste).

- Dans la section 4, nous avons dévelopé cette notion d'équilibrage entre égoisme et altruisme pour le MIMO-IC-SUD. Nous avons proposé un algorithme de conception émetteur-récepteur itératif qui choisit les poids alloués à chaque lien dans les réseaux asymétriques et optimise la performance de la somme des débits. Ces poids dépendent des statistiques des canaux, au lieu des réalisations instantanées des canaux, ce qui diminue la quantité d'information sur le canal échangée par rapport aux autres algorithmes dans la littérature. Dans le régime de haut SNR, l'algorithme proposé aligne l'interférence s'il est possible de le faire, ce qui guarantit une somme des débits qui croît linéairement avec le SNR. Dans les scénarios où il est impossible d'aligner l'interférence, nous proposons un simple algorithme d'allocation binaire de puissance qui a pour objectif de restaurer la faisabilité de l'alignement d'interférence. Les résultats de nos simulations montrent qu'avec une controle binaire de la puissance de transmission, le design proposé en émission et en réception pour balancer entre góisme et altruisme réussit à restaurer la faisabilité de l'alignement de l'interférence et atteint des sommes de débits supérieures à celles des autres algorithmes.

- Dans la section 5, nous donnons aux récepteurs la possibilité de décoder l'interférence. Nous considérons le cas d'un canal MISO-IC à deux utilisateurs avec IDC et proposons 4 structures de décodage, chaque récepteur choisit soit de décoder l'interférence et de la soustraire du signal reçu avant de décoder son signal propre soit de traiter l'interférence comme du bruit. Nous trouvons la région des débits réalisable par ces différentes stratégies et la frontière Pareto correspondante. Les vecteurs de beamforming et l'allocation de puissance de transmission qui permettent d'atteindre la frontière Pareto ont été caracterisées. Nous avons démontré que les vecteurs Pareto optimaux sont des combinaisons positives linéaires de deux canaux, conformément aux résultats obtenus pour le MISO-IC-SUD [31]. Nous utilisons la caractérisation obtenue de la frontière Pareto pour caractériser le point de somme des débits maximale et obtenons un ensemble réduit de vecteurs de beamforming qui contient la solution optimale. Ceci réduit de façon significative l'espace de recherche du problème initial qui est NP-difficile [39]. Afin de trouver une méthode de transmission aussi simple que possible, nous avons étudié les conditions de canal dans lesquelles les stratégies MRT sont optimales en termes de somme des débits. Inspirés par ces résultats, nous proposons une méthode de transmission très simple avec un groupe restreint de choix de vecteurs de beamforming. Les résultats de simulations confirment que sous certaines conditions de canal, le schème proposé a une performance en termes de somme des débits très encourageante.

Abstract

In this thesis, we aim to optimize transmit and receive strategies in a network where there is little or no centralized resource management unit and nodes have limited knowledge of the channel states and limited backhaul communication among each other. In particular, the transmitters have mostly locally available channel state information (CSI) and we assume no data sharing or joint transmit strategies design among transmitters, thus prohibiting joint MIMO transmission.

As transmitters must share the same system resources e.g. time and frequency, they generate interference in the process of communicating with the receivers making interference management essential. In a game theoretic perspective of the beamforming design problem over the interference channel, extreme egoistic and altruistic strategies can be defined. Egoistic transmitters act selfishly and maximize their own SINR despite the interference generated to the remaining of the network whereas altruistic transmitters exploit all resources to null out interference generated towards other receivers. It is intuitive to see that none of the above two strategies is generally sum rate optimal. A recent work [31] shows that in the transmit beamforming vector design problem in the MISO-IC with single user decoding (SUD), balancing egoism and altruism brings the operating point on the Pareto boundary, which is the boundary of the achievable rate region assuming linear pre-processing. With this concept in mind, we investigate distributed transmit beamforming designs in the MISO-IC-SUD in Chapter 3. We develop an iterative algorithm that starts at the Nash equilibrium (egoistic extreme) and in each iteration moves towards the zero-forcing solution (altruistic extreme) with a fixed step size. The algorithm ends if one of the transmitters experiences a decrease of rates, thus mimicking the effects of bargaining. The proposed algorithm achieves an operating point close to the Pareto boundary and each user experiences a higher rate than the Nash equilibrium. We thus demonstrate that on the MISO-IC-SUD, players (transmit-receive pairs) can achieve higher rates by cooperating and maintaining a balance between egoism and altruism.

As an extension of the beamforming problem on the MISO-IC-SUD, we design the transmit and receive strategies on the MIMO-IC-SUD in Chapter 4. Assuming mostly local CSIT, we model the problem as a Bayesian game which takes the unknown channel knowledge into consideration and where players maximize the expected utility function based on the statistics of the unknown channel. We derive the equilibria of the Bayesian games and revisit the sum rate maximization problem on the K users MIMO-IC-SUD. We observe that the sum rate maximization solution can be interpreted as a balance between the egoistic and altruistic equilibria. With this analysis, we provide an algorithm which allows the transmitters and receivers to optimize the transmit and receive beamformers iteratively. At convergence, the algorithm achieves interference alignment in high SNR regime which allows the sum rate to scale indefinitely with SNR, with the number of degrees of freedom (DOF) as slope. In low SNR regime, we outperform conventional inter-

ference alignment schemes as our proposed algorithm balances the egoistic and altruistic components of the metric. In particular, the proposed algorithm achieves close to optimal performances in asymmetric networks, in which some receivers experience stronger uncontrolled background noise.

Then we proceed to allow the receivers to have interference decoding capability (IDC) in the MISO-IC in Chapter 5. This additional degree of freedom allows receivers to decode interference and subtract it from the received signal and thus enjoy interference free communication when the channel realizations allow it. However, the receivers' choices of action depend on the design of the transmit precoders. With each choice of the transmit beamformers, we form a new SISO-IC which has a different capacity region. Thus, with each MISO channel realization, we must choose the beamforming vector and transmit power such that the achievable sum rate is the highest after taking into account all possible receivers actions (decode interference or treat interference as noise). There are three design parameters: the receivers decoding structure, the transmit beamforming vector and the transmit power. However, the optimal choice of the three parameters is coupled with each other and its computation is shown to be NP-hard [39]. Nevertheless, we simplify the analysis by first formulating the achievable rate region of a two-user MISO-IC-IDC as a union of regions with different decoding structures. Then, we characterize the boundaries of achievable rate regions of each decoding structure and thus the overall Pareto boundary. We parameterize the transmit power and beamforming vectors that attain the Pareto boundary. The Pareto optimal beamforming vectors are positive linear combinations of two channel vectors with weights depending only on two real-valued scalars that range from zero to one. This refines the search space of potential Pareto boundary attaining solutions. As a direct application of the Pareto boundary characterization, we characterize the maximum sum rate point, whose solution set is a strict subset of that of the Pareto boundary, thus significantly reducing the search space of the originally NP-hard problem.

Acknowledgements

I would like to dedicate this thesis to my parents who support me with all of their hearts. If it had not been them, it would not be possible for me to finish my thesis. I would like to thank them for their faith and patience with me. I would also like to thank my sister Xandre and brother Adam for their love and the fun time we always have when I am at home. I must also thank Pawel Zawisza for his love, care and support.

Also, I would like to thank two very important persons who contributed a lot in this thesis, Prof. David Gesbert and Prof. Eduard Jorswieck. David has been a very nice thesis supervisor not only in the academic field but also in life. Apart from giving me guidance in my thesis, he teaches me to relax and keep a distance from work occasionally. It is through this isolation, we keep a clear head and maintain the passion of research. David has always brilliance and a strong intuition and guides me to the right path throughout these 3 years in EURECOM, France. In the near end of my thesis, we started a collaboration between EURECOM and TU Dresden. Hadn't it been for Eduard who helped me a lot in the last few months, the second part of thesis would not exist. Although we only collaborate for a short period of time, Eduard has amazed me with his board and solid knowledge in the areas, his thoroughness and serious working attitude. I am looking forward to our collaborations in the near future.

Then, I would like to thank all my friends in France and Germany: Ikbal, Randa, Sara, Carina, Jin-hui, Sabrina and Ralph, Anne, Shen Fei, Xiao Lei, Kostas, Shakti, Umer, Najim, Rizwan, all my Chinese friends and many others. Thank you for keeping me mentally healthy and motivated in work. Also, I need to thank my friends in Hong Kong for their support: Hang, Roderick, Peter, Herbert, Tin and Ernest and many others.

Last by not least, I would like to thank my mentors in the past, Prof. Vincent Lau, Prof. Roger Cheng and Mr. William Wong for all the motivation, encouragement and share of knowledge. I would like to thank especially Mr. H.C Tsang for the first inspiration of pursuing electronic engineering and encourage my curiosity in mathematics and problem solving.

Contents

List of Figures

Acronyms

Here are the main acronyms used in this document. The meaning of an acronym is usually indicated once, when it first occurs in the text. The English acronyms are also used for the French summary.

app.	Appendix.
AWGN	Additive White Gaussian Noise.
BC	Broadcast Channel.
BS	Base Station.
cdf	cumulative density function.
DL	Downlink.
i.i.d.	independent and identically distributed.
IC	Interference Channel.
IDC	Interference Decoding Capability.
l.f.s	left hand side.
MIMO	Multiple Input Multiple Output.
MISO	Multiple Input Single Output.
MMSE	Minimum Mean Square Error.
MS	Mobile Station.
pdf	probability density function.
r.h.s.	right hand side.
Rx	Receiver(s).
SIMO	Single Input Multiple Output.
SNR	Signal-to-Noise Ratio.
SISO	Single-Input Single-Output.
s.t.	such that.
SVD	Singular Value Decomposition.
SUD	Single User Detection.
Tx	Transmitter(s).
w.r.t.	with respect to.

Notation

Throughout this thesis, calligraphic upper-case letters denote sets. Upper case and lower case boldface symbols will represent matrices and column vectors respectively.

$\mathrm{tr}\{\cdot\}$	Trace of the matrix in brackets.
$\det\{\cdot\}$	Determinant of the matrix in brackets.
$\lvert a\rvert$	Absolute value of a.
$\lVert\mathbf{a}\rVert$	Euclidean norm of vector $\mathbf{a}$.
$\lVert\mathbf{A}\rVert$	Frobenius norm of matrix $\mathbf{A}$.
$\lvert\mathbb{S}\rvert$	The cardinality of set $\mathbb{S}$.
$\mathbf{A}^*$	The complex conjugate of matrix $\mathbf{A}$.
$\mathbf{A}^H$	The complex conjugate transpose (Hermitian) of matrix $\mathbf{A}$.
$\mathbf{A}^t$	The transpose of matrix $\mathbf{A}$.
$\mathbf{A}^{-1}$	The inverse of matrix $\mathbf{A}$.
$[\mathbf{A}]_{(k:l,m:n)}$	A submatrix of $\mathbf{A}$ containing the common elements of rows k-l and columns m-n.
$\mathbf{A} = \mathrm{diag}\,(\mathbf{a})$	The diagonal matrix with the entries of vector $\mathbf{A}$ along its main diagonal, if the latter is defined.
$\mathbf{a} = \mathrm{diag}\,(\mathbf{A})$	The vector equal to the main diagonal of $\mathbf{A}$, if the latter is defined.
$\mathcal{E}\{\cdot\}$	Expected value of the random variable in brackets.
$\mathcal{CN}(\mathbf{m}, \mathbf{C})$	Circularly symmetric complex Gaussian random vector of mean $\mathbf{m}$ and covariance matrix $\mathbf{C}$.
$\max, \min$	Maximum and minimum.
$\arg\max\{\cdot\}$	Argument that maximizes the function(al) in brackets.
$\bigcup$	set union operation.
$\bigcap$	set intersection operation.
$\boldsymbol{\nu}(\mathbf{A})$	returns the dominant eigenvector of matrix $\mathbf{A}$.
$\Leftrightarrow$	The *if-and-only-if* relationship of two statements.
$Re(z)$	The real part of a complex number z.
$Im(z)$	The imaginary part of a complex number z.
$\arg(z)$	The phase of the complex number z.

Symbol Index

The definition of symbols that are repeated throughout this thesis are given in the tables below. There will be a few exceptions, where these symbols will denote something different than what is described below. For these exceptions, the definition will be given at the place of their occurrence.

Sets	
$\mathbb{R}, \mathbb{C}$	The set of all real and complex numbers, respectively.
$\mathbb{R}^{m\times n}$	The set of $m \times n$ real matrices.
$\mathbb{C}^{m\times n}$	The set of $m \times n$ matrices with complex-valued entries.
$\mathbb{Z}$	Set of integer numbers

Scalar Parameters	
j	subscript used for transmitter or receiver in the system.
i	subscript used for transmitter or receiver in the system.
k	subscript used for transmitter or receiver in the system.
N_t	Number of transmit antennas.
N_r	Number of receive antennas.
K	Number of transmitter-receiver pairs.

(Column) Vectors	
$\mathbf{h}_{ji}$	channel vector from transmitter i to receiver j.
$\mathbf{w}_i$	transmit beamforming vector of transmitter i.
$\mathbf{v}_j$	receive beamforming vector of receiver j.

Matrices	
$\mathbf{I}$	Identity matrix.
$\mathbf{H}_{ji}$	Channel matrix from transmitter i to receiver j.
$\mathbf{\Pi}_{\mathbf{x}}$	The projection matrix on vector $\mathbf{x}$.

$\mathbf{\Pi}_{\mathbf{x}}^{\perp}$ The orthogonal projection matrix on vector $\mathbf{x}$.

Chapter 1

Introduction

In a network without centralized resource management, transmitter and receiver nodes are isolated, in the sense that they do not exchange information, and are thus required to design transmit and receive strategies based on locally available information. This information includes channel state information (CSI) which is either estimated using uplink pilots in time-division-duplex systems (TDD) or obtained by feedback from receivers in frequency-division-duplex systems (FDD). With only locally available CSI, transmitters are not aware of other important information such as other transmitters' data or channel realizations. To obtain such non-local information, some backhaul communication is required. As backhaul communication among transmitters consumes system resources or may not be possible in certain situations, such as spectrum sharing among different operators, in this manuscript, we do not consider user payload data sharing that would allow for strong cooperation schemes such as joint transmit strategy designs, e.g. network MIMO.

We assume that the transmitters have a common objective, such as the system sum rate. In a competitive game theoretic framework (which has been considered for this type of channel in the literature) one may assume that the transmitters have an egoistic incentive and maximize their own rate while ignoring the excess interference generated towards other receivers in the network. However, if every transmitter in the network is egoistic and transmit at its best response strategies, the system converges to the Nash Equilibrium, assuming its existence. At the Nash Equilibrium, no transmitters (or players) have incentive to deviate from this operating point and it can be shown that this point generally results in a high amount of interference for all receivers. Hence, it is reasonable for the transmitters to cooperate and have a common objective, as long as there is a reward of cooperation compared to the Nash Equilibrium.

In this thesis, we consider point-to-point transmission in the network which is a general model with applications such as the cellular network and focus on the spatial structure of the interference channel. In the multiple-input-multiple-output interference channel (MIMO-IC), the multiple antennas at each node can be exploited to improve the information theoretic capacity by choosing the transmit and receive strategy carefully. Interference alignment (IA) is one example where the transmit and receive beamformers are chosen such that the interference signals at each receiver in the network align within a subspace with smaller dimension than the number of receive antennas. In this case, the interference can be nulled out by a simple zero-forcing receive beamforming vector. By sacrificing some degrees of freedom (DOF) for interference nulling, the transmitters and receivers in the network enjoy interference free communication, assuming the feasibility of interference alignment. However, interference alignment does not maximize sum rate in all SNR

regimes. In particular, in the low and medium SNR regimes, maximum-ratio-transmission (MRT) is a more reasonable transmission strategy as the interference power is negligible comparing to the noise power. Moreover, interference alignment tends to treat every link in the system equally which is not sum rate optimal in asymmetric networks where some links are weaker due to uncontrolled noise or shadowing. Hence, it is essential to have an adaptive strategy which adapts to both SNR and link priorities in both symmetric and asymmetric networks. This is the focus of Chapter 4 in this thesis.

Although the importance and relevance of the interference channel have been well established, the capacity region or the sum rate capacity of the most basic form of the interference channel, the single-input-single-output (SISO) IC, is still an open problem, except for some special cases. As an extension of the SISO-IC, the capacity of the MISO and MIMO IC remains unknown. Although the exact capacity is not known, there exist several capacity outer bounds and researchers are motivated to provide the best inner bounds or achievable rate region possible: schemes that achieve the highest weighted sum rates, in different network settings. The achievable rate region we consider in this manuscript is different from the achievable rate region in the information theoretic definition in the sense that we assume Gaussian codebooks other than optimizing over possible codebooks. In Chapter 3 and 4, we consider beamforming optimization problems in the MISO-IC and MIMO-IC with single user decoding (SUD) where linear filters are applied to both Txs and Rxs. In Chapter 5, we relax this constraint and allow interference decoding capability at the receivers, although linear filters are applied to the received signal, the overall interference decode and remove post-processing is not linear.

1.1 Problem Statement

In this thesis, we consider the scenario in which transmitters are not under centralized resource management and the transmit strategies must be designed in a semi-distributed fashion. This is relevant to the scenario of a large network where the backhaul networks between transmitters cannot support full cooperation among all nodes or in a more practical scenario where transmitters (e.g. mobiles or base stations) are not under the same service providers (e.g. operators in the cognitive radio networks).

In order to focus on the study of the spatial structure of the problem, we assume linear pre-processing (and linear post-processing in Chapter 3 and 4 and non-linear post-processing in Chapter 5) of the signals through multiple antenna combining; Gaussian codebooks (complex Gaussian input alphabets) in order to simplify the rate expressions and additive white Gaussian noise (AWGN). With only locally[1] available CSI, we design transmit and receive strategies, e.g. beamforming vectors, so as to maximize the system sum rate or obtain an operating point that is close to the Pareto boundary. [2]

[1] the notion of "local" information may have several possible definitions. Ours is defined later in this document.

[2] In most scenarios, the sum rate is an attractive metric. However, in the SISO-IC, the maximum sum rate point may be a "single-user" point in which one of the users have to be shut off. This will not be interesting to the system as the transmitters only cooperate if the resulting operating point provides benefits over the Nash Equilibrium point for each transmitter. As a consequence, we rather consider the Pareto boundary, which is the set of operating points where one transmitter cannot increase its rate without causing decrease to other transmitter rates.

1.2 Related Work

In this section, we give a brief summary of a few different lines of work on the interference channel. Since the literature on this topic is already so rich, we present here only the areas that are closely related to this manuscript: distributed transceiver design on the multi-antennas IC. In Section 1.2.1, we present some well known work on the achievable rate region and capacity of specific cases of the interference channel. Note that, we assume Gaussian codebooks and additive white Gaussian noise (AWGN) whereas the references in Section 1.2.1 optimize over coding structures and input alphabet distributions which give further insight into the fundamental limits of the performance of the IC. In Section 1.2.2, we provide references that characterize the frontier of the achievable rate region of the IC, the Pareto boundary, under the assumption of linear precoding. These works are the inspiration of this manuscript; the study of the Pareto boundary and its characterization are still an on-going and popular research topic. In Section 1.2.3, we briefly discuss some game theoretic and bargaining problems for the case of more than two users on the IC where Tx-Rx pairs must share the system resources including space, time and frequency and generate interference towards each other. Game theory comes as a natural tool to model this conflict between Tx-Rx pairs, or players. When the Tx-Rx pairs are willing to and able to cooperate, bargaining theory offers an optimization framework for cooperative strategies. Closely related to our work, we present some important works on interference alignment in both the SISO and MIMO-IC in Section 1.2.4. In Section 1.2.5, we discuss briefly the optimization problems on the IC when partial CSIT (incomplete or outdated CSIT) is considered. Then, in Section 1.2.6, we include some work on the deterministic interference channel whereas in Section 1.2.7, we briefly discuss the large system analysis which considers for the case when the number of antennas and/or the number of links on the interference channel grows large.

1.2.1 Achievable rate region and capacity of IC

The notion of interference channel is introduced by Shannon [58]. In [11], Caleial discusses in details different achievable rates regions on the 2-user SISO-IC with deterministic channel gains. The impact and performance of different decoding schemes, such as full or no interference decoding, partial interference decoding and different capacity outer bounds such as a multiple access channel outer bound, are discussed. Then, the capacity region in the strong interference scenario was proposed by Sato [51] and Han and Kobayashi [21]. The capacity region in the strong interference case is a pentagon which contains the subcase of the very strong interference scenario which has a capacity region of a rectangle. By allowing rate splitting and partial interference decoding, Han and Kobayashi proposed an achievable scheme which achieves the best inner bound to date. These results are then extended the results to the Gaussian Interference channel [16].

However, the capacity of the SISO interference channel is still an open problem, except for several special cases, such as the noisy or low interference regime in which treating interference as noise and employing Gaussian input alphabets achieve capacity [4, 55]; the strong and very strong interference regime in which decoding interference and then subtract it from the received signal before decoding the desired signal is optimal [11,21,52]; the mixed interference regime, where one cross interference gain is stronger than direct channel gain and the other link weaker, in which case the sum rate capacity is shown to be attained by one user decoding interference and the other user treating interference as

noise [4, 67].

The results for scalar Gaussian interference channel are extended to the vector Gaussian channel [5] in which the authors showed that the sum rate optimal transmit covariance matrix of the MISO-IC with strong interference has rank less than or equal to the number of transmitters in the network; and to MIMO-IC [57] in which the authors provide the capacity regions of the MIMO-IC with very strong interference or aligned strong interference. Note that the study of sum rate is different from the study of achievable rate regions or capacity regions. The former is only one point in the capacity region but has the highest sum rate whereas the capacity region includes the maximum sum rate point and many other rate points. Any operating point outside the capacity region is not achievable and results in non-reducible decoding errors. The capacity region is the union of all possible achievable rate regions.

1.2.2 The Pareto boundary characterization of the MISO-IC

Since the establishment of the IC capacity region in the most general information theoretic sense is still an open and difficult problem, we address here a sub-region of the capacity region (denoted as MISO-IC and MIMO-IC) assuming simple linear pre-processing and zero or full interference decoding at the receiver. Note that since we do not consider partial interference decoding at the receivers, we are considering an achievable rate region *within* the Han-Kobayashi region. Although we sacrifice some achievable rate points, this assumption allows us to simplify the formulations and focus on the spatial structure of the problem.

We emphasize the importance of the boundary of such an achievable rate region, which we denote as the Pareto boundary. It holds importance in both information theory and bargaining theory as any point on the Pareto boundary satisfies the following definitions: assuming transmit and receive beamforming vectors, it is impossible for any player to increase its rate without decreasing other players rate. The Pareto boundary of MISO-IC and its characterization have gained much attention in the communication theory community since its introduction in [31, 73].

The authors, in particular [31], characterize the Pareto boundary in the general K users MISO-IC by providing a parameterization of the transmit beamforming vectors as a linear combination of interference channel coefficients with complex weights. In the two-user case, the Pareto optimal beamforming vectors of each Tx only depend on one real-valued parameter that takes values between zero and one. On the other hand, in [73], the authors draw the connection between the MISO-IC Pareto boundary characterization and the sum rate optimization problems on the cognitive radio. The Pareto boundary attaining beamforming vectors are the optimal solutions of the sum rate optimization problems with given interference temperature constraints. The resulting characterization of the beamforming vectors are different from [31]; the characterization in [31] uses $K(K-1)$ complex coefficients for the K-user MISO-IC but can be generated directly from the parameterization of the beamforming vectors whereas the characterization in [73] uses $K(K-1)$ real coefficients but the beamforming vectors are the solutions of some optimization problems. Both approaches provide insights into the problem structure and algorithms to operate arbitrarily close to the Pareto boundary. On the other hand, the computation of the maximum sum rate point and the corresponding beamforming vectors, is shown to be a NP-hard problem [39].

Although the rate functions on the interference channel have been proved to be non-

convex over transmit power or transmit beamforming vectors in general, researchers have developed relaxations and approximations of such problems to offer valuable insights. In [56], the authors consider the Pareto optimal transmit covariance matrices of the MISO-IC-SUD where interference is treated as noise. The Pareto boundary attaining transmit covariance matrices are the solutions of a rate optimization problem subject to interference temperature constraints. By converting the non-convex rate optimization problem into a family of convex optimization problems, the authors show that the optimal transmit covariance matrices are rank one and therefore it is sufficient to consider the transmit beamforming vector for Pareto optimality and sum rate maximization. Inspired by [31, 56], in Chapter 5, we convert the Pareto optimality problem in the MISO-IC-IDC to a family of convex optimization problems and prove that the Pareto optimal transmit covariance matrices are rank one in the MISO-IC-IDC where interference can be decoded and removed.

1.2.3 Game theoretic and bargaining problems

Game theory is a powerful tool for resource allocation and optimization problems on the interference channel where the transmitters (players) are individuals that have conflicts over the system resources such as time and bandwidth. It can be shown that the Nash Equilibrium is not avoidable in zero-sum games when each player acts selfishly with its best-response strategy but can bring tremendous loss to all players in non-zero sum games such as the rate optimization problems in the interference channels. In such problems, cooperation among players can help improve the utilities of all players. It is through bargaining theory that we model how players bargain and cooperate in order to improve the utilities in a stable way. Through series of bargaining, at convergence, players reach an outcome, called the Nash Bargaining solution, which is shown to outperform the Nash equilibrium at which the transmitters all act selfishly. In [2], the authors show the existence of the Nash Bargaining solution for a two-user SISO-IC where players are using time-division-multiple-access (TDMA) or frequency-division-multiple-access (FDMA) strategies. In [72], the authors provide alternative bargaining solutions to the same channel settings but with asymmetric users requirements. On the other hand, pricing is a popular technique in bargaining theory. In [61], the authors propose to use the pricing technique such that transmitters can reach the maximum sum rate point on the MIMO-IC, through iterations of bargaining process. At high SNR, this pricing algorithm comes to the interference alignment solution such that all receivers enjoy interference-free communications.

Although bargaining theory provides an extensive optimization framework in which convergence and performance of the algorithm can be analyzed, it relies heavily on the design of a heuristic utility which may be different from the original objective. Each choice of such heuristic utility functions gives a different convergence behavior and solution. Also, the resulting bargaining solution may require full channel state information exchange. In this thesis, inspired by the bargaining theory, we tackle the distributed beamforming design problem on the vector interference channel in an iterative fashion among Txs and Rxs, with the sum rate and the Pareto boundary as the objectives. The bargaining solution of the maximum sum rate problem on the MIMO-IC-SUD [61] , requiring full CSI exchange, is considered as a performance upper bound to our distributed beamforming design algorithm in Chapter 4.

1.2.4 Interference alignment

In [60, 66] , it is shown that interference alignment allows transmitters and receivers to achieve $K/2$ degrees of freedom, also known as multiplexing gains, on the K-user time-varying SISO-IC . Interference alignment is a promising technique that gives the highest achievable degrees of freedom which is especially important in the high SNR regime as the sum capacity scales linearly with SNR, with a slope equal to the number of degrees of freedom. In the following, we outline several different forms of interference alignment.

1.2.4.1 Time domain interference alignment

The *time, frequency-domain interference alignment* is applied on the time-varying or frequency-varying SISO-IC [60, 66]. The transmitters expand the transmit symbols in the time / frequency domain to big super-symbols that consume some consecutive time / frequency slots in which each slot experiences a different channel fading. This time / frequency diversity allows the super-symbols to be in different dimensions. Through interference alignment, the interference symbols align into a smaller subspace than the receiver dimension. In this case, zero-forcing is implemented at the receiver to remove interference completely [66]. The number of degrees of freedom in a K-user time-varying SISO-IC is shown to be $K/2$. In [60] the authors modify the algorithm in [66] to further improve the sum rate while maintaining the same degree of freedom.

1.2.4.2 Signal domain interference alignment

In *signal domain interference alignment*, signals are encoded using different codes such as lattice codes [30, 63] or random codes [8] such that the interference signals are aligned in the codes level. In [8], the authors show that random codes achieve capacity on the 3-user many-to-one deterministic SISO-IC in the noisy-interference regime. In [30, 63], on the other hand, lattice codes are applied to a class of three-user Gaussian and K-user symmetric interference channels, respectively. Although in this thesis, we do not consider coding and maintain our focus on the spatial domain of the distributed transceiver design problem, aligning interference on the signal level provides insight into the optimization problems. The combinations of the signal level alignment and the spatial domain alignment is yet to be seen.

1.2.4.3 Spatial domain interference alignment

In a MIMO-IC, the *spatial domain Interference alignment* may be employed: the transmit and receive beamforming vectors are exploited such that interference signals align in a reduced-dimension subspace and can therefore be nulled out by the receive beamforming vectors, [20, 24, 25, 49, 53, 59]. Interference alignment is achieved by iteratively minimizing interference power at each receiver [20], minimizing leakage interference power [49], jointly minimizing sum minimum mean squared error (MSE) [59] or with a least squares approach [70]. In [35, 53], the authors proposed an improved interference alignment scheme in terms of sum rate performance. In conventional spatial interference alignment scheme, the received interference signals are aligned into a subspace as small as possible. The proposed interference alignment scheme [35] provides an extra step of aligning the desired signal space as orthogonal as possible to the received interference subspace. In [53], the authors proposed to reduce the number of transmit data streams with interference alignment so

that the sum rate performance in low and medium SNR is higher than the sum rate achieved with full number of degrees of freedom.

Note that, although interference alignment maximizes the number of degrees of freedom, it does not maximize sum rate in all SNR regimes. In particular, in the low and medium SNR regimes, maximum-ratio-transmission (MRT) is a more reasonable transmission strategy as the interference has power smaller than the noise power. Moreover, interference alignment tends to treat every link in the system equally which is not sum rate optimal in an asymmetric network where some links are weaker due to uncontrolled noise or shadowing. Hence, it is essential to have an adaptive strategy which adapts to both SNR and link priorities in asymmetric networks. This is the focus of Chapter 4 in this thesis.

1.2.5 Partial CSIT analysis on interference channel

In distributed networks, as perfect and complete CSIT may not always be available, it is important to consider the robustness of the proposed algorithms with respect to incomplete CSIT. The research topics discussed above, such as the Pareto boundary characterization and interference alignment have been studied carefully for the partial CSIT case [27, 38]. In [27], the authors proposed an interference alignment scheme using lattice code on the MIMO-IC with imperfect CSI whereas in [38], the authors characterize the Pareto boundary on the MISO-IC when only statistical CSIT is available. In [64], the authors consider the frequency selective SISO-IC-SUD with limited broadcast feedbacks from Rxs. The number of feedback bits required to achieve interference alignment is shown to be $N(L-1)\log(P)$ where L is the number of taps and P is the transmit power. In this thesis, we assume perfect but not complete CSI of the network in the sense that each Tx or Rx can only obtain channel information of the channels it connects to, termed as local CSI. This assumption enforces practicality of the algorithm in the scenario where full and complete CSI of the whole network is available at every node, which is highly unlikely.

1.2.6 The deterministic channel approach

The Host-Madsen-Nosratinia conjecture [26] states that the degree of freedom in fully connected wireless interference networks with a single antenna per node and constant channel coefficients is one. Aiming to settle this conjecture, the deterministic channel approach offers a good approximation of the sum capacity of interference channel. In the deterministic channel approach, the input-output relationship of the channel is modeled as a bit-shifting operation [9, 17, 29]. This abstraction allows detailed study of the degree of freedom of the IC. In [17], the two-user SISO-IC sum capacity is approximated to within one bit using the deterministic channel approach. This result is extended in [29] such that the generalized degree of freedom (GDOF) of the symmetric Gaussian K-user SISO-IC is computed. The capacity of many-to-one and one-to-many Gaussian interference channel is approximated in [7].

The deterministic approach focus on the theoretical limit of the interference channel in terms of capacity and the degrees of freedom. In this thesis, we aim to provide practical algorithms which achieve performance as close as possible to such limits.

1.2.7 Large System Analysis

In [53], the authors address the tradeoff between the degrees of freedom and the rate offset in the MIMO-IC. The authors show that although it is possible to achieve $2N-1$ DOF in a symmetric K-user MIMO-IC with each node equipped with N antennas, a scheme that achieves DOF N may outperform the scheme with DOF $2N-1$ in low and medium SNR regime (the rate offset). The authors propose a large system approximation of the scheme with DOF N when the number of users K and the number of antennas N grow large. On the other hand, the authors in [48] employ interference alignment on the secondary link with respect to the primary link in a MIMO cognitive radio setting. The achievable transmission rate is approximated using large system analysis in the regime of large number of antennas.

The large system analysis provides a good reference point in the extreme of large networks or large number of antennas. Although the focus of this thesis is on the medium size networks, the large system analysis can be a potential extension of our work.

1.3 Scope of this work and contributions

In this thesis, we study distributed transmit strategies (also receive strategies in some cases) in the MISO and MIMO IC. In Chapter 2, we provide some brief background of the interference channel and definitions. The key contributions are organized around three main chapters (3, 4 and 5). The contributions are given in details below. In the remainder of the thesis, we assume that there is no data sharing and joint encoding among the transmitters.

In Chapter 3, we start by studying the two-user MISO-IC with single user decoding. As a basic set-up, we assume that the receivers have single antenna and single user decoding ability. In this setting, the Pareto boundary attaining beamforming vectors were shown to be a linear combination of selfish maximum-ratio-transmission (MRT) and altruistic zero-forcing (ZF) [31]. However, the closed form solution of the Pareto boundary attaining beamforming vectors are not provided in [31] and this is the aim of Chapter 3. We construct a simple algorithm which balances egoism and altruism and achieves operating points close to the Pareto boundary. The work is presented in the following publications:

- Z.K.M. Ho and D. Gesbert, *Spectrum sharing in multiple antenna channels: a distributed cooperative game theoretic approach*, in Proceedings of PIMRC, 19th IEEE international Symposium on Personal, Indoor and Mobile Radio Communications, pp. 1-5, September 15-18, 2008.

- R. Zakhour, Z.K.M. Ho and D. Gesbert, *Distributed beamforming coordination in multicell MIMO channels*, in Proceedings of VTC 2009, IEEE 69th Vehicular Technology Conference, pp. 1-5, April 26-29, 2009.

In Chapter 4, we extend the work in Chapter 3 by studying the MIMO-IC-SUD. Both the transmitters and receivers have multiple antennas and therefore the ability to improve the system efficiency. In particular, we aim to provide a game theoretic view of the sum rate maximization problem. We show that in asymmetric networks, different links in the system (each transmitter-receiver pair is considered as a link) should be weighted differently in the sum rate optimization problem, which is a concept not taken into account by existing

IA-based techniques which treat all links equally. By carefully balancing between egoism and altruism on each link, we achieve close to optimal performance in both symmetric and asymmetric MIMO-IC-SUD. As a special case, we look at the scenario in which the network is "over-crowded" and the interference alignment is infeasible and we provide a simple power control algorithm which restores the feasibility of interference alignment and allows the system sum rate to scale indefinitely with the system SNR. This work is presented in the following publications:

- Z.K.M. Ho, M. Kaynia and D. Gesbert, *Distributed power control and beamforming on MIMO Interference channels*, in Proceedings of EW 2010, 16th European Wireless Conference, pp. 654-660, April 12-15, 2010.

- Z.K.M. Ho and D.Gesbert, *Balancing Egoism and Altruism on Interference channel: the MIMO case*, in Proceedings of ICC 2010, IEEE International Conference on Communications, pp. 1-5, May 23-27, 2010.

- Z.K.M. Ho and D. Gesbert, *Balancing Egoism and Altruism on the single beam MIMO Interference Channel* , submitted to IEEE Transaction on Wireless Communications, 2011.

In Chapter 5, we study the two-user MISO-IC with interference decoding capability (IDC). With the IDC at the receivers, the performance of the system is an upper bound of the one without IDC, such as the scenario considered in Chapter 4. Although SISO-IC with SUD has been extensively studied, the MISO-IC-IDC has received little attention. The particularly intriguing problem arising in the multi-antenna IC with IDC is that transmitters may now have the incentive to *amplify* the interference generated at the non-intended receivers, in the hope that Rxs have a high chance of decoding the interference and removing it. This notion completely changes the previous paradigm of balancing between maximizing one's user's desired power and reducing the generated interference by opening up a new dimension for the beamforming design strategy. The fundamental question becomes *"when should a cooperating transmitter increase the generated interference?"*

We proposed and formulated an achievable rate region as a union of four possible decoding structures: receivers 1 and 2 choose to decode interference (D) or treat interference as noise (N). We then characterized the corresponding Pareto boundary and show that the Pareto boundary attaining beamforming vectors are positive linear combinations of specific vectors. As an application of the Pareto boundary characterization, we characterize the maximum sum rate point and obtain a solution set that is a strict subset of the previous. This shows a significant improvement, as the maximum sum rate operating point of such system is proved to be NP-hard. This work is presented in the following publications:

- Z.K.M. Ho, D. Gesbert, E. Jorswieck and R. Mochaourab, *Beamforming on the MISO Interference Channel with multi-user decoding capabability*, in Proceedings of Asilomar 2010.

- Z.K.M. Ho, D. Gesbert, E. Jorswieck and R. Mochaourab, *On the MISO Interference Channel with interference decoding*, submitted to IEEE Transaction on Information Theory, 2010.

In Chapter 6, we summarize the contributions of the thesis and provide an overview of possible future research directions.

Chapter 2

The Interference Channel

In this chapter, we introduce the system model of a general interference channel investigated in the following chapters of this manuscript. This chapter introduces our key simplifying assumptions and notations.

2.1 Channel model

In a network of $2N$ nodes where N nodes are transmitters and the remaining N nodes are receivers, we assume that the transmitters are equipped with N_t antennas and receivers are equipped with N_r antennas each. Each transmitter has a target receiver and each transmitter-receiver pair forms a link in the network. For each Tx i, $i = 1, \ldots, N$, the Gaussian fading channel to Rx j, $j = 1, \ldots, N$, is denoted as

$$\mathbf{H}_{ji} = \sqrt{\alpha_{ji}}\mathbf{G}_{ji} \tag{2.1}$$

where $\mathbf{G}_{ji}$ is a $N_r \times N_t$ matrix with independent identically distributed (i.i.d.) elements that are complex Gaussian random variables with zero mean and unit variance. The variable α_{ji} is the long term fading coefficient that depends on the path loss and the shadowing of the link between Tx i and Rx j.

We assume an individual power constraint P_i for each Tx i, which has an application in cellular systems where each base station or mobile station has an individual battery. In this manuscript, we focus on linear precoding strategies. Denote the precoders and decoders at Tx i and Rx i by $\mathbf{W}_i \in \mathbb{C}^{N_t \times N_{si}}$ and $\mathbf{V}_i \in \mathbb{C}^{N_r \times N_{si}}$ respectively, where N_{si} is the number of data streams Tx i intend to transmit. Without loss of generality, the precoders must satisfy the power constraint,

$$tr(\mathbf{W}_i\mathbf{W}_i^H) = 1. \tag{2.2}$$

Let $\mathbf{w}_{ij}$ and $\mathbf{v}_{ij}$ denote the column vectors of $\mathbf{W}_i$ and $\mathbf{V}_i$ respectively, i.e. the vectors corresponding to the transmission and decoding of the j-th symbol of link i, as follows

$$\begin{aligned} \mathbf{W}_i &= [\mathbf{w}_{i1}, \ldots, \mathbf{w}_{iN_{si}}] \\ \mathbf{V}_i &= [\mathbf{v}_{i1}, \ldots, \mathbf{v}_{iN_{si}}]\,. \end{aligned} \tag{2.3}$$

Clearly, $N_{si} \leq \min(N_t, N_r)$. Note that each column vector in $\mathbf{W}_i$ and $\mathbf{V}_i$ corresponds to a symbol in the symbol vector $\mathbf{x}_i$ from Tx i. The symbols are assumed to be unit power.

One can choose $\mathbf{W}_i$ and $\mathbf{V}_i$ carefully so that the signal-to-interference-plus-noise-ratio (SINR) of this link is improved.

The received signal at Rx j is

$$\mathbf{y}_j = \sum_{i=1}^{N} \mathbf{V}_j^H \mathbf{H}_{ji} \mathbf{W}_i \mathbf{x}_i + \mathbf{n}_j \tag{2.4}$$

where $\mathbf{n}_j$ is the thermal noise at Rx j and is assumed to be statistically independent to channel coefficients. The elements in $\mathbf{n}_j$ are i.i.d complex Gaussian distributed with zero mean and variance σ^2. We can rewrite the received signal to distinguish the desired signal from the interference and noise,

$$\mathbf{y}_j = \underbrace{\mathbf{V}_j^H \mathbf{H}_{jj} \mathbf{W}_j \mathbf{x}_j}_{\text{desired signal}} + \underbrace{\sum_{i=1, i\neq j}^{N} \mathbf{V}_j^H \mathbf{H}_{ji} \mathbf{W}_i \mathbf{x}_i}_{\text{interference signal}} + \mathbf{n}_j. \tag{2.5}$$

Assuming that the receivers are single-user-detection (SUD) receivers, the SINR of symbol k, $k = 1, \ldots, N_{sj}$, at receiver j is therefore

$$\gamma_{jk}(\mathbf{W}, \mathbf{V}, \sigma^2) = \frac{|\mathbf{v}_{jk}^H \mathbf{H}_{jj} \mathbf{w}_{jk}|^2}{\sum_{k'\neq k}^{N_{sj}} |\mathbf{v}_{jk}^H \mathbf{H}_{jj} \mathbf{w}_{jk'}|^2 + \sum_{i\neq j}^{N} \sum_{k'=1}^{N_{si}} |\mathbf{v}_{jk}^H \mathbf{H}_{ji} \mathbf{w}_{ik'}|^2 + \|\mathbf{v}_{jk}\|^2 \sigma^2} \tag{2.6}$$

where $\mathbf{W} = [\mathbf{W}_1, \ldots, \mathbf{W}_N]$ and $\mathbf{V} = [\mathbf{V}_1, \ldots, \mathbf{V}_N]$. The channel model of a system of $N = 3$ Tx-Rx pairs with $N_t = N_r = 2$ and $N_{si} = 1, i = 1, 2, 3$ is shown in Fig. 2.1. The circles illustrated the locally available channel knowledge at Tx 1: $\{\mathbf{H}_{i1}, i = 1, 2, 3\}$ and at Rx 3: $\{\mathbf{H}_{3i}, i = 1, 2, 3\}$.

2.1.1 Local channel knowledge

In this subsection, we give the formal definitions of local channel knowledge assumption which is employed throughout the remaining of the thesis. Let the local channel information available at Tx i to be $\mathbb{B}_i$,

$$\mathbb{B}_i = \{\mathbf{H}_{ji}, \quad j = 1, \ldots, N_c\}, \qquad i = 1, \ldots, N_c. \tag{2.7}$$

Similarly the unknown channel knowledge at Tx i is

$$\mathbb{B}_i^{\perp} = \{\mathbf{H}_{jk}, \quad j, k = 1, \ldots, N_c\} \setminus \mathbb{B}_i. \tag{2.8}$$

2.1.2 An achievable rate region and its Pareto boundary

The achievable rate region, assuming linear transceivers and single-user-detection at Rxs, is the set of rates achieved by exhausting the transmit and receive matrices that satisfy the power constraints. Letting

$$R_i(\mathbf{W}, \mathbf{V}, \sigma^2) = \sum_{k=1}^{N_{si}} \log_2(1 + \gamma_{ik}(\mathbf{W}, \mathbf{V}, \sigma^2)), \qquad i = 1, \ldots, N, \tag{2.9}$$

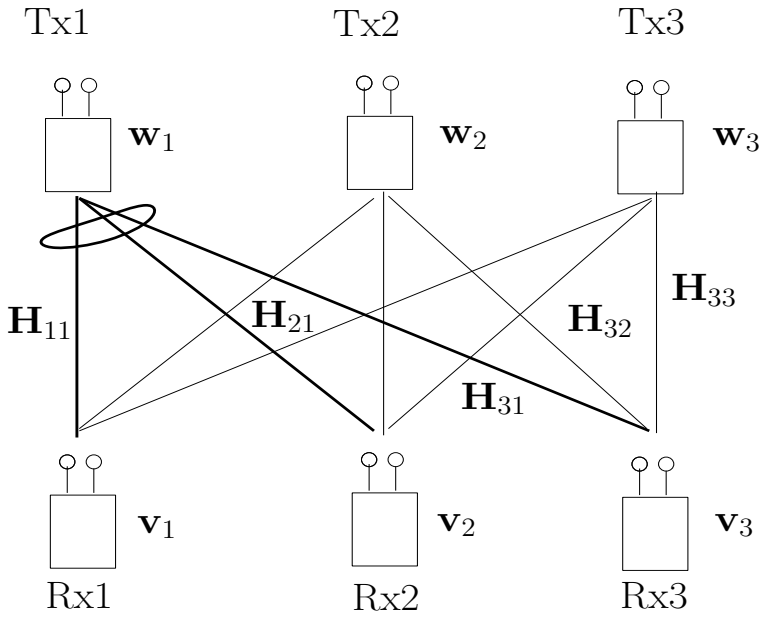

Figure 2.1: The channel model of a system of three Tx-Rx pairs with two antennas at each node. The bold lines indicate the locally available channel state information at Tx 1.

be the rate achieved at user i for Tx and Rx matrices $\mathbf{W}$ and $\mathbf{V}$, the rate region is:

$$\mathcal{R}^{SUD} = \left\{ (R_1(\mathbf{W}, \mathbf{V}, \sigma^2), \ldots, R_N(\mathbf{W}, \mathbf{V}, \sigma^2)) : tr\left(\mathbf{W}_i \mathbf{W}_i^H\right) = 1, i = 1, \ldots, N; \mathbf{V} \in \mathbb{C}^{N_r \times \bar{N}_s} \right\} \tag{2.10}$$

where $\bar{N}_s$ is the total number of streams in the system,

$$\bar{N}_s = \sum_{i=1}^{N} N_{si}. \tag{2.11}$$

The Pareto boundary, $\mathcal{B}(\mathcal{R})$ is the boundary of the achievable rate region $\mathcal{R}$ and can be represented mathematically as follows.

$$\begin{aligned} \mathcal{B}(\mathcal{R}) = \big\{ &(R_1, \ldots, R_N) \in \mathcal{R} : \text{there does not exist } (r_1', \ldots, r_N') \in \mathcal{R} \\ &\text{such that } (r_1', \ldots, r_N') \geq (R_1, \ldots, R_N) \text{ with one straight inequality,} \big\} \end{aligned} \tag{2.12}$$

where we write R_i instead of $R_i(\mathbf{W}, \mathbf{V}, \sigma^2)$ for brief notations and $\geq$ is an component-wise inequality.

2.1.3 The maximum sum rate of the interference channel with linear processing

Note that the maximum sum rate with linear processing discussed here is smaller than the information theoretic ergodic capacity of the interference channel, which is still an open problem [1]. We assume linear pre- and post processing, Gaussian codebooks and additive

[1] The ergodic capacity is the maximum achievable sum rate optimizing over the source alphabets and possible processing techniques linear or non-linear.

white Gaussian noise that is independent of the source alphabets, and limited transmit power at each transmitter. Under these assumptions, the maximum sum rate is a function depending on the system SNR $\frac{1}{\sigma^2}$:

$$\begin{aligned} \mathcal{C}^{SUD}(\sigma^2) = \quad & \max_{\mathbf{W},\mathbf{V}} \sum_{i=1}^{N} \sum_{k=1}^{N_{si}} \log_2\left(1+\gamma_{ik}(\mathbf{W},\mathbf{V},\sigma^2)\right) \\ \text{subject to} \quad & tr\left(\mathbf{W}_i\mathbf{W}_i^H\right)=1, \qquad i=1,\ldots,N. \end{aligned} \tag{2.13}$$

The maximum sum rate defined in (2.13) assumes perfect channel state information at the transmitter (CSIT) and at the receivers (CSIR). In general, the perfect channel state information may not be available at the transmitters. One can formulate the maximum sum rate of IC with statistical CSIT by maximizing the averaged sum rate over different channel realizations.

$$\begin{aligned} \mathcal{C}^{Stat}(\sigma^2) = \quad & \max_{\mathbf{W},\mathbf{V}} \sum_{i=1}^{N} \sum_{k=1}^{N_{si}} \mathcal{E}_{\{\mathbf{H}_{mn},m,n=1,\ldots,N\}} \log_2\left(1+\gamma_{ik}(\mathbf{W},\mathbf{V},\sigma^2)\right) \\ \text{subject to} \quad & tr\left(\mathbf{W}_i\mathbf{W}_i^H\right)=1, \qquad i=1,\ldots,N. \end{aligned} \tag{2.14}$$

However, with only statistical CSIT, the optimized precoders and receivers can lead to channel outage by transmitting at a rate higher than the instantaneous capacity of the channel.

2.1.4 The degrees of freedom

The degrees of freedom (DOF) of the interference channel with SUD is the number of data streams the system can support without causing error at the receivers in the high SNR regime. It is widely used to approximate sum rate performance asymptotically,

$$DOF = \lim_{\sigma^2\to 0} -\frac{C^{SUD}(\sigma^2)}{\log\sigma^2} \tag{2.15}$$

where $C^{SUD}(\sigma^2)$ is defined in (2.13).

2.1.5 Spatial interference alignment

The spatial interference alignment scheme is a scheme that allows the system to operate with maximum multiplexing gains or degree of freedom on the interference channel [20, 49, 61]. In the MIMO-IC, interference alignment schemes jointly optimize the transmit and receive matrices such that the interference signals align or collapse into a subspace with a smaller dimension than the number of antennas at each receiver. For a general K-user MIMO-IC, there is no closed form solution of the transmit and receive matrices that achieve interference alignment, except for $K = 3$ symmetric MIMO-IC. The interference alignment solution can be described as the solution that satisfies the following criteria, for a predefined tuple of degree of freedom $(d_1,\ldots,d_N)$:

$$\begin{cases} rank(\mathbf{V}_i^H\mathbf{H}_{ii}\mathbf{W}_i) = d_i \\ \mathbf{V}_i^H\mathbf{H}_{ij}\mathbf{W}_j = \mathbf{0}, \qquad i,j=1,\ldots,N, i\neq j. \end{cases} \tag{2.16}$$

The feasibility of the constraints in (2.16) is termed the feasibility problem of IA and is a very important and well studied problem in its own right. We do not elaborate on this

topic so as to focus on beamforming optimization on the interference channel. For details, please refer to [44, 69] and the references therein.

Interference alignment is a necessary condition in high SNR regime as it allows the sum rate to scale indefinitely with the SNR with slope equal to the number of degrees of freedom in the system.

In the following, we give some simple receiver designs given the knowledge of the Tx beamformers.

2.1.6 The matched filter receiver

For receivers that have simple design and may not be able to afford complicated computations, the matched filter design is preferred:

$$\mathbf{v}_{ik} = \mathbf{H}_{ii}\mathbf{w}_{ik}. \tag{2.17}$$

The corresponding SINR can be written as

$$\gamma_{ik}^{MF} = \frac{\|\mathbf{H}_{ii}\mathbf{w}_{ik}\|^4}{\sum_{k'\neq k}^{N_{si}} |\mathbf{w}_{ik}^H\mathbf{H}_{ii}^H\mathbf{H}_{ii}\mathbf{w}_{ik'}|^2 + \sum_{j\neq i}^{N}\sum_{k'=1}^{N_{sj}} |\mathbf{w}_{ik}^H\mathbf{H}_{ii}^H\mathbf{H}_{ij}\mathbf{w}_{jk'}|^2 + \|\mathbf{H}_{ii}\mathbf{w}_{ik}\|^2\sigma^2} \tag{2.18}$$

2.1.7 The minimum-mean-squared error receiver

In this subsection, we introduce the minimum-mean-squared error receiver (MMSE) which is the solution of the mean-squared error minimization problem. We start with introducing the mean-squared error metric

$$MSE_{jk} = \mathcal{E}_{\{\mathbf{x}_{jk},\mathbf{n}_{jk}\}}\left(\left\|\mathbf{v}_{jk}^H\left(\sum_{i=1}^{N}\sum_{k'=1}^{N_{si}}\mathbf{H}_{ji}\mathbf{w}_{ik'}x_{jk'} + n_{jk}\right) - x_{jk}\right\|^2\right) \tag{2.19}$$

and the minimization problem is

$$\begin{aligned} \min_{\mathbf{v}_{jk},j=1,\ldots,N} \quad & MSE_{jk} \\ \text{subject to} \quad & tr(\mathbf{V}_j) = 1. \end{aligned} \tag{2.20}$$

We can expand the MSE_{jk} to the following:

$$\begin{aligned} MSE_{jk} &= \mathcal{E}_{\{x_{jk},n_{jk}\}}\left(\mathbf{v}_{jk}^H\mathbf{M}_{jk}\mathbf{M}_{jk}^H\mathbf{v}_{jk} - 2Re\left(\mathbf{v}_{jk}^H\mathbf{M}_{jk}x_{jk}\right) + \|x_{jk}\|^2\right) \\ &= \mathbf{v}_{jk}^H\mathcal{E}_{\{x_{jk},n_{jk}\}}\left(\mathbf{M}_{jk}\mathbf{M}_{jk}^H\right)\mathbf{v}_{jk} - 2Re\left(\mathbf{v}_{jk}^H\mathbf{H}_{jj}\mathbf{w}_{jk}\right) + 1 \\ &= \mathbf{v}_{jk}^H\left(\sum_{i=1}^{N}\sum_{k'=1}^{N_{si}}\mathbf{H}_{ji}\mathbf{w}_{ik'}\mathbf{w}_{ik'}^H\mathbf{H}_{ji}^H + \sigma^2\mathbf{I}\right)\mathbf{v}_{jk} - 2Re\left(\mathbf{v}_{jk}^H\mathbf{H}_{jj}\mathbf{w}_{jk}\right) + 1 \end{aligned} \tag{2.21}$$

where $\mathbf{M}_{jk} = \sum_{i=1}^{N}\sum_{k'=1}^{N_{si}}\mathbf{H}_{ji}\mathbf{w}_{ik'}x_{ik'} + n_{jk}$. Hence, the optimal $\mathbf{v}_{jk}$ that minimizes (2.21) is

$$\mathbf{v}_{jk} = \left(\sum_{i=1}^{N}\sum_{k'=1}^{N_{si}}\mathbf{H}_{ji}\mathbf{w}_{ik'}\mathbf{w}_{ik'}^H\mathbf{H}_{ji}^H + \sigma^2\mathbf{I}\right)^{-1}\mathbf{H}_{jj}\mathbf{w}_j. \tag{2.22}$$

The resulting SINR for symbol k at receiver j is

$$\gamma_{jk}^{MMSE} = \mathbf{w}_j^H\mathbf{H}_{jj}^H\left(\sum_{i=1}^{N}\sum_{k'=1}^{N_{si}}\mathbf{H}_{ji}\mathbf{w}_{ik'}\mathbf{w}_{ik'}^H\mathbf{H}_{ji}^H + \sigma^2\mathbf{I}\right)^{-1}\mathbf{H}_{jj}\mathbf{w}_j. \tag{2.23}$$

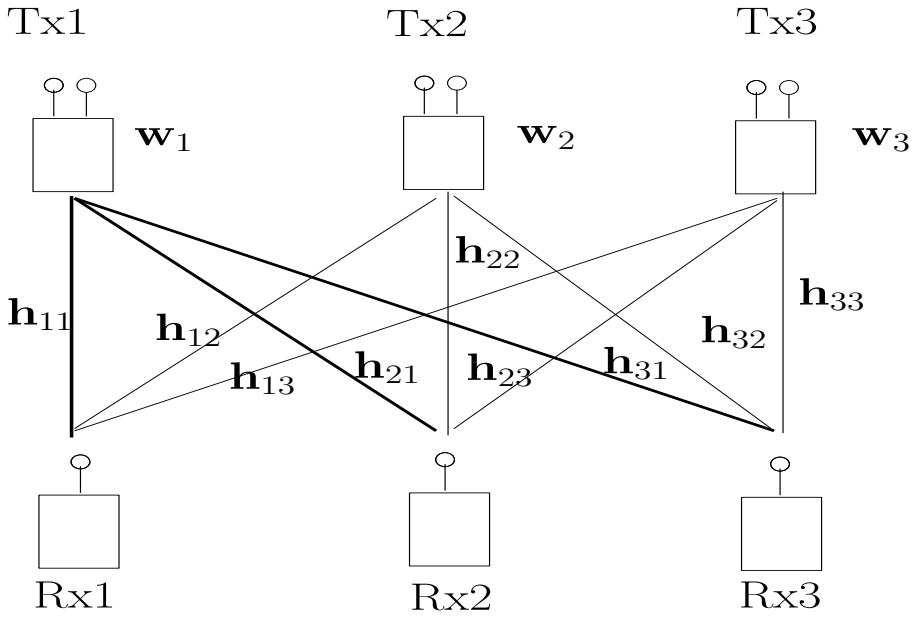

Figure 2.2: The channel model of the MISO-IC with $N = 3$ and $N_t = 2$.

2.1.8 The maximum SINR receiver

The maximum SINR receiver is the receiver that maximizes (2.6):

$$\mathbf{v}_{jk} = \left(\mathbf{F} - \mathbf{H}_{jj}\mathbf{w}_{jk}\mathbf{w}_{jk}^H\mathbf{H}_{jj}^H\right)^{-1}\mathbf{H}_{jj}\mathbf{w}_j \tag{2.24}$$

where $\mathbf{F} = \sum_{i=1}^{N}\sum_{k'=1}^{N_{si}}\mathbf{H}_{ji}\mathbf{w}_{ik'}\mathbf{w}_{ik'}^H\mathbf{H}_{ji}^H + \sigma^2\mathbf{I}$. The resulting SINR is

$$\gamma_{jk}^{MaxSINR} = \mathbf{w}_i^H\mathbf{H}_{jj}^H\left(\mathbf{F} - \mathbf{H}_{jj}\mathbf{w}_{jk}\mathbf{w}_{jk}^H\mathbf{H}_{jj}^H\right)^{-1}\mathbf{H}_{jj}\mathbf{w}_{jk}. \tag{2.25}$$

Note that the MMSE receiver in (2.22) is a scaled version of the maximum SINR receiver (2.24). To see this, we start from the *un-normalized* MaxSINR receiver:

$$\begin{aligned}
\mathbf{v}_{jk}^{MaxSINR} &= \left(\mathbf{F} - \mathbf{H}_{jj}\mathbf{w}_{jk}\mathbf{w}_{jk}^H\mathbf{H}_{jj}^H\right)^{-1}\mathbf{H}_{jj}\mathbf{w}_{jk} \\
&\overset{(a)}{=} \left(\mathbf{F}^{-1} + \frac{\mathbf{F}^{-1}\mathbf{H}_{jj}\mathbf{w}_{jk}\mathbf{w}_{jk}^H\mathbf{H}_{jj}^H\mathbf{F}^{-1}}{1 - \mathbf{w}_{jk}^H\mathbf{H}_{jj}^H\mathbf{F}^{-1}\mathbf{H}_{jj}\mathbf{w}_{jk}}\right)\mathbf{H}_{jj}\mathbf{w}_{jk} \\
&= \mathbf{F}^{-1}\mathbf{H}_{jj}\mathbf{w}_{jk} + a'\mathbf{F}^{-1}\mathbf{H}_{jj}\mathbf{w}_{jk} \\
&= (1 + a')\mathbf{F}^{-1}\mathbf{H}_{jj}\mathbf{w}_{jk} \\
&= (1 + a')\mathbf{v}_{jk}^{MMSE}
\end{aligned} \tag{2.26}$$

where (a) is due to the matrix inversion lemma and the variable $a' = \frac{\mathbf{w}_{jk}^H\mathbf{H}_{jj}^H\mathbf{F}^{-1}\mathbf{H}_{jj}\mathbf{w}_{jk}}{1-\mathbf{w}_{jk}^H\mathbf{H}_{jj}^H\mathbf{F}^{-1}\mathbf{H}_{jj}\mathbf{w}_{jk}}$.

2.2 The MISO-IC

In the scenario where Rxs are equipped with only one antenna, we obtain a MISO-IC, as shown in Fig. 2.2. The received signal at Rx i is

$$y_i = \mathbf{h}_{ii}^H \mathbf{w}_i x_i + \sum_{j=1, j\neq i}^{N} \mathbf{h}_{ij}^H \mathbf{w}_j x_j + n_i \tag{2.27}$$

where each Tx only transmits a single symbol and the channel from Tx j to Rx i is a vector Gaussian channel denoted as $\mathbf{h}_{ij}$. The beamforming vectors are subject to a power constraint: $\|\mathbf{w}_i\|^2 \leq 1, i = 1, \ldots, N$ and the noise n_i is a complex Gaussian random variable with zero mean and variance σ^2. The transmit symbol x_i is assumed to have unit power. Assuming SUD and treating interference as noise, the SINR of the i-th link is therefore:

$$\gamma_i(\mathbf{W}, \sigma^2) = \frac{|\mathbf{h}_{ii}^H \mathbf{w}_i|^2}{\sum_{j=1, j\neq i}^{N} |\mathbf{h}_{ij}^H \mathbf{w}_j|^2 + \sigma^2} \tag{2.28}$$

where $\mathbf{W} = [\mathbf{w}_1, \ldots \mathbf{w}_N]$. Note that each Rx has only one antenna and therefore has no ability to null out interference. This channel model is relevant in Chapter 3 in which we discuss the transmit beamforming design on the 2-user MISO-IC with SUD. We define here the Pareto boundary of the MISO-IC , $\mathcal{B}(\mathcal{R})$ to be the boundary of the achievable rate region $\mathcal{R}$:

$$\mathcal{R} = \left\{ (R_1(\mathbf{W}), \ldots, R_N(\mathbf{W})) : R_i(\mathbf{W}) = \log_2(1+\gamma_i), \|\mathbf{w}_i\|^2 \leq 1, i = 1, \ldots, N \right\}. \tag{2.29}$$

2.2.1 The power gain region

The power gain region is a set of rate tuples achieved by any beamforming vectors that satisfy the power constraints for any given channel realizations. For a N-user MISO-IC, the power gain region Φ_i of Tx i is

$$\Phi_i = \left\{ \left(|\mathbf{h}_{1i}^H \mathbf{w}_i|^2, \ldots, |\mathbf{h}_{Ni}^H \mathbf{w}_i|^2 \right) : \|\mathbf{w}_i\|^2 \leq 1 \right\} \tag{2.30}$$

for arbitrary fixed channel gains $\mathbf{h}_{1i}, \ldots, \mathbf{h}_{Ni}$. The power gain region Φ_i is shown to be a convex compact region [42]. Also, for SUD, the authors [42] show that the beamforming vectors that attain the Pareto boundary are on the boundary of Φ_i. This is relevant to the discussion of MISO-IC-IDC in Chapter 5. In Chapter 5, we employ the power gain region Φ_i to illustrate the Pareto boundary attaining beamforming vectors when interference decoding is allowed.

Chapter 3

MISO-IC with Single User Decoding

In this chapter, the Txs face the choice of competition or cooperation in the way they choose their transmission parameters (here beamforming vectors) to communicate with their respective users. We build on interesting recently published work [31] analyzing the gains of cooperation in this context and propose novel techniques for beamforming on the MISO-IC with single user decoding (SUD). The proposed techniques outperform classical non-cooperative game solutions and mimic known cooperative game solutions while introducing a distributed aspect for the algorithm.

As the Txs have the selfish goal of maximizing their own performance, this results in a conflict situation between the transmitter-receiver pairs. The classical way of analyzing performance optimization in this scenario is through the so called non-cooperative games [15,46] . The optimal operation point is known to be the Nash equilibrium solution (NE), defined to be the set of transmission strategies such that any unilateral deviation from it by anyone of the players cannot result in an increase of his/her utility (here, rate). Although NE is an unavoidable outcome in zero-sum games, it is not the case in non-zero sum games such as spectrum sharing problems in the interference channel. In this context, the NE , as a result of players' selfish behaviors, can often be seen as a worst case scenario, over which improvements can be made by using concepts of bargaining and learning [37].

A cooperative game is a game where some form of trust is established between players for the sake of maximizing their utilities jointly. Such games have been brought up recently in the wireless networking literature [1, 40, 50]. The trust is exploited to allow bargaining between the players in an iterative manner. The optimal point at convergence is analyzed in the game theory literature and referred to as the Nash bargaining (NB) point. The application of cooperative games and NB theory to the spectrum sharing problem is undertaken in [28, 31, 36, 45]. The advantage of the NB point over the classical NE is that it is possible to operate on the Pareto boundary of the rate region. However, the computation of the NB-achieving strategies requires a full exchange of channel state information between the users, which is not ideal in situations where backhaul communication between Txs is limited or not possible, especially in the context of cognitive radio where different users belong to different operators. Hence, at one extreme where NE does not require exchange of information and is easy to implement but may lead to bad performance. At the other extreme, NB solution requires full exchange of channel information but allow players (Txs) to cooperate and result in a much better operating point. This constitute to

a trade-off between cooperation and distributedness of the bargaining algorithms. In this chapter, we explore semi-distributed techniques that exploit cooperation in the spectrum sharing context and are reminiscent of bargaining methods while not requiring the full centralized CSIT of actual cooperative game theoretic equilibria.

More specifically, we consider multiple antenna transmitters and single antenna receivers. The choice of transmission parameter (from the base to the terminal) is limited to the choice of a beamforming vector, subject to a transmit power constraint. We propose an iterative beamforming algorithm where each transmitter updates its beamforming vector as a function of a single bit of feedback provided by the intended terminal. This bit of feedback provides the transmitters information of the channel realizations which can be used to improve it's transmit strategy, while maintaining semi-distributedness. At all instance of the algorithm, feedback is exploited in order to adjust the transmit beamforming vector as a linear combination of the NE solution and the so-called zero forcing solution.

Although mainly heuristic in nature, this algorithm finds some theoretical justification in the recently published literature [31,36]. The authors of [31,36] showed that all beamforming strategies attaining the boundary of the rate region of a 2-user MISO-IC-SUD (so-called Pareto boundary) are composed of a positive linear combination of the zero-forcing solution (ZF) and maximum-ratio-transmission solution (MRT). But in principle, the construction of such beamformer with an algorithm other than exhaustive search or some other centralized techniques, remains an open problem. Our solution thus serves as an practical alternative solution to exploit cooperation and to explore the trade-off between selfishness and altruism over the MISO-IC channels.

3.1 System model

As introduced in Section 2.2, we consider a set of N links, each featuring a downlink communication between a base station, equipped with N_t antennas, and one receiver node with only a single antenna, all sharing the same frequency band in a given geographical area. We recall the main definitions here for the convenience of the readers. The MISO channel between receiver node i and transmitter node j is a vector denoted as $\mathbf{h}_{ij} \in \mathcal{C}^{N_t \times 1}$ for $i, j = 1, \ldots, N$,

$$\mathbf{h}_{ij} = \sqrt{\alpha_{ij}}\mathbf{g}_{ij} \tag{3.1}$$

where α_{ij} denotes the path loss attenuation between transmitter j and receiver i. The vector $\mathbf{g}_{ij}$ is a vector with each element an independently identically distributed (i.i.d) complex Gaussian random variable with zero mean and unit variance. We assume that the transmit symbol x_i is from a Gaussian codebook and has unit power $\mathcal{E}\{|x_i|^2\} = 1$. The receive signal of user i is

$$y_i = \mathbf{h}_{ii}^H \mathbf{w}_i x_i + \sum_{j=1, j\neq i}^{N} \mathbf{h}_{ij}^H \mathbf{w}_j x_j + n_i. \tag{3.2}$$

where the variable n_i denotes a complex Gaussian noise with zero mean and variance σ^2. In this chapter, we assume a symmetric channel model in a sense that the noise power at each receiver is on average the same. In the next chapter, we discuss the egoism and altruism balancing problems on the MIMO-IC in an asymmetric network in which some links suffer stronger uncontrolled noise than other links in the network. See Chapter 4 for details.

As introduced in (2.28), the Signal-to-Interference-and-Noise-Ratio (SINR) at Rx i, assuming treating interference as thermal noise, is

$$\gamma_i = \gamma_i(\mathbf{W}) = \frac{|\mathbf{h}_{ii}^H \mathbf{w}_i|^2}{\sum_{j\neq i}^{N} |\mathbf{h}_{ij}^H \mathbf{w}_j|^2 + \sigma^2}, \tag{3.3}$$

where $\mathbf{W} = [\mathbf{w}_1, \ldots, \mathbf{w}_N]$. We drop the notation of the noise power σ^2 from now on to focus on the design of beamforming vectors. Assuming Gaussian inputs and single user decoding, the theoretic data rate of the Tx-Rx pair i is

$$r_i(\mathbf{W}) = \log_2(1 + \gamma_i(\mathbf{W})) \tag{3.4}$$

and system sum rate is therefore

$$R = \sum_{i=1}^{N} r_i. \tag{3.5}$$

3.1.1 Local Channel Information

Similar to the local channel information for the MIMO-IC defined in Section 2.1.1, we give in the following the local channel information definition in the MISO-IC. The local channel information of Tx i is denoted as the set of channel vectors $\mathbb{B}_i$, which includes the direct channel $\mathbf{h}_{ii}$ and the interference channel to other receiver nodes $\mathbf{h}_{ki}, k \neq i$. Hence, we have

$$\mathbb{B}_i = \{\mathbf{h}_{ki}, k = 1, \ldots N\}, \qquad i = 1, \ldots, N. \tag{3.6}$$

Note that Tx i does not know the direct channel of other users $\mathbf{h}_{kk}$ or the interference channel from others to its receiver $\mathbf{h}_{ki}$. We denote the unknown channel knowledge of Tx i to be $\mathbb{B}_i^{\perp}$:

$$\mathbb{B}_i^{\perp} = \{\mathbf{h}_{ki},\ i, k = 1, \ldots, N\} \setminus \mathbb{B}_i. \tag{3.7}$$

Furthermore, we assume that each receiver is able to measure its local signal to interference and noise ratio (SINR). The goal of the transmitters is to choose a beamforming vector based on limited information, $\mathbb{B}_i$, so as to reach *good* points in the achievable rate region. There may be numerous desirable points in the achievable rate region depending on the objective of the system. In a spectrum sharing scenario with independent operators, it is more reasonable to consider a trade-off between sum rate and fairness, rather than to maximize sum rate alone. It is because, in the two-user MISO-IC-SUD, the maximum sum rate operating point can be the single user point, in which one of the Tx is shut off. This is not desirable in our context as Txs, or players, only cooperate if the cooperation brings increase in their utilities. In the following, we assume that each Tx has its data rate as the utility function, hence selfish in nature, but is willing to cooperate or bargain, as long as the bargaining outcome is beneficial: the rate outcome is higher than the non-cooperating rate, e.g. the NE.

3.2 Achievable rate region and Pareto boundary

We assume that no interference precancellation is allowed and the interference from other transmitter nodes is treated as noise. We recall the definition of the achievable rate region

of MISO-IC-SUD $\mathcal{R}$ in 2.29 which is characterized by a set of all possible rate tuples $\mathbf{r}$ such that each rate element r_i, as defined in (3.4), satisfies the power constraint,

$$\mathcal{R} = \left\{ \mathbf{r}\left(\mathbf{W}\right) = \left(r_1\left(\mathbf{W}\right), \ldots, r_N\left(\mathbf{W}\right)\right) : \|\mathbf{w}_i\|^2 \leq 1, 1 \leq i \leq N \right\}. \tag{3.8}$$

The Pareto boundary $\mathcal{B}\left(\mathcal{R}\right)$ is simply the boundary of the achievable rate region $\mathcal{R}$, as defined similarly in (2.12).

3.3 Particular solutions

In this section, we discuss some particular solutions with the application in the MISO-IC-SUD. These solutions are not always good ones, but have the merit of being simple to understand and they bear strong connections with game theory. These solutions are generalized readily from classical single cell MIMO theory.

3.3.1 The zero-forcing solution

The philosophy behind the zero-forcing solution (ZF) is *altruism* in a game theory sense. This means that each transmitter selects a beamforming vector so that no interference is created to other receivers. The ZF beamformer is in the null space of the channel matrix between transmitter i and the receivers, excluding its intended receiver i. Define the following channel matrix $\mathbf{H}_{-i}$ with its columns being channel vectors from Tx i to other receivers.

$$\mathbf{H}_{-i} = [\mathbf{h}_{1i}, \ldots, \mathbf{h}_{(i-1)i}, \mathbf{h}_{(i+1)i}, \ldots, \mathbf{h}_{Ni}]. \tag{3.9}$$

Assume $N_t \geq N$ and thus the following projection matrices onto the column space of H_{-i} exist, we have

$$\mathbf{\Pi}_{-i} = \mathbf{H}_{-i}\left(\mathbf{H}_{-i}^H\mathbf{H}_{-i}\right)^{-1}\mathbf{H}_{-i}^H \tag{3.10}$$

and the orthogonal complement

$$\mathbf{\Pi}_{-i}^{\perp} = \mathbf{I} - \mathbf{H}_{-i}\left(\mathbf{H}_{-i}^H\mathbf{H}_{-i}\right)^{-1}\mathbf{H}_{-i}^H. \tag{3.11}$$

The ZF solution is therefore

$$\mathbf{w}_i^{ZF} = \frac{\mathbf{\Pi}_{-i}^{\perp}\mathbf{h}_{ii}}{\|\mathbf{\Pi}_{-i}^{\perp}\mathbf{h}_{ii}\|} \tag{3.12}$$

which satisfy the power constraint $\|\mathbf{w}_i^{ZF}\| = 1$. Note that if the null space of H_{-i} has dimension larger than one, the ZF solution is the projection of $\mathbf{h}_{ii}$ onto the null space such that $|\mathbf{h}_{ii}^H\mathbf{w}_i^{ZF}|$ is the largest. Note that the ZF solution only requires local information at Tx i, $\mathbb{B}_i$.

3.3.2 The Maximum-Ratio-Transmission

The maximum-ratio-transmission (MRT) beamformer is employed to maximize the desired signal power at the user, by aligning the direction of the beamformer and the desired channel, ignoring the interference generated to other receivers. In a game theory sense, this forms an *egoistic* solution. Also, it coincides with the Nash Equilibrium (NE) in a non-cooperative strategic game [31, 36].

The MRT beamformer $\mathbf{w}_i^{MRT}$ for base station i is

$$\mathbf{w}_i^{MRT} = \frac{\mathbf{h}_{ii}}{\|\mathbf{h}_{ii}\|}. \tag{3.13}$$

Similar to the ZF solution, the computation of the MRT solution only requires channel knowledge which is locally observable at Tx i (at least in a TDD mode), $\mathbb{B}_i$. The following theorem gives an intriguing characterization of the Pareto optimal beamforming strategies. It serves as a justification for the algorithm proposed later on.

Theorem 5. *Any rate point on the Pareto Boundary of a two-user MISO-IC-SUD is attained by beamforming vectors which are a linear combination of the ZF solutions and the MRT solutions with weights between zero and one [31]. For any* $\mathbf{r} \in \mathcal{B}(\mathcal{R})$*,*

$$r_i = \log_2(1 + \gamma_i(\mathbf{w}_1, \mathbf{w}_2)),\ i = 1, 2 \tag{3.14}$$

with

$$\mathbf{w}_i = \frac{\lambda_i \mathbf{w}_i^{ZF} + (1-\lambda_i)\mathbf{w}_i^{MRT}}{\left\|\lambda_i \mathbf{w}_i^{ZF} + (1-\lambda_i)\mathbf{w}_i^{MRT}\right\|}, \quad 0 \le \lambda_i \le 1, i = 1, 2. \tag{3.15}$$

Proof. As the argument of the proof is highly related to this chapter and Chapter 5, we adopt the proof from [31] at the end of this chapter for completeness. □

Thm. 5 states that by combining the ZF and MRT solutions, one can construct a beamforming vector that attains the Pareto boundary of a two-user MISO-IC-SUD. Although this only applies to the two-user case, we propose the following algorithm which bears a similar concept but on the N-user MISO-IC-SUD. When $N = 2$, the following algorithm provides a practical alternative solution to perform close to Pareto boundary.

3.4 Distributed Algorithms

In this section, we present a heuristic (although intuitively motivated) distributed bargaining solution (DBS) and we will compare it to the non-cooperative NE and altruistic solutions above presented. The difficulty is that the optimum cooperative points (on the Pareto boundary) are given by a linear combination between the ZF and the MRT beamformers where the weights are a function of the complete, centralized CSIT. To preserve semi-distributedness, we introduce the idea of a limited feedback link from each user and its *serving* base. The second novel aspect is the idea of iterative bargaining where the transmitters simultaneously realize small increments of their beamformer in a direction leading to improvements for all parties involved. Users are expected to monitor their rates and indicate to their serving base whether the bargaining is successful or not (via a single bit of feedback). In the proposed framework, a loss of rate by one of the users will cause this user to cease the cooperation.

3.4.1 The DBS algorithm

We provide an iterative algorithm which approaches the Pareto boundary by incrementally steering the beamforming vector in each iteration so that *every* transmitter and receiver pair would have a higher transmission rate.

Denote the beamforming vector of transmitter i in iteration j by $\mathbf{w}_i(j)$. Intuitively, it is reasonable to initialize the beamforming vectors $\mathbf{w}_i(0)$ to be the MRT solutions $\mathbf{w}_i^{MRT}$

because players start with a non-cooperative setting. However they can also initialize in an joint altruistic setting (see later).

The beamforming vector is updated at each iteration j by

$$\mathbf{w}_i(j) = \mathbf{w}_i(j-1) + \delta_w(j) \tag{3.16}$$

$$\mathbf{w}_i(j) \to \frac{\mathbf{w}_i(j)}{\|\mathbf{w}_i(j)\|} \tag{3.17}$$

where $\delta_w(j)$ is a computed vector based on the available local channel state information. At each iteration j, each receivers computes its rate using locally available information ,

$$r_i^{(j)} = log_2\left(1 + \frac{|\mathbf{h}_{ii}^H \mathbf{w}_i(j)|^2}{I_i(j)}\right) \tag{3.18}$$

where $I_i(j)$ is the measured interference and noise power at receiver i at j-th iteration,

$$I_i(j) = \sum_{k \neq i}^{N} |\mathbf{h}_{ik}^H \mathbf{w}_k(j)|^2 + \sigma^2. \tag{3.19}$$

Then, Rx i reports to Tx i a single bit to inform the base about its satisfaction: increment of data rates (1) or decrement of data rates (0).

3.4.2 Iterative Bargaining

In low SNR regime, interference power is negligible comparing to the noise power and the MRT solution achieves a higher rate performance than the ZF solution as it maximizes the desired signal energy while ignoring the interference. On the other hand, in the high SNR regime, the system becomes interference limited. The ZF solution mitigates interference and achieves a higher rate performance than the MRT solution. With this concept in mind, we propose the following initialization policy which adapts to system SNR assuming the SINR of employing ZF and MRT are known:

$$\mathbf{w}_i(0) = \begin{cases} \mathbf{w}_i^{ZF} & \text{if } R^{ZF} > R^{MRT}; \\ \mathbf{w}_i^{MRT} & \text{otherwise.} \end{cases} \tag{3.20}$$

where

$$\begin{aligned} R^{ZF} &= \sum_{i=1}^{N} \log_2\left(1 + \gamma_i\left(\mathbf{w}_1^{ZF}, \ldots, \mathbf{w}_N^{ZF}\right)\right) \\ R^{MRT} &= \sum_{i=1}^{N} \log_2\left(1 + \gamma_i\left(\mathbf{w}_1^{MRT}, \ldots, \mathbf{w}_N^{MRT}\right)\right). \end{aligned} \tag{3.21}$$

It is interesting to note that different update-mechanics in (3.16) would result in a different data rates trajectory (data rate improvement curve) and would result in a different converged system sum rate. Here we provide two simple examples of $\delta_{w_i(j)}$ which will be shown later to perform better than the non-cooperative and altruistic solutions. Both of these algorithm provide with a trajectory linking the MRT and the ZF operating points in the rate region.

3.4.2.1 Zero-Forcing Increment (ZFI)

In ZFI, assuming we start with the MRT solution, the beamforming vector is steered towards the ZF solution in each iteration. Intuitively, the transmitters are willing to cooperate by decreasing the interference level generated to other receivers as long as they get benefits, increment in transmission rates, in the process. The beamforming vector of transmitter i in iteration j is updated as

$$\mathbf{w}_i(j+1) = \mathbf{w}_i(j) + \alpha_i \mathbf{w}_i^{ZF} \tag{3.22}$$

where α_i is a preset step size constant. The beamforming vector is then normalized as in equation (3.17). On the other hand, if we start with ZF solution, the beamformer is steered towards the MRT solution in each iteration.

3.4.2.2 Orthogonal Bases Increment (OBI)

In OBI, the beamforming vectors are a linear combination of the ZF solution and a vector that is in the span of the interference signals, as designed in (3.28):

$$\begin{aligned} \mathbf{w}_i^{ZF} &= \frac{\mathbf{\Pi}_{-i}^{\perp}\mathbf{h}_{ii}}{\|\mathbf{\Pi}_{-i}^{\perp}\mathbf{h}_{ii}\|} \\ \bar{\mathbf{w}}_i^{ZF} &= \frac{\mathbf{\Pi}_{-i}\mathbf{h}_{ii}}{\|\mathbf{\Pi}_{-i}\mathbf{h}_{ii}\|}. \end{aligned} \tag{3.23}$$

The beamforming vector of transmitter i at iteration j be

$$\mathbf{w}_i(j) = \sqrt{\beta_i(j)}\mathbf{w}_i^{ZF} + \sqrt{1-\beta_i(j)}\bar{\mathbf{w}}_i^{ZF} \tag{3.24}$$

As illustrated in [31] [36], to achieve Pareto optimality, it is sufficient to vary $\beta_i(j)$ between $0 \le \beta_i(j) \le \tilde{\beta}_i$, where $l_1 = |\Pi_{-i}\mathbf{h}_{ii}|^2$, $l_2 = |\Pi_{-i}^{\perp}\mathbf{h}_{ii}|^2$ and $\tilde{\beta}_i = \frac{l_1}{l_1+l_2}$. To initialize, the beamformer equals

$$\beta_i(0) = \begin{cases} \tilde{\beta}_i & \text{if } R^{MRT} > R^{ZF} \\ 0 & \text{Otherwise.} \end{cases} \tag{3.25}$$

At iteration $j+1$,

$$\beta_i(j+1) = \begin{cases} \beta_i(j) - \delta_\beta & \text{if } R^{MRT} > R^{ZF} \\ \beta_i(j) + \delta_\beta & \text{Otherwise.} \end{cases} \tag{3.26}$$

where δ_β is a predefined constant. The beamformer is then normalized as in (3.17).

3.4.3 Stopping Condition

A stopping condition is implemented so that the beamformer trajectory is halted as near as possible to the Pareto boundary. The stopping condition reflects the sharing policy and many options are available. A reasonable and intuitive stopping condition is that each transmitter would stop cooperating and terminates the algorithm when it encounters a decrement of transmission rate. User i, $1 \le i \le N$ stops cooperating if

$$\frac{|\mathbf{h}_{ii}^H \mathbf{w}_i(j)|^2}{I_i(j)} > \frac{|\mathbf{h}_{ii}^H \mathbf{w}_i(j+1)|^2}{I_i(j+1)} \tag{3.27}$$

where $I_i(j)$ is the measured interference and noise energy in (3.19).

3.5 Results and Discussion

In this section, we illustrate the dynamics (trajectory in the rate region) and the sum rate performance of DBS.

3.5.1 Dynamics of DBS

In figure 3.1, the achievable rate region for a particular channel realization is plotted for the two-user MISO-IC-SUD. The ZF solution and the MRT solution are marked as a circle and a triangle respectively, inside the achievable rate region. The system SNR is 15dB. In this channel realization, neither the ZF nor the MRT is reaching the Pareto boundary. The trajectory of rate bargaining at each iteration, starts at the MRT solution. The solid line is the trajectory with stopping condition which ensures the bargaining stops when one of the transmitters has rate decrement. The dotted line is the trajectory path without stopping condition. As seen, the path eventually goes to the ZF point but there is no guarantee of each transmitters' rates. Note that the beamforming vector is steered towards ZF beamformer. Yet, it stops before reaching the ZF solution because one of the transmitter encounters rate decrement which results in a higher sum rate operating point and close to the Pareto boundary. As shown in the figure, the resulting rate is higher than both ZF solution and MRT solution. Note that DBS reaches close to the Pareto boundary in 3 iterations in this realization which means that only 3 bits of feedback are required to improve the performance.

3.5.2 Performance Comparison of DBS

The sum rate comparison between DBS, the ZF and the MRT solutions in the MISO-IC-SUD against SNR is illustrated in Fig. 3.2. In the low SNR regime, SNR $<$ 9dB, the interference is weak, the MRT solution outperforms the ZF solution which confirms our intuition. We see that both ZFI and OBI outperform the non-cooperative NE, the MRT solution. In medium and high SNR regime, the ZF solution outperforms the MRT because the interference power is stronger than noise power and mitigation of interference improves performance.

In figure 3.3, the sum rate of DBS, the ZF and MRT schemes are plotted against the distance between two transmitters. The distance is calculated as a multiple of the coverage of the transmitter. As the distance increases, interference becomes weaker. The MRT solution and DBS both improve in performance and DBS outperforms MRT. On the other hand, the ZF solution does not take into account the strength of interference and consumes all transmitter power to mitigate a weak interference, resulting in a constant performance.

3.6 Conclusion

In an interference channel where Txs are competing for frequency resource selfishly, with a lack of network structure, a distributive interference mitigation algorithm is essential to improve the system performance. We provided two simple distributed bargaining solutions which build on balancing between the egoism solution (MRT) and the altruistic solution (ZF). In the following chapter, we investigate the concept of egoism and altruism balancing on the MIMO-IC-SUD.

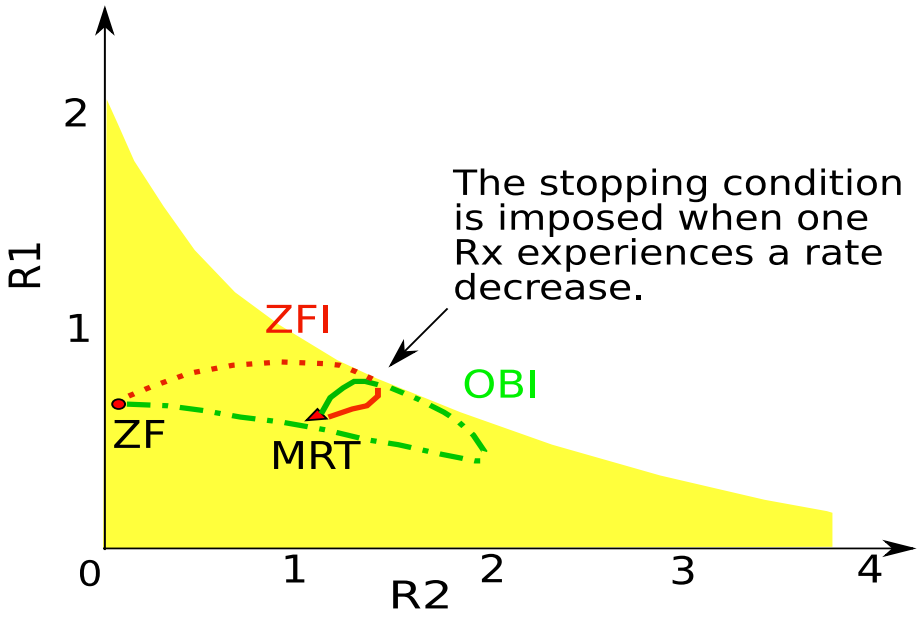

Figure 3.1: The trajectory of DBS within the rate region in the 2-user MISO-IC-SUD at SNR 15dB. The trajectories of both ZFI and OBI, starting at the MRT point (triangle), are illustrated in solid lines, with colors red and green respectively, whereas if there are no stopping conditions, the trajectories continue and end at the ZF point (circle) and are shown in dotted lines. As shown in the figure, the algorithms stop close to the Pareto boundary.

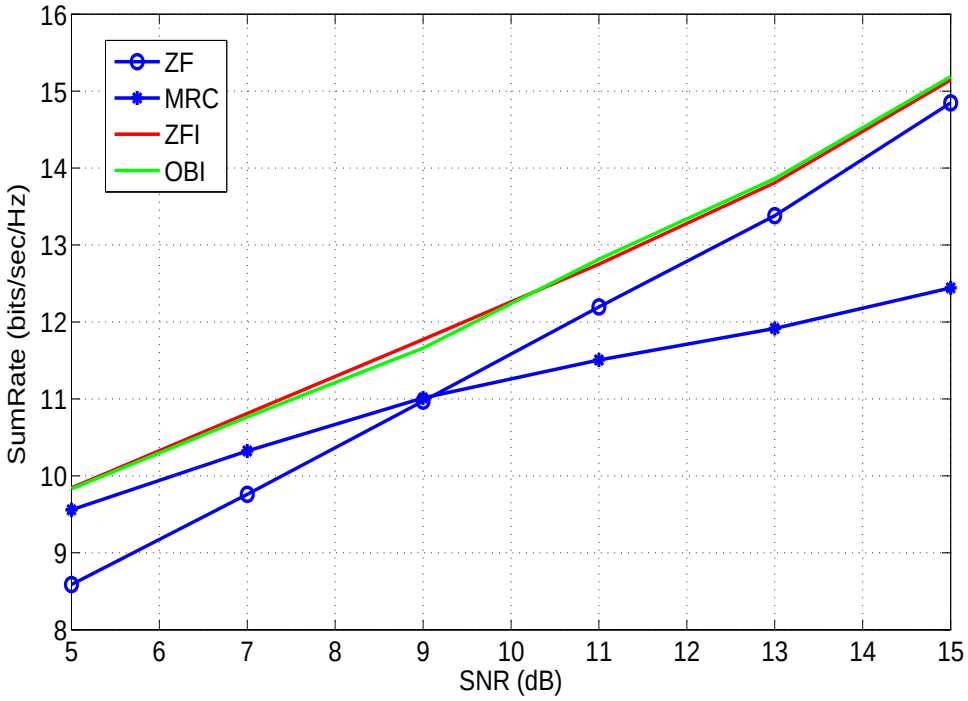

Figure 3.2: The performance comparison of DBS against SNR (dB). The two version of DBS, namely ZFI and OBI, outperform the Nash equilibrium (MRT) and the altruistic (ZF) solution.

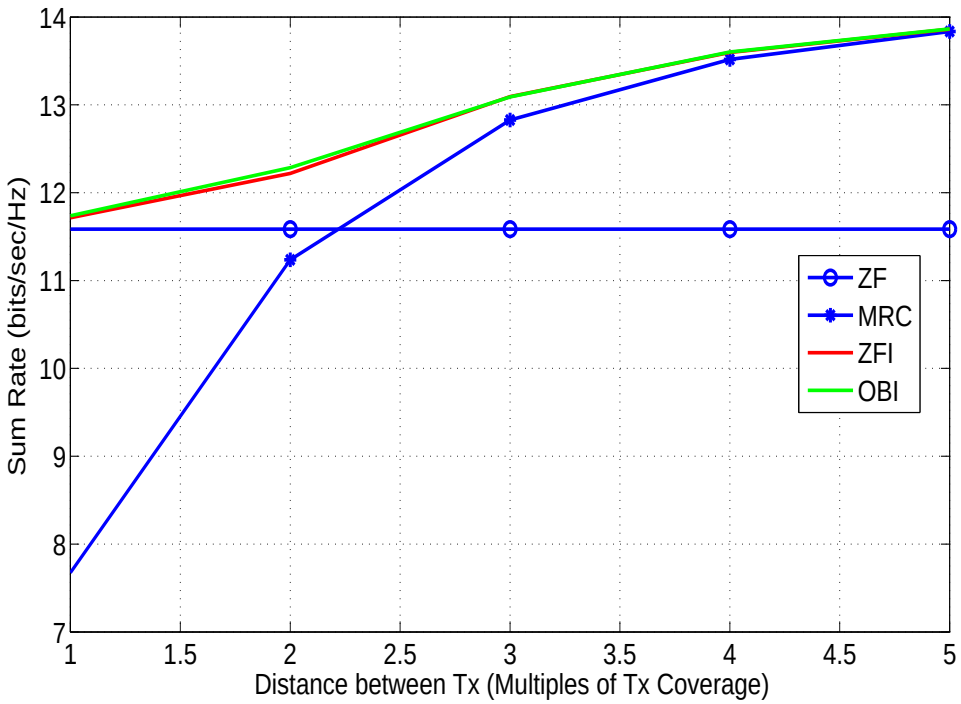

Figure 3.3: The performance comparison of DBS against distance between transmitters at SNR 10dB.

3.7 Proof of Thm. 5

We first prove that the Pareto boundary attaining beamforming vectors take the following form:

$$\mathbf{w}_i = \sqrt{\mu_i}\frac{\mathbf{\Pi}_{-i}^{\perp}\mathbf{h}_{ii}}{\|\mathbf{\Pi}_{-i}^{\perp}\mathbf{h}_{ii}\|} + \sqrt{1-\mu_i}\frac{\mathbf{\Pi}_{-i}\mathbf{h}_{ii}}{\|\mathbf{\Pi}_{-i}\mathbf{h}_{ii}\|}, \quad 0 \le \mu_i \le 1, i = 1, 2. \tag{3.28}$$

Then, we show that the set of solutions parameterized in (3.15) is a subset of solutions parameterized in (3.28) which attain the Pareto boundary

As $N = 2$, for $j \neq i$, $\mathbf{\Pi}_{-i} = \frac{\mathbf{h}_{ji}\mathbf{h}_{ji}^H}{\|\mathbf{h}_{ji}\|^2}$ and $\mathbf{\Pi}_{-i}^{\perp} = \mathbf{I} - \mathbf{\Pi}_{-i}$. We start by contradictions. Assume the Pareto boundary attaining beamforming vectors are

$$\mathbf{w}_i = a_1\frac{\mathbf{\Pi}_{-i}\mathbf{h}_{ii}}{\|\mathbf{\Pi}_{-i}\mathbf{h}_{ii}\|} + a_2\frac{\mathbf{\Pi}_{-i}^{\perp}\mathbf{h}_{ii}}{\|\mathbf{\Pi}_{-i}^{\perp}\mathbf{h}_{ii}\|} + a_3\boldsymbol{\nu}_3 + \ldots + a_{N_t}\boldsymbol{\nu}_{N_t} \tag{3.29}$$

with at least one a_j non-zero and $\boldsymbol{\nu}_j$ are mutually orthogonal and orthogonal to $\frac{\mathbf{\Pi}_{-i}\mathbf{h}_{ii}}{\|\mathbf{\Pi}_{-i}\mathbf{h}_{ii}\|}$ and $\frac{\mathbf{\Pi}_{-i}^{\perp}\mathbf{h}_{ii}}{\|\mathbf{\Pi}_{-i}^{\perp}\mathbf{h}_{ii}\|}$, $3 \le j \le N_t$. The coefficients $a_1, \ldots, a_N$ are complex and satisfy the power constraint,

$$|a_1|^2 + \ldots, |a_N|^2 = 1. \tag{3.30}$$

Without loss of generality, assume $a_3 \neq 0$. We can construct $\mathbf{w}_i' = \mathbf{w}_i - \epsilon\boldsymbol{\nu}_3$ with ϵ chosen such that $\mathbf{w}_i'$ satisfies the power constraint. Note that, for $i, k = 1, 2, k \neq i$,

$$\begin{aligned} \left|\mathbf{h}_{ii}^H\mathbf{w}_i'\right| &= \left|\mathbf{h}_{ii}^H\mathbf{w}_i\right| \\ \left|\mathbf{h}_{ki}^H\mathbf{w}_i'\right| &= \left|\mathbf{h}_{ki}^H\mathbf{w}_i\right|. \end{aligned} \tag{3.31}$$

Then, we can choose $\mathbf{w}_i'' = \mathbf{w}_i' + \epsilon e^{j\phi}\frac{\mathbf{\Pi}_{-i}\mathbf{h}_{ii}}{\|\mathbf{\Pi}_{-i}\mathbf{h}_{ii}\|}$ where ϵ is chosen such that $\mathbf{w}_i''$ satisfies the power constraint. We obtain

$$\begin{aligned} \left|\mathbf{h}_{ii}^H\mathbf{w}_i''\right| &= \left|\mathbf{h}_{ii}^H\left(\mathbf{w}_i' + \epsilon e^{j\phi}\frac{\mathbf{\Pi}_{-i}\mathbf{h}_{ii}}{\|\mathbf{\Pi}_{-i}\mathbf{h}_{ii}\|}\right)\right| \\ &= \left|\mathbf{h}_{ii}^H\mathbf{w}_i' + \epsilon e^{j\phi}\|\mathbf{\Pi}_{-i}\mathbf{h}_{ii}\|\right| \\ &\overset{(a)}{=} \left|\mathbf{h}_{ii}^H\mathbf{w}_i'\right| + \epsilon\|\mathbf{\Pi}_{-i}\mathbf{h}_{ii}\| \\ &\ge \left|\mathbf{h}_{ii}^H\mathbf{w}_i'\right| = \left|\mathbf{h}_{ii}^H\mathbf{w}_i\right|, \\ \left|\mathbf{h}_{ki}^H\mathbf{w}_i''\right| &= \left|\mathbf{h}_{ki}^H\mathbf{w}_i'\right| = \left|\mathbf{h}_{ki}^H\mathbf{w}_i\right| \end{aligned} \tag{3.32}$$

where (a) is due to the selection of $\phi = \arg(\mathbf{h}_{ii}^H\mathbf{w}_i')$. Note that $\mathbf{w}_i''$ achieves a higher power gain $\left|\mathbf{h}_{ii}^H\mathbf{w}_i''\right|$ than $\left|\mathbf{h}_{ii}^H\mathbf{w}_i\right|$ while keeping the interference gain constant. This violates the assumption that $\mathbf{w}_i$ attains the Pareto boundary. Hence, we have $a_3 = 0$. By the similar argument, we have $a_j = 0, j = 3, \ldots, N_t$ and obtain

$$\mathbf{w}_i = a_1\frac{\mathbf{\Pi}_{-i}\mathbf{h}_{ii}}{\|\mathbf{\Pi}_{-i}\mathbf{h}_{ii}\|} + a_2\frac{\mathbf{\Pi}_{-i}^{\perp}\mathbf{h}_{ii}}{\|\mathbf{\Pi}_{-i}^{\perp}\mathbf{h}_{ii}\|} \tag{3.33}$$

with $|a_1|^2 + |a_2|^2 = 1$. Now we prove that a_1, a_2 are be chosen real, instead of complex coefficients. With (3.33), we have

$$\begin{aligned} |\mathbf{h}_{ii}^H\mathbf{w}_i| &= \left|a_1\|\mathbf{\Pi}_{-i}\mathbf{h}_{ii}\| + a_2\|\mathbf{\Pi}_{-i}^{\perp}\mathbf{h}_{ii}\|\right| \overset{(a)}{\le} |a_1|\|\mathbf{\Pi}_{-i}\mathbf{h}_{ii}\| + |a_2|\|\mathbf{\Pi}_{-i}^{\perp}\mathbf{h}_{ii}\| \\ |\mathbf{h}_{ki}^H\mathbf{w}_i| &= \left|a_1\frac{\mathbf{\Pi}_{-i}\mathbf{h}_{ii}}{\|\mathbf{\Pi}_{-i}\mathbf{h}_{ii}\|}\right| = |a_1|. \end{aligned} \tag{3.34}$$

Equality is set at (a) is the phase of a_1, a_2 are the same: $\arg(a_1) = \arg(a_2)$. Note that the phase of a_1 does not affect the interference gain $\left|\mathbf{h}_{ki}^H \mathbf{w}_i\right|$ and hence we have a_1, a_2 real coefficients and we denote $a_1 = \sqrt{1-\mu_i}$ and $a_2 = \sqrt{\mu_i}$.

Now, we show that the set of solutions in (3.15) is a subset of the set of solutions parameterized in (3.28). We start with (3.28),

$$\begin{aligned}
\mathbf{w}_i &= \sqrt{\mu_i}\frac{\mathbf{\Pi}_{-i}^{\perp}\mathbf{h}_{ii}}{\|\mathbf{\Pi}_{-i}^{\perp}\mathbf{h}_{ii}\|} + \sqrt{1-\mu_i}\frac{\mathbf{\Pi}_{-i}\mathbf{h}_{ii}}{\|\mathbf{\Pi}_{-i}\mathbf{h}_{ii}\|} \\
&= \sqrt{\mu_i}\frac{\mathbf{\Pi}_{-i}^{\perp}\mathbf{h}_{ii}}{\|\mathbf{\Pi}_{-i}^{\perp}\mathbf{h}_{ii}\|} + \sqrt{1-\mu_i}\frac{\mathbf{h}_{ii}}{\|\mathbf{\Pi}_{-i}\mathbf{h}_{ii}\|} - \sqrt{1-\mu_i}\frac{\mathbf{\Pi}_{-i}^{\perp}\mathbf{h}_{ii}}{\|\mathbf{\Pi}_{-i}\mathbf{h}_{ii}\|} \\
&= \left(\sqrt{\mu_i} - \sqrt{1-\mu_i}\frac{\|\mathbf{\Pi}_{-i}^{\perp}\mathbf{h}_{ii}\|}{\|\mathbf{\Pi}_{-i}\mathbf{h}_{ii}\|}\right)\frac{\mathbf{\Pi}_{-i}^{\perp}\mathbf{h}_{ii}}{\|\mathbf{\Pi}_{-i}^{\perp}\mathbf{h}_{ii}\|} + \frac{\sqrt{1-\mu_i}\|\mathbf{h}_{ii}\|}{\|\mathbf{\Pi}_{-i}\mathbf{h}_{ii}\|}\frac{\mathbf{h}_{ii}}{\|\mathbf{h}_{ii}\|} \qquad (3.35) \\
&= b_i\frac{\mathbf{\Pi}_{-i}^{\perp}\mathbf{h}_{ii}}{\|\mathbf{\Pi}_{-i}^{\perp}\mathbf{h}_{ii}\|} + d_i\frac{\mathbf{h}_{ii}}{\|\mathbf{h}_{ii}\|} \\
&= b_i\mathbf{w}_i^{ZF} + d_i\mathbf{w}^{MRT}
\end{aligned}$$

where $0 \le b_i, d_i \le 1$ if $0 \le \mu_i \le \frac{|\mathbf{h}_{ji}^H \mathbf{h}_{ii}|^2}{\|\mathbf{h}_{ji}\|^2\|\mathbf{h}_{ii}\|^2}$. Rewriting the coefficients in terms of λ_i and we obtain (3.15).

Chapter 4

MIMO-IC with Single User Decoding

In previous chapter, we have discussed the egoism and altruism balancing in the MISO-IC, in the goal of operating close to the Pareto boundary. In this chapter, we consider the multiple-input-multiple-output interference channel (MIMO-IC) and shed more light on these game-theoretic concepts in the more general context of MIMO channels and more particularly when not all CSI is shared by coordinating parties by using the framework of Bayesian games. In particular, this allows us to derive distributed beamforming techniques. We draw parallels with existing work on the MIMO-IC, including rate-optimizing and interference-alignment precoding techniques, showing how such techniques may be improved or re-interpreted through a common prism based on balancing egoistic and altruistic beamforming. Our analysis and simulations currently limited to single stream transmission per user attest the improvements over known interference alignment based methods in terms of sum rate performance in the case of so-called asymmetric networks.

Recently, coordination on the MIMO-IC-SUD has emerged as a very popular topic in its own right, with several important non-game related contributions shedding light on rate-scaling optimal precoding strategies based on so-called interference alignment, subspace optimization, alternated maximum SINR optimization, [20, 41, 49] and rate-maximizing precoding strategies [61, 68], to cite just a few examples.

Interference alignment based strategies exhibit the designed feature of rendering interference cancelable (when feasible, according to the available degrees of freedom) at both the transmitter and receiver side. Such a behavior is optimal in the large signal to noise ratio (SNR) region when Rxs have single user decoder and interference is the key bottleneck. At finite SNR, various strategies exist which aim at maximizing a link quality metric individually over each link, while taking interference into account. This often takes the form of maximizing the link's SINR or minimizing minimum-mean-square-error (MMSE). This approach provides good rates in symmetric networks where all links are subject to impairments (noise, average interference) of similar level. In more general and practical situations however, we argue that a better sum rate may be obtained from a proper and different weighting of the egoistic and altruistic objective at each individual link. This situation is particularly important when more links are subject to statistically stronger interference than others, a case which has so far received little attention and which we shall refer here as asymmetric networks. For this purpose, we suggest to re-visit the problem of coordinated beamforming design by directly building on the game theoretic concept of

egoistic and altruistic game equalibria. Because our focus is on scenarios where CSI is not fully available, we consider a class of games suitable to the case of partial information-based decision making, called Bayesian games. Note that this is different from the limited CSI feedback scenario studied by previous authors [64] who consider channel quantization requirement as function of SNR. Our approach is two-fold, first derive analytically the game equalibria. Second, exploit the obtained equilibria solution into heuristic design of a practical beamforming technique. The behavior of our solution is then studied both theoretically (large SNR regime) and tested by simulations.

The road-map of this chapter is:

- We define the egoistic and altruistic objective functions and derive analytically the equilibria of so-called egoistic and altruistic Bayesian games [22], in Section 4.2.
- Based on the equilibria, we propose a practical distributed beamforming scheme, in Section 4.3, which provides a game-theoretic interpretation of the distributed sum rate maximization problem the MIMO-IC, such as [61].
- The proposed techniques allows a tradeoff between the reduced complexity/feedback and the rate maximization offered by [61].
- We show that our algorithm exhibits the same rate scaling (when SNR grows) as shown by recent interesting interference alignment based methods [20, 41, 49] which operates on the same feedback assumption as the proposed beamforming scheme. At finite SNR, we show improvements in terms of sum rate, especially in the case of asymmetric networks where interference-alignment methods are unable to properly weigh the contributions on the different interfering links to maximize the sum rate. This situation is particularly relevant. In practical contexts where for complexity limitation reasons only a subset of cells (links) is coordinated across, while other uncoordinated links contribute to additional unequal amounts of unstructured interference.

4.1 Bayesian Games Definition on interference channel

Let $\mathcal{N} = \{1, \ldots, N\}$ be a set containing a finite set $\mathcal{N}_c$, with cardinality $N_c \leq N$, of cooperating transmitters (Txs), also termed as players. From now on, we use players and Txs interchangeably. We call the set $\mathcal{N}_c$ a coordination cluster and Txs outside the cluster will contribute to uncontrolled interference. The provided model has general applications in which the Txs can be base stations in cellular downlink where typically coordination is restricted to a subset of neighboring cell sites while more distant sites cannot be coordinated over [19] ; nodes in ad-hoc network and cognitive radio.

Each Tx is equipped with N_t antennas and the Rx with N_r antennas. Each Tx communicates with a unique Rx at a time. Txs are not allowed or able to exchange users' packet (message) information, giving rise to an interference channel over which we seek some form of beamforming-based coordination. Recall from the definition in (2.1), the channel from Tx i to Rx j $\mathbf{H}_{ji} \in \mathcal{C}^{N_r \times N_t}$ is given by:

$$\mathbf{H}_{ji} = \sqrt{\alpha_{ji}}\mathbf{G}_{ji}, \quad i, j = 1, \ldots, N_c \tag{4.1}$$

Each element in channel matrix $\mathbf{G}_{ji}$ is an independent identically distributed complex Gaussian random variable with zero mean and unit variance and α_{ji} denotes the slow-

varying shadowing and pathloss attenuation. The probability density of $\mathbf{G}_{ji}$ is

$$f_{\mathbf{G}_{ji}}(\mathbf{H}) = \frac{1}{\pi^{N_t N_r}} \exp(-Tr\left(\mathbf{H}\mathbf{H}^H\right)). \tag{4.2}$$

4.1.1 Limited Channel knowledge

As introduced in Section 2.1.1, the local channel knowledge is defined in (2.7) which we recall here. The set of CSI locally available (resp. not available) at Tx i denoted by $\mathbb{B}_i$ (resp. $\mathbb{B}_i^{\perp}$) is denoted by:

$$\mathbb{B}_i = \{\mathbf{H}_{ji}\}_{j=1,\ldots,N_c} \; ; \; \mathbb{B}_i^{\perp} = \{\mathbf{H}_{kl}\}_{k,l=1\ldots N_c} \setminus \mathbb{B}_i \tag{4.3}$$

By construction here, locally available channel knowledge, $\mathbb{B}_i$, is only known to Tx i but *not* other Txs. We call this knowledge $\mathbb{B}_i$ the *type* of player (Tx) i, in the game theoretic terminology [22].

In the view of Tx i, the decision to be made shall be based on its type $\mathbb{B}_i$ and its *beliefs* on *other* Txs types. Since Tx i does not know other Txs types (channel realizations), we assume that Tx i has the probability densities (beliefs) of its unknown channels, $\mathbb{B}_i^{\perp}$. For simplicity, we assume that these *beliefs* are symmetric: these unknown channels are all complex Gaussian distributed. The asymmetric path loss attenuation variables α_{ji} are assumed to be long term statistics and known to the Txs. And we assume that the channel coefficients in the network are statistically independent from each other. We define here the joint beliefs (probability density) at Tx i:

$$\mu_i = p(\mathbb{B}_i^{\perp}) = f_{\mathbf{G}_{ji}}(\mathbf{H})^{N_c(N_c-1)} = \mu. \tag{4.4}$$

The Tx index i is dropped because the beliefs are symmetric among Txs, given the asymmetric path loss coefficients α_{ji}. $p(.)$ is a probability measure and $f_{\mathbf{G}_{ji}}(\mathbf{H})$ is density of a complex Gaussian channel defined in (4.2). The second equality relies on the assumptions that the channel coefficients from any Tx to any Rx are independent.

Without any further information, Tx i designs the transmit beamforming vector, $\mathbf{w}_i \in \mathcal{C}^{N_t \times 1}$, so as to optimize the expected value of a certain utility over such *belief*. As in several important contributions dealing with coordination on the interference channel [14,18,20,31,34,62,71], we assume linear beamforming. We call the transmit beamforming vector $\mathbf{w}_i$ an action of Tx i and denote the set of all possible actions by $\mathcal{A}$ at any Tx.

$$\mathcal{A} = \left\{\mathbf{w} \in \mathcal{C}^{N_t \times 1} : |\mathbf{w}|^2 \leq 1\right\} \tag{4.5}$$

The received signal at Rx i is therefore

$$y_i = \mathbf{v}_i^H \mathbf{H}_{ii} \mathbf{w}_i x_i \sqrt{P} + \sum_{j \neq i}^{N_c} \mathbf{v}_i^H \mathbf{H}_{ij} \mathbf{w}_j x_j \sqrt{P} + n_i \tag{4.6}$$

where $x_k, k = 1, \ldots, N_c$ are the transmit symbols, n_i is a complex Gaussian noise with zero mean and variance σ_i^2. Note that the noise levels σ_i^2 depend on the link index which was not considered in previous work on transmitter coordination. We assume that the Txs are transmitting with full power P. The Rxs are assumed to employ maximum SINR (Max-SINR) beamforming throughout the paper so as to also maximize the link rates [47]. The receive beamformer $\mathbf{v}_i$ is classically given by:

$$\mathbf{v}_i = \frac{\mathbf{C}_{Ri}{}^{-1} \mathbf{H}_{ii} \mathbf{w}_i}{\left\| \mathbf{C}_{Ri}{}^{-1} \mathbf{H}_{ii} \mathbf{w}_i \right\|} \tag{4.7}$$

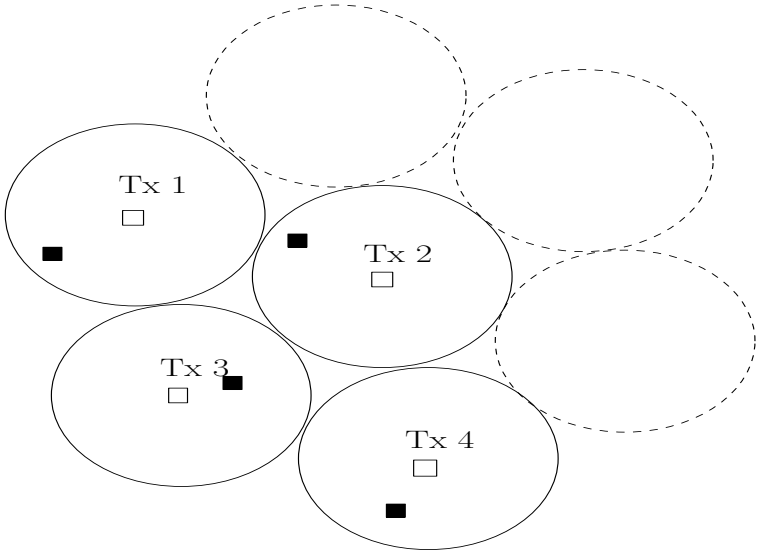

Figure 4.1: This figure illustrates a system of $N = 7$ cells where $N_c = 4$ cells form a coordination cluster. Empty squares represent transmitters whereas filled squares represent receivers. The noise power (which includes out-of-cluster interference) undergone in each cell varies from link to link.

where $\mathbf{C}_{Ri}$ is the covariance matrix of received interference and noise

$$\mathbf{C}_{Ri} = \sum_{j \neq i}^{N_c} \mathbf{H}_{ij} \mathbf{w}_j \mathbf{w}_j^H \mathbf{H}_{ij}^H P + \sigma_i^2 \mathbf{I}. \tag{4.8}$$

P is the transmit power.

Importantly, the noise will in practice capture thermal noise effects but also any interference originating from the rest of the network, i.e. coming from transmitters located beyond the coordination cluster. Thus, depending on the path loss and shadowing effects, the $\{\sigma_i^2\}$ may be quite different from each other [43]. Fig. 4.3 illustrates a system of $N = 7$ cells where $N_c = 4$ cells form a coordination cluster. Note that for simplification of analysis, we consider the sum of uncoordinated source of interference and thermal noise to be spatially white.

Receiver feedback vs. Reciprocal Channel: In the case of reciprocal channels (TDD), the feedback requirement to obtain $\mathbb{B}_i$ can be replaced by a channel estimation step based on uplink pilot sequences. Additionally, it will be classically assumed that the receivers are able to estimate the covariance matrix of the interference signals, based on, for instance, transmit pilot sequences.

We can now define the Bayesian game on the interference channel as a 5-tuple.

Definition 2.

$$G =< \mathcal{N}_c, \mathcal{A}, \{\mathbb{B}_i\}, \mu, \{u_i\} > . \tag{4.9}$$

μ denotes the beliefs *of the players and $\{u_i\}$ denotes the utility functions of the players, which can be either egoistic or altruistic.*

Specific definitions of u_i will be given in the following sections. The players are assumed to be *rational* as they maximize their own utility based on their *types* and *beliefs*.

Definition 3. *A pure-strategy of player i, $s_i : \mathbb{B}_i \to \mathcal{A}_i$ is a deterministic choice of action given information $\mathbb{B}_i$ of player i.*

Definition 4. *A strategy profile $\mathbf{s}^* = (s_i^*, s_{-i}^*)$ achieves a Bayesian Equilibrium if s_i^* is the best response of player i given strategy tuple s_{-i}^* for all other players and is characterized by*

$$s_i^* = \arg\max \mathcal{E}_{\mathbb{B}_i^\perp} \left\{ u_i(s_i, s_{-i}^*) \right\}, \qquad i = 1, \ldots, N_c. \tag{4.10}$$

Note that, intuitively, the player's strategy is optimized by averaging over the *beliefs* (the distribution of all missing state information) while in a standard game, such expectation is not required.

In the following sections, we derive the equilibria for egoistic and altruistic Bayesian games respectively. These equilibria constitute extreme strategies which in general do not perform optimally in terms of the overall network performance, yet can be exploited as components of a more general beamforming-based coordination technique which is then proposed in Section 4.4.

4.2 Bayesian Games with Receiver Beamformer Feedback

We assume that Tx has the local channel state information $\mathbb{B}_i$ and the added knowledge of receive beamformers through a feedback channel. Note that in the case of reciprocal channels, the receive beamformer feedback is *not* required.

4.2.1 Egoistic Bayesian game

Definition 5. *Denote the set of transmit beamforming vectors of players $j, j \neq i$, by $\mathbf{w}_{-i}$. The egoistic utility function for Tx i is defined as its received SINR*

$$u_i(\mathbf{w}_i, \mathbf{w}_{-i}) = \frac{|\mathbf{v}_i^H \mathbf{H}_{ii} \mathbf{w}_i|^2 P}{\sum_{j \neq i}^{N_c} |\mathbf{v}_i^H \mathbf{H}_{ij} \mathbf{w}_j|^2 P + \sigma_i^2}. \tag{4.11}$$

Based on Tx i's belief, Tx i maximizes the utility function in (4.11) *where $\mathbf{v}_i$ is a known quantity.*

Lemma 2. *There exists at least one Nash equilibrium in the egoistic Bayesian game G* (4.9) *with utility function defined in* (4.11).

Proof. $\mathcal{A}_i$ is convex, closed and bounded for all players i and the egoistic utility function $u_i(\mathbf{w}_i, \mathbf{w}_{-i})$ is continuous in both $\mathbf{w}_i$ and $\mathbf{w}_{-i}$. The utility function is concave in $\mathbf{w}_i$ for any set $\mathbf{w}_{-i}$. Thus, at least one Nash equilibrium (NE) exists [23, 46]. □

Theorem 6. *The unique best-response strategy of player i in the egoistic Bayesian game G* (4.9) *with utility function* (4.11) *is to maximize the utility function based on its belief:*

$$\mathbf{w}_i^{Ego} = \arg\max_{\|\mathbf{w}_i\| \leq 1} \mathcal{E}_{\mathbb{B}_i^\perp} \left\{ u_i(\mathbf{w}_i, \mathbf{w}_{-i}) \right\}. \tag{4.12}$$

The best-response strategy of player i is

$$\mathbf{w}_i^{Ego} = V^{(max)}(\mathbf{E}_i) \tag{4.13}$$

where $\mathbf{E}_i$ *denotes the* egoistic equilibrium matrix *for Tx* i*, given by*

$$\mathbf{E}_i = \mathbf{H}_{ii}^H \mathbf{v}_i \mathbf{v}_i^H \mathbf{H}_{ii}.$$

Proof. The knowledge of receive beamformers decorrelates the maximization problem which can be written as

$$\mathbf{w}_i^{Ego} = \underset{\|\mathbf{w}_i\| \leq 1}{\arg\max}\, \mathcal{E}_{\mathbb{B}_i^{\perp}} \left\{ \frac{1}{\sum_{j \neq i}^{N_c} |\mathbf{v}_i^H \mathbf{H}_{ij} \mathbf{w}_j|^2 P + \sigma_i^2} \right\} \mathbf{w}_i^H \mathbf{H}_{ii}^H \mathbf{v}_i \mathbf{v}_i^H \mathbf{H}_{ii} \mathbf{w}_i. \tag{4.14}$$

The egoistic-optimal transmit beamformer is therefore the dominant eigenvector of $\mathbf{H}_{ii}^H \mathbf{v}_i \mathbf{v}_i^H \mathbf{H}_{ii}$. □

4.2.2 Altruistic Bayesian game

Definition 6. *The utility of the altruistic game is defined here so as to minimize the sum of interference powers caused to other receivers.*

$$u_i(\mathbf{w}_i, \mathbf{w}_{-i}) = -\sum_{j \neq i}^{N_c} \left| \mathbf{v}_j^H \mathbf{H}_{ji} \mathbf{w}_i \right|^2 \tag{4.15}$$

Lemma 3. *There exist at least one NE in the altruistic Bayesian game* G (4.9) *with utility function defined in* (4.15)*.*

Proof. $\mathcal{A}_i$ is convex, closed and bounded for all players i and the altruistic utility function $u_i(\mathbf{w}_i, \mathbf{w}_{-i})$ is continuous in both $\mathbf{w}_i$ and $\mathbf{w}_{-i}$. The utility function is concave in $\mathbf{w}_i$ for any set $\mathbf{w}_{-i}$. Thus, at least one NE exists [23, 46]. □

Theorem 7. *Based on belief* μ*, Tx* i *seeks to maximize the utility function defined in* (4.15)*. The best-response strategy is*

$$\mathbf{w}_i^{Alt} = V^{(min)} \left(\sum_{j \neq i}^{N_c} \mathbf{A}_{ji} \right) \tag{4.16}$$

where $\mathbf{A}_{ji}$ *denotes the* altruistic equilibrium matrix for Tx i towards Rx j*, defined by* $\mathbf{A}_{ji} = \mathbf{H}_{ji}^H \mathbf{v}_j \mathbf{v}_j^H \mathbf{H}_{ji}$.

Proof. Recall the utility function to be $-\sum_{j \neq i}^{N_c} |\mathbf{v}_j^H \mathbf{H}_{ji} \mathbf{w}_i|^2 = -\sum_{j \neq i}^{N_c} \mathbf{w}_i^H \mathbf{A}_{ji} \mathbf{w}_i$. Since $\mathbf{v}_j$ are known from feedback or estimation in reciprocal channels, the optimal $\mathbf{w}_i$ is the least dominant eigenvector of the matrix $\sum_{j \neq i}^{N_c} \mathbf{A}_{ji}$. □

4.3 Sum rate Maximization with Receive Beamformer Feedback

From the results above, it can be seen that balancing altruism and egoism for player i can be done by trading-off between setting the beamformer close to the dominant eigenvectors of the egoistic equilibrium $\mathbf{E}_i$ or that of the negative altruistic equilibrium $\{-\mathbf{A}_{ji}\}$ $(j \neq i)$ matrices in (4.42). Interestingly, it can be shown that, in later sections, sum rate

maximizing precoding for the MIMO-IC does exactly that. Thus we hereby briefly re-visit rate-maximization approaches such as [61] with this perspective.

Denote the sum rate by $\bar{R} = \sum_{i=1}^{N_c} R_i$ where $R_i = \log_2\left(1 + \frac{|\mathbf{v}_i^H \mathbf{H}_{ii}\mathbf{w}_i|^2 P}{\sum_{j\neq i}^{N_c} |\mathbf{v}_i^H \mathbf{H}_{ij}\mathbf{w}_j|^2 P + \sigma_i^2}\right)$.

Lemma 4. *The transmit beamforming vector which maximizes the sum rate $\bar{R}$ is the dominant eigenvector of a matrix, which is a linear combination of $\mathbf{E}_i$ and $\mathbf{A}_{ji}$:*

$$\left(\mathbf{E}_i + \sum_{j\neq i}^{N_c} \lambda_{ji}^{opt} \mathbf{A}_{ji}\right) \mathbf{w}_i = \mu_{max}\mathbf{w}_i \tag{4.17}$$

where

$$\lambda_{ji}^{opt} = -\frac{|\mathbf{v}_j^H \mathbf{H}_{jj}\mathbf{w}_j|^2 P}{\sum_{k=1}^{N_c} |\mathbf{v}_j^H \mathbf{H}_{jk}\mathbf{w}_k|^2 P + \sigma_j^2} \frac{\sum_{k=1}^{N_c} |\mathbf{v}_i^H \mathbf{H}_{ik}\mathbf{w}_k|^2 P + \sigma_i^2}{\sum_{k\neq j}^{N_c} |\mathbf{v}_j^H \mathbf{H}_{jk}\mathbf{w}_k|^2 P + \sigma_j^2} \tag{4.18}$$

and μ_{max} is defined in the proof.

Proof. see Section 4.8.1. □

Note that the balancing between altruism and egoism in sum rate maximization is done using the dominant eigenvector of a simple *linear combination* of the altruistic and egoistic equilibrium matrices. The balancing parameters, $\{\lambda_{ji}^{opt}\}$, can be shown simply to coincide with the pricing parameters invoked in the iterative algorithm proposed in [61]. Clearly, these parameters plays a key role, however their computation is a function of the *global* channel state information and requires additional message (price) exchange. Instead, we seek below a suboptimal egoism-altruism balancing technique which only requires statistical channel information, while exhibiting the right performance scaling when SNR grows large.

4.4 A practical distributed beamforming algorithm: *DBA*

We are proposing the following distributed beamforming algorithm (*DBA*) where one computes the transmit and receive beamformers iteratively as:

$$\mathbf{w}_i = V^{max}\left(\mathbf{E}_i + \sum_{j\neq i}^{N_c} \lambda_{ji}\mathbf{A}_{ji}\right) \tag{4.19}$$

$$\mathbf{v}_i = \frac{\mathbf{C}_{Ri}^{-1}\mathbf{H}_{ii}\mathbf{w}_i}{\left\|\mathbf{C}_{Ri}^{-1}\mathbf{H}_{ii}\mathbf{w}_i\right\|} \tag{4.20}$$

where λ_{ji} shall be made to depend on channel statistics only. At this stage, it is interesting to compare with previous schemes based on interference alignment such as the practical algorithms proposed in [49]. In such schemes, the transmit beamformer $\mathbf{w}_i$ is taken independent of $\mathbf{H}_{ii}$. Note that here however, $\mathbf{w}_i$ is correlated to the direct channel gain $\mathbf{H}_{ii}$ through the egoistic matrix $\mathbf{E}_i$ in *DBA*. The correlation is useful in terms of sum rate as it allows proper weighting between the contributions of the egoistic and altruistic matrices in a link specific manner.

4.4.1 The egoism-altruism balancing parameters λ_{ji}

The egoism-altruism balancing parameters λ_{ji} are now found heuristically based on the statistical channel information. Recall from (4.18) that

$$\lambda_{ji}^{opt} = -\frac{S_j}{S_j + I_j + \sigma_j^2} \frac{S_i + I_i + \sigma_i^2}{I_j + \sigma_j^2} \tag{4.21}$$

where $S_j = |\mathbf{v}_j^H \mathbf{H}_{jj} \mathbf{w}_j|^2 P$ and $I_j = \sum_{k \neq j}^{N_c} |\mathbf{v}_j^H \mathbf{H}_{jk} \mathbf{w}_k|^2 P$.

Following the principle behind sum rate maximization, we conjecture that at convergence, residual coordinated interference shall be proportionate to the noise and out-of-cluster interference, i.e. $I_j = O(\sigma_j^2)$. Note that this should not be interpreted as an assumption in a proof but rather as a proposed design guideline. Based on this, we propose the following characterization:

$$\lambda_{ji}^{opt} = -\frac{S_j}{S_j + O(\sigma_j^2)} \frac{S_i + O(\sigma_i^2)}{O(\sigma_j^2)}. \tag{4.22}$$

By Jensen's inequality, a lower bound on the average λ_{ji}^{opt} is found by:

$$\mathcal{E}\left(\lambda_{ji}^{opt}\right) \geq -\frac{1}{1 + \frac{O(\sigma_j^2)}{\mathcal{E}S_j}} \frac{1 + \frac{O(\sigma_i^2)}{\mathcal{E}S_i}}{\frac{O(\sigma_j^2)}{\mathcal{E}S_i}}. \tag{4.23}$$

Although $\mathcal{E}S_i$ is not known explicitly, it is strongly related to the strength of the direct channel $P\alpha_{ii}$. Let $\gamma_i = \frac{P\alpha_{ii}}{\sigma_i^2}$. In order to obtain an exploitable formulation for λ_{ji}, we replace $\mathcal{E}S_i$ by $P\alpha_{ii}$ and $O(\sigma_i^2)$ by σ_i^2, to derive:

$$\lambda_{ji} = -\frac{1}{1 + \gamma_j^{-1}} \frac{1 + \gamma_i^{-1}}{\frac{\sigma_j^2}{P\alpha_{ii}}}. \tag{4.24}$$

Interestingly, in the special case where direct channels have the same average strength, we obtain a simple expression

$$\lambda_{ji} = -\frac{1 + \gamma_i^{-1}}{1 + \gamma_j^{-1}} \gamma_j. \tag{4.25}$$

The above result suggests Tx i to behave more altruistically towards link j when the SNR of link j is high or when the SNR of link i is comparatively lower. This is in accordance with the intuition behind rate maximization over parallel Gaussian channels.

DBA iterates between optimizing the transmit and receive beamformers, as summarized in Algorithm 1. Iterative optimization of the transmit and receive beamformers is reminiscent of recent interference-alignment based methods [20, 49]. However here, interference alignment is *not* a design criterion. In [20], an improved interference alignment technique based on alternately maximizing the SINR at both transmitter and receiver sides is proposed. In contrast, here the Max-SINR criterion is only used at the receiver side. Although the distinction is unimportant in the large SNR case (see below), it dramatically changes performance in certain situations at finite SNR (see Section 4.6).

Algorithm 1 DBA

1) Initialize beamforming vectors $\mathbf{w}_i, i = 1, \ldots, N_c$, to be predefined vectors.
2) For each Rx i, compute $\mathbf{v}_i = \frac{\mathbf{C}_{Ri}^{-1}\mathbf{H}_{ii}\mathbf{w}_i}{|\mathbf{C}_{Ri}^{-1}\mathbf{H}_{ii}\mathbf{w}_i|}$ where $\mathbf{C}_{Ri}$ is computed with $\mathbf{w}_i$ in previous step.
3) For each Tx i, compute $\mathbf{w}_i = V^{max}\left(\mathbf{E}_i + \sum_{j\neq i}^{N_c}\lambda_{ji}\mathbf{A}_{ji}\right)$ where λ_{ji} are computed from statistical parameters (4.24).
4) Repeat step 2 and 3 until convergence.

4.4.2 Asymptotic Interference Alignment

One important aspect of the algorithm above is whether it achieves the interference alignment in high SNR regime [20]. The following theorem answers this question positively.

Definition 7. *Define the set of beamforming vectors solutions in downlink (respectively uplink) interference alignment to be [20]*

$$\mathcal{IA}^{DL} = \left\{(\mathbf{w}_1, \ldots, \mathbf{w}_{N_c}) : \sum_{k\neq i}^{N_c}\mathbf{H}_{ik}\mathbf{w}_k\mathbf{w}_k^H\mathbf{H}_{ik}^H \text{ is low rank, } \forall i\right\} \tag{4.26}$$

$$\mathcal{IA}^{UL} = \left\{(\mathbf{v}_1, \ldots, \mathbf{v}_{N_c}) : \sum_{k\neq i}^{N_c}\mathbf{H}_{ki}^H\mathbf{v}_k\mathbf{v}_k^H\mathbf{H}_{ki} \text{ is low rank, } \forall i\right\}. \tag{4.27}$$

Thus, for all $(\mathbf{w}_i, \ldots, \mathbf{w}_{N_c}) \in \mathcal{IA}^{DL}$, there exist receive beamformers $\mathbf{v}_i, i = 1, \ldots, N_c$ such that the following is satisfied:

$$\mathbf{v}_i^H\mathbf{H}_{ij}\mathbf{w}_j = 0 \ \ \forall i, j \neq i. \tag{4.28}$$

Note that the uplink alignment solutions are defined for a virtual uplink having the same frequency and only appear here as a technical concept helping with the proof.

Theorem 8. *Assume the downlink interference alignment set is non-empty (interference alignment is feasible). Denote average SNR of link i by $\gamma_i = \frac{P\alpha_{ii}}{\sigma_i^2}$. Let $\lambda_{ji} = -\frac{1+\gamma_i^{-1}}{1+\gamma_j^{-1}}\gamma_j$, then in the large SNR regime, $P \to \infty$, any transmit beamforming vector in $\mathcal{IA}^{DL}$ is a convergence (stable) point of* DBA.

Proof. see Section 4.8.2. □

Note that this does not prove global convergence, but local convergence, as is the case for other IA or rate maximization techniques [20, 49, 61]. Another way to characterize local convergence is as follows: assuming interference alignment is feasible ($\mathcal{IA}^{DL}$ is non-empty), the first algorithm in [20] was shown to converge to transmit beamformers belonging to $\mathcal{IA}^{DL}$ and the receivers are based on the minimum eigenvector of the downlink interference covariance matrix, which tends to be low-rank. However, *DBA* selects its receive beamformer from the Max-SINR criterion which, in the large SNR situation, is also identical to selecting receive beamformers in the null space of the interference covariance matrix. Therefore when interference alignment is feasible, the algorithm in [20] and *DBA* coincide at large SNR. This aspect is confirmed by our simulations (see section 4.6).

4.5 Multi streams transmission

In this section, we extend the previous discussion to the multi-streams per Tx-Rx pair scenario. Hence, we recall the received signal at Rx i from (2.4) to

$$\mathbf{y}_i = \mathbf{H}_{ii}\mathbf{W}_i\mathbf{x}_i\sqrt{P} + \sum_{j\neq i}^{N_c}\mathbf{H}_{ij}\mathbf{W}_j\mathbf{x}_j\sqrt{P} + \mathbf{n}_i. \tag{4.29}$$

Here, we assume equal power allocation among the streams that belong to the same Tx. The pre-coder $\mathbf{W}_i$ is a $N_t \times N_{si}$ matrix with N_{si} being the number of streams Tx i wishes to transmit to Rx i. The N_{si} transmit symbols are denoted as a vector $\mathbf{x}_i$. The pre-coders are subject to the power constraint,

$$tr\left(\mathbf{W}_i\mathbf{W}_i^H\right) = 1, \qquad i = 1, \ldots, N_c. \tag{4.30}$$

Each element in the noise vector at Rx i is a complex Gaussian random variable with zero mean and variance σ_i^2 which captures both the thermal noise and the uncontrolled interference from out-of-cluster interference sources. Similarly, we define the receive matrix at Rx i to be $\mathbf{V}_i$ which is a $N_r \times N_{si}$ matrix. We assume that interference is treated as noise and the interference power for stream k at Rx i is defined as

$$\mathcal{I}_{ik} = \sum_{(j,m)\in\mathbb{I}_{ik}} \left|\mathbf{v}_{ik}^H\mathbf{H}_{ij}\mathbf{w}_{jm}\right|^2 \tag{4.31}$$

where $\mathbb{I}_{ik}$ is the set of interfering links with respect to stream k of Rx i, defined as

$$\mathbb{I}_{ik} = \{(j,m) : j = 1, \ldots, N_c, m = 1, \ldots, N_{sj}\} \setminus \{(i,k)\}. \tag{4.32}$$

Now, we define the SINR of stream k of Tx-Rx pair i to be

$$\gamma_{ik} = \frac{\left|\mathbf{v}_{ik}^H\mathbf{H}_{ii}\mathbf{w}_{ik}\right|^2}{\mathcal{I}_{ik} + \sigma_i^2} \tag{4.33}$$

and the corresponding received interference covariance matrix

$$C_{Rik} = \sum_{(j,m)\in\mathbb{I}_{ik}} \mathbf{H}_{ij}\mathbf{w}_{jm}\mathbf{H}_{ij}^H\mathbf{w}_{jm}^H. \tag{4.34}$$

To avoid repetitions, we give the extensions briefly. Recall the Bayesian games definition in (4.9), each Tx-Rx pair is a player. However, in the multi-stream scenario, each stream belonging to Tx-Rx pair i, in the total of N_{si} streams, has conflict among each other as there is interference among these streams. To avoid such confusion, we propose to model *each stream as a player*.

A strategy of player l, here refers to beamforming design, $\mathbf{w}_{ik}$ (see table 4.1), is a deterministic choice of action given information $\mathbb{B}_i$. A strategy profile $\mathbf{W}^* = (\mathbf{w}_{ik}^*, \mathbf{w}_{-ik}^*)$ achieves the Bayesian Equilibrium if $\mathbf{w}_{ik}^*$ is the best response of player l given strategies $\mathbf{w}_{-ik}^*$ for all other players. The optimal transmit beamformer of player l, $\mathbf{w}_{ik}^*$, is characterized by the argument maximization of the expectation of the utility function $u(.)$:

$$\mathbf{w}_{ik}^* = \arg\max \mathcal{E}_{\mathbb{B}_i^\perp}\left\{u(\mathbf{w}_{ik}, \mathbf{w}_{-ik}^*, \mathbb{B}_i, \mathbb{B}_i^\perp)\right\}. \tag{4.35}$$

We can formulate the bayesian game as

$$G^B = \left[\mathcal{M}, \mathbb{A}, \mathbb{B}_i^\perp, \{u\}\right]. \tag{4.36}$$

player l	data stream k of Tx i where $l = \sum_{j=1}^{i-1} N_{si} + k$ $l \in \mathcal{M} = \{1, \ldots, \bar{N}_s\}$
action set	$\mathbb{A} = \{\mathbf{w} \in \mathbb{C}^{N_t \times 1} : \|\mathbf{w}\|^2 = 1\}$
strategy	beamforming vector of stream k of Tx i, $\mathbf{w}_{ik} \in \mathbb{A}$
utility function egoistic : altruistic :	$u : \mathbb{A}^{N_s} \to \mathbb{R}$ received SINR of stream l (4.37) negative interference caused by stream l (4.15)
Belief	unknown channel statistics $\mathbb{B}_i^{\perp}$ as a Gaussian distribution
common knowledge	utility function and channel statistics

Table 4.1: Summary of the multi-stream Bayesian game

4.5.1 Egoistic Bayesian Game

Given receive beamformers as a common knowledge, the best response strategy of stream k of Tx i which maximizes the utility function, i.e. its own SINR,

$$u(\mathbf{w}_{ik}, \mathbf{w}_{-ik}, \mathbb{B}_i, \mathbb{B}_i^{\perp}) = \frac{\left|\mathbf{v}_{ik}^H H_{ii} \mathbf{w}_{ik}\right|^2 P_{ik}}{\mathcal{I}_{ik} + \sigma_i^2}, \tag{4.37}$$

is the following:

Theorem 9. *The best-response strategy of stream k of Tx i in the egoistic Bayesian game is*

$$\mathbf{w}_{ik}^{Ego} = V^{(max)}(\mathbf{E}_{ik}) \tag{4.38}$$

where $\mathbf{E}_{ik}$ *will denote the* egoistic equilibrium matrix *for stream k of Tx i, given by*

$$\mathbf{E}_{ik} = \mathbf{H}_{ii}^H \mathbf{v}_{ik} \mathbf{v}_{ik}^H \mathbf{H}_{ii} \tag{4.39}$$

and the corresponding Rx is given by $\mathbf{v}_{ik} = \frac{{C_{Rik}}^{-1} \mathbf{H}_{ii} \mathbf{w}_{ik}^{Ego}}{\|{C_{Rik}}^{-1} \mathbf{H}_{ii} \mathbf{w}_{ik}^{Ego}\|}$.

Proof. The knowledge of receive beamformers decorrelates the maximization problem. The maximization problem can be written as

$$\mathbf{w}_{ik}^{Ego} = \underset{\|\mathbf{w}_{ik}\| \leq 1}{\arg\max}\, \mathcal{E}_{\mathcal{B}_i^{\perp}} \left\{ \frac{P_{ik}}{\mathcal{I}_{ik} + \sigma_i^2} \right\} \mathbf{w}_{ik}^H \mathbf{E}_{ik} \mathbf{w}_{ik}. \tag{4.40}$$

The egoistic-optimal transmit beamformer is the dominant eigenvector $\mathbf{w}_{ik}^{Ego} = V^{(max)}(\mathbf{E}_{ik})$. □

4.5.2 Altruistic Bayesian Game

The altruistic utility of stream k at Tx i is defined here in the sense of minimizing the expectation of the sum of interference power towards other streams.

$$u(\mathbf{w}_{ik}, \mathbf{w}_{-ik}, \mathbb{B}_i, \mathbb{B}_i^{\perp}) = - \sum_{(j,m) \in \mathbb{I}_{ik}} \left|\mathbf{v}_{jm}^H \mathbf{H}_{ji} \mathbf{w}_{ik}\right|^2 \tag{4.41}$$

Theorem 10. *The best-response strategy of stream k of Tx i in the altruistic Bayesian game is given by:*

$$\mathbf{w}_{ik}^{Alt} = V^{(min)}\left(\sum_{(j,m)\in\mathbb{I}_{ik}} \mathbf{A}_{jmik}\right) \tag{4.42}$$

where $\mathbf{A}_{jmik}$ will denote the altruistic equilibrium matrix for stream k of Tx i towards stream m of Rx j, *defined by*

$$\mathbf{A}_{jmik} = \mathbf{H}_{ji}^H \mathbf{v}_{jm}\mathbf{v}_{jm}^H \mathbf{H}_{ji}. \tag{4.43}$$

The corresponding receiver is $\mathbf{v}_{ik} = \frac{C_{Rik}^{-1}\mathbf{H}_{ii}\mathbf{w}_{ik}}{\left\|C_{Rik}^{-1}\mathbf{H}_{ii}\mathbf{w}_{ik}\right\|}$.

Proof. The altruistic utility can be rewritten as $-\mathbf{w}_{ik}^H(\sum_{(j,m)\in\mathbb{I}_{ik}} \mathbf{A}_{jmik})\mathbf{w}_{ik}$. Since the $\mathbf{v}_{jm}$ are known from feedback, the optimal $\mathbf{w}_{ik}$ is the least dominant eigenvector of the matrix $\sum_{(j,m)\in\mathbb{I}_{ik}} \mathbf{A}_{jmik}$. □

4.5.3 Multi-stream DBA

Similar to (4.44), we have the following beamforming vector that coincides to sum rate maximization in the multi-stream scenario, as the eigenvector of a linear combination of the egoistic matrix and altruistic matrix defined in the multi-stream scenario in (4.39) and (4.43) respectively:

$$\mathbf{w}_{ik} = V^{max}\left(\mathbf{E}_{ik} + \sum_{(j,m)\in\mathbb{I}_{ik}} \lambda_{ji}\mathbf{A}_{jmik}\right) \tag{4.44}$$

where λ_{ji} is computed as in Thm. 8. The receiver beamforming vector is matched with the corresponding transmit beamforming vector,

$$\mathbf{v}_{ik} = \frac{{C_{Rik}}^{-1}\mathbf{H}_{ii}\mathbf{w}_{ik}}{\left\|{C_{Rik}}^{-1}\mathbf{H}_{ii}\mathbf{w}_{ik}\right\|}. \tag{4.45}$$

4.5.4 Feasibility of interference alignment

As described in (2.16), the feasibility problem of interference alignment for a given tuple of degrees of freedom, here the number of data streams $d_i = N_{si}$, is whether the following constraints can be satisfied simultaneously:

$$\begin{cases} rank(\mathbf{V}_i^H\mathbf{H}_{ii}\mathbf{W}_i) = N_{si} \\ \mathbf{V}_i^H\mathbf{H}_{ij}\mathbf{w}_j = \mathbf{0}, \qquad i,j = 1,\ldots,N, i \neq j. \end{cases} \tag{4.46}$$

The feasibility problem depends on all of the following parameters: $N_c, N_t, N_r, N_{s1}, \ldots N_{N_c}$. If the constraints in (4.46) cannot be satisfied, then we say that interference alignment is infeasible in this channel setting.

4.5.5 Binary power control

In the channel settings that render infeasibility of interference alignment, the residual interference saturates the sum rate performance in the high SNR regime. To scale the sum rate indefinitely in the IA infeasible regime, we propose a binary power control to

restore the feasibility of IA. Note that binary power control is shown to be sum rate optimal in 2 cells scenario and near-optimal in multi cell scenario [32]. Here, we propose to consider a subset of the transmit streams to be shut down in order to allow a perfect interference removal at the receive side in the IA infeasible and high SNR regime.

In order to obtain equations which are amenable to a simple power control scheme, we advocate a design guideline by which the residual interference at each Rx should be made on the same order of magnitude as the thermal noise (as opposed to making it zero, as the cost of degrees of freedom on the optimization of the beamforming coefficients). To check whether at least one stream should be turned off, we can easily check by comparing the received interference power to noise. Thus, according to our designing rule, the stream k of user i will be shut down when

$$P_{ik} = 0 \quad \text{if} \quad \mathcal{I}_{ik} > \sigma_i^2 \text{ and } \gamma_{ik} < \gamma_{jm}, \qquad (j,m) \in \mathbb{I}_{ik}. \tag{4.47}$$

To fulfill the transmit power constraint, equal power is allocated to the remaining streams at each Tx.

The proposed beamforming and power control algorithm can be summarized as follows:

1. Initialization: For each user $i \in \mathbb{N}_c$, initialize transmit power for each stream $k = 1 \dots N_s$ with equal power allocation $P_{ik} = \frac{P}{N_s}$. Initialize transmit beamformer $\mathbf{w}_{ik}$ to a predefined vector and the receive beamformer $\mathbf{v}_{ik}$ is a max-SINR receiver in the form of (4.45).

2. DBA: Start the iterative beamforming procedure using (4.44) and (4.7).

3. Power Control: When DBA converges, check power control criteria (4.47). If at least one stream is shut down, repeat DBA until power control criteria is satisfied.

4.5.6 Low Complexity of Binary Power Control

We include here briefly the pricing algorithm in [61] in the following, for details, please refer to section III B in [61].

Algorithm 2 Distributed Bargaining Algorithm through Pricing [61]

1) Initialization of precoding matrices, interference prices, power profiles and receive filters.
2) Iteration: for each user,

1. optimize beamformers based on given interference prices and power profile.

2. optimize power profile by maximizing a non-convex surplus function .

3. recompute all interference prices and receive filters.

Repeat until convergence.

The Binary power optimization offers a complexity reduction advantage over a search over the continuous power domain proposed in [61].

4.5.7 Restoring IA feasibility in high SNR

Both [61] and DBA restore IA feasibility in the high SNR regime. In the high SNR or high interference regime, the individual rates become more sensitive towards the received interference. By definition, the prices are increased and force the transmit power of some Tx to decrease. In Fig. 4.7, we illustrate the sum rate performance of [61] with binary power allocation. As the sum rate scales indefinitely with SNR, the IA feasibility is restored. However, this binary power control in [61] can be affected by fast fading gains and thus in some channel realizations, some links remain transmitting even if the sum rate could be higher if they are shut down. Comparing to DBA, the binary power control criteria seems to be more effective and achieve a better sum rate in high SNR and IA unfeasibility region. (see later for details)

4.6 Simulation Results

In this section, we investigate the sum rate performances of *DBA* in comparison with several related methods, namely the *Max-SINR* method [20], the alternated-minimization (*Alt-Min*) method for interference alignment [49] and the sum rate optimization method (*SR-Max*) [61]. The *SR-Max* method is by construction optimal but is more complex and requires extra sharing or feedback of pricing information among the transmitters. To ensure a fair comparison, all the algorithms in comparisons are initialized to the same solution and have the same stopping condition. The algorithms are considered to reach convergence if the sum rates achieved between successive iterations have difference less than 0.001. We perform sum rate comparisons in both symmetric channels and asymmetric channels where links undergo different levels of out-of-cluster noise. Define the Signal to Interference ratio of link i to be $SIR_i = \frac{\alpha_{ii}}{\sum_{j\neq i}^{N_c} \alpha_{ij}}$. The SIR is assumed to be 1 for all links, unless otherwise stated. Denote the difference in SNR between two links in asymmetric channels by ΔSNR. Note that the proposed algorithm is not limited to the following settings, but can be applied to network with arbitrary players and number of antennas.

4.6.1 Symmetric Channels

Fig. 4.2 illustrates the sum rate comparison of *DBA* with *Max-SINR*, *Alt-Min* and *SR-Max* in a system of 3 links and each Tx and Rx have 2 antennas. Since interference alignment is feasible in this case, the sum rate performance of *SR-Max* and *Max-SINR* increases linearly with SNR. *DBA* achieves sum rate performance with the same scaling as *Max-SINR* and *SR-Max* (i.e. multiplexing gain of 3). Therefore these methods seem to perform similarly in symmetric channels.

4.6.2 Asymmetric Channels

In the asymmetric system, some links undergo uneven levels of noise and uncontrolled interference. Another aspect is that more links can experience greater path loss or shadowing than others. Here we consider a few typical scenarios for which could constitute asymmetric networks, as shown in Fig. 4.3.

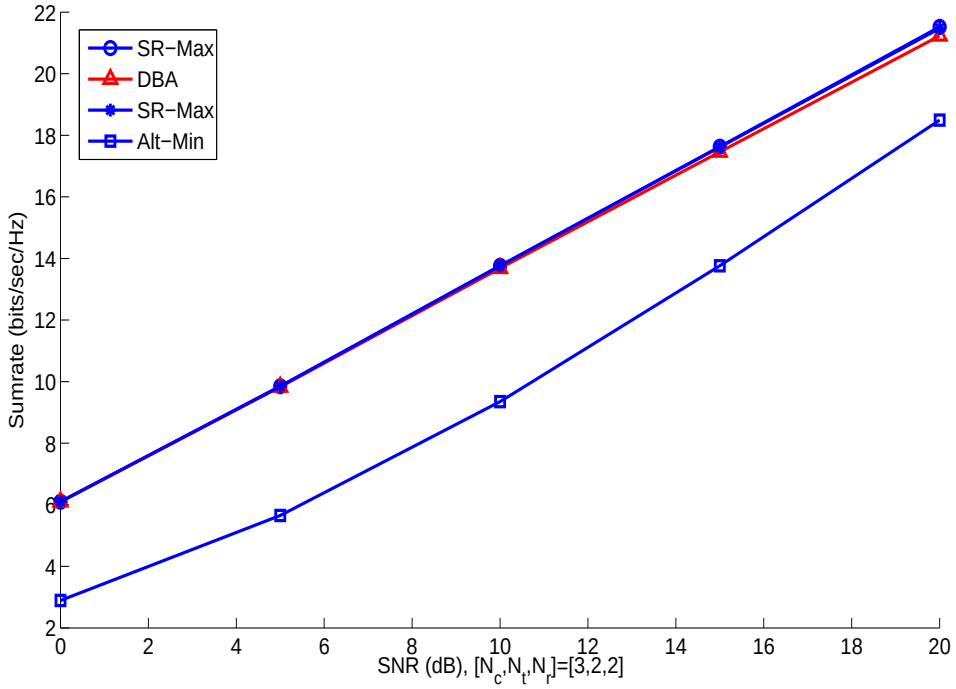

Figure 4.2: Sum rate comparison in multi links systems is illustrated in Fig. 4.2 with $[N_c, N_t, N_r] = [3, 2, 2]$ with increasing SNR. *DBA*, *SR-Max* and *Max-SINR* achieve very close performance.

4.6.2.1 Asymmetric uncontrolled interference power, illustrated in Fig. 4.3a

In Fig. 4.4, there are 3 links in the system in which the noise and unstructured interference in one of the links are 20dB stronger than the other two links. This set up captures the scenario that one link is at the boundary of the coordination cluster and suffer from strong out-of-cluster noise. The SIR of every link is assumed to be 10 dB. in this scenario, *DBA* outperforms interference alignment based methods because they are unable to properly weigh the importance of each link in the overall sum rate. *SR-Max* is by construction sum rate optimal. However, in the asymmetric network, we observe by simulation that the convergence may require more iterations than other algorithms and the increment in sum rate per iteration can be small in some channel realizations.

4.6.2.2 Asymmetric uncontrolled interference power and interference within cluster, illustrated in Fig. 4.3b

In Fig. 4.5, we compare the sum rate performance in the same set up as in Fig. 4.4, except that the SIR's of the links are $[10, 10, 0.1]$ respectively. Thus, link 3 not only suffers from strong out of cluster noise, but also suffers from strong interference within the cluster. The asymmetry penalizes the *Max-SINR* and interference alignment methods because they are unable to properly weigh the contributions of the weaker link in the sum rate. The *Max-SINR* strategy turns out to make link 3 very egoistic in this example, while its proper behavior should be altruistic. In contrast, *DBA* exploits useful statistical information, allowing weaker link to allocate their spatial degrees of freedom wisely towards helping stronger links and vice versa, yielding a better sum rate for the same feedback budget. The performance is very close to *SR-Max*, with less information exchange.

4.6.2.3 Asymmetric desired channel power, illustrated in Fig. 4.3c

In Fig. 4.6, there are 3 links cooperating in the system. Each Tx and Rx has 2 antennas and has 1 stream transmission. The noise at each Rx is the same. The system is asymmetric in a sense that the direct channel gain H_{11} of link 1 is 30dB weaker than other links in the network. This set up models a realistic environment where the user suffers strong shadowing. *DBA* achieves sum rate closed to *SR-Max* and much better than other interference alignment based schemes *Max-SINR* and *Alt-Min*.

4.6.3 Restoring IA feasibility by power control

In Fig 4.7, the sum rate performance of *SR-Max* is compared with *DBA* in a IA unfeasibility region, namely a 4 links system with each Tx and Rx equipped with 2 antennas and 1 stream transmission. The system SNR is allowed to increase to a high value which is plotted as the x-axis. The link qualities in the network are assumed to be equal, $\Delta SNR = 0$. To illustrate the design difference, we compare the performance of *SR-Max* with both continuous and binary power allocation. The continuous power allocation in [61] is a non-convex optimization. For implementation, the continuous power allocation is implemented as an exhaustive search over a quantized search space. We include here the performance of *SR-Max* with power control with 1 bit (binary), 2 bits and 3 bits quantization. As the system SNR increase, the sum rate becomes more sensitive towards the interference which increase the *price* in *SR-Max*. This forces some of the users to decrease their transmit power. However, the IA unfeasibility may not be fully restored in some channel realizations and may offer a lower performance compare with *DBA*.

In Fig. 4.8, the sum rate performance of *DBA* is plotted with and without power control in a 5 links system with each Tx and Rx equipped with two antennas. As shown in the figure, the proposed scheme with power control improve the sum rate by turning off non-contributing links. As SNR grows, the scenario of IA feasibility has to be restored in order to have the maximum sum rate scaling. Depending on the system SNR, the proposed scheme adaptively turn off 1 or more non-contributing links and restore the sum rate scaling.

4.7 Conclusion

We model the distributed beamforming optimization problem on MIMO interference channel using the framework of Bayesian Games which allow players to have incomplete information of the game, in this case the channel state information. Based on the incentives of the players, we proposed two games: the Egoistic Bayesian Game (players selfishly maximize its rate) and the Altruistic Bayesian Game (players altruistically minimize interference generated towards other players). We proved the existence of equilibria of such games and the best response strategy of players are computed. Inspired from the equilibria, a beamforming technique based on balancing the egoistic and the altruistic behavior with the aim of maximizing the sum rate is proposed. Such beamforming algorithm exhibits the same optimal rate scaling (when SNR grows) shown by recent iterative interference-alignment based methods. The proposed beamforming algorithm achieves close to optimal sum rate maximization method [61] without additional pricing feedbacks from users and outperform interference alignment based methods in terms of sum rate in asymmetric networks.

4.8 Proofs

4.8.1 Proof of Lemma 4

Define the Largrangian of the sum rate maximization problem for Tx i to be $\mathcal{L}(\mathbf{w}_i, \mu) = \bar{R} - \mu_{max}(\mathbf{w}_i^H \mathbf{w}_i - 1)$. The necessary condition of Largrangian $\frac{\partial}{\partial \mathbf{w}_i^H}\mathcal{L}(\mathbf{w}_i, \mu) = 0$ gives: $\frac{\partial}{\partial \mathbf{w}_i^H} R_i + \sum_{j\neq i}^{N_c} \frac{\partial}{\partial \mathbf{w}_i^H} R_j = \mu_{max}\mathbf{w}_i$. With elementary matrix calculus,

$$\frac{\partial}{\partial \mathbf{w}_i^H} R_i = \frac{P}{\sum_{k=1}^{N_c} |\mathbf{v}_i^H \mathbf{H}_{ik}\mathbf{w}_k|^2 P + \sigma_i^2} \mathbf{E}_i \mathbf{w}_i \tag{4.48}$$

$$\frac{\partial}{\partial \mathbf{w}_i^H} R_j = -\frac{|\mathbf{v}_j^H \mathbf{H}_{jj}\mathbf{w}_j|^2 P}{\sum_{k=1}^{N_c} |\mathbf{v}_j^H \mathbf{H}_{jk}\mathbf{w}_k|^2 P + \sigma_j^2} \frac{P}{\sum_{k\neq j}^{N_c} |\mathbf{v}_j^H \mathbf{H}_{jk}\mathbf{w}_k|^2 P + \sigma_j^2} \mathbf{A}_j \mathbf{w}_i \tag{4.49}$$

where λ_{ji}^{opt} is a function of all channel states information and beamformer feedback:

$$\lambda_{ji}^{opt} = -\frac{|\mathbf{v}_j^H \mathbf{H}_{jj}\mathbf{w}_j|^2 P}{\sum_{k=1}^{N_c} |\mathbf{v}_j^H \mathbf{H}_{jk}\mathbf{w}_k|^2 P + \sigma_j^2} \frac{\sum_{k=1}^{N_c} |\mathbf{v}_i^H \mathbf{H}_{ik}\mathbf{w}_k|^2 P + \sigma_i^2}{\sum_{k\neq j}^{N_c} |\mathbf{v}_j^H \mathbf{H}_{jk}\mathbf{w}_k|^2 P + \sigma_j^2}. \tag{4.50}$$

Thus, the gradient is zero for any $\mathbf{w}_i$ eigenvector of the matrix shown on the L.H.S. of (4.17). Among all stable points, the global maximum of the cost function is reached by selecting the dominant eigenvector of $E_i + \sum_{j\neq i} \lambda_{ji} A_{ji}$.

4.8.2 Proof of Theorem 8: convergence points of *DBA*

To prove that interference alignment forms a convergence set of *DBA*, we will prove that if *DBA* achieves interference alignment, *DBA* will not deviate from the solution (stable point).

Assumed interference alignment is reached and let $(\mathbf{w}_1^{IA}, \ldots, \mathbf{w}_{N_c}^{IA}) \in \mathcal{IA}^{DL}$ and $(\mathbf{v}_1^{IA}, \ldots, \mathbf{v}_{N_c}^{IA}) \in \mathcal{IA}^{UL}$. Let $\mathbf{Q}_i^{DL} = \sum_{k\neq i}^{N_c} \mathbf{H}_{ik}\mathbf{w}_k^{IA}\mathbf{w}_k^{IA,H}\mathbf{H}_{ik}^H$ and $\mathbf{Q}_i^{UL} = \sum_{k\neq i}^{N_c} \mathbf{H}_{ki}^H\mathbf{v}_k^{IA}\mathbf{v}_k^{IA,H}\mathbf{H}_{ki}$.

Given receivers $(\mathbf{v}_1^{IA}, \ldots, \mathbf{v}_{N_c}^{IA})$, we compute new transport beamformers. In high SNR regime, $\lambda_{ji} \to -\infty$ and *DBA* gives $\mathbf{w}_i = V^{min}(\mathbf{Q}_i^{UL})$ (4.44). By (4.26), $\mathbf{Q}_i^{UL}$ is low rank and thus $\mathbf{w}_i$ is in the null space of $\mathbf{Q}_i^{UL}$. In direct consequence, the conditions of interference alignment (4.28) are satisfied. Thus, $(\mathbf{w}_1, \ldots, \mathbf{w}_{N_c}) \in \mathcal{IA}^{DL}$.

Given transmitters $(\mathbf{w}_1^{IA}, \ldots, \mathbf{w}_{N_c}^{IA})$, we compute new receive beamformers. The receive beamformer is defined as $\mathbf{v}_i = \arg\max \frac{\mathbf{v}_i^H\mathbf{H}_{ii}\mathbf{w}_i^{IA}\mathbf{w}_i^{IA,H}\mathbf{H}_{ii}^H\mathbf{v}_i}{\mathbf{v}_i^H\mathbf{Q}_i^{DL}\mathbf{v}_i}$. Since $\mathbf{Q}_i^{DL}$ is low rank, the optimal $\mathbf{v}_i$ is in the null space of $\mathbf{Q}_i^{DL}$. Hence, $\mathbf{v}_i \in \mathcal{IA}^{UL}$.

Since both $\mathbf{w}_i$ and $\mathbf{v}_i$ stays within $\mathcal{IA}^{DL}$ and $\mathcal{IA}^{UL}$, interference alignment is a convergence point of DBA-RF in high SNR.

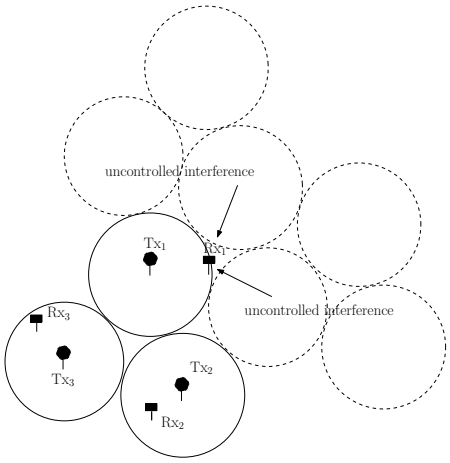

(a) Asymmetric uncontrolled interference

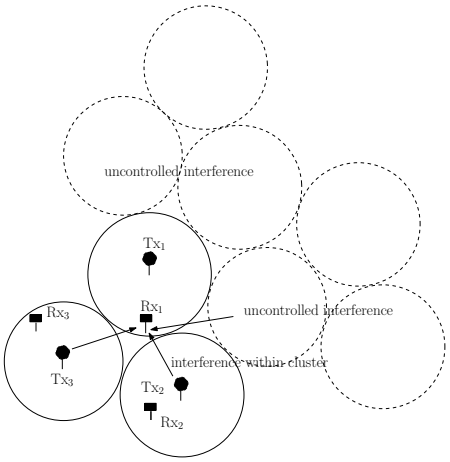

(b) Asymmetric uncontrolled interference and interference within cluster

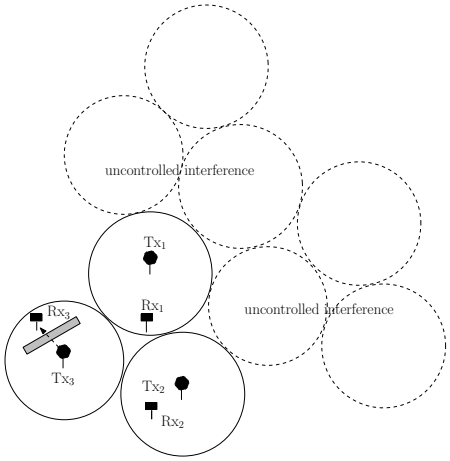

(c) Asymmetric desired channel power

Figure 4.3: Scenarios where asymmetry of channels are illustrated. Fig. 4.3a illustrates asymmetry of uncontrolled interference. Fig. 4.3b illustrates asymmetry of both uncontrolled interference and interference within cluster. Fig 4.3c illustrates the asymmetric strength of desired channel power.

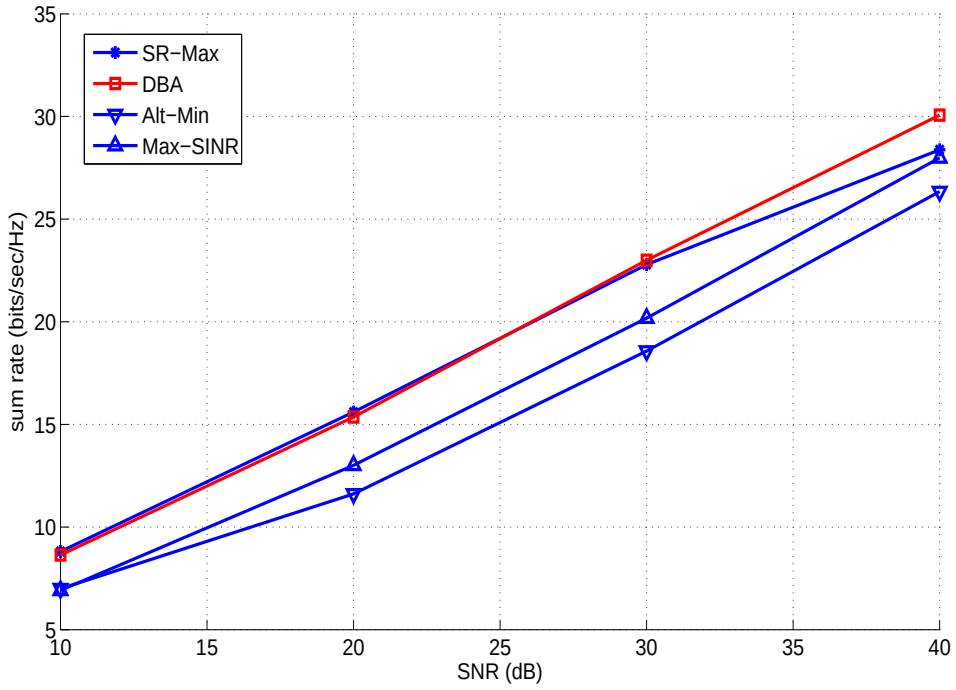

Figure 4.4: Sum rate performance for asymmetric channel, with one link under strong noise, is illustrated. The strong noise, from out of cluster interference, is 20dB stronger than other links. *DBA* outperforms standard *IA* methods thanks to a proper balance between egoistic and altruistic beamforming algorithm.

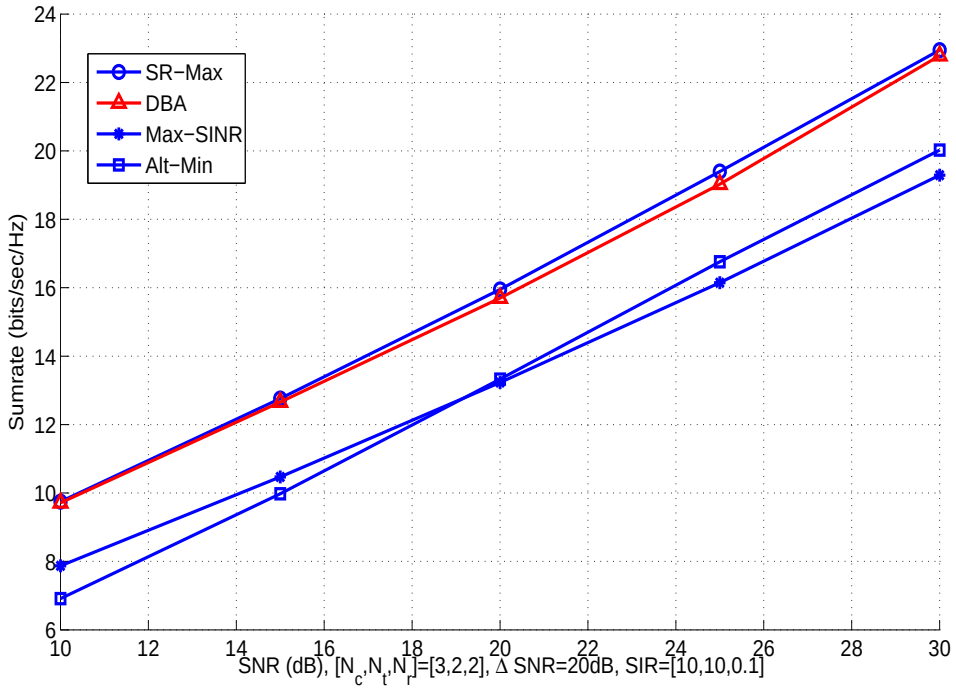

Figure 4.5: Sum rate performance for asymmetric channel, with one link under strong interference within the cooperating cluster, is illustrated.

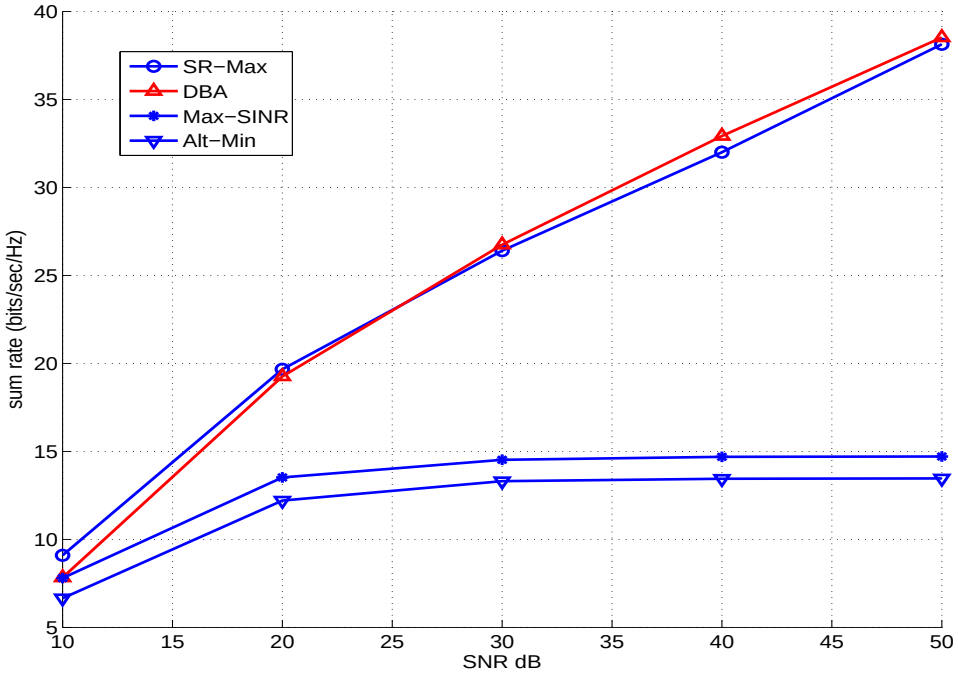

Figure 4.6: Sum rate performance for asymmetric channel is illustrated. The direct channel gain of link 1 is 30dB weaker than other links.

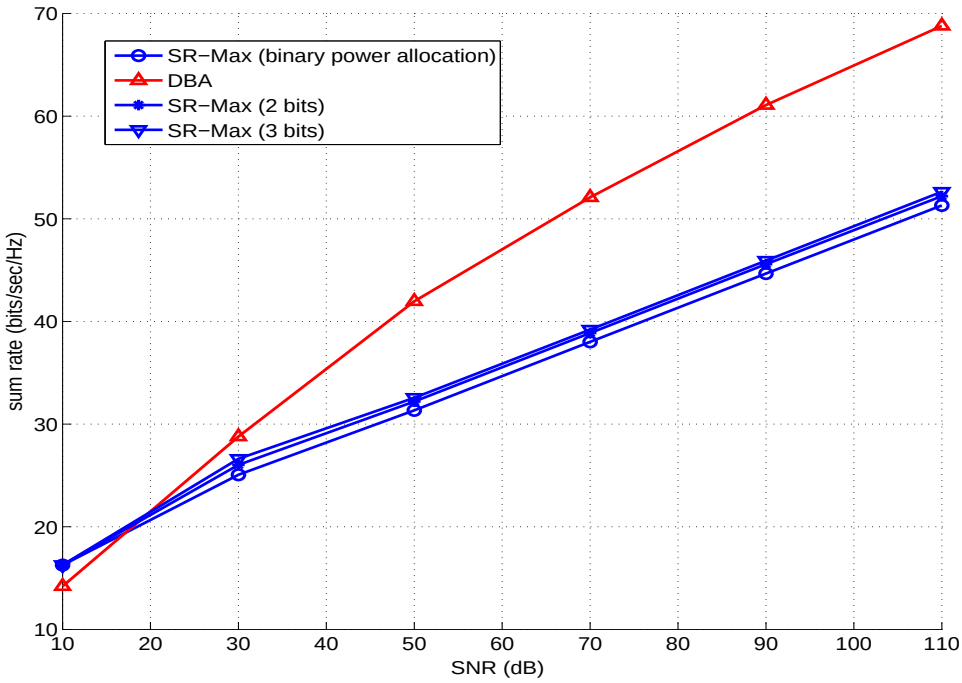

Figure 4.7: Sum rate performance for symmetric channel of 6 links system. *DBA* achieves a higher sum rate than *SR-Max* with continuous power allocation in IA unfeasibility and high SNR regime.

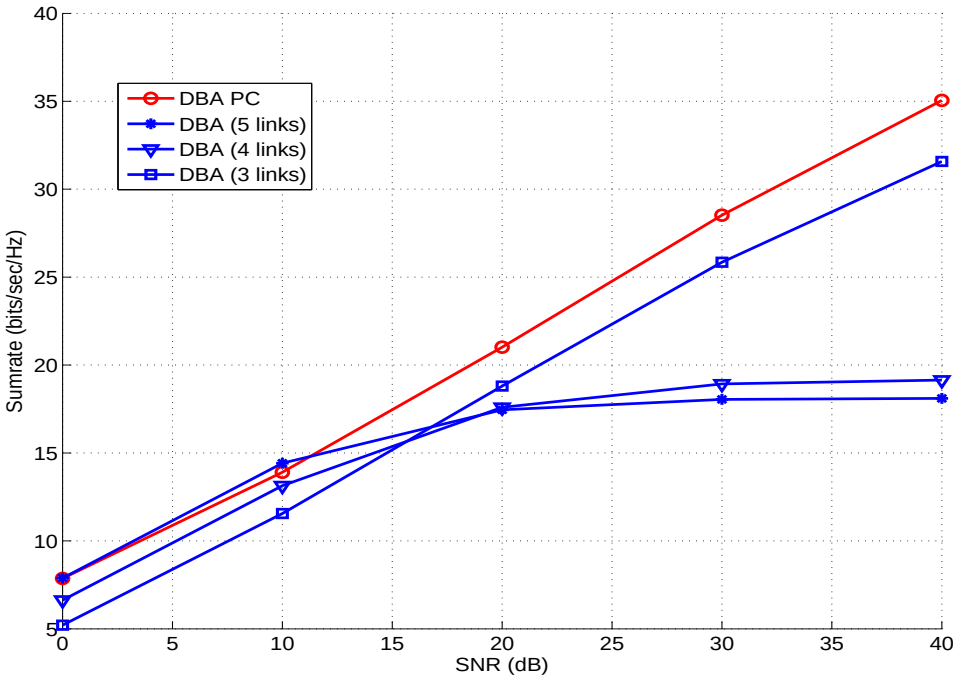

Figure 4.8: Sum rate performance for asymmetric channel of 5 links system. *DBA* with power control improves the *DBA* without power control.

Chapter 5

MISO-IC with Interference Decoding Capability

In this chapter, we consider receivers with interference decoding capability (IDC) so that the interference signal can be decoded and subtracted from the received signal. Although the capacity region of the SISO-IC-IDC has been extensively studied, the optimal power allocation and beamforming strategies which achieve the Pareto boundary of the MISO-IC-IDC have received little attention. On the MISO-IC with single user decoding, transmit beamforming vectors are designed to reach a compromise between mitigating the generated interference (zero forcing of the interference) or maximizing the energy at the desired user. With IDC, receivers can potentially decode interference and yield a higher data rate. Yet, when a user decides to decode the interference signal, it poses a rate constraint on the interferer because the interference should be received sufficiently strongly (or with a rate sufficiently low) which in turn dramatically affects the strategies for precoders design at all transmitters. The particularly intriguing problem arising in the multi-antenna IC with IDC is that transmitters may now have the incentive to amplify the interference generated at the non-intended receivers, in the hope that Rxs have a high chance of decoding the interference and removing it. This notion completely changes the previous paradigm of balancing between maximizing ones users desired energy and reducing the generated interference by opening up a new dimension for the beamforming design strategy. The fundamental question becomes: *when should the beamforming vectors be designed to amplify interference to improve performance and when to mitigate interference?*

The optimal rank of the transmit precoder in the MISO-IC with IDC is still an open problem. We proceed by proving that the optimal rank of the transmit precoders, optimal in the sense of Pareto optimality and therefore sum rate optimality, is rank one. Then, we investigate suitable transmit beamforming strategies for different decoding structures and characterize its Pareto boundary by parameterizing the set of beamforming vectors that achieves this Pareto boundary of the MISO-IC-IDC, termed *the candidate set of the Pareto boundary*. As an application of this characterization, we obtain the *candidate set of the maximum sum rate point* which is a strict subset of the candidate set of the Pareto boundary. We derived the MRT optimality conditions which are the constraints on channel coefficients that guarantee the sum rate optimality of the MRT strategies. Inspired by the MRT optimality conditions, we propose a simple algorithm that achieves maximum sum rate in certain scenarios and suboptimal, but fairly good performance, in other scenarios comparing to the maximum sum rate.

We consider the two transmitter-receiver (Tx-Rx) pairs interference channel with interference decoding capability (IDC). Each receiver can choose to decode interference (D) or treat interference as noise (N). The main contributions of this chapter are:

- In Section 5.2, we describe an achievable rate region of the MISO-IC with IDC, with the assumption of linear precoding, taking into account of receivers choice of actions, D or N.
- We study and characterize its Pareto boundary in Section 5.5.1, in terms of beamforming vectors design and power allocation. We characterize the set Ω of tuples of beamforming vectors and power allocation which attain the Pareto boundary.
- As a special case, in Section 5.6, we characterize the set of beamforming vectors which attain the maximum sum rate point as the candidate set $\tilde{\Omega}$ of maximum sum rate point. As the maximum sum rate problem is non-convex, conventional solutions rely on different searching techniques. Note that $\tilde{\Omega} \subset \Omega$. The cardinality of $\tilde{\Omega}$ is much smaller than the cardinality of Ω which provides a significant reduction of searching. Further, we prove that with IDC full power must be used at each Tx to attain the maximum sum rate point. This result is interesting as non-full power should be employed in some Txs to achieve the maximum sum rate point in the SISO-IC-SUD [13, 33].
- In Section 5.7, we investigate the conditions of channel parameters for which simple strategies are sum rate optimal. In particular, we study the matched filter (MF) with respect to the desired channel and the MF with respect to the interference channel, which are termed as the maximum-ratio-transmission (MRT) schemes. We define the MRT optimality conditions as the conditions, on channel coefficients, of the MRT schemes attaining maximum sum rate.
- Inspired by the MRT optimality conditions, we propose a suboptimal but very low complexity algorithm in Section 5.8. The suboptimal algorithm shows a promising tradeoff between complexity and performance, as illustrated by simulation results.
- In Section 5.9, we provide simulations and discussions which illustrate cases where interference decoding is beneficial to sum rate performances.

5.1 Channel model

We assume a simple system of two transmitter-receiver (Tx-Rx) pairs in which each Tx has N transmit antennas and each Rx has only one receive antenna. This results in a two-user Multiple-Input-Single-Output Interference Channel (MISO-IC), which is illustrated in Fig. 5.1 as an example with $N = 3$. We assume that the Txs are using commonly known codebooks and therefore the Rx, if the channel qualities allow, can decode the interference and subtract it from the received signal. Also, we assume that the interference is successfully decoded if the rate of the interference signal is smaller than the Shannon capacity of the interference channel.

In the MISO-IC-SUD, it has been shown that the optimal transmit precoders are rank 1 and therefore beamforming attains the Pareto boundary. However, whether his conclusion holds in the MISO-IC-IDC is not known yet. We answer this question in the following by starting with a general transmit covariance matrix. Denote the transmit covariance matrix

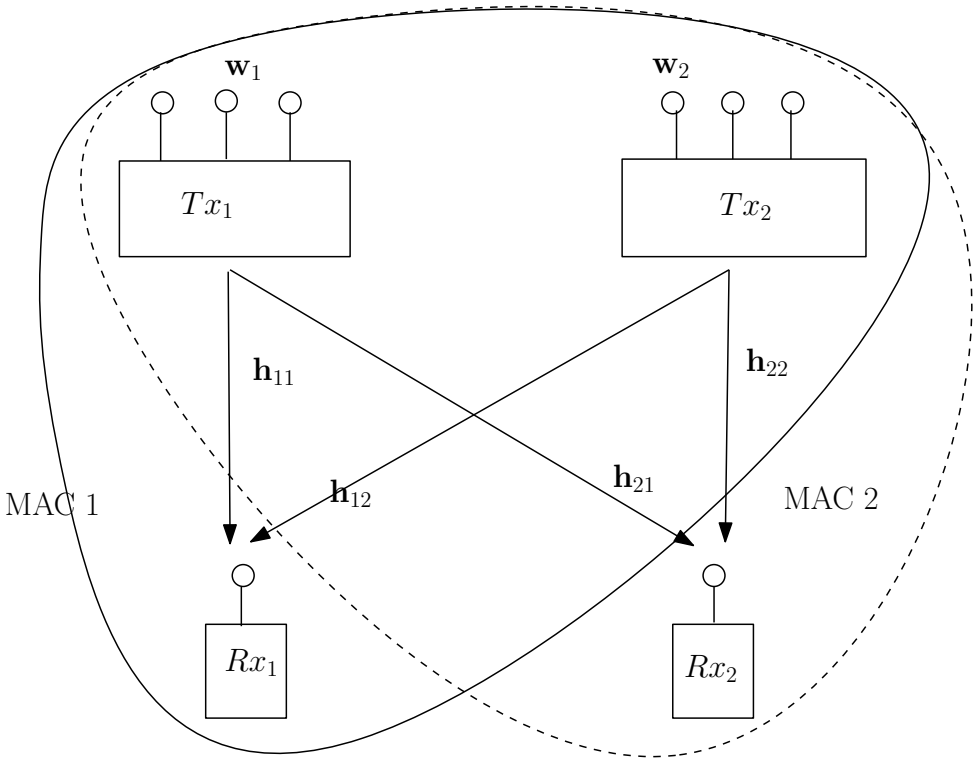

Figure 5.1: The 2 users MISO-IC where Txs are equipped with 3 antennas.

of Tx i by $\mathbf{S}_i$ and the channel from Tx i to Rx $\bar{i}$, where $i \in \{1,2\}, \bar{i} \neq i$, $\mathbf{h}_{\bar{i}i} \in \mathbb{C}^{N\times 1}$. Note that the channel gains are i.i.d complex Gaussian coefficients with zero mean and unit variance. The received signal at Rx i is therefore

$$y_i = \mathbf{h}_{ii}^H \mathbf{S}_i^{1/2} \mathbf{x}_i + \mathbf{h}_{i\bar{i}}^H \mathbf{S}_{\bar{i}}^{1/2} \mathbf{x}_{\bar{i}} + n_i. \tag{5.1}$$

The noise n_i is a complex Gaussian random variable with zero mean and unit variance. The symbol $\mathbf{x}_i$ is the transmit symbol at Tx i with unit power. Denote the set of the transmit covariance matrices that satisfy the power constraint $tr(\mathbf{S}_i) \leq P_{max}$ to be

$$\mathcal{S} = \left\{ \mathbf{S} \in \mathbb{C}^{N\times N} : \mathbf{S} \geq 0, tr(\mathbf{S}) \leq P_{max} \right\}, \; i = \{1,2\}. \tag{5.2}$$

5.2 Achievable Rate Region

We propose the following four decoding structures corresponding to the Rxs. actions: (N,N), (N,D), (D,N) and (D,D) [10], with "N" stands for treating interference as noise and "D" stands for decoding and removing interference. Thus, (D,N) means Rx 1 decodes and removes interference and Rx 2 treats interference as noise. In [10], these four decoding structures are proposed and its corresponding rate points are shown to be achievable in the SISO-IC. We extend the concept to the MISO-IC and define the following important

quantities:

$$\begin{aligned}
C_1(\mathbf{S}_1) &\triangleq \log_2(1+\mathbf{h}_{11}^H\mathbf{S}_1\mathbf{h}_{11}),\\
C_2(\mathbf{S}_2) &\triangleq \log_2(1+\mathbf{h}_{22}^H\mathbf{S}_2\mathbf{h}_{22}),\\
D_1(\mathbf{S}_1,\mathbf{S}_2) &\triangleq \log_2\left(1+\frac{\mathbf{h}_{11}^H\mathbf{S}_1\mathbf{h}_{11}}{\mathbf{h}_{12}^H\mathbf{S}_2\mathbf{h}_{12}+1}\right),\\
D_2(\mathbf{S}_1,\mathbf{S}_2) &\triangleq \log_2\left(1+\frac{\mathbf{h}_{22}^H\mathbf{S}_2\mathbf{h}_{22}}{\mathbf{h}_{21}^H\mathbf{S}_1\mathbf{h}_{21}+1}\right),\\
T_2(\mathbf{S}_1,\mathbf{S}_2) &\triangleq \log_2\left(1+\frac{\mathbf{h}_{12}^H\mathbf{S}_2\mathbf{h}_{12}}{\mathbf{h}_{11}^H\mathbf{S}_1\mathbf{h}_{11}+1}\right),\\
T_1(\mathbf{S}_1,\mathbf{S}_2) &\triangleq \log_2\left(1+\frac{\mathbf{h}_{21}^H\mathbf{S}_1\mathbf{h}_{21}}{\mathbf{h}_{22}^H\mathbf{S}_2\mathbf{h}_{22}+1}\right).
\end{aligned} \tag{5.3}$$

C_1 and C_2 are the *single user rates*, the largest rate user 1 and 2 can achieve without the influence of interference. D_1 and D_2 are the rates corresponding to decoding the desired signal while treating interference as thermal noise and T_1 and T_2 are the rate corresponding to decoding the interference while treating the desired signals as noise.

Consequently, if both receivers decode interference, user i must transmit at a rate that ensures interference decoding at Rx $\bar{i}$, thus we have the following:

$$\begin{aligned}
R_1 &\leq \min\left\{C_1(\mathbf{S}_1), T_1(\mathbf{S}_1,\mathbf{S}_2)\right\}\\
R_2 &\leq \min\left\{C_2(\mathbf{S}_2), T_2(\mathbf{S}_1,\mathbf{S}_2)\right\}.
\end{aligned} \tag{5.4}$$

Denote the rate region with interference decoding at both receivers by the Decode-Decode (DD) region:

$$\mathcal{R}^{dd} = \bigcup_{\mathbf{S}_1,\mathbf{S}_2\in\mathcal{S}} \left\{(R_1,R_2) \leq \left(\min\left\{C_1(\mathbf{S}_1), T_1(\mathbf{S}_1,\mathbf{S}_2)\right\}, \min\left\{C_2(\mathbf{S}_2), T_2(\mathbf{S}_1,\mathbf{S}_2)\right\}\right)\right\}. \tag{5.5}$$

Remark 1. *For each selected pair of transmit beamformers, a corresponding rate region which satisfies the inequalities* (5.4) *is obtained. The achievable rate region* $\mathcal{R}^{dd}$ *is defined as the union of all regions achieved by all possible transmit beamformers.*

On the other hand, if both Rxs choose to treat interference as noise, we obtain the NN region,

$$\mathcal{R}^{nn} = \bigcup_{\mathbf{S}_1,\mathbf{S}_2\in\mathcal{S}} \left\{(R_1,R_2) \leq \big(D_1(\mathbf{S}_1,\mathbf{S}_2), D_2(\mathbf{S}_1,\mathbf{S}_2)\big)\right\}. \tag{5.6}$$

If Rx 1 decodes interference but Rx 2 treats interference as noise, Tx 2 must transmit at a rate that ensures interference decoding at Rx 1. Thus, the DN region is obtained as,

$$\mathcal{R}^{dn} = \bigcup_{\mathbf{S}_1,\mathbf{S}_2\in\mathcal{S}} \left\{(R_1,R_2) \leq \left(C_1(\mathbf{S}_1), \min\left\{D_2(\mathbf{S}_1,\mathbf{S}_2), T_2(\mathbf{S}_1,\mathbf{S}_2)\right\}\right)\right\}. \tag{5.7}$$

Remark 2. $\mathcal{R}^{dn}(\mathbf{S}_1,\mathbf{S}_2)$ *is the rate region that the inequalities in* (5.7) *are satisfied for specific transmit covariance matrices* $(\mathbf{S}_1,\mathbf{S}_2)$*. It can be an empty region if the inequalities cannot be satisfied at the same time. This corresponds to the situation where the data rate of Tx 2 is too high for Rx 1 to decode.*

Similarly, we have for the ND region,

$$\mathcal{R}^{nd} = \bigcup_{\mathbf{S}_1,\mathbf{S}_2\in\mathcal{S}} \left\{ (R_1, R_2) \leq \left(\min\left\{ D_1(\mathbf{S}_1, \mathbf{S}_2), T_1(\mathbf{S}_1, \mathbf{S}_2) \right\}, C_2(\mathbf{S}_1) \right) \right\}. \tag{5.8}$$

Finally, one achievable rate region of the MISO-IC with interference decoding capability is therefore the union of the above regions:

$$\mathcal{R} = \mathcal{R}^{nn} \cup \mathcal{R}^{dd} \cup \mathcal{R}^{dn} \cup \mathcal{R}^{nd}. \tag{5.9}$$

We now turn our attention to the Pareto boundary of the rate region. To find the boundary achieving solutions, we proceed by identifying a set of smaller dimension than $\mathcal{S} \times \mathcal{S}$ but is guaranteed to contain the Pareto optimal solutions. Consequently, the candidate set offers a subtantial reduction of complexity compared with the exhaustive search over the full set $\mathcal{S} \times \mathcal{S}$.

Definition 8. *Denote the set of points on the Pareto boundary by $\mathcal{B}(\mathcal{R})$. If the rate pair $(r_1, r_2) \in \mathcal{R}$ is on the boundary, $(r_1, r_2) \in \mathcal{B}(\mathcal{R})$, then there does not exist a rate pair $(r_1', r_2') \in \mathcal{R}$ such that $(r_1', r_2') \geq (r_1, r_2)$, with one strict inequality. Using $\mathcal{R}$ in* (5.9)*,*

$$\mathcal{B}(\mathcal{R}) \subset \mathcal{B}(\mathcal{R}^{nn}) \cup \mathcal{B}(\mathcal{R}^{dd}) \cup \mathcal{B}(\mathcal{R}^{dn}) \cup \mathcal{B}(\mathcal{R}^{nd}) \tag{5.10}$$

Definition 9. *The transmit covariance matrices $\mathbf{S}_1, \mathbf{S}_2$ are Pareto optimal in the rate region $\mathcal{R}$ if*

$$\left(R_1(\mathbf{S}_1, \mathbf{S}_2), R_2(\mathbf{S}_1, \mathbf{S}_2) \right) \in \mathcal{B}(\mathcal{R}). \tag{5.11}$$

Definition 10. *The candidate set of $\mathcal{B}(\mathcal{R}^{xy})$, $x, y \in \{n, d\}$, is a set of transmit covariance matrices that contains the transmit covariance matrices that attain the Pareto boundary of $\mathcal{R}^{xy}$. If $(\mathbf{S}_1, \mathbf{S}_2)$ are Pareto optimal, then $(\mathbf{S}_1, \mathbf{S}_2) \in \Omega^{xy}$. Similarly, the candidate of $\mathcal{B}(\mathcal{R})$ is Ω which contains all pairs of $(\mathbf{S}_1, \mathbf{S}_2)$ which are Pareto optimal in the region $\mathcal{R}$.*

5.3 The Pareto optimal transmit covariance matrices

In this section, we study the transmit covariance matrices that attain the Pareto boundary and prove that they are rank one.

Theorem 11. *The Pareto boundaries of the NN region, the DN region and the DD region are attained by rank 1 matrices. Consequently, the Pareto boundary of MISO-IC-IDC, defined in* (5.10)*, is attained by rank one transmit covariance matrices, or transmit beamforming.*

Proof. Here, we provide a sketch of the proof. For details, please refer to Appendix 5.11.1. We first show that the boundaries of rate region $\mathcal{R}^{nd}$ and $\mathcal{R}^{dd}$ are attained by rank one matrices. By exchanging the roles of the transmitters, we obtain that $\mathcal{B}(\mathcal{R}^{dn})$ is attained by rank one matrices. From [42, 54], it is shown that the boundary in the NN region is attained by rank one matrices. Hence, the boundaries of all decoding structures are attained by rank one transmit covariance matrices. Since the Pareto boundary of the proposed achievable rate region in the MISO-IC-IDC, defined in (5.10), is a subset of the union of the above boundaries, we conclude that this Pareto boundary is attained by rank one transmit covariance matrices, or transmit beamforming. □

From Theorem 11, we have established that the Pareto boundary is attained by transmit beamforming vectors. To facilitate the following discussions, we define the transmit beamforming vectors $\mathbf{w}_i$ and transmit power P_i, for $i = 1, 2$,

$$\mathbf{S}_i = \mathbf{w}_i \mathbf{w}_i^H P_i \tag{5.12}$$

with $\|\mathbf{w}_i\|^2 = 1$. As an abuse of notation, we write $\mathcal{S}$ as the set of all possible beamforming vectors,

$$\mathbf{w}_i \in \mathcal{S}, \qquad \mathcal{S} = \left\{ \mathbf{w} \in \mathbb{C}^{N\times 1} : \|\mathbf{w}\| = 1 \right\}. \tag{5.13}$$

Consequently, we redefine the candidate sets in terms of transmit power allocations and beamforming vectors. The candidate set of $\mathcal{B}(\mathcal{R}^{xy}), x, y \in \{n, d\}$ contains the Pareto optimal beamforming vectors and transmit power allocations.

$$\Omega^{xy} \supset \left\{ (\mathbf{w}_1, \mathbf{w}_2, P_1, P_2) : \big(R_1(\mathbf{w}_1, \mathbf{w}_2, P_1, P_2), R_2(\mathbf{w}_1, \mathbf{w}_2, P_1, P_2)\big) \in \mathcal{B}(\mathcal{R}^{xy}) \right\} \tag{5.14}$$

and the candidate set of $\mathcal{B}(\mathcal{R})$ is

$$\Omega \supset \left\{ (\mathbf{w}_1, \mathbf{w}_2, P_1, P_2) : \big(R_1(\mathbf{w}_1, \mathbf{w}_2, P_1, P_2), R_2(\mathbf{w}_1, \mathbf{w}_2, P_1, P_2)\big) \in \mathcal{B}(\mathcal{R}) \right\}. \tag{5.15}$$

In the following sections, we study the Pareto boundary in terms of power allocation and transmit beamforming vectors in different decoding structures namely $\mathbf{R}^{nd}$ and $\mathbf{R}^{dd}$. $\mathbf{R}^{nn}$ is the case of MISO-IC-SUD and is well studied in [31]. $\mathbf{R}^{dn}$ is symmetric to $\mathbf{R}^{nd}$ and is therefore omitted here. Then as a special case, we discuss the characterization of the maximum sum rate point in each decoding structures.

5.4 The power gain region

The power gain region was first proposed in [42] as a powerful tool to illustrate the dependency between the power gains and the Pareto boundary on the K-user MISO-IC-SUD. The power gain tuple at one receiver includes the received power from the desired signal and the received power from the interference signal(s). In a two-user MISO-IC, we can illustrate the power gain region as a two-dimensional plot, as shown in Fig. 5.2. Mathematically, the power gain region of user i for the two-user MISO-IC is defined as:

$$\Phi_i = \left\{ \left(|\mathbf{h}_{ii}^H \mathbf{w}_i|^2 P_i, |\mathbf{h}_{ji}^H \mathbf{w}_i|^2 P_i \right) : \mathbf{w}_i \in \mathcal{S}, 0 \le P_i \le P_{max} \right\} \tag{5.16}$$

where the desired channel power of user i is $|\mathbf{h}_{ii}^H \mathbf{w}_i|^2 P_i$ and the interference channel power of user i is $|\mathbf{h}_{ji}^H \mathbf{w}_i|^2 P_i$.

The importance and relevance of the power gain region can be summarized in the following.

The boundary of power gain region and the Pareto boundary: The received power region is a convex and compact region with respect to the received power values. The Pareto boundary of the MISO-IC-SUD with linear pre-coding, the NN region here, is shown to be attained by the received power values *on the boundary of the received power region* [31].

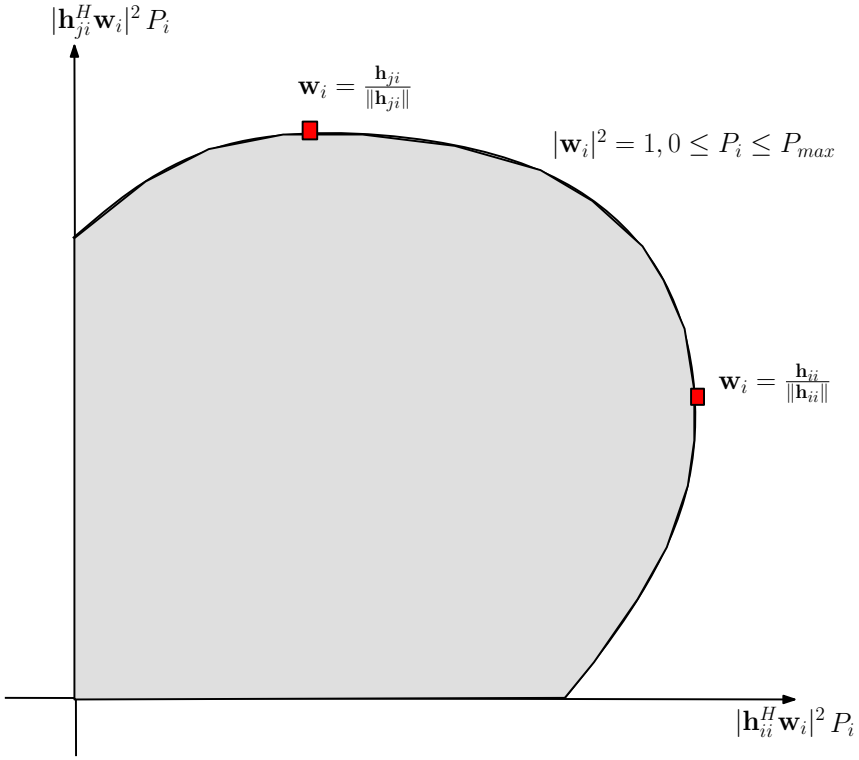

Figure 5.2: The power gain region for Tx i.

Monotonicity of rates: The rate metrics defined in (5.3) are either *monotonically increasing or decreasing* with the channel powers. The optimization of such rates can be simplified by first computing the optimized channel powers and then the corresponding beamforming vectors that achieve such channel powers.

Now we define the power gain region achieved by beamforming vectors inside the Pareto boundary candidate set, Ω,

$$\Phi(\Omega) = \left\{ \left(|\mathbf{h}_{11}^H \mathbf{w}_1|^2 P_1, |\mathbf{h}_{21}^H \mathbf{w}_1|^2 P_1, |\mathbf{h}_{22}^H \mathbf{w}_2|^2 P_2, |\mathbf{h}_{12}^H \mathbf{w}_2|^2 P_2 \right) : (\mathbf{w}_1, \mathbf{w}_2, P_1, P_2) \in \Omega \right\}. \tag{5.17}$$

Immediately, we have the following relations: the Pareto boundary candidate set achieves a power gain region which is a subset of the Cartesian product of the power gain regions for Rx 1 and 2, Φ_1 and Φ_2,

$$\Phi(\Omega) \subset \Phi_1 \times \Phi_2. \tag{5.18}$$

The beamforming vectors and power allocations in $\Phi_1 \times \Phi_2$ contribute to the whole achievable rate region whereas the tuples in $\Phi(\Omega)$ only attain the Pareto boundary. This means that if we know $\Phi(\Omega)$, we can achieve the Pareto boundary without searching over that potential candidates in the remaining space in $\Phi_1 \times \Phi_2$. This reduces the search space from $\Phi_1 \times \Phi_2$ significantly.

In the following sections, we compute $\Omega^{nn}, \Omega^{dn}, \Omega^{nd}, \Omega^{dd}$ which are the candidate sets of the Pareto boundary of the corresponding regions: NN, DN, ND and DD. The candidate

$$\mathcal{W}_i = \left\{ \mathbf{w}_i : \mathbf{w}_i = \sqrt{\lambda_i}\frac{\Pi_{ji}\mathbf{h}_{ii}}{\|\Pi_{ji}\mathbf{h}_{ii}\|} + \sqrt{1-\lambda_i}\frac{\Pi_{ji}^{\perp}\mathbf{h}_{ii}}{\|\Pi_{ji}^{\perp}\mathbf{h}_{ii}\|} \; ; \; 0 \le \lambda_i \le 1 \right\}, \quad i,j = 1,2, i \ne j. \tag{5.21}$$

set of the overall Pareto boundary, Ω, is the union of the candidate sets mentioned above:

$$\Omega = \bigcup_{x,y \in \{n,d\}} \Omega^{xy}. \tag{5.19}$$

5.5 The Pareto boundary characterization

5.5.1 Pareto boundary characterization in the ND region

With decoding structure $\mathbf{R}^{nd}$, Rx 1 treats interference as noise and Rx 2 decodes and subtracts the interference signal from the received signal before decoding the desired signal.

Theorem 12. *The Pareto boundary $\mathcal{B}(\mathcal{R}^{nd})$ is attained by candidate set Ω^{nd}*

$$\Omega^{nd} = \{\mathcal{W}_1, \mathcal{W}_2, P_1 = P_{max}, 0 \le P_2 \le P_{max}\} \tag{5.20}$$

where $\mathcal{W}_1, \mathcal{W}_2$ defined in (5.21)*, are sets of beamforming vectors composed of linear combinations of two channel vectors; to attain the Pareto boundary, Tx 1 transmits with full power P_{max} whereas Tx 2 transmits with less than full power $P_2 \le P_{max}$.*

Proof. See Appendix 5.11.2. □

In the ND region, Rx 1 treats interference as noise and Rx 2 decodes interference. As described by Thm. 12, the Pareto optimal transmit power for Tx 1 is to transmit at full power P_{max} and less than full power for Tx 2. The interpretation is that Tx 1's transmit power does not affect the rate performance of Rx 2 as the interference from Tx 1 is decoded and removed. On the other hand, Tx 2 is not advised to transmit at full power because its increase of power will increase the interference power at Rx 1 and hence reduce the achievable rate of Rx 1.

The Pareto optimal transmit beamforming vectors are parameterized in the sets $\mathcal{W}_1, \mathcal{W}_2$ as positive linear combinations of two orthogonal vectors. These two vectors are the desired channel projection onto the span and the null space of the interference channel. As shown in Fig. 5.3, the vectors in $\mathcal{W}_1$ and $\mathcal{W}_2$ are represented by blue regions. The blue regions cover from the point of zero interference power (Point A in Fig. 5.3) to the point of maximum desired channel power (Point B) and the point of maximum interference power (Point C). Moving from point A to B and C on the Pareto boundary in Fig. 5.3, the interference power increases monotonically. On the left figure of Figure 5.3, we show the received power region of Tx 1, the channel powers between A and B correspond to a strong desired channel power of Tx 1 and a relatively small interference channel power from Tx 1 to Rx 2. These points may attain the Pareto boundary if the desired channel power of Tx 2 is weak. On the other hand, if Tx 2's desire channel power is large, the interference power from Tx 1 to Rx 2 must be increased to increase to interference rate T_1 which limits rate rate of R_1 as $R_1 = \min(T_1, D_1)$. This is a novel concept comparing

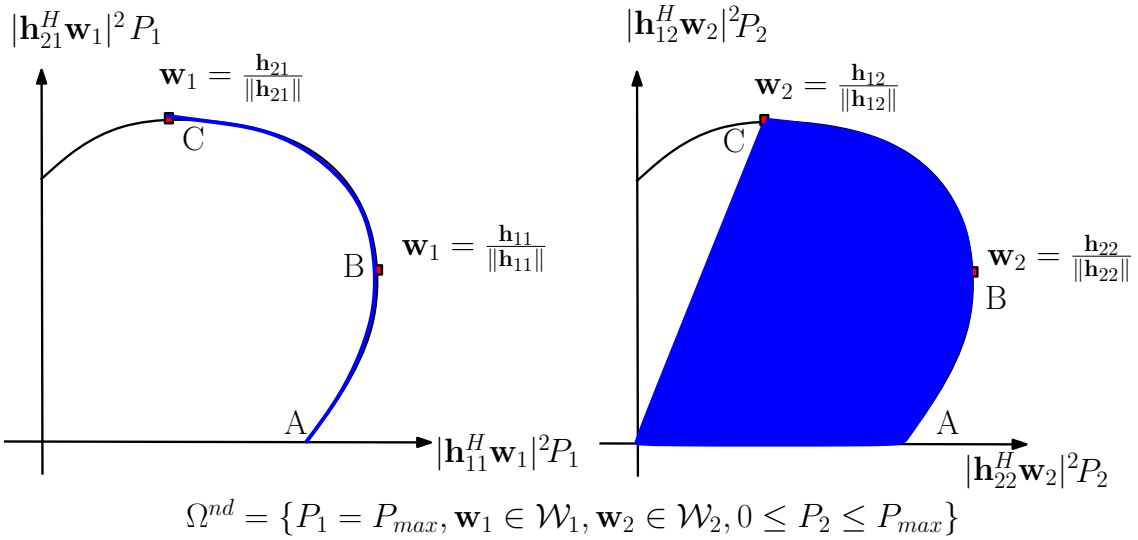

$$\Omega^{nd} = \{P_1 = P_{max}, \mathbf{w}_1 \in \mathcal{W}_1, \mathbf{w}_2 \in \mathcal{W}_2, 0 \leq P_2 \leq P_{max}\}$$

Figure 5.3: The graphical illustration of the candidate set Ω^{nd} as the shaded area which is a subset of the received power regions Φ_i.

to the conventional single user decoding interference channel, the increase in interference power here is beneficial as it facilitates interference decoding and removal.

In the next section, we investigate the Pareto boundary attaining beamforming vectors in the DD region.

5.5.2 The Pareto boundary characterization in the DD region

With decoding structure $\mathbf{R}^{dd}$, both Rx's decode interference. The Pareto boundary attaining solutions are:

Theorem 13. *The Pareto boundary $\mathcal{B}(\mathcal{R}^{dd})$ is attained by candidate set*

$$\Omega^{dd} = \{\mathbf{w}_1 \in \mathcal{V}_1, \mathbf{w}_2 \in \mathcal{V}_2, 0 \leq P_1, P_2 \leq P_{max}\}, \tag{5.22}$$

with Pareto boundary attaining beamforming vectors composed of two orthogonal channel vectors, specifically for $i = 1, 2$,

$$\mathcal{V}_i = \left\{\mathbf{w} \in \mathcal{S} : \mathbf{w} = \sqrt{\lambda_i}\frac{\Pi_{ii}\mathbf{h}_{ji}}{\|\Pi_{ii}\mathbf{h}_{ji}\|} + \sqrt{1-\lambda_i}\frac{\Pi_{ii}^{\perp}\mathbf{h}_{ji}}{\|\Pi_{ii}^{\perp}\mathbf{h}_{ji}\|}, 0 \leq \lambda_i \leq 1\right\}, \tag{5.23}$$

and both Txs transmit at less than full power.

Proof. See Appendix 5.11.3. □

Remark 3. *Note that $\mathcal{W}_i$ in Thm. 12 and $\mathcal{V}_i$ defined here are different candidate sets. In particular, $\mathcal{W}_i$ is a set of vectors that are the positive linear combinations of $\Pi_{ji}\mathbf{h}_{ii}$ and $\Pi_{ji}^{\perp}\mathbf{h}_{ii}$ whereas $\mathcal{V}_i$ is a set of vectors that are the positive linear combinations of $\Pi_{ii}\mathbf{h}_{ji}$ and $\Pi_{ii}^{\perp}\mathbf{h}_{ji}$. This difference is shown graphically in Fig. 5.3 and 5.4.*

In the DD region, both Tx 1 and 2 decode interference and their choice of actions are symmetric. As described by Thm. 13, the Pareto optimal transmit power for Tx 1 and 2

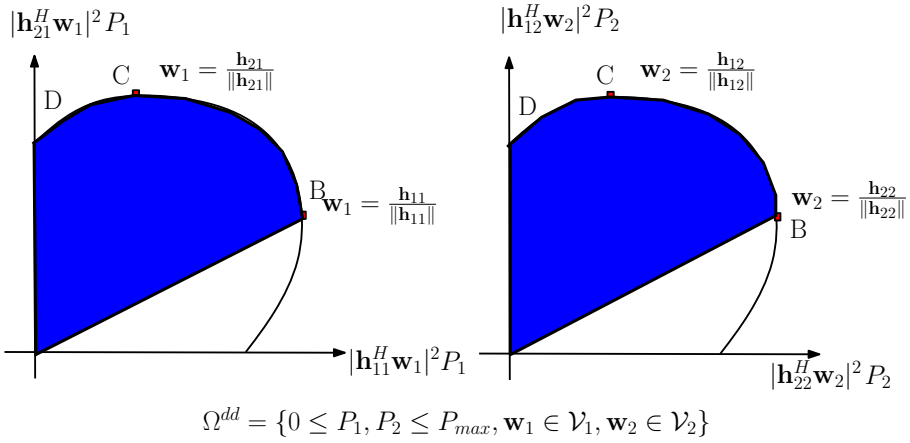

$$\Omega^{dd} = \{0 \leq P_1, P_2 \leq P_{max}, \mathbf{w}_1 \in \mathcal{V}_1, \mathbf{w}_2 \in \mathcal{V}_2\}$$

Figure 5.4: The graphical illustration of candidate set Ω^{dd} as the shaded area which is a subset of the received power regions Φ_i.

are to transmit at less than full power. The Pareto optimal transmit beamforming vectors are parameterized in the sets $\mathcal{V}_1, \mathcal{V}_2$ as positive linear combinations of two orthogonal vectors. These two vectors are the interference channel projection onto the span and the null space of the desired channel. As shown in Fig. 5.4, the vectors in $\mathcal{V}_1$ and $\mathcal{V}_2$ are represented by blue regions. The blue regions cover from the point where the point of maximum desired channel power (Point B) to the point of maximum interference power (Point C) and the point of zero desired channel power (Point D).

Notice that the points where the interference channel powers are zero is not Pareto optimal. It is because minimizing the interference power in the DD region makes decoding interference more difficult. This choice of action is not Pareto optimal. From the received power region representation in Fig. 5.4, we can see that the interference channel power should be maximized despite the values of the direct channel gain. It means that for each achievable desired channel power value, the interference channel power should be increased for easy interference decoding and removal.

5.5.3 The Pareto boundary characterization

From Thm. 12 and 13, we have presented the Pareto boundary characterization in ND and DD region. We can easily obtain the candidate set Ω^{dn} by reversing the role of Tx 1 and 2 from Ω^{nd} in Thm. 12. Also, the candidate set Ω^{nn} is shown to be the following [31]:

$$\Omega^{nn} = \{\mathcal{W}_1, \mathcal{W}_2, P_1 = P_2 = P_{max}\} \tag{5.24}$$

where $\mathcal{W}_1, \mathcal{W}_2$ are defined in Thm. 12.

By definition in (10) , the candidate set of the Pareto boundary $\mathcal{B}(\mathcal{R})$ is the union of the candidate sets in each decoding region. Hence, we have characterized the Pareto boundary $\mathcal{B}(\mathcal{R})$. In the candidate sets of the Pareto boundary, the beamforming vectors are parameterized with positive real scalars $0 \leq \lambda_1, \lambda_2 \leq 1$. By varying λ_1, λ_2 from zero to one and P_2 from zero to P_{max}, we obtain all beamforming vectors that may attain the the boundary in each decoding region and in turn the overall Pareto boundary. Intuitively, it means that the boundary attaining beamforming vectors in each decoding region exist

only in a two-dimensional subspace, spanned by the direct channel and the interference channel, in a N-dimensional signal space.

As a direct application of the Pareto boundary characterization, we characterize the maximum sum rate point in the following section. Since the maximum sum rate point is always on the Pareto boundary, the candidate set of the maximum sum rate point is therefore a subset of the candidate set derived above. We reduce the size of the candidate set by eliminating beamforming vectors in the candidate set that achieve a smaller sum rate than other vectors in the set.

5.6 The maximum sum rate point characterization

In this section, we characterize the candidate sets of the maximum sum rate point by first illustrating that Txs. should always transmit with full power, in Section 5.6.1. Then, we study the candidates sets of the boundaries of ND and DD regions by eliminating vectors that attain a smaller sum rate than other vectors in the candidate sets and obtain the candidate sets of maximum sum rate point in $\mathcal{B}(\mathcal{R}^{nd})$ and $\mathcal{B}(\mathcal{R}^{dd})$ respectively, in Section 5.6.2 and 5.6.3.

5.6.1 Full power transmission

We observe that the maximum sum rate point is attained by maximum transmit power at each transmitter. To see this, we combine the power constraints and beamformer norm constraints:

$$\|\mathbf{w}_i\|^2 \leq P_i. \tag{5.25}$$

Assume that the sum rate optimal beamformer is not transmitting at maximum power: $\|\mathbf{w}_i\|^2 = p < P_i$. We can choose a beamformer $\mathbf{w}_i' = \mathbf{w}_i + \epsilon e^{j\phi}\Pi_{ji}^{\perp}\mathbf{h}_{ii}$ where ϵ is chosen such that $\|\mathbf{w}_i'\|^2 = P_i$ and $\phi = \arg(\mathbf{h}_{ii}^H\mathbf{w}_i)$. Notice that $|\mathbf{h}_{ii}^H\mathbf{w}_i'|^2 \geq |\mathbf{h}_{ii}^H\mathbf{w}_i|^2$ and $|\mathbf{h}_{ji}^H\mathbf{w}_i'|^2 = |\mathbf{h}_{ji}^H\mathbf{w}_i|^2$. Or, we can choose $\mathbf{w}_i'' = \mathbf{w}_i + \epsilon' e^{j\phi'}\Pi_{ii}^{\perp}\mathbf{h}_{ji}$ with $\phi' = \arg(\mathbf{h}_{ji}^H\mathbf{w}_i)$ to increase $|\mathbf{h}_{ji}^H\mathbf{w}_i|^2$ and keep $|\mathbf{h}_{ii}^H\mathbf{w}_i|^2$ constant. Thus, it contradicts that $\mathbf{w}_i$ is on the Pareto boundary. From now on, we set $P_i = P_{max}, i = 1, 2$. Note that the argument above is limited to non-parallel channels, for parallel channels (e.g. $\mathbf{h}_{ji}^H\mathbf{h}_{ii} = 0$), it reduces to SISO-IC where the maximum sum rate point is attained by one Tx transmitting with full power whereas the other Txs. transmit at less than full power [6].

In the following sections, we characterize the candidate sets that attain the maximum sum rate point. Note that, the candidate sets attaining the maximum sum rate point is a strict subset of those attaining the Pareto boundary. The sum rate metric does not distinguish between Tx 1 and 2's rate and therefore we can identify a much smaller candidate set as illustrated in the following sections. This is particularly useful for system optimization which does not put emphasis on user fairness.

Note that the computation of the global optimal solution

$$\boldsymbol{\omega}^* = \arg\max_{\mathbf{w}_1,\mathbf{w}_2\in\mathcal{S}} \bar{R}^{nd}(\mathbf{w}_1, \mathbf{w}_2) \tag{5.26}$$

is in general NP-hard [39], even though there exist channels for which the solution is easily obtained (e.g. orthogonal channels). Here, we would like to reduce the search space and characterize the solutions set.

5.6.2 The maximum sum rate point characterization in the ND region

Theorem 14. *The candidate set of maximum sum rate $\bar{R}^{nd}$ denoted as $\tilde{\Omega}^{nd}$, hence $\boldsymbol{\omega}^* \subset \tilde{\Omega}^{nd} \subset \Omega^{nd}$, is given by*

$$\tilde{\Omega}^{nd} = \left\{\tilde{\mathcal{W}}_1, \tilde{\mathcal{W}}_2, P_{max}, P_{max}\right\} \tag{5.27}$$

where Ω^{nd} is the candidate set of Pareto boundary $\mathcal{B}(\mathcal{R}^{nd})$ in (5.20). In particular, $\tilde{\mathcal{W}}_1$ is the following set with cardinality three:

$$\tilde{\mathcal{W}}_1 = \left\{\frac{\mathbf{h}_{11}}{||\mathbf{h}_{11}||}, \frac{\mathbf{h}_{21}}{||\mathbf{h}_{21}||}, \mathbf{w}_1(\lambda_1^{(b)})\right\} \tag{5.28}$$

with $\lambda_1^{(b)} = \frac{c_1||\Pi_{21}^{\perp}\mathbf{h}_{11}||^2}{c_2||\mathbf{h}_{21}||^2 - 2\sqrt{c_1c_2}|\mathbf{h}_{21}^H\mathbf{h}_{11}| + c_1||\mathbf{h}_{11}||^2}$. The candidate set $\tilde{\mathcal{W}}_2$ is a set of beamforming vectors characterized by a parameter λ_2 in a smaller range than the range in $\mathcal{W}_2$:

$$\tilde{\mathcal{W}}_2 = \left\{\mathbf{w}_2 \in \mathcal{S} : \mathbf{w}_2 = \sqrt{\lambda_2}\frac{\Pi_{12}\mathbf{h}_{22}}{\|\Pi_{12}\mathbf{h}_{22}\|} + \sqrt{1-\lambda_2}\frac{\Pi_{12}^{\perp}\mathbf{h}_{22}}{\|\Pi_{12}^{\perp}\mathbf{h}_{22}\|}\ ;\ \lambda_2^{(b)} \le \lambda_2 \le \lambda_2^{\mathrm{MRT}}\right\} \tag{5.29}$$

where $\lambda_2^{\mathrm{MRT}} = \frac{|\mathbf{h}_{12}^H\mathbf{h}_{22}|}{||\mathbf{h}_{12}||||\mathbf{h}_{22}||}$ is a parameter that gives the beamforming solution towards channel $\mathbf{h}_{22}$ and $\mathbf{w}_2(\lambda_2^{(b)}) = \frac{\tilde{b}}{\sqrt{\tilde{a}+\tilde{b}}}\mathbf{v}_a + \frac{e^{j\phi}\tilde{a}}{\sqrt{\tilde{a}+\tilde{b}}}\mathbf{v}_b$ for some eigenvectors $\mathbf{v}_a, \mathbf{v}_b$ and positive scalars $\tilde{a}, \tilde{b}$. The vectors $\mathbf{v}_a, \mathbf{v}_b$ are the most and least dominant eigenvectors of the matrix $\mathbf{S} = \mathbf{h}_{22}\mathbf{h}_{22}^H - \frac{g_{21}}{g_{11}}\mathbf{h}_{12}\mathbf{h}_{12}^H$.

Proof. See Appendix 5.11.4. □

Remark 4. *Note that for some channel realizations and chosen $\mathbf{w}_2$, $\mathbf{w}_1(\lambda_1^{(b)})$ may be equal to the maximum ratio transmission solutions $\frac{\mathbf{h}_{11}}{\|\mathbf{h}_{11}\|}$ or $\frac{\mathbf{h}_{21}}{\|\mathbf{h}_{21}\|}$. But we distinguish between them in the candidate sets to illustrate that for most channel realizations and $\mathbf{w}_2$, $\mathbf{w}_1(\lambda_1^{(b)}) \notin \left\{\frac{\mathbf{h}_{11}}{\|\mathbf{h}_{11}\|}, \frac{\mathbf{h}_{21}}{\|\mathbf{h}_{21}\|}\right\}$.*

It is interesting to see that the sum rate optimal beamforming vector of Tx 1 is either the beamforming vector towards the desired channel or the beamforming vector towards the interference channel or a beamforming vector that balances the interference decoding rate T_i and the treating interference as noise rate D_i in a weighted manner with weights c_1, c_2 which depend on the choice of the beamforming vector at Tx 2.

Comparing the candidate set of the Pareto boundary to the candidate set of the maximum sum rate point of the ND region, namely $\tilde{\Omega}^{nd}$ and Ω^{nd}, we observe the following:

- For each Tx i, the candidate set $\tilde{\Omega}^{nd}$ consists of only *three* closed-form beamforming vectors whereas Ω^{nd} consists of a set of beamforming vectors characterized by a real-valued parameter spanned between zero and one, as shown in Fig. 5.5.

- An interesting question rises: what are the conditions of each of these potential sum rate optimal solutions being sum rate optimal? We give the discussion in Section 5.7.

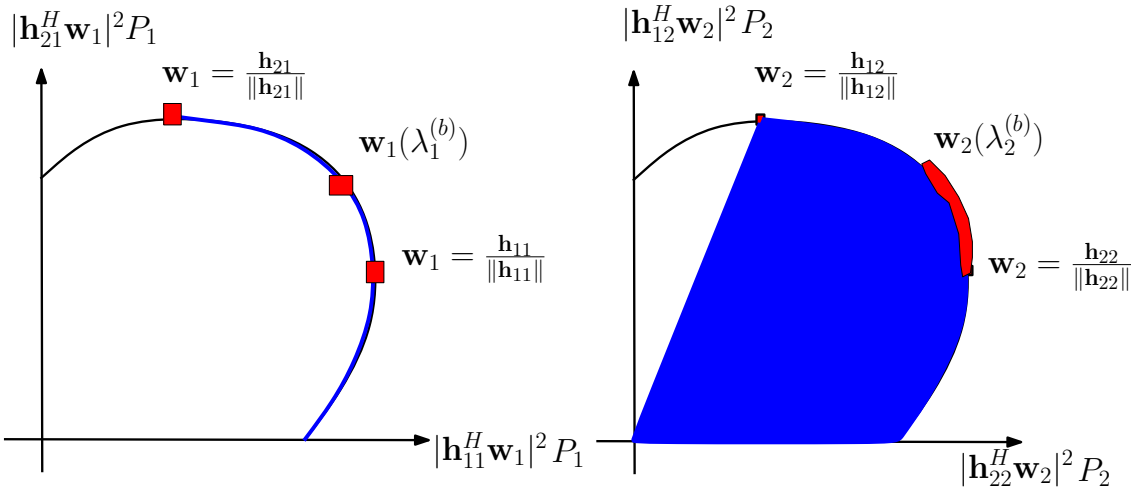

$$\Omega^{nd} = \{P_1 = P_{max}, \mathbf{w}_1 \in \mathcal{W}_1, \mathbf{w}_2 \in \mathcal{W}_2, 0 \leq P_2 \leq P_{max}\}$$
$$\tilde{\Omega}^{nd} = \left\{\mathcal{W}_1^{nd}, \mathcal{W}_2^{nd}\right\}$$

Figure 5.5: The illustration of the candidate set of the maximum sum rate point of ND region in red and the candidate set of the Pareto boundary $\mathcal{B}(\mathcal{R}^{nd})$ in blue. The cardinality of the candidate set for $\mathbf{w}_1$ of the maximum sum rate point is only three, conditioned on $\mathbf{w}_2$.

5.6.3 The maximum sum rate point characterization in the DD region

In this section, we compute the candidate set that attains the maximum sum rate point of the DD region.

Theorem 15. *The candidate set of the maximum sum rate in* $\mathbf{R}^{dd}$ *is*

$$\tilde{\Omega}^{dd} = \left\{\mathcal{V}_1^{dd}, \mathcal{V}_2^{dd}, P_{max}, P_{max}\right\} \tag{5.30}$$

where for user $i = 1, 2$*, the sum rate optimal beamforming vectors are either a linear combination of two orthogonal vectors or maximizing the desired channel power or a specific vector:*

$$\mathcal{V}_i^{dd} = \left\{\tilde{\mathcal{V}}_i, \frac{\mathbf{h}_{ii}}{\|\mathbf{h}_{ii}\|}, \mathbf{w}_i(\lambda_i^A)\right\} \tag{5.31}$$

$$\tilde{\mathcal{V}}_i = \left\{\mathbf{w}_i : \sqrt{\lambda_i}\frac{\Pi_{ii}\mathbf{h}_{ji}}{\|\Pi_{ii}\mathbf{h}_{ji}\|} + \sqrt{1-\lambda_i}\frac{\Pi_{ii}^{\perp}\mathbf{h}_{ji}}{\|\Pi_{ii}^{\perp}\mathbf{h}_{ji}\|}, \lambda_i^A \leq \lambda_i \leq \lambda_i^{\text{MRT}}\right\} \tag{5.32}$$

where $\lambda_i^{\text{MRT}} = \frac{|\mathbf{h}_{ii}^H\mathbf{h}_{ji}|^2}{\|\mathbf{h}_{ii}\|^2\|\mathbf{h}_{ji}\|^2}$ *and* $\lambda_i^A = \frac{\|\Pi_{ii}^{\perp}\mathbf{h}_{ji}\|}{\|\mathbf{h}_{ji}\|^2+(1+g_{jj})\|\mathbf{h}_{ii}\|^2-2|\mathbf{h}_{ii}^H\mathbf{h}_{ji}|\sqrt{1+g_{jj}}}$.

Proof. see Appendix 5.11.5. □

Remark 5. *Note that* $\mathbf{w}_i(\lambda_i^A)$ *may not be a element of* $\mathcal{V}_i$ *because* λ_i^A *may not be smaller than* λ_i^{mrt} *and in this case* $\tilde{\mathcal{V}}_i$ *is empty. The vector* $\mathbf{w}_i(\lambda_i^A)$ *is a beamforming vector that balance the interference decoding rate* T_i *and the treating interference as noise rate* D_i *in a weighted manner. See Appendix 5.11.5 for more details.*

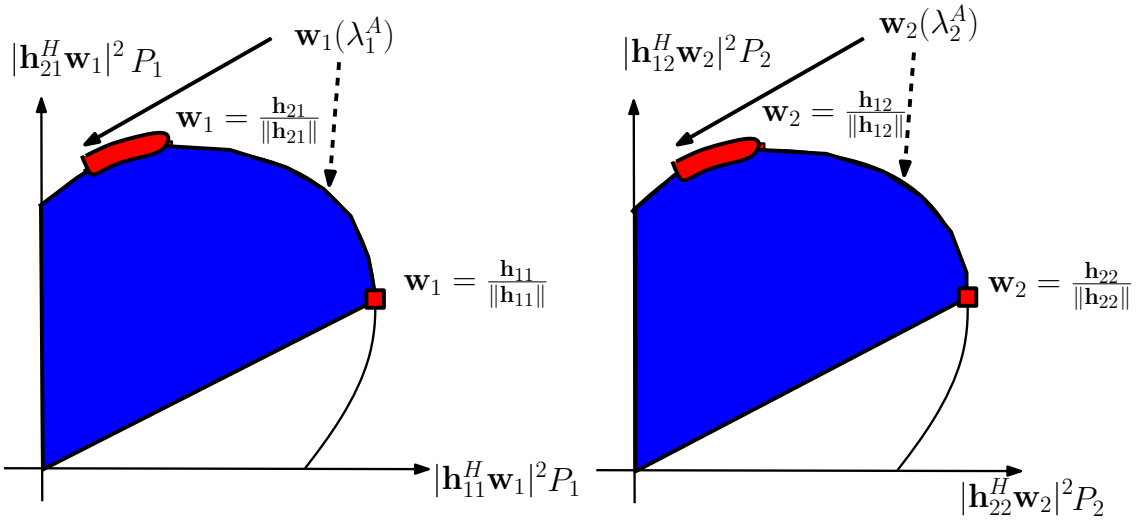

$$\Omega^{dd} = \{0 \leq P_1, P_2 \leq P_{max}, \mathbf{w}_1 \in \mathcal{V}_1, \mathbf{w}_2 \in \mathcal{V}_2\}$$
$$\tilde{\Omega}^{dd} = \{\mathcal{V}_1, \mathcal{V}_2\}$$

Figure 5.6: The illustration of the candidate set of the maximum sum rate point of the DD region, in red, and the candidate set of the Pareto boundary $\mathcal{B}(\mathcal{R}^{dd})$ in blue. If $\lambda_i^A \leq \lambda_i^{\text{MRT}}$, then the candidate set consists of the set $\tilde{V}_i$ and $\mathbf{w}_i = \frac{\mathbf{h}_{ii}}{\|\mathbf{h}_{ii}\|}$ as illstrated by the red area in the figure. When $\lambda_i^A > \lambda_i^{\text{MRT}}$, the candidate set becomes 3 beamforming vectors: $\frac{\mathbf{h}_{ii}}{\|\mathbf{h}_{ii}\|}, \mathbf{w}(\lambda_i^A)$ and $\mathbf{w}_i = \frac{\mathbf{h}_{ji}}{\|\mathbf{h}_{ji}\|}$.

In Fig. 5.6, we illustrate the reduction of the candidate set of the maximum sum rate point of the DD region, in red, comparing to the candidate set of the Pareto boundary of the DD region, in blue. As shown in Fig. 5.6, the beamforming vectors in $\tilde{\mathcal{V}}$ achieve channel powers that are in the direction of minimizing the direct channel power while maximizing the interference channel power.

To summarize, we obtain the candidate set of the maximum sum rate point in the ND and DD region, in Thm. 14 and Thm. 15 respectively. We can exchange the role of Tx 1 and 2 in Thm. 14 to obtain the candidate set of maximum sum rate point in the DN region, $\tilde{\Omega}^{dn}$. For the NN region, the candidate set of the maximum sum rate point is identical to the candidate set of the Pareto boudary, Ω^{nn}. Thus, we can have candidate set of the maximum sum rate point of MISO-IC-IDC as $\tilde{\Omega}$:

$$\tilde{\Omega} = \tilde{\Omega}^{nd} \bigcup \tilde{\Omega}^{dn} \bigcup \tilde{\Omega}^{dd} \bigcup \Omega^{nn}. \tag{5.33}$$

In the next section, we apply the results obtained above: from the candidate set of the maximum sum rate point in different decoding structures, we identify the conditions in which the MRT strategies are sum rate optimal. Such strategies are attractive because of their simplicity and the MRT optimality conditions answer the following two interesting questions: *When is selfishness sum rate optimal? When is interference amplification sum rate optimal?*

5.7 MRT optimality conditions

In this section, we investigate the conditions in which the MRT strategies at both Tx 1 and 2 are sum rate optimal. For clarification, MRT strategies can mean two strategies, one to beamform to the direct channel $\mathbf{h}_{ii}$ and the other to beamform to the interference channel $\mathbf{h}_{ji}$. We characterize the MRT optimality conditions in terms of the *separation* between the desired channel and the interference channel, θ_i:

$$\theta_i = \cos^{-1}\left(\frac{|\mathbf{h}_{ji}^H \mathbf{h}_{ii}|}{\|\mathbf{h}_{ji}\|\|\mathbf{h}_{ii}\|}\right). \tag{5.34}$$

Theorem 16. *The MRT optimality conditions for decoding structure $\mathbf{R}^{nd}$ are:*

- $\left(\frac{\mathbf{h}_{11}}{\|\mathbf{h}_{11}\|}, \frac{\mathbf{h}_{22}}{\|\mathbf{h}_{22}\|}\right)$ *is optimal if and only if*

$$\frac{c_1\|\Pi_{21}^{\perp}\mathbf{h}_{11}\|^2}{c_2\|\mathbf{h}_{21}\|^2 - 2\sqrt{c_1c_2}|\mathbf{h}_{21}^H\mathbf{h}_{11}| + c_1\|\mathbf{h}_{11}\|^2} < \cos^2(\theta_1) \leq \frac{(1+\|\mathbf{h}_{22}\|^2 P_{max})\|\mathbf{h}_{11}\|^2}{(1+\|\mathbf{h}_{12}\|^2\cos^2(\theta_2)P_{max})\|\mathbf{h}_{21}\|^2} \tag{5.35}$$

- $\left(\frac{\mathbf{h}_{21}}{\|\mathbf{h}_{21}\|}, \frac{\mathbf{h}_{22}}{\|\mathbf{h}_{22}\|}\right)$ *is optimal if and only if*

$$\|\mathbf{h}_{21}\|^2 \leq (1+\|\mathbf{h}_{22}\|^2 P_{max})\frac{\|\Pi_{21}\mathbf{h}_{11}\|^2}{1+\|\mathbf{h}_{12}\|^2\cos^2(\theta_2)P_{max}} \tag{5.36}$$

where $c_1 = \frac{P_{max}}{\|\mathbf{h}_{12}\|^2\cos^2(\theta_2)P_{max}+1}$ *and* $c_2 = \frac{P_{max}}{\|\mathbf{h}_{22}\|^2 P_{max}+1}$.

Proof. See Appendix 5.11.6. □

Now, we provide the MRT optimality conditions for $\mathbf{R}^{dd}$.

Theorem 17. *The MRT optimality conditions for $\mathbf{R}^{dd}$ are:*

$$\mathbf{w}_i = \frac{\mathbf{h}_{ji}}{\|\mathbf{h}_{ji}\|} \text{ is optimal if } \quad \frac{g_{ij}}{g_{jj}} - 1 \leq \|\mathbf{h}_{ii}\|^2\cos^2(\theta_i) \leq \frac{\|\mathbf{h}_{ji}\|^2}{1+g_{jj}} \tag{5.37}$$

$$\mathbf{w}_i = \frac{\mathbf{h}_{ii}}{\|\mathbf{h}_{ii}\|} \text{ is optimal if } \quad (1+g_{jj})\|\mathbf{h}_{ii}\|^2 \leq \|\mathbf{h}_{ji}\|^2\cos^2(\theta_i) \tag{5.38}$$

for $i,j = 1,2$ and $g_{ij} = |\mathbf{h}_{ij}^H\mathbf{w}_j|^2$. To be more specific:

$$\left(\frac{\mathbf{h}_{11}}{\|\mathbf{h}_{11}\|}, \frac{\mathbf{h}_{22}}{\|\mathbf{h}_{22}\|}\right) \text{ is optimal if and only if} \begin{cases} \cos^2(\theta_1) \geq \dfrac{(1+\|\mathbf{h}_{22}\|^2)\|\mathbf{h}_{11}\|^2}{\|\mathbf{h}_{21}\|^2} \\ \cos^2(\theta_2) \geq \dfrac{(1+\|\mathbf{h}_{11}\|^2)\|\mathbf{h}_{22}\|^2}{\|\mathbf{h}_{12}\|^2}. \end{cases} \tag{5.39}$$

$$\left(\frac{\mathbf{h}_{21}}{\|\mathbf{h}_{21}\|}, \frac{\mathbf{h}_{12}}{\|\mathbf{h}_{12}\|}\right) \text{ is optimal if and only if}$$

$$\begin{cases} \|\mathbf{h}_{12}\|^2 - \|\mathbf{h}_{22}\|^2\cos^2(\theta_2) \leq \|\mathbf{h}_{11}\|^2\|\mathbf{h}_{22}\|^2\cos^2(\theta_1)\cos^2(\theta_2) & \leq \dfrac{\|\mathbf{h}_{21}\|^2\|\mathbf{h}_{22}\|^2\cos^2(\theta_2)}{1+\|\mathbf{h}_{22}\|^2\cos^2(\theta_2)} \\ \|\mathbf{h}_{21}\|^2 - \|\mathbf{h}_{11}\|^2\cos^2(\theta_1) \leq \|\mathbf{h}_{11}\|^2\|\mathbf{h}_{22}\|^2\cos^2(\theta_1)\cos^2(\theta_2) & \leq \dfrac{\|\mathbf{h}_{12}\|^2\|\mathbf{h}_{11}\|^2\cos^2(\theta_1)}{1+\|\mathbf{h}_{11}\|^2\cos^2(\theta_1)}. \end{cases} \tag{5.40}$$

Proof. see Appendix 5.11.7. □

5.8 A simple transmit strategy

In this Section, we propose a very simple transmission strategy with only countable number of beamforming vector choices. Although the performance will be suboptimal, the beamforming vector choices are proposed below in the hope that it achieves maximum sum rate in certain channel conditions and achieve close to maximum sum rate in other scenarios.

This transmission strategy is inspired by the parameterization of each decoding structure. We propose to select only two beamforming vectors in each candidate set. Given the channel states information, we compare the sum rate performance of these eight beamforming vectors and choose the beamforming vector and the corresponding decoding structure which achieves the highest sum rate.

- NN region: $\left(\frac{\Pi_{21}^{\perp}\mathbf{h}_{11}}{\|\Pi_{21}^{\perp}\mathbf{h}_{11}\|}, \frac{\Pi_{12}^{\perp}\mathbf{h}_{22}}{\|\Pi_{12}^{\perp}\mathbf{h}_{22}\|}\right)$ and $\left(\frac{\mathbf{h}_{11}}{\|\mathbf{h}_{11}\|}, \frac{\mathbf{h}_{22}}{\|\mathbf{h}_{22}\|}\right)$.
- ND region: $\left(\frac{\mathbf{h}_{21}}{\|\mathbf{h}_{21}\|}, \frac{\mathbf{h}_{22}}{\|\mathbf{h}_{22}\|}\right)$ and $\left(\frac{\mathbf{h}_{11}}{\|\mathbf{h}_{11}\|}, \frac{\mathbf{h}_{22}}{\|\mathbf{h}_{22}\|}\right)$.
- DN region: $\left(\frac{\mathbf{h}_{11}}{\|\mathbf{h}_{11}\|}, \frac{\mathbf{h}_{12}}{\|\mathbf{h}_{12}\|}\right)$ and $\left(\frac{\mathbf{h}_{11}}{\|\mathbf{h}_{11}\|}, \frac{\mathbf{h}_{22}}{\|\mathbf{h}_{22}\|}\right)$.
- DD region: $\left(\frac{\mathbf{h}_{21}}{\|\mathbf{h}_{21}\|}, \frac{\mathbf{h}_{12}}{\|\mathbf{h}_{12}\|}\right)$ and $\left(\frac{\mathbf{h}_{11}}{\|\mathbf{h}_{11}\|}, \frac{\mathbf{h}_{22}}{\|\mathbf{h}_{22}\|}\right)$.
- TDMA: a time sharing scheme between single user points and therefore $\mathbf{w}_i = \frac{\mathbf{h}_{ii}}{\|\mathbf{h}_{ii}\|}$.

In the NN region, we propose to choose either the interference nulling solution or the desired channel gain maximizing solution. It has been shown in previous literature that in MISO-IC-SUD and low SNR regime, maximizing desired channel gain is sum rate optimal whereas in high SNR regime, interference nulling is sum rate optimal.

It was shown in SISO-IC that the DD scheme is sum rate optimal among all four decoding structures when the strength of both interference channels are strong and the DN or ND scheme is sum rate optimal when one interference channel is strong and the other interference channel is weak comparing to the desired channel. The interference maximizing beamforming solution and the desired channel power gain beamforming solution are chosen in DN, ND and DD regions in the proposed algorithm to verify the analogy from SISO-IC to MISO-IC.

5.9 Simulation Results

In this section, we provide simulation results regarding to the proposed parameterization. By varying the beamforming vectors and power allocation, according to the proposed parameterization, we plot the achievable rate region for each decoding structure for a particular channel realization in Section 5.9.1. The maximum sum rate point and the MRT points in each decoding structure are plotted on the corresponding achievable rate region. In Section 5.9.2, we compute the empirical frequency of MRT strategies in $\mathbf{R}^{nd}$ and $\mathbf{R}^{dd}$ averaged over 500 channel realizations. In Section 5.9.3, we allow the channels to be correlated and we see that the sum rate optimal decoding structure changes with the strength of the interference channel, agreeing with the observations with SISO-IC.

5.9.1 Achievable rate region and maximum sum rate point

In Fig. 5.7, we plot the achievable rate region of the decoding structure $\mathbf{R}^{nd}$, $\mathbf{R}^{dn}$, $\mathbf{R}^{dd}$ and $\mathbf{R}^{nn}$ in Fig. 5.7a, 5.7b, 5.7c and 5.7d respectively. We assume $N = 3$ transmit antennas and SNR=0dB. We exhaust λ_1 and λ_2 to take 20 values between zero and one, inclusively. For each pair of (λ_1, λ_2), beamforming vectors $\mathbf{w}_1, \mathbf{w}_2$ are generated and the corresponding rates with transmit powers P_1, P_2 are plotted. Depending on the candidate set in each decoding structure, the transmit powers can be less than maximum power or equal to the maximum power P_{max}. For example, in $\mathbf{R}^{nn}$, maximum power is used: $P_1 = P_2 = P_{max}$, whereas in $\mathbf{R}^{nd}$, $P_1 = P_{max}$ and $0 \leq P_2 \leq P_{max}$ and in $\mathbf{R}^{dd}$, $0 \leq P_1, P_2 \leq P_{max}$. For simulation purposes, we allow the transmit powers to take 10 values between 0 and P_{max}, inclusively. The rate points plotted are achieved by the proposed Pareto boundary parameterization and the red asterisk is the maximum sum rate point by employing the maximum sum rate point parameterization where as the red square is the MRT strategies: $\left(\mathbf{w}_1 = \frac{\mathbf{h}_{21}}{\|\mathbf{h}_{21}\|}, \mathbf{w}_2 = \frac{\mathbf{h}_{22}}{\|\mathbf{h}_{22}\|}\right)$ in $\mathbf{R}^{nd}$; $\left(\mathbf{w}_1 = \frac{\mathbf{h}_{11}}{\|\mathbf{h}_{11}\|}, \mathbf{w}_2 = \frac{\mathbf{h}_{12}}{\|\mathbf{h}_{12}\|}\right)$ in $\mathbf{R}^{dn}$ and $\left(\mathbf{w}_1 = \frac{\mathbf{h}_{11}}{\|\mathbf{h}_{11}\|}, \mathbf{w}_2 = \frac{\mathbf{h}_{22}}{\|\mathbf{h}_{22}\|}\right)$ in $\mathbf{R}^{dd}$ and $\mathbf{R}^{nn}$.

5.9.2 Empirical Frequency of MRT strategies

In Fig. 5.8, we demonstrate the variation of the empirical frequency of MRT strategies in $\mathbf{R}^{nd}$ when SNR increases. In $\mathbf{R}^{nd}$, the empirical frequency of beamforming vectors pair $\left(\frac{\mathbf{h}_{21}}{\|\mathbf{h}_{21}\|}, \frac{\mathbf{h}_{22}}{\|\mathbf{h}_{22}\|}\right)$ is 50% when SNR goes to infinity where as the empirical frequency o f$\left(\frac{\mathbf{h}_{11}}{\|\mathbf{h}_{11}\|}, \frac{\mathbf{h}_{22}}{\|\mathbf{h}_{22}\|}\right)$ is 10%. It shows that with $\mathbf{R}^{nd}$, in high SNR, Tx 1 should amplify interference signal by beamforming at the interference channel and Tx 2 should amplify desired signal by beamforming at the desired channel and by doing so, it achieves maximum sum rate on average 50% of the channel realizations.

In Fig. 5.9, we compare the maximum sum rate and the rates achieved by MRT strategies in $\mathbf{R}^{dd}$: $(\mathbf{w}_1 = \frac{\mathbf{h}_{11}}{\|\mathbf{h}_{11}\|}, \mathbf{w}_2 = \frac{\mathbf{h}_{22}}{\|\mathbf{h}_{22}\|})$ and $(\mathbf{w}_1 = \frac{\mathbf{h}_{21}}{\|\mathbf{h}_{21}\|}, \mathbf{w}_2 = \frac{\mathbf{h}_{12}}{\|\mathbf{h}_{12}\|})$. In the x-axis, we plot the percentage of the average maximum sum rate whereas the y-axis is the percentage of channel realizations such that the MRT rates are less than a certain percentage of the maximum sum rate. Simulations show that the sum rate achieved by MRT strategies are less than 20% to 80% of the maximum sum rate. Since maximizing direct channel gain or interference gain do not reach maximum sum rate, it seems to imply that in $\mathbf{R}^{dd}$, interference should not be maximized or minimized and should be balanced instead.

In Fig. 5.10, we plotted the averaged difference between the maximum sum rate and MRT strategies in $\mathbf{R}^{nd}$ and $\mathbf{R}^{dd}$ respectively. From Fig. 5.10a, the rate difference between MRT strategies and the maximum sum rate decreases with SNR and reaches to about 2% and 4% at 40dB SNR. Thus, even if the empirical frequency is about 50% and 10%, MRT strategies only lose about 2% and 4% of the maximum sum rate of $\mathbf{R}^{nd}$. On the other hand, from Fig. 5.10b, it shows that the rate difference between MRT strategies and the maximum sum rate in $\mathbf{R}^{dd}$ increases with SNR and we conclude that MRT strategies are not sum rate optimal in $\mathbf{R}^{dd}$.

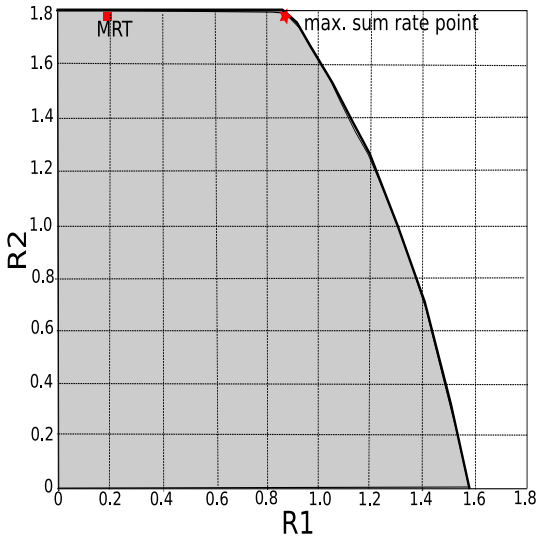

(a) Achievable rate region of $\mathbf{R}^{nd}$: proposed parameterization achieves the Pareto Boundary and maximum sum rate point.

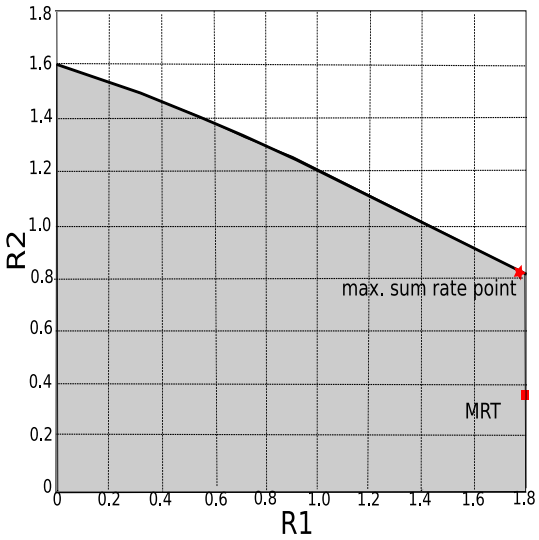

(b) Achievable rate region of $\mathbf{R}^{dn}$: proposed parameterization achieves the Pareto Boundary and maximum sum rate point.

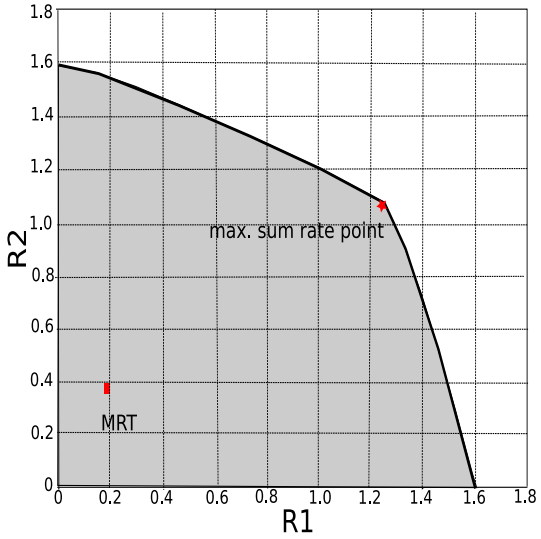

(c) Achievable rate region of $\mathbf{R}^{dd}$: proposed parameterization achieves the Pareto Boundary and maximum sum rate point.

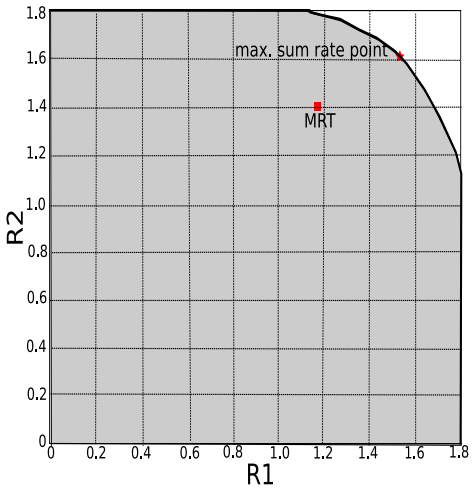

(d) Achievable rate region of $\mathbf{R}^{nn}$: proposed parameterization achieves the Pareto Boundary and maximum sum rate point.

Figure 5.7: Achievable rate region of different decoding structures.

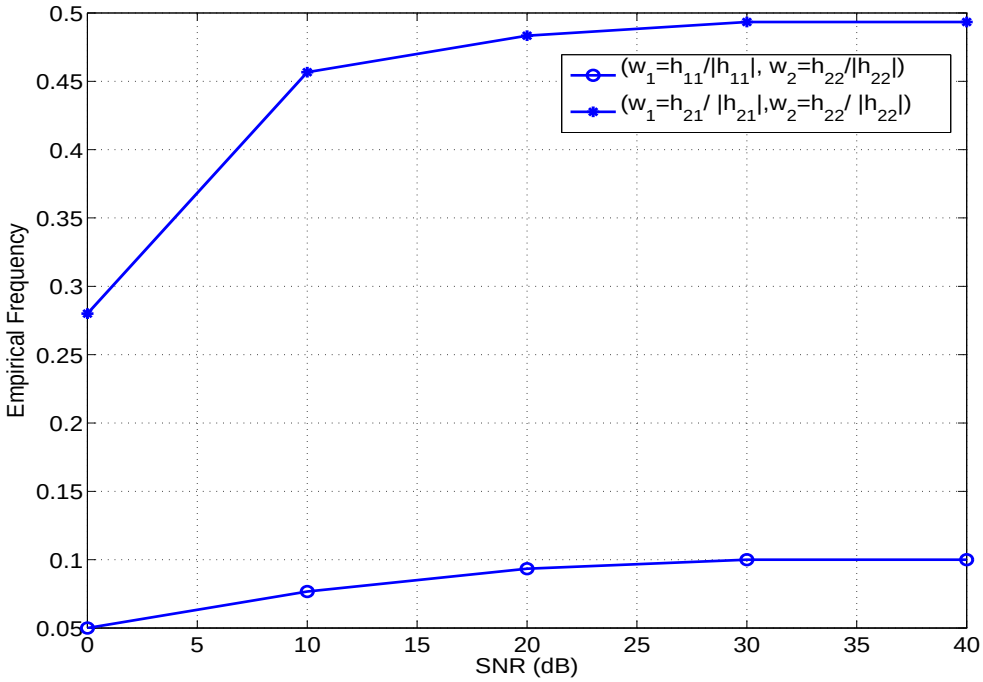

Figure 5.8: MRT optimality in $\mathbf{R}^{nd}$ when SNR increases: interference should be maximized half of the time when SNR goes to infinity.

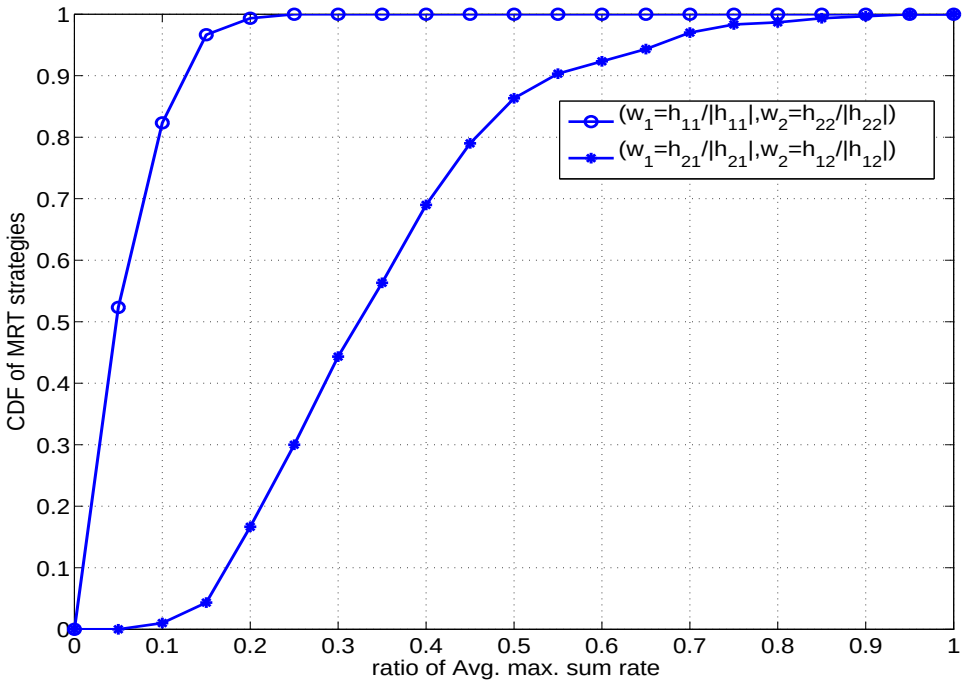

Figure 5.9: Maximum sum rate plots in different channel realizations. MRT strategies are not sum rate optimal in $\mathbf{R}^{dd}$.

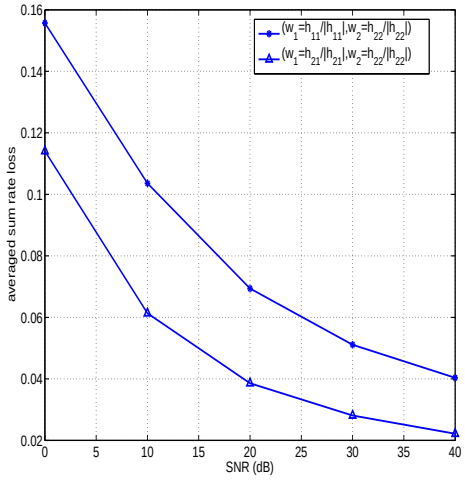

(a) The averaged sum rate difference between maximum sum rate point and MRT strategies in $\mathbf{R}^{nd}$.

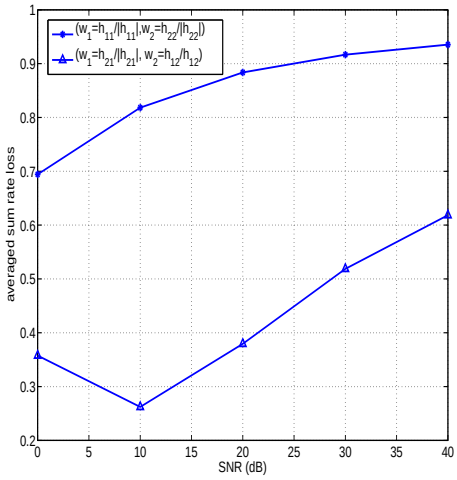

(b) The averaged sum rate difference between maximum sum rate point and MRT strategies in $\mathbf{R}^{dd}$.

Figure 5.10: The averaged sum rate difference between maximum sum rate point and MRT strategies in $\mathbf{R}^{nd}$ and $\mathbf{R}^{dd}$.

5.9.3 Correlated Channels and Sum Rate optimal decoding structures

In this section, we assume a symmetric channel [3] in which the direct channels, $\mathbf{h}_{ii}$, are i.i.d complex gaussian vector channels. The interference channel $\mathbf{h}_{ji}$ has a projection angle θ_i with the direct channel $\mathbf{h}_{ii}$:

$$|\mathbf{h}_{ji}^H \mathbf{h}_{ii}| = \|\mathbf{h}_{ii}\| \|\mathbf{h}_{ji}\| \cos(\theta_i). \tag{5.41}$$

Moreover, we define the signal to interference ratio SIR as

$$\text{SIR} = \frac{\|\mathbf{h}_{ii}\|^2}{\|\mathbf{h}_{ji}\|^2}. \tag{5.42}$$

In Fig. 5.11, we compare the sum rate achieved by $\mathbf{R}^{nn}$, $\mathbf{R}^{dd}$ and TDMA. When the strength of the interference channel increases, there is a transition from $\mathbf{R}^{nn}$ to TDMA to $\mathbf{R}^{dd}$: treating interference as noise is sum rate optimal in low interference regime and then time sharing should be performed and then decoding interference is sum rate optimal in high interference regime. When the angle between the interference channel increases to $\theta = 0.15\pi$, about 27 degrees, there is a direct transition between treating interference as noise and decoding interference. Thus, when the direct channel and the interference channel are more *apart*, time sharing is not sum rate optimal and outperformed by the other decoding structures.

In Fig. 5.12, we compare the maximum sum rate achieved in different decoding structures with TDMA when the system SNR increases. When the interference channel is as strong as the direct channel SIR= 1, treating interference as noise is sum rate optimal in all SNR range. When the interference channel power increases $\text{SIR}^{-1} = 5, 10, 20$, both Rxs. decoding interference is sum rate optimal in low SNR whereas one Rx treating interference as noise and one Rx decoding interference is sum rate optimal in high SNR.

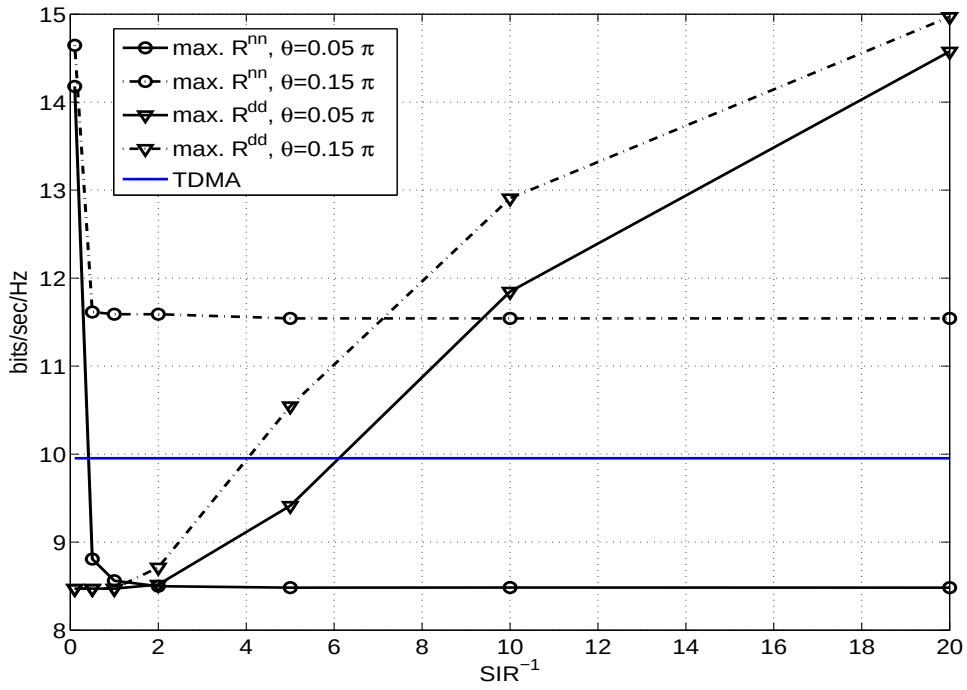

Figure 5.11: The averaged sum rate of different decoding structure comparing to TDMA in symmetric channel when the strength of the interference channel increases.

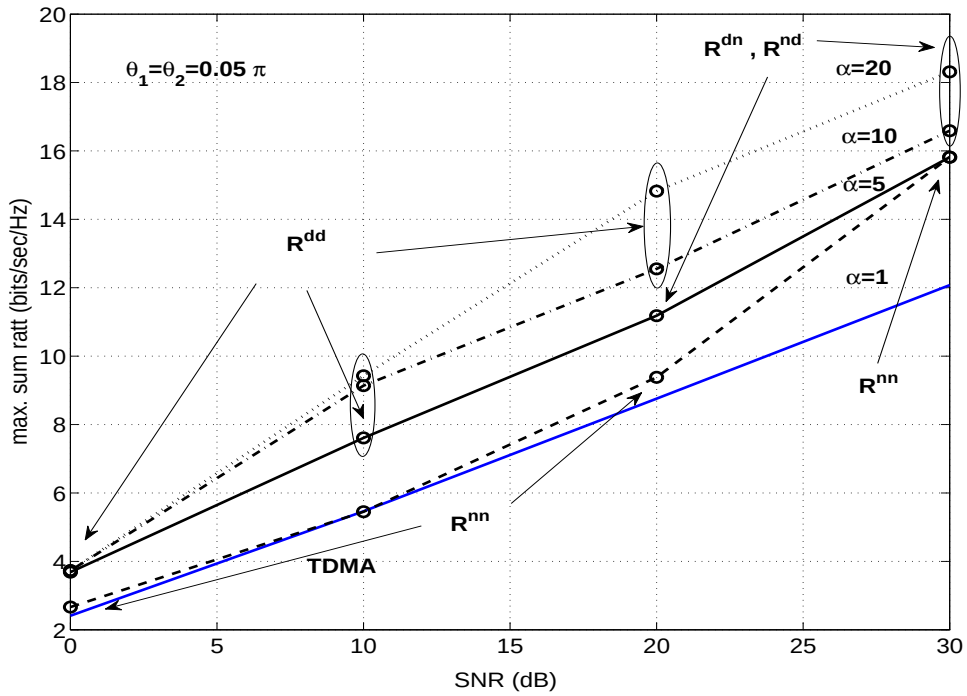

Figure 5.12: The averaged sum rate of different decoding structure comparing to TDMA in symmetric channel when the system SNR increases.

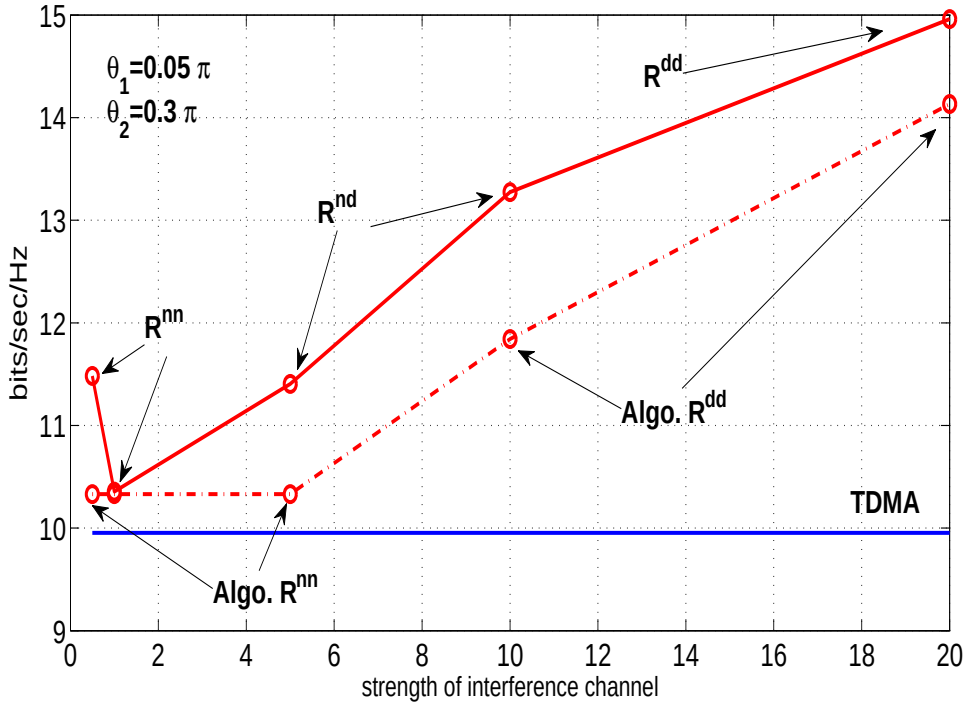

Figure 5.13: Sum rate optimal decoding structures when the strength of interference channel increases.

5.9.4 Performance of suboptimal algorithm

In Fig. 5.13, we plotted the maximum sum rate achieved by different decoding structure and compare it with the proposed simple algorithm when SIR decreases. We see that when the interference is weak, it is sum rate optimal to treat interference as noise and when the interference strength increases, sum rate can be increased by allowing one of the Rx to decode interference and in the strong interference regime, both Rxs. decoding interference achieves the highest sum rate. Depending on the channel coefficients, TDMA may outperform $\mathbf{R}^{nn}$ and $\mathbf{R}^{dd}$ in the medium interference regime. Note that the computation of the maximum sum rate point is NP-hard. However, we see the the proposed simple algorithm achieves nice sum rate performance with only five choices of beamforming vectors.

5.10 Conclusion and future work

The interference decoding capability brings additional freedom to the Rxs. which either decode interference or treat interference as noise. However, it is not trivial when Txs. should avoid interference and when should amplify interference power. To answer this question, we formulate the achievable rate region for a two-user MISO-IC-SUD. We provide an in-depth analysis of the achievable rate region, as a union of different decoding structures. The Pareto boundary is then characterized in terms of both power allocation and beamforming vectors. As a direct application of the Pareto boundary characterization, we characterize the maximum sum rate points. The candidate set to the maximum

sum rate point is a strict subset of the the candidate set of the Pareto boundary. With the maximum sum rate characterization, we derive the MRT optimality conditions which describe the conditions in which simple MRT strategies are sum rate optimal. We conclude the paper by providing simulation results which shed some insights into the question " *When is selfishness sum rate optimal?*". Results show that MRT strategies have only 2% to 4% rate loss comparing to the maximum sum rate point in high SNR if one Rx decodes interference and the other treats interference as noise. On the other hand, MRT is not sum rate optimal if both Rxs. decode interference. In symmetric channels, there is a transition in decoding structure from treating interference as noise to TDMA to decoding interference at both Rxs. when the strength of interference increases.

The achievable rate problem for the K-user MISO-IC-IDC is not simple as the number of possible interference decoding order increases exponentially with the number of users. It is not easy to see which decoding order is better than the others and whether this decoding order in this decoding structure is better than other decoding structures. This extension to the K-user case is currently under preparation.

5.11 Appendix

5.11.1 Proof of Thm. 11

In this sequel, we are going to prove that the Pareto boundary in NN region, DN region and DD region are attained by rank 1 matrices.

Lemma 5. *In the NN region, where Rx 1 and Rx 2 treat interference as noise, the Pareto boundary attaining transmit covariance matrices are rank one.*

Proof. See reference [42, 54]. □

To prove that the Pareto optimal transmit covariance matrices in DN and DD regions are rank one, we follow and modify slightly the proof from [42]. To facilitate the discussion, we define the following received channel power region for Tx i, assuming transmit power being one,

$$\Phi_i^s = \left\{ (\mathbf{h}_{ii}^H \mathbf{S}_i \mathbf{h}_{ii}, \mathbf{h}_{ji}^H \mathbf{S}_i \mathbf{h}_{ji}) : \mathbf{S}_i \in \mathcal{S} \right\}. \tag{5.43}$$

For each received channel power $g_{ji} = \mathbf{h}_{ji}^H \mathbf{S}_i \mathbf{h}_{ji}$, $i, j = 1, 2$, there is a set $\mathcal{K}_{ji}^{\uparrow}$ such that each utility u_k, $k \in \mathcal{K}_{ji}^{\uparrow}$, is monotonically increasing with received channel power g_{ji},

$$u_k(g_{ii}, g_{ji}, g_{ij}, g_{jj}) \leq u_k(g_{ii}, g'_{ji}, g_{ij}, g_{jj}) \tag{5.44}$$

if $g_{ji} \leq g'_{ji}$. Similarly, there is a set $\mathcal{K}_{ji}^{\downarrow}$ such that each utility u_k, $k \in \mathcal{K}_{ji}^{\downarrow}$, is monotonically decreasing with received channel power g_{ji}.

Lemma 6. *For an arbitrary fixed Tx i, if there exist a received channel power g_{ji}, $j = 1, 2$, such that the number of utilities that are monotonically increasing and decreasing with g_{ji} are both larger than zero and the number of such received channel power g_{ji} is not larger than one, e.g.*

$$\mathcal{N}_i = \left\{ k : \left| \mathcal{K}_{ki}^{\uparrow} \right| > 0, \left| \mathcal{K}_{ki}^{\downarrow} \right| > 0 \right\}, \|\mathcal{N}_i\| \leq 1, \qquad i = 1, 2, \tag{5.45}$$

then the Pareto optimal transmit covariance matrices with respect to these utilities are rank one and attain the boundary of the corresponding received channel power regions Φ_i^s.

Proof. We proceed by separating the cases where the some utilities are increasing or decreasing with the received channel power g_{ji}, for $i, j = 1, 2$.

- If $\left|\mathcal{K}_{ji}^{\uparrow}\right| \neq 0$ and $\left|\mathcal{K}_{ji}^{\downarrow}\right| = 0$, then the Pareto optimal transmit covariance matrix $\mathbf{S}^*$ attains the boundary of the received channel power region Φ_i^s. It is because for each utility $u_k(g_{ii}, g_{ji}, g_{ij}, g_{jj})$ such that $k \in \mathcal{K}_{ji}^{\uparrow}$, if g_{ji} is not on the boundary of Φ_i^s, we can choose a transmit covariance matrix $\mathbf{S}^*$ such that $g_{ji}^* = \mathbf{h}_{ji}^H \mathbf{S}^* \mathbf{h}_{ji} \geq g_{ji}$ which increases the value of the utility $u_k(g_{ii}, g_{ji}, g_{ij}, g_{jj}) \leq u_k(g_{ii}, g_{ji}^*, g_{ij}, g_{jj})$. Since $\left|\mathcal{K}_{ji}^{\downarrow}\right| = 0$, no utilities are decreased by modifying the transmit covariance matrix from $\mathbf{S}$ to $\mathbf{S}^*$.
- If $\left|\mathcal{K}_{ji}^{\downarrow}\right| \neq 0$ and $\left|\mathcal{K}_{ji}^{\uparrow}\right| = 0$, then the Pareto optimal transmit covariance matrix $\mathbf{S}^*$ attains the boundary of the received channel power region Φ_i^s. It is because for each utility $u_k(g_{ii}, g_{ji}, g_{ij}, g_{jj})$ such that $k \in \mathcal{K}_{ji}^{\uparrow}$, if g_{ji} is not on the boundary of Φ_i^s, we can choose a transmit covariance matrix $\mathbf{S}^*$ such that $g_{ji}^* = \mathbf{h}_{ji}^H \mathbf{S}^* \mathbf{h}_{ji} \leq g_{ji}$ which increases the value of the utility $u_k(g_{ii}, g_{ji}, g_{ij}, g_{jj}) \leq u_k(g_{ii}, g_{ji}^*, g_{ij}, g_{jj})$. Since $\left|\mathcal{K}_{ji}^{\uparrow}\right| = 0$, no utilities are decreased by modifying the transmit covariance matrix from $\mathbf{S}$ to $\mathbf{S}^*$.
- According to the assumption (5.45), for each Tx i, there exist at most one j such that $\left|\mathcal{K}_{ji}^{\downarrow}\right| \neq 0$ and $\left|\mathcal{K}_{ji}^{\uparrow}\right| \neq 0$. In this case, the received channel power with transmit power, $g_{ji}P_i$ has value between 0 and $\|\mathbf{h}_{ji}\|^2 P_{max}$ which can be achieved by setting g_{ji} to be on the boundary of Φ_i^s and letting P_i vary from 0 to P_{max}. Hence, we can put the Pareto optimal transmit covariance matrix $\mathbf{S}^*$ on the boundary of the received channel power region Φ_i^s by allowing power control $0 \leq P_i \leq P_{max}$.

From [42, Lemma 3], the received channel powers on the boundary of the received channel power region Ψ_i^s are attained by rank one transmit covariance matrices, which completes the proof. □

In the following, we are going to show that the Pareto optimality problem in DN region and DD region respectively satisfy the assumption in Lemma 6 and therefore the Pareto optimal transmit covariance matrices are rank one.

5.11.1.1 In the DN region

Rx 1 decodes interference and Rx 2 treats interference as noise and the Pareto boundary attaining transmit covariance matrices are rank one. To see this, we recall the achievable rates in $\mathbf{R}^{dn}$:

$$\begin{aligned} u_1(g_{11}, g_{21}, g_{12}, g_{22}) &= \log_2(1 + g_{11}P_1) \\ u_2(g_{11}, g_{21}, g_{12}, g_{22}) &= \min\left(\log_2\left(1 + \frac{g_{12}P_2}{g_{11}P_1 + 1}\right), \log_2\left(1 + \frac{g_{22}P_2}{1 + g_{21}P_1}\right)\right). \end{aligned} \tag{5.46}$$

and therefore we have

$$\begin{aligned} &\mathcal{K}_{11}^{\uparrow} = \{1\}; \quad \mathcal{K}_{11}^{\downarrow} = \{2\}; \quad \mathcal{K}_{21}^{\uparrow} = \{\emptyset\}; \quad \mathcal{K}_{21}^{\downarrow} = \{2\}; \\ &\mathcal{K}_{12}^{\uparrow} = \{2\}; \quad \mathcal{K}_{12}^{\downarrow} = \{\emptyset\}; \quad \mathcal{K}_{22}^{\uparrow} = \{2\}; \quad \mathcal{K}_{22}^{\downarrow} = \{\emptyset\}. \end{aligned} \tag{5.47}$$

Since the assumption (5.45) is satisfied, by Lemma 6, we have the Pareto optimal transmit covariance matrices in DN region as rank one.

5.11.1.2 In DD region

Rx 1 and 2 decode interference and the Pareto boundary attaining transmit covariance matrices are rank one. To see this, we recall the achivable rates in $\mathbf{R}^{dd}$:

$$\begin{aligned} u_1(g_{11}, g_{21}, g_{12}, g_{22}) &= \min\left(\log_2(1+g_{11}), \log_2\left(1+\frac{g_{21}}{1+g_{22}}\right)\right) \\ u_2(g_{11}, g_{21}, g_{12}, g_{22}) &= \min\left(\log_2(1+g_{22}), \log_2\left(1+\frac{g_{12}}{1+g_{11}}\right)\right). \end{aligned} \tag{5.48}$$

Hence we have

$$\begin{aligned} &\mathcal{K}_{11}^{\uparrow} = \{1\}; \quad &&\mathcal{K}_{11}^{\downarrow} = \{2\}; \quad &&\mathcal{K}_{21}^{\uparrow} = \{1\}; \quad &&\mathcal{K}_{21}^{\downarrow} = \{\emptyset\}; \\ &\mathcal{K}_{12}^{\uparrow} = \{2\}; \quad &&\mathcal{K}_{12}^{\downarrow} = \{\emptyset\}; \quad &&\mathcal{K}_{22}^{\uparrow} = \{2\}; \quad &&\mathcal{K}_{22}^{\downarrow} = \{1\}. \end{aligned} \tag{5.49}$$

Since the assumption (5.45) is satisfied, by Lemma 6, we have the Pareto optimal transmit covariance matrices in DD region are rank one.

5.11.2 Proof of Thm. 12

The Pareto optimal beamforming vectors can be presented as the solutions of the following optimization problems, for some feasible value r_i, $i, j = 1, 2, j \neq i$,

$$\begin{aligned} \max_{\mathbf{w}_1, \mathbf{w}_2, P_1, P_2} \quad & R_j(\mathbf{w}_1, \mathbf{w}_2, P_1, P_2) \\ \text{subject to} \quad & R_i(\mathbf{w}_1, \mathbf{w}_2, P_1, P_2) \geq r_i, \\ & \|\mathbf{w}_1\| = 1, \|\mathbf{w}_2\| = 1, \\ & 0 \leq P_1 \leq P_{max}, 0 \leq P_2 \leq P_{max}. \end{aligned} \tag{5.50}$$

With different decoding structure, the achievable rates R_1, R_2 are substituted with different rate expressions. However, both the ND and DD case resemble closely to the maximization problem of channel power and the optimal solution can be characterized in a linear combination of some specific vectors.

Lemma 7. *Define a maximization problem of channel power in the following:*

$$\begin{aligned} \max_{\mathbf{w}} \quad & t \\ \textit{subject to} \quad & |\mathbf{u}^H\mathbf{w}|^2 \geq ut, |\mathbf{v}^H\mathbf{w}|^2 \geq vt \\ & \|\mathbf{w}\|^2 \leq 1 \end{aligned} \tag{5.51}$$

for some arbitrary fixed scalars $u \geq 0$ and $v \geq 0$. The solutions $\mathbf{w}^*$ must be in the following set $\mathcal{W}$,

$$\mathcal{W} = \left\{\mathbf{w} \in \mathbb{C}^{N\times 1} : \mathbf{w} = \sqrt{\mu}\frac{\Pi_u \mathbf{v}}{\|\Pi_u \mathbf{v}\|} + \sqrt{1-\mu}\frac{\Pi_u^{\perp}\mathbf{v}}{\|\Pi_u^{\perp}\mathbf{v}\|}, 0 \leq \mu \leq 1\right\}. \tag{5.52}$$

Corollary 1. *Reversing the signs of the inequality in* (5.51) *to* $|\mathbf{u}^H\mathbf{w}|^2 \leq ut, |\mathbf{v}^H\mathbf{w}|^2 \leq vt$ *does not change the characterization of the solutions in* (5.52)*.*

Proof. We proceed by writing the Lagrangians of the problem, with Lagrange multipliers $\boldsymbol{\lambda} = [\lambda_1, \lambda_2, \lambda_3]$,

$$L(\mathbf{w}, \boldsymbol{\lambda}) = t - \lambda_1\left(ut - |\mathbf{u}^H\mathbf{w}|^2\right) - \lambda_2\left(vt - |\mathbf{v}^H\mathbf{w}|^2\right) - \lambda_3(\|\mathbf{w}\|^2 - 1). \tag{5.53}$$

Now, we compute the vanishing point of the Lagragian derivative which is a necessary condition of the optimal solution, $\frac{\partial L(\mathbf{w}_1,\boldsymbol{\lambda})}{\partial \mathbf{w}^H} = \lambda_1 \mathbf{u}\mathbf{u}^H\mathbf{w} + \lambda_2 \mathbf{v}\mathbf{v}^H\mathbf{w} - \lambda_3\mathbf{w} = 0$. We can write $\lambda_1 \mathbf{u}\mathbf{u}^H\mathbf{w} + \lambda_2 \mathbf{v}\mathbf{v}^H\mathbf{w} = \lambda_3\mathbf{w}$ and adjusting the constant scaling, we have $\lambda_1\|\mathbf{u}\|^2 \frac{\mathbf{u}\mathbf{u}^H}{\|\mathbf{u}\|^2}\mathbf{w} + \lambda_2\|\mathbf{v}\|^2 \frac{\mathbf{v}\mathbf{v}^H}{\|\mathbf{v}\|^2}\mathbf{w} = \lambda_3\mathbf{w}$. Therefore, the eigenvector $\mathbf{w}$ is a composition of its projection on $\mathbf{u}$ and $\mathbf{v}$:

$$\lambda_1\|\mathbf{u}\|^2\Pi_u\mathbf{w} + \lambda_2\|\mathbf{v}\|^2\Pi_v\mathbf{w} = \lambda_3\mathbf{w}. \tag{5.54}$$

Since $\lambda_i \geq 0, i = 1, 2, 3$, we can write, for some complex-valued μ_1, μ_2,

$$\mathbf{w} = \frac{\mu_1 \frac{\mathbf{u}}{\|\mathbf{u}\|} + \mu_2 \frac{\mathbf{v}}{\|\mathbf{v}\|}}{\left\| \mu_1 \frac{\mathbf{u}}{\|\mathbf{u}\|} + \mu_2 \frac{\mathbf{v}}{\|\mathbf{v}\|} \right\|}. \tag{5.55}$$

Now we define the set of beamforming vectors that satisfy (5.55), $\mathcal{U} = \left\{ \mathbf{w} : \mathbf{w} = \frac{\mu_1 \frac{\mathbf{u}}{\|\mathbf{u}\|} + \mu_2 \frac{\mathbf{v}}{\|\mathbf{v}\|}}{\left\| \mu_1 \frac{\mathbf{u}}{\|\mathbf{u}\|} + \mu_2 \frac{\mathbf{v}}{\|\mathbf{v}\|} \right\|}, \mu_1, \mu_2 \in \mathbb{C} \right\}$. Then, we show in the following that $\mathcal{U}$ is a subset of $\mathcal{W}$ in Lemma 7. We start with

$$\begin{aligned}
\mathbf{w} &= \mu_1 \frac{\mathbf{u}}{\|\mathbf{u}\|} + \mu_2 \frac{\mathbf{v}}{\|\mathbf{v}\|} \\
&\overset{(a)}{=} \frac{\mu_1}{\|\mathbf{u}\|}\left(\Pi_v + \Pi_v^{\perp}\right)\mathbf{u} + \mu_2 \frac{\|\mathbf{v}\|^2}{|\mathbf{v}^H\mathbf{u}|} e^{-j\phi_{uv}} \Pi_v \mathbf{u} \\
&= \left(\frac{\mu_1}{\|\mathbf{u}\|} + \mu_2 \frac{\|\mathbf{v}\|^2}{|\mathbf{v}^H\mathbf{u}|} e^{-j\phi_{uv}} \right) \Pi_v\mathbf{u} + \Pi_v^{\perp}\mathbf{u} \\
&= z_1 \frac{\Pi_v\mathbf{u}}{\|\Pi_v\mathbf{u}\|} + z_2 \frac{\Pi_v^{\perp}\mathbf{u}}{\|\Pi_v^{\perp}\mathbf{u}\|}
\end{aligned} \tag{5.56}$$

where (a) is due to $\mathbf{v} = \frac{\Pi_{\mathbf{v}}\mathbf{u}\|\mathbf{v}\|^2}{\mathbf{v}^H\mathbf{u}}$ and $\phi_{uv} = \arg(\mathbf{v}^H\mathbf{u})$. The parameter z_1 is complex and z_2 is real; the values of z_1 and z_2 are scaled such that $\|\mathbf{w}\| = 1$. Notice that $|\mathbf{u}^H\mathbf{w}| = \left| z_1\|\Pi_v\mathbf{u}\| + z_2\|\Pi_v^{\perp}\mathbf{u}\| \right| \overset{(a)}{\leq} |z_1|\|\Pi_v\mathbf{u}\| + z_2\|\Pi_v^{\perp}\mathbf{u}\|$ and $|\mathbf{v}^H\mathbf{w}| = \left| z_1 \frac{\mathbf{v}^H\mathbf{u}}{\|\Pi_v\mathbf{u}\|} \right| = |z_1| \frac{|\mathbf{v}^H\mathbf{u}|}{\|\Pi_v\mathbf{u}\|}$. Note that equality at (a) when z_1 is real and the phase of z_1 does not affect $|\mathbf{v}^H\mathbf{w}|$. Hence, z_1 can be chosen real and since the two basis are orthogonal, the power constraint of $\mathbf{w}$ is satisfied when $z_1^2 + c_2^2 = 1$ and thus, we can write $z_1 = \sqrt{\mu}$ and $c_2 = \sqrt{1-\mu}$ for $0 \leq \mu \leq 1$.

If the signs of inequalities are reversed and we have $|\mathbf{u}^H\mathbf{w}|^2 \leq ut, |\mathbf{v}^H\mathbf{w}|^2 \leq vt$ in the constraints in (5.51), then the corresponding signs changes to minus from positive in the Lagrangian but does not affect the discussion above and the characterization of the Pareto optimal solutions holds. □

Substitute the rate definitions (5.3) into (5.50) and maximizing R_1 subjecting to a constraint on R_2, we let $z_{22}^2 = |\mathbf{h}_{22}^H\mathbf{w}_2|^2 P_2$ and $z_{12}^2 = |\mathbf{h}_{12}^H\mathbf{w}_2|^2 P_2$ and we focus on the subproblem that concerns $\mathbf{w}_1$,

$$\begin{aligned}
\max_{\mathbf{w}_1} \quad & t \\
\text{subject to} \quad & |\mathbf{h}_{21}^H\mathbf{w}_1|^2 \geq (z_{22}^2 + 1)t, \\
& |\mathbf{h}_{11}^H\mathbf{w}_1|^2 \geq (z_{12}^2 + 1)t, \\
& \|\mathbf{w}_1\|^2 \leq 1.
\end{aligned} \tag{5.57}$$

This has the same formulation as in Lemma 7. By substituting $\mathbf{u} = \mathbf{h}_{21}$ and $\mathbf{v} = \mathbf{h}_{11}$, we obtain the characterization of the Pareto optimal beamforming vectors as a linear

combination of the vectors $\Pi_{21}\mathbf{h}_{11}$ and $\Pi_{21}^{\perp}\mathbf{h}_{11}$. Now we reverse the optimization order : maximize R_2 subject to a constraint on R_1. After some manipulations, we obtain for some z_{11}^2, z_{21}^2,

$$\begin{aligned} \max_{\mathbf{w}_2, P_2} \quad & |\mathbf{h}_{22}^H \mathbf{w}_2|^2 P_2 \\ \text{subject to} \quad & |\mathbf{h}_{22}^H \mathbf{w}_2|^2 P_2 \leq \frac{z_{21}^2}{2^{r_1}-1} - 1, \\ & |\mathbf{h}_{12}^H \mathbf{w}_2|^2 P_2 \leq \frac{z_{11}^2}{2^{r_1}-1} - 1, \\ & \|\mathbf{w}_2\| \leq 1, 0 \leq P_2 \leq P_{max}. \end{aligned} \tag{5.58}$$

By Corollary 1, we have

$$\mathbf{w}_2 = \sqrt{\mu_2}\frac{\Pi_{12}\mathbf{h}_{22}}{\|\Pi_{12}\mathbf{h}_{22}\|} + \sqrt{1-\mu_2}\frac{\Pi_{12}^{\perp}\mathbf{h}_{22}}{\|\Pi_{12}^{\perp}\mathbf{h}_{22}\|} \tag{5.59}$$

for $0 \leq \mu_2 \leq 1$.

5.11.3 Proof of Theorem 13

The following proof is similar to the approach in Appendix 5.11.2, to avoid repetitions we only highlight the main differences in the following. The Pareto optimality problem in the DD region is written as a maximization of R_1 subject to $R_2 \geq r_2$ and after some manipulation, we focus on the subproblem optimizing $\mathbf{w}_1$:

$$\begin{aligned} \max_{\mathbf{w}_1, P_1} \quad & t \\ \text{subject to} \quad & |\mathbf{h}_{11}^H \mathbf{w}_1|^2 P_1 \geq t, \\ & |\mathbf{h}_{11}^H \mathbf{w}_1|^2 P_1 \leq \frac{z_{12}^2 P_2}{2^{r_2}-1} - 1, \\ & |\mathbf{h}_{21}^H \mathbf{w}_1|^2 P_1 \geq t(z_{22}^2+1), \\ & \|\mathbf{w}_1\| \leq 1, 0 \leq P_1 \leq P_{max} \end{aligned} \tag{5.60}$$

for some z_{12}^2, z_{22}^2. Similar to Lemma 7, we write the Lagrangian and set the derivative with respect to $\mathbf{w}_1^H$ to zero, and obtian $\left(P_1(\lambda_1-\lambda_2)\mathbf{h}_{11}\mathbf{h}_{11}^H + \lambda_3 P_1 \mathbf{h}_{21}\mathbf{h}_{21}^H\right)\mathbf{w}_1 = \lambda_4 \mathbf{w}_1$. We add $P_1\lambda_2\|\mathbf{h}_{11}\|^2\mathbf{w}_1$ to both sides and obtain

$$\left(P_1\lambda_1\|\mathbf{h}_{11}\|^2\Pi_{11} + P_1\lambda_2\|\mathbf{h}_{11}\|^2\Pi_{11}^{\perp} + \lambda_3 P_1\|\mathbf{h}_{21}\|^2\Pi_{21}\right)\mathbf{w}_1 = (\lambda_4 + P_1\lambda_2\|\mathbf{h}_{11}\|^2)\mathbf{w}_1. \tag{5.61}$$

Hence, we see that the optimal solution is composed of its projection on the subspace spanned by $\mathbf{h}_{11}, \mathbf{h}_{21}$ and the orthogonal subspace of $\mathbf{h}_{11}$, which can be represented by the following:

$$\mathbf{w}_1 = \mu_1\frac{\Pi_{11}\mathbf{h}_{21}}{\|\Pi_{11}\mathbf{h}_{21}\|} + \mu_2\frac{\Pi_{11}^{\perp}\mathbf{h}_{21}}{\|\Pi_{11}^{\perp}\mathbf{h}_{21}\|} \tag{5.62}$$

for some $\mu_1, \mu_2 \in \mathbb{C}$ and $|\mu_1|^2 + |\mu_2|^2 = 1$.

Similar to the arguments before in Appendix 5.11.2, we omit the details here to avoid repetitions. The values μ_1, μ_2 can be chosen real-valued and the Pareto boundary of $\mathbf{R}^{dd}$ attaining beamforming vectors are

$$\mathbf{w}_1 \in \mathcal{V}_1 = \left\{\mathbf{w} = \sqrt{\nu_1}\frac{\Pi_{11}\mathbf{h}_{21}}{\|\Pi_{11}\mathbf{h}_{21}\|} + \sqrt{1-\nu_1}\frac{\Pi_{11}^{\perp}\mathbf{h}_{21}}{\|\Pi_{11}^{\perp}\mathbf{h}_{21}\|}, 0 \leq \nu_1 \leq 1\right\}. \tag{5.63}$$

5.11.4 Proof of Theorem 14

Before we go into details of computing the candidate set of the maximum sum rate in the ND region, we present the following lemma which holds importance in the discussions later.

Lemma 8. *Consider two functions $f_1(x), f_2(x)$ where $f_1(x)$ is concave and $f_2(x)$ is linearly increasing with $x \in \mathcal{X} \subset \mathbb{R}$. Define*

$$x_1^* = \arg\max_{x\in\mathcal{X}} f_1(x), \quad x_2^* = \arg\max_{x\in\mathcal{X}} f_2(x) \quad \textit{and} \quad \mathbb{X} = \{x \in \mathcal{X} : f_1(x) = f_2(x)\} \tag{5.64}$$

If $\hat{x} = arg\max \min(f_1(x), f_2(x))$, then

$$\hat{x} \subset \{x_1^*, x_2^*, \mathbb{X}\} \tag{5.65}$$

Proof. Notice that since $f_1(x)$ is concave, there are at most two intersection points. If there are no intersection points, then $\hat{x} \subset \{x_1^*, x_2^*\}$. If there is one intersection point $\bar{x}$, then one of the following orderings is true:

- $\bar{x} < x_1^* < x_2^*$: since there is only one intersection point, $f_2(x_2^*) < f_1(x_2^*)$ and thus $\hat{x} = x_2^*$.
- $x_1^* < \bar{x} < x_2^*$: let $x^- < \bar{x} < x^+$ and we have $f_1(x^-) > f_1(\bar{x}) > f_1(x^+)$ and $f_2(x^-) < f_2(\bar{x}) < f_2(x^+)$. Thus, $\hat{x} = \bar{x}$.

Note that $f_2(x)$ is linearly increasing with x and therefore x_2^* is the boundary of $\mathcal{X}$ and thus $x_2^* > x_1^*$ and $x_2^* > \bar{x}$. If there are two intersection points, then we have $\hat{x} \subset \mathbb{X}$. □

Note that the global optimal solution $\boldsymbol{\omega}^*$ must be in the solutions set of $\mathcal{B}(\mathbf{R}^{nd})$:

$$\boldsymbol{\omega}^* \subset \Omega^{nd} \tag{5.66}$$

where Ω^{nd} is defined in Thm. 12. Thus, we can refine the constraint set in the maximum sum rate problem in the ND region to

$$\bar{R}^{nd}(\mathbf{w}_1, \mathbf{w}_2) = \max_{(\mathbf{w}_1,\mathbf{w}_2)\in\Omega^{nd}} C_2(\mathbf{w}_2) + \min\{T_1(\mathbf{w}_1, \mathbf{w}_2), D_1(\mathbf{w}_1, \mathbf{w}_2)\} \tag{5.67}$$

which can be decomposed to the following:

$$\max_{\mathbf{w}_2\in\mathcal{W}_2} \left\{ C_2(\mathbf{w}_2) + \max_{\mathbf{w}_1\in\mathcal{W}_1} \min\{T_1(\mathbf{w}_1, \mathbf{w}_2), D_1(\mathbf{w}_1, \mathbf{w}_2)\} \right\} \tag{5.68}$$

where the inner maximin problem is maximized over $\mathbf{w}_1$ for *each* $\mathbf{w}_2$. With each given $\mathbf{w}_2$, we define $c_1 = \frac{P_{max}}{|\mathbf{h}_{12}^H \mathbf{w}_2|^2 P_{max}+1}$ and $c_2 = \frac{P_{max}}{|\mathbf{h}_{22}^H \mathbf{w}_2|^2 P_{max}+1}$ and we rewrite T_1 and D_1 to the following: $\tilde{D}_1 = 2^{D_1} - 1 = c_1|\mathbf{h}_{11}^H \mathbf{w}_1|^2$ and $\tilde{T}_1 = 2^{T_1} - 1 = c_2|\mathbf{h}_{21}^H \mathbf{w}_1|^2$. Thus, the maximin problem in (5.68) is equivalent to

$$\max_{\mathbf{w}_1\in\mathcal{W}_1} \min\{c_1|\mathbf{h}_{11}^H \mathbf{w}_1|^2, c_2|\mathbf{h}_{21}^H \mathbf{w}_1|^2\}, \quad \text{for arbitrary fixed } \mathbf{w}_2 \in \mathcal{S}. \tag{5.69}$$

Lemma 9. *The candidate set of the maximin problem in* (5.69) *and therefore maximum sum rate problem in* (5.68) *can be reduced from* $\mathcal{W}_1 \in \Omega^{nd}$ *to* $\tilde{\mathcal{W}}_1$ *which is a candidate set with cardinality three containing at least the maximum sum rate solution:* $|\tilde{\mathcal{W}}_1| = 3$*,*

$$\tilde{\mathcal{W}}_1 = \left\{ \frac{\mathbf{h}_{11}}{||\mathbf{h}_{11}||}, \frac{\mathbf{h}_{21}}{||\mathbf{h}_{21}||}, \mathbf{w}_1(\lambda_1^{(b)}) \right\} \tag{5.70}$$

with

$$\lambda_1^{(b)} = \frac{c_1||\Pi_{21}^{\perp}\mathbf{h}_{11}||^2}{c_2||\mathbf{h}_{21}||^2 - 2\sqrt{c_1c_2}|\mathbf{h}_{21}^H\mathbf{h}_{11}| + c_1||\mathbf{h}_{11}||^2}. \tag{5.71}$$

Proof. Because of the formulation of $\mathbf{w}_1 \in \mathcal{W}_1$, we can write the beamforming vector as a function of a real-valued parameter λ_1, $\mathbf{w}_1(\lambda_1)$. Using the result in Lemma 7, we define $f_1(\lambda_1) = c_1|\mathbf{h}_{11}^H\mathbf{w}_1(\lambda_1)|^2$ and $f_2(\lambda_1) = c_2|\mathbf{h}_{21}^H\mathbf{w}_1(\lambda_1)|^2$. It is easy to see that $f_1(\lambda_1)$ is concave in λ_1 and $f_2(\lambda_1)$ is linearly increasing with λ_1. The function $f_1(\lambda_1) = c_1|\mathbf{h}_{11}^H\mathbf{w}_1(\lambda_1)|^2$ attains maximum when $w_1(\lambda_1) = \frac{\mathbf{h}_{11}}{\|\mathbf{h}_{11}\|}$. Similarly, $f_2(\lambda_2)$ attains maximum when $w_1(\lambda_1) = \frac{\mathbf{h}_{21}}{\|\mathbf{h}_{21}\|}$. Now we compute $\lambda_1^{(b)}$ which satisfies $c_1|\mathbf{h}_{11}^H\mathbf{w}_1(\lambda_1^{(b)})|^2 = c_2|\mathbf{h}_{21}^H\mathbf{w}_1(\lambda_1^{(b)})|^2$.

To proceed, we compute the channel powers $|\mathbf{h}_{11}^H\mathbf{w}_1|^2 = \left(\sqrt{\lambda_1^{(b)}}\|\Pi_{21}\mathbf{h}_{11}\| + \sqrt{1-\lambda_1^{(b)}}\|\Pi_{21}^{\perp}\mathbf{h}_{11}\|\right)^2$ and $|\mathbf{h}_{21}^H\mathbf{w}_1|^2 = \lambda_1^{(b)}\|\mathbf{h}_{21}\|^2$. Notice that $\|\Pi_{21}\mathbf{h}_{11}\| = \|\mathbf{h}_{21}\|\cos(\phi)$ and $\|\Pi_{21}^{\perp}\mathbf{h}_{11}\| = \|\mathbf{h}_{21}\|\sin(\phi)$ where $|\mathbf{h}_{21}^H\mathbf{h}_{11}| = \|\mathbf{h}_{21}\|\|\mathbf{h}_{11}\|\cos(\phi)$ and by definition $\cos(\phi)$ is positive. Rewrite $\lambda_1^{(b)} = \cos^2(\theta)$ where $0 \le \theta \le \pi/2$. Thus, we can rewrite the channel powers to

$$\begin{aligned} |\mathbf{h}_{11}^H\mathbf{w}_1|^2 &= \|\mathbf{h}_{11}\|^2\cos^2(\theta-\phi), \\ |\mathbf{h}_{21}^H\mathbf{w}_1|^2 &= \cos^2(\theta)\|\mathbf{h}_{21}\|^2. \end{aligned} \tag{5.72}$$

Thus, $c_1|\mathbf{h}_{11}^H\mathbf{w}_1(\lambda_1^{(b)})|^2 = c_2|\mathbf{h}_{21}^H\mathbf{w}_1(\lambda_1^{(b)})|^2$ is equivalent to $\sqrt{c_1}\|\mathbf{h}_{11}\|\cos(\theta-\phi) = \sqrt{c_2}\cos(\theta)\|\mathbf{h}_{21}\|$ which is due to the fact that $\cos(\theta-\phi)$ and $\cos(\theta)$ are by definition positive. Putting the sinusoids one side and we obtain $\frac{\cos(\theta-\phi)}{\cos(\theta)} = \frac{\sqrt{c_2}\|\mathbf{h}_{21}\|}{\sqrt{c_1}\|\mathbf{h}_{11}\|}$. If we expand $\cos(\theta-\phi) = \cos(\theta)\cos(\phi) + \sin(\theta)\sin(\phi)$, we have

$$\tan(\theta) = \frac{\sqrt{c_2}\|\mathbf{h}_{21}\| - \sqrt{c_1}\|\mathbf{h}_{11}\|\cos(\phi)}{\sqrt{c_1}\|\mathbf{h}_{11}\|\sin(\phi)}. \tag{5.73}$$

Use the Pythagorus theorem, if $\tan(\theta) = \frac{a}{b}$ then $\cos(\theta) = \frac{b}{\sqrt{a^2+b^2}}$ and therefore

$$\lambda_1^{(b)} = \cos^2(\theta) = \frac{c_1\|\Pi_{21}^{\perp}\mathbf{h}_{11}\|^2}{c_2\|\mathbf{h}_{21}\|^2 - 2\sqrt{c_1c_2}|\mathbf{h}_{21}^H\mathbf{h}_{11}| + c_1\|\mathbf{h}_{11}\|^2}. \tag{5.74}$$

□

If we reverse the maximization order in (5.67), we obtain:

$$\bar{R}^{nd}(\mathbf{w}_1,\mathbf{w}_2) = \max_{\mathbf{w}_1\in\tilde{\mathcal{W}}_1}\max_{\mathbf{w}_2\in\mathcal{W}_2}\min\{C_2(\mathbf{w}_2)+T_1(\mathbf{w}_1,\mathbf{w}_2), C_2(\mathbf{w}_2)+D_1(\mathbf{w}_1,\mathbf{w}_2)\} \tag{5.75}$$

Lemma 10. *The optimal solutions to* $\bar{R}^{nd}$ *in* (5.75) *can be reduced from* $\mathcal{W}_2 \in \Omega^{nd}$ *to* $\tilde{\mathcal{W}}_2$*, a set of beamforming vectors that includes the beamforming vector towards the desired channel* $\mathbf{h}_{22}$*,*

$$\tilde{\mathcal{W}}_2 = \left\{ \mathbf{w}_2 \in \mathcal{S} : \mathbf{w}_2 = \sqrt{\lambda_2}\frac{\Pi_{12}\mathbf{h}_{22}}{\|\Pi_{12}\mathbf{h}_{22}\|} + \sqrt{1-\lambda_2}\frac{\Pi_{12}^{\perp}\mathbf{h}_{22}}{\|\Pi_{12}^{\perp}\mathbf{h}_{22}\|} \;;\; \lambda_2^{(b)} \le \lambda_2 \le \lambda_2^{\mathrm{MRT}} \right\} \tag{5.76}$$

where $\lambda_2^{\mathrm{MRT}} = \frac{|\mathbf{h}_{12}^H \mathbf{h}_{22}|}{||\mathbf{h}_{12}||||\mathbf{h}_{22}||}$ *is parameter that gives the beamforming solution towards channel* $\mathbf{h}_{22}$ *and*

$$\mathbf{w}_2(\lambda_2^{(b)}) = \frac{\tilde{b}}{\sqrt{\tilde{a}+\tilde{b}}}\mathbf{v}_a + \frac{e^{j\phi}\tilde{a}}{\sqrt{\tilde{a}+\tilde{b}}}\mathbf{v}_b \tag{5.77}$$

for some eigenvectors $\mathbf{v}_a, \mathbf{v}_b$ *and positive scalars* $\tilde{a}, \tilde{b}$*. The vectors* $\mathbf{v}_a, \mathbf{v}_b$ *are the most and least dominant eigenvectors of the matrix* $\mathbf{S} = \mathbf{h}_{22}\mathbf{h}_{22}^H - \frac{g_{21}}{g_{11}}\mathbf{h}_{12}\mathbf{h}_{12}^H$*.*

Proof. $\bar{R}^{nd}$ in (5.75) is equivalent to compute

$$\max_{\mathbf{w}_2|\mathbf{w}_1} \min \left\{ 1 + g_{21} + |\mathbf{h}_{22}^H \mathbf{w}_2|^2 P_2, (1 + |\mathbf{h}_{22}^H \mathbf{w}_2|^2 P_{max}) \left(1 + \frac{g_{11}}{1 + |\mathbf{h}_{12}^H \mathbf{w}_2|^2 P_{max}} \right) \right\}, \tag{5.78}$$

where the notation $\max_{\mathbf{w}_2|\mathbf{w}_1}$ denotes maximization over $\mathbf{w}_2$ for some given $\mathbf{w}_1$ and can be decomposed into the following two subproblems:

$$\begin{cases} \max_{\mathbf{w}_2|\mathbf{w}_1} 1 + g_{21} + |\mathbf{h}_{22}^H \mathbf{w}_2|^2 P_{max} & \text{if } |\mathbf{h}_{22}^H \mathbf{w}_2|^2 P_{max} \geq \frac{g_{21}}{g_{11}} - 1 + \frac{g_{21}}{g_{11}} |\mathbf{h}_{12}^H \mathbf{w}_2|^2 P_{max} \\ \max_{\mathbf{w}_2|\mathbf{w}_1} (1 + |\mathbf{h}_{22}^H \mathbf{w}_2|^2 P_2) \left(1 + \frac{g_{11}}{1 + |\mathbf{h}_{12}^H \mathbf{w}_2|^2 P_{max}} \right) & \text{if } |\mathbf{h}_{22}^H \mathbf{w}_2|^2 P_{max} \leq \frac{g_{21}}{g_{11}} - 1 + \frac{g_{21}}{g_{11}} |\mathbf{h}_{12}^H \mathbf{w}_2|^2 P_{max} \end{cases}. \tag{5.79}$$

The first subproblem has optimum solution $\frac{\mathbf{h}_{22}}{\|\mathbf{h}_{22}\|}$. For the second subproblem, the optimal λ_2 must be in the region $\Lambda = \{\lambda_2 : \lambda_2^{(b)} \leq \lambda_2 \leq \lambda_2^{\mathrm{MRT}}\}$ where $\mathbf{w}_2(\lambda_2^{\mathrm{MRT}}) = \frac{\mathbf{h}_{22}}{\|\mathbf{h}_{22}\|}$ and $|\mathbf{h}_{22}^H \mathbf{w}_2(\lambda_2^{(b)})|^2 P_{max} = \frac{g_{21}}{g_{11}} - 1 + \frac{g_{21}}{g_{11}} |\mathbf{h}_{12}^H \mathbf{w}_2(\lambda_2^{(b)})|^2 P_{max}$. To see this, we write the metric in the second subproblem as a function of λ_2:

$$F(\lambda_2) = (1 + |\mathbf{h}_{22}^H \mathbf{w}_2(\lambda_2)|^2 P_{max}) \left(1 + \frac{g_{11}}{1 + |\mathbf{h}_{12}^H \mathbf{w}_2(\lambda_2)|^2 P_{max}} \right)$$

Assume $\lambda^+, \lambda^- \notin \Lambda$, in particular, $\lambda^+ \geq \lambda_2^{\mathrm{MRT}}$ and $\lambda^- \leq \lambda_2^{(b)}$, we have

$$|\mathbf{h}_{12}^H \mathbf{w}_2(\lambda^+)|^2 = \lambda^+ \|\mathbf{h}_{12}\|^2 \geq \lambda^{\mathrm{MRT}} \|\mathbf{h}_{12}\|^2 \tag{5.80}$$

$$|\mathbf{h}_{22}^H \mathbf{w}_2(\lambda^+)|^2 \leq |\mathbf{h}_{22}^H \mathbf{w}_2(\lambda^{\mathrm{MRT}})|^2 = \|\mathbf{h}_{22}\|^2. \tag{5.81}$$

Thus, any λ^+ achieves $F(\lambda^+)$ smaller than $F(\lambda^{\mathrm{MRT}})$. Note that for any $\lambda^- \leq \lambda_2^{(b)}$, $\mathbf{w}_2(\lambda_2^-)$ is not in the constraint set of the second optimization problem. It is because $|\mathbf{h}_{22}^H \mathbf{w}_2(\lambda)|^2$ is concave in λ and attains the maximum at λ_2^{MRT} and $|\mathbf{h}_{12}^H \mathbf{w}_2(\lambda)|^2$ is linearly increasing with λ. Since $\lambda_2^{(b)} < \lambda_2^{\mathrm{MRT}}$, for points $\lambda^- \leq \lambda_2^{(b)}$, we have $|\mathbf{h}_{22}^H \mathbf{w}_2(\lambda^-)|^2 > \frac{g_{21}}{g_{11}} - 1 + \frac{g_{21}}{g_{11}} |\mathbf{h}_{12}^H \mathbf{w}_2(\lambda^-)|^2$.

Unfortunately, the direct computation of $\lambda_2^{(b)}$ is tedious and does not give much insight. Here, we provide a cleaner method of computing $\mathbf{w}_2(\lambda^{(b)})$ directly. Denote $g = \frac{g_{21}}{g_{11}}$. We compute the beamforming vector $\mathbf{w}_2$ such that

$$|\mathbf{h}_{22}^H \mathbf{w}_2|^2 P_2 = g - 1 + g |\mathbf{h}_{12}^H \mathbf{w}_2|^2 P_2. \tag{5.82}$$

Define $\mathbf{S} = \mathbf{h}_{22}\mathbf{h}_{22}^H - g\mathbf{h}_{12}\mathbf{h}_{12}$, $\tilde{\mathbf{S}} = \mathbf{S} - (g-1)\mathbf{I}$.

$$\mathbf{w}_2^H \tilde{\mathbf{S}} \mathbf{w}_2 = 0 \tag{5.83}$$

is a necessary condition for satisfying (5.82).

From the definition of $\mathbf{S}$, we know that $\mathbf{S}$ is rank two with one positive eigenvalue and one negative eigenvalue [42]. Denote the non-zero eigenvalues of $\mathbf{S}$ by a and $-b$ where $a, b > 0$. Employ eigenvalue decomposition on $\mathbf{S}$ and we have

$$\mathbf{S} = [\mathbf{v}_a \mathbf{v}_b | \mathbf{V}] \begin{bmatrix} a & 0 & \mathbf{0}_{1\times(N-2)} \\ 0 & -b & \mathbf{0}_{1\times(N-1)} \\ 0 & 0 & \mathbf{0}_{(N-2)\times(N-2)} \end{bmatrix} [\mathbf{v}_a \mathbf{v}_b | \mathbf{V}]^H \tag{5.84}$$

where $\mathbf{V}$ is the N by $N-2$ matrix with column vectors of eigenvectors of $\mathbf{S}$ that are orthogonal to $\mathbf{v}_a$, $\mathbf{v}_b$. With the same eigenvectors, we can write $\tilde{\mathbf{S}}$ as the following:

$$\tilde{\mathbf{S}} = [\mathbf{v}_a \mathbf{v}_b | \mathbf{V}] \begin{bmatrix} a-(g-1) & 0 & \mathbf{0}_{1\times(N-2)} \\ 0 & -b-(g-1) & \mathbf{0}_{1\times(N-1)} \\ 0 & 0 & -(g-1)\mathbf{I}_{(N-2)\times(N-2)} \end{bmatrix} [\mathbf{v}_a \mathbf{v}_b | \mathbf{V}]^H \tag{5.85}$$

Let $\tilde{a} = a-(g-1), \tilde{b} = b-(g-1)$. The beamforming vector $\mathbf{w}_2$ of the following form

$$\mathbf{w}_2 = \frac{1}{\sqrt{\tilde{a}}}\mathbf{v}_a + \frac{e^{j\phi}}{\sqrt{\tilde{b}}}\mathbf{v}_b \tag{5.86}$$

satisfies $\mathbf{w}_2^H \tilde{\mathbf{S}} \mathbf{w}_2 = 0$, where $j = \sqrt{-1}$ and ϕ is a phase angle between 0 to π. Notice that if $\mathbf{w}_2$ has any power on the remaining orthogonal subspace spanned by $\mathbf{V}$, $\mathbf{w}_2$ also satisfies (5.82) but the value of $|\mathbf{h}_{22}^H \mathbf{w}_2|^2$ is smaller and therefore cannot achieve the maximum sum rate. It is easy to see the result by direct computation: $\mathbf{w}_2^H \tilde{\mathbf{S}} \mathbf{w}_2 = \left(\frac{1}{\sqrt{\tilde{a}}}\mathbf{v}_a^H + \frac{e^{-j\phi}}{\sqrt{\tilde{b}}}\mathbf{v}_b^H\right)[\mathbf{v}_a \mathbf{v}_b] \begin{bmatrix} \tilde{a} & 0 \\ 0 & -\tilde{b} \end{bmatrix} [\mathbf{v}_a \mathbf{v}_b]^H \left(\frac{1}{\sqrt{\tilde{a}}}\mathbf{v}_a + \frac{e^{j\phi}}{\sqrt{\tilde{b}}}\mathbf{v}_b\right) = 0$ for given angle ϕ. The formulation in (5.86) gives a family of beamforming vectors, each with a different value of ϕ. To fine the unique ϕ and therefore $\mathbf{w}_2$ that maximizes sum rate, we rewrite the optimization problem in (5.69) to

$$\begin{aligned} \max_{\phi} \quad & |\mathbf{h}_{22}^H \mathbf{w}_2(\phi)|^2 \\ \text{such that} \quad & \mathbf{w}_2 = \tfrac{1}{\sqrt{\tilde{a}}}\mathbf{v}_a + \tfrac{e^{j\phi}}{\sqrt{\tilde{b}}}\mathbf{v}_b. \end{aligned} \tag{5.87}$$

Define the following phase angles, $\phi_a = \arg(\mathbf{h}_{22}^H \mathbf{v}_a), \phi_b = \arg(\mathbf{h}_{22}^H \mathbf{v}_b)$ and therefore

$$\phi_m = \arctan\left(\frac{Im(\mathbf{h}_{22}^H \mathbf{v}_m)}{Re(\mathbf{h}_{22}^H \mathbf{v}_m)}\right) + \begin{cases} \pi & Re(\mathbf{h}_{22}^H \mathbf{v}_m) < 0 \\ 0 & \text{otherwise.} \end{cases}, \quad m = a, b.$$

The optimization problem in (5.87) is therefore equivalent to

$$\max_{\phi} |\mathbf{h}_{22}^H \mathbf{w}_2|^2 = \max_{\phi} \left| \frac{1}{\sqrt{\tilde{a}}} |\mathbf{h}_{22}^H \mathbf{v}_a| e^{j\phi_a} + \frac{e^{j\phi}}{\sqrt{\tilde{b}}} |\mathbf{h}_{22}^H \mathbf{v}_b| e^{j\phi_b} \right|^2 = \max_{\phi} \left| \frac{1}{\sqrt{\tilde{a}}} |\mathbf{h}_{22}^H \mathbf{v}_a| + \frac{e^{j(\phi+\phi_b-\phi_a)}}{\sqrt{\tilde{b}}} |\mathbf{h}_{22}^H \mathbf{v}_b| \right|^2.$$

Thus, the optimal phase angle ϕ is

$$\phi = \phi_a - \phi_b. \tag{5.88}$$

To satisfy the norm constraint, we can scale the beamforming vector with a positive scalar, which does not change the direction of the vector.

$$\mathbf{w}_2 = \frac{\tilde{b}}{\sqrt{\tilde{a}+\tilde{b}}}\mathbf{v}_a + \frac{e^{j\phi}\tilde{a}}{\sqrt{\tilde{a}+\tilde{b}}}\mathbf{v}_b. \tag{5.89}$$

□

Note that if $\lambda_2^b > \lambda_2^{mrt}$, then $\tilde{\mathcal{W}}_2$ has only one element, i.e. $\frac{\mathbf{h}_{22}}{\|\mathbf{h}_{22}\|}$. Lemma 9 gives the optimal candidate set for $\mathbf{w}_1$ for arbitrary fixed $\mathbf{w}_2$ whereas Lemma 10 gives the optimal candidate set for $\mathbf{w}_2$ for arbitrary fixed $\mathbf{w}_1$. Combining both Lemmas, we obtain the maximum sum rate candidate sets for both $\mathbf{w}_1$ and $\mathbf{w}_2$.

Remark 6. *The authors in [65] provided a general solution of* (5.69)*, in the context of a multicast SNR balancing problem. The authors transformed the channel powers balancing problem to a weighted sum channel powers maximization problem for some positive weights w_1, w_2. The optimal beamforming vector is then characterized as a dominant eigenvector of some matrices, depending on w_1, w_2. However, the computation of such weights w_1, w_2 is not provided or trivial. In this paper, due to the beamforming vectors parameterization proposed in Thm. 12 and 13, we obtained the closed form solution of such channel powers balancing beamforming vectors.*

5.11.5 Proof of Thm. 15

In this section, we provide the proof of Thm. 15. We start by identifying four constraint sets of beamforming vectors $\Omega^{00}, \Omega^{01}, \Omega^{10}, \Omega^{11}$ where the sum rate function is a different function in each set. In other words, when the beamforming vectors vary, the sum rate function being a sum of two minimum of rate functions, may change from one rate expression to another rate expression. The constraint sets are the set of beamforming vectors for which the sum rate function remains at one rate function. In the following, we provide the analysis for $\mathbf{w}_2$ but the sum rate function $\bar{R}^{dd}$ is symmetric with Tx 1 and 2. Therefore, we can exchange the role of Tx 1 and 2 and obtain the candidate sets for $\mathbf{w}_1$. The sum rate in the DD region is:

$$\begin{aligned}\bar{R}^{dd} &= \min\{C_1, T_1\} + \min\{C_2 + T_2\} \\ &= \min\{\underbrace{C_1 + C_2}_{Z_1}, \underbrace{C_1 + T_2}_{Z_2}, \underbrace{T_1 + C_2}_{Z_3}, \underbrace{T_1 + T_2}_{Z_4}\}.\end{aligned} \tag{5.90}$$

We analyze each term and define $\tilde{Z}_i = 2^{Z_i}, i = 1, \ldots, 4$

$$\begin{aligned}\tilde{Z}_1 &= (1 + |\mathbf{h}_{11}^H \mathbf{w}_1|^2 P)(1 + |\mathbf{h}_{22}^H \mathbf{w}_2|^2 P) \\ \tilde{Z}_2 &= 1 + |\mathbf{h}_{11}^H \mathbf{w}_1|^2 P + |\mathbf{h}_{12}^H \mathbf{w}_2|^2 P \\ \tilde{Z}_3 &= 1 + |\mathbf{h}_{21}^H \mathbf{w}_1|^2 P + |\mathbf{h}_{22}^H \mathbf{w}_2|^2 P \\ \tilde{Z}_4 &= \left(1 + \frac{|\mathbf{h}_{21}^H \mathbf{w}_1|^2 P}{1 + |\mathbf{h}_{22}^H \mathbf{w}_2|^2 P}\right)\left(1 + \frac{|\mathbf{h}_{12}^H \mathbf{w}_2|^2 P}{1 + |\mathbf{h}_{11}^H \mathbf{w}_1|^2 P}\right) \\ &= \frac{\tilde{Z}_2 \tilde{Z}_3}{\tilde{Z}_1}.\end{aligned} \tag{5.91}$$

Notice that $\tilde{Z}_1 < \tilde{Z}_2$ is equivalent to $\tilde{Z}_3 < \tilde{Z}_4$ and $\tilde{Z}_1 < \tilde{Z}_3$ is equivalent to $\tilde{Z}_2 < \tilde{Z}_4$. We summarize to the following lemma.

Lemma 11. *Let $g_{11} = |\mathbf{h}_{11}^H \mathbf{w}_1|^2 P_1$ and $g_{21} = |\mathbf{h}_{21}^H \mathbf{w}_1|^2 P_1$.*

$$\begin{aligned}\tilde{Z}_1 \leq \tilde{Z}_2 &\Leftrightarrow \tilde{Z}_3 \leq \tilde{Z}_4 \\ &\Leftrightarrow (1 + g_{11})|\mathbf{h}_{22}^H \mathbf{w}_2|^2 \leq |\mathbf{h}_{12}^H \mathbf{w}_2|^2 \\ \tilde{Z}_1 \leq \tilde{Z}_3 &\Leftrightarrow \tilde{Z}_2 \leq \tilde{Z}_4 \\ &\Leftrightarrow |\mathbf{h}_{22}^H \mathbf{w}_2|^2 P_2 \leq \frac{g_{21}}{g_{11}} - 1\end{aligned}$$

Proof. It is by direct manipulation of the definitions. □

To facilitate representation, we denote the following two indicators and the corresponding candidate sets:

$$A = \begin{cases} 1 & \text{if } (1+g_{11})|\mathbf{h}_{22}^H\mathbf{w}_2|^2P_2 \le |\mathbf{h}_{12}^H\mathbf{w}_2|^2P_2 \\ 0 & \text{otherwise.} \end{cases} \quad (5.92)$$

$$B = \begin{cases} 1 & \text{if } |\mathbf{h}_{22}^H\mathbf{w}_2|^2P_2 \le \frac{g_{21}}{g_{11}} - 1 \\ 0 & \text{otherwise.} \end{cases} \quad (5.93)$$

$$\Omega^{ab} = \{\mathbf{w}_2 : \|\mathbf{w}_2\| = 1, A = a, B = b\} \quad (5.94)$$

Notice that $\Omega^{ab}, a, b = 0, 1$, gives four constraint sets. By Lem. 11, we can decompose the optimization problem in (5.90) to the following:

$$\bar{R}^{dd} = \log_2\left(\max_{\mathbf{w}_1\in\mathcal{S}}\max_{\mathbf{w}_2\in\mathcal{S}|\mathbf{w}_1}\min\{\tilde{Z}_1,\tilde{Z}_2,\tilde{Z}_3,\tilde{Z}_4\}\right)$$
$$= \begin{cases} \log_2\left(\max_{\mathbf{w}_1}\max_{\mathbf{w}_2\in\Omega^{11}}\tilde{Z}_1\right) & \text{if } A=1, B=1 \\ \log_2\left(\max_{\mathbf{w}_1}\max_{\mathbf{w}_2\in\Omega^{01}}\tilde{Z}_2\right) & \text{if } A=0, B=1 \\ \log_2\left(\max_{\mathbf{w}_1}\max_{\mathbf{w}_2\in\Omega^{10}}\tilde{Z}_3\right) & \text{if } A=1, B=0 \\ \log_2\left(\max_{\mathbf{w}_1}\max_{\mathbf{w}_2\in\Omega^{00}}\tilde{Z}_4\right) & \text{if } A=0, B=0 \end{cases}.$$

Now, we proceed with the proof of Thm. 15 in two parts: first, in Section 5.11.5.1, we identify the candidate sets for each of the subproblems $\tilde{Z}_i, i = 1, \ldots, 4$; second, in Section 5.11.5.2, we combine these candidate sets to one superset by eliminating beamforming vectors, which are on the boundary of the constraint sets, if they achieve smaller sum rate than other beamforming vectors.

5.11.5.1 The candidate sets of subproblems $\tilde{Z}_i$

The candidate sets for each of the subproblem is as follows:

- If $\mathbf{w} = \arg\max_{\mathbf{w}_2\in\Omega^{11}}\tilde{Z}_1$, then $\mathbf{w} \in \Omega^A \bigcup \Omega^B \bigcup \frac{\mathbf{h}_{22}}{\|\mathbf{h}_{22}\|}$
- If $\mathbf{w} = \arg\max_{\mathbf{w}_2\in\Omega^{01}}\tilde{Z}_2$, then $\mathbf{w} \in \mathbf{w}_2(\lambda_2^A) \bigcup \mathbf{w}_2^{AB} \bigcup \frac{\mathbf{h}_{12}}{\|\mathbf{h}_{12}\|}$.
- If $\mathbf{w} = \arg\max_{\mathbf{w}_2\in\Omega^{10}}\tilde{Z}_3$, then $\mathbf{w} \in \mathbf{w}_2(\lambda_2^A) \bigcup \frac{\mathbf{h}_{22}}{\|\mathbf{h}_{22}\|}$.
- If $\mathbf{w} = \arg\max_{\mathbf{w}_2\in\Omega^{00}}\tilde{Z}_4$, then $\mathbf{w} \in \Omega^A \bigcup \tilde{\mathcal{W}}_2^{dd}$

where the constraints Ω^A and Ω^B are the set of beamforming vectors that satisfy the constraints by equality $\Omega^A = \left\{\mathbf{w}_2 : (1+g_{11})|\mathbf{h}_{22}^H\mathbf{w}_2|^2 = |\mathbf{h}_{12}^H\mathbf{w}_2|^2\right\}$ and $\Omega^B = \left\{\mathbf{w}_2 : |\mathbf{h}_{22}^H\mathbf{w}_2|^2P_2 = \frac{g_{21}}{g_{11}} - 1\right\}$. The beamforming vector $\mathbf{w}_2(\lambda_2^A)$ is the beamforming vector in Ω^A that maximizes the desired channel power, $\mathbf{w}_2(\lambda_2^A) = \arg\max_{\mathbf{w}_2\in\Omega^A}(1+g_{11})|\mathbf{h}_{22}^H\mathbf{w}_2|^2$. The beamforming vector $\mathbf{w}_2^{AB}$ is a unique vector that is a member of both Ω^A and Ω^B, $\mathbf{w}_2^{AB} = \Omega^A \bigcap \Omega^B$. Lastly, we have $\tilde{\mathcal{V}}_2$ which is a subset of $\mathcal{V}_2$, $\tilde{\mathcal{V}}_2 = \left\{\mathbf{w}_2 : \sqrt{\lambda_2}\frac{\Pi_{22}\mathbf{h}_{12}}{\|\Pi_{22}\mathbf{h}_{12}\|} + \sqrt{1-\lambda_2}\frac{\Pi_{22}^{\perp}\mathbf{h}_{12}}{\|\Pi_{22}^{\perp}\mathbf{h}_{12}\|}, \lambda_2^A \le \lambda_2 \le \lambda_2^{\mathrm{MRT}}\right\}$ where $\lambda_2^{\mathrm{MRT}} = \frac{|\mathbf{h}_{22}^H\mathbf{h}_{12}|^2}{\|\mathbf{h}_{22}\|^2\|\mathbf{h}_{12}\|^2}$.

Notice that beamforming vectors in Ω^A, Ω^B satisfy the constraints in (5.92) with equality. To see this, we have the following observations:

1. $\tilde{Z}_1$ is monotonically increasing with $|\mathbf{h}_{22}^H \mathbf{w}_2|^2$. If the constraints are not active, the optimal solution is $\frac{\mathbf{h}_{22}}{\|\mathbf{h}_{22}\|}$. If the constraints are active, $\tilde{Z}_1$ is maximized over constraint set Ω^{11} and therefore the optimal solutions are in $\Omega^A \bigcup \Omega^B$.

2. $\tilde{Z}_2$ is monotonically increasing with $|\mathbf{h}_{12}^H \mathbf{w}_2|^2$in constraint set Ω^{01}. If the constraints are not active, the optimal solution is $\frac{\mathbf{h}_{12}}{\|\mathbf{h}_{12}\|}$. There are an upper bound on $|\mathbf{h}_{12}^H \mathbf{w}_2|^2$ and an upper bound on $|\mathbf{h}_{22}^H \mathbf{w}_2|^2$ which in turn upper bound $|\mathbf{h}_{12}^H \mathbf{w}_2|^2$. If the constraint for $|\mathbf{h}_{12}^H \mathbf{w}_2|^2$ is active, the solution is $\mathbf{w}_2(\lambda_2^A)$. If both are active, the solution is $\mathbf{w}_2^{AB}$. Thus, the candidate set is $\left\{\mathbf{w}_2(\lambda_2^A), \mathbf{w}_2^{AB}, \frac{\mathbf{h}_{12}}{\|\mathbf{h}_{12}\|}\right\}$.

3. $\tilde{Z}_3$ is monotonically increasing with $|\mathbf{h}_{22}^H \mathbf{w}_2|^2$ in constraint set Ω^{10}. There is only one constraint that upper bound the value of $|\mathbf{h}_{22}^H \mathbf{w}_2|^2$, the optimal solution is in set Ω^A which at the same time maximizes $|\mathbf{h}_{22}^H \mathbf{w}_2|^2$, denote as $\mathbf{w}_2(\lambda_2^A)$. If the constraints are not active, we have $\frac{\mathbf{h}_{22}}{\|\mathbf{h}_{22}\|}$.

4. $\tilde{Z}_4$ is monotonically increasing with $|\mathbf{h}_{12}^H \mathbf{w}_2|^2$ and decreasing with $|\mathbf{h}_{22}^H \mathbf{w}_2|^2$ in constraint set Ω^{00}. If the constraints are active, the optimal solutions are in Ω^A. If the constraints are not active, the optimal solutions are in $\tilde{\mathcal{V}}_2$. Similar to the case of $\bar{\mathcal{R}}^{nd}$, any $\lambda \notin (\lambda_2^A \leq \lambda_2 \leq \lambda_2^{\mathrm{MRT}})$ cannot attain maximum value of $\tilde{Z}_4$ in Ω^{00}. Notice that for any $\lambda \geq \lambda^{mrt}$, $|\mathbf{h}_{12}^H \mathbf{w}_2(\lambda)|^2 \leq |\mathbf{h}_{12}^H \mathbf{w}_2(\lambda_2^{\mathrm{MRT}})|^2$ and $|\mathbf{h}_{22}^H \mathbf{w}_2(\lambda)|^2 = \lambda \|\mathbf{h}_{12}\|^2 \geq \lambda_2^{\mathrm{MRT}} \|\mathbf{h}_{12}\|^2 = |\mathbf{h}_{12}^H \mathbf{w}_2(\lambda_2^{mrt})|^2$. Thus, $\tilde{Z}_4(\lambda) \leq \tilde{Z}_4(\lambda_2^{\mathrm{MRT}})$, for any $\lambda \geq \lambda_2^{\mathrm{MRT}}$. Also, for any $\lambda < \lambda_2^A$, $(1+g_{11})|\mathbf{h}_{22}^H \mathbf{w}_2(\lambda)|^2 \leq |\mathbf{h}_{12}^H \mathbf{w}_2(\lambda)|^2$. It is because $|\mathbf{h}_{12}^H \mathbf{w}_2(\lambda)|^2$ is concave in λ and attains maximum at λ_2^{MRT} whereas $|\mathbf{h}_{22}^H \mathbf{w}_2(\lambda)|^2$ is linearly increasing with λ. Since the intersection point $\lambda_2^A \leq \lambda_2^{mrt}$, we have $(1+g_{11})|\mathbf{h}_{22}^H \mathbf{w}_2(\lambda)|^2 \leq |\mathbf{h}_{12}^H \mathbf{w}_2(\lambda)|^2$ which violates the constraint set requirement.

5.11.5.2 Eliminating non-sum-rate optimal solutions

Now, we combine the above results. For any solutions $\omega \in \Omega^A$, we have $\omega \in \Omega^{0b}$ and $\omega \in \Omega^{1b}$ for $b = 0, 1$. This is because ω is on the boundary separating Ω^{0b}, Ω^{1b}. Thus, if ω is sum rate optimal in Ω^{0b} but *not* sum rate optimal in Ω^{1b}, then the sum rate optimal solutions in Ω^{1b} achieves a higher sum rate than ω which is in the *same* constraint set. Then, ω can be removed from the candidate sets of the maximum sum rate point over constraint sets $\Omega^{0b} \bigcup \Omega^{1b}$. Applying this argument, we combine the following:

For any $\omega \in \Omega^A$ which maximizes $\tilde{Z}_4$ in Ω^{00} is also in Ω^{10} and achieves a *smaller* $\tilde{Z}_3$ than other sum rate optimal solutions in Ω^{10}, namely $\mathbf{w}_2(\lambda_2^A) \bigcup \frac{\mathbf{h}_{22}}{\|\mathbf{h}_{22}\|}$. Thus, we have:

$$\text{If } \omega = \arg \max_{\mathbf{w}_2 \in \Omega^{10} \bigcup \Omega^{00}} \min \left\{\tilde{Z}_3, \tilde{Z}_4\right\}, \text{ then } \omega \in \mathbf{w}_2(\lambda_2^A) \bigcup \frac{\mathbf{h}_{22}}{\|\mathbf{h}_{22}\|} \bigcup \tilde{\mathcal{V}}_2^{dd} \tag{5.95}$$

Similarly, for any $\omega \in \Omega^B$ which maximizes $\tilde{Z}_2$ in the constraint set Ω^{01} is also in Ω^{00} and achieves a smaller $\tilde{Z}_4$ than other solutions. Thus, we have:

$$\text{If } \omega = \arg \max_{\mathbf{w}_2 \in \Omega^{01} \bigcup \Omega^{10} \bigcup \Omega^{00}} \min \left\{\tilde{Z}_2, \tilde{Z}_3, \tilde{Z}_4\right\}, \text{ then } \omega \in \mathbf{w}_2(\lambda_2^A) \bigcup \frac{\mathbf{h}_{22}}{\|\mathbf{h}_{22}\|} \bigcup \tilde{\mathcal{V}}_2^{dd}. \tag{5.96}$$

The candidate set remains unchanged because $\mathbf{w}_2^{AB}$ performs worse than other solutions and $\frac{\mathbf{h}_{12}}{\|\mathbf{h}_{12}\|} \in \tilde{\mathcal{V}}_2^{dd}$.

Lastly, for any $\omega_b \in \Omega^B$ which maximizes $\tilde{Z}_1$ in constraint set Ω^{11} is also in Ω^{10} and achieves a smaller $\tilde{Z}_3$ than other solutions. And for $\omega_a \in \Omega^A$ which maximizes $\tilde{Z}_1$ in constraint set Ω^{11} is also in Ω^{01} and achieves a less $\tilde{Z}_2$ than other solutions. Thus, we have:

$$\text{If } \omega = \arg \max_{\mathbf{w}_2 \in \Omega^{11} \bigcup \Omega^{01} \bigcup \Omega^{10} \bigcup \Omega^{00}} \min\left\{\tilde{Z}_1, \tilde{Z}_2, \tilde{Z}_3, \tilde{Z}_4\right\}, \text{ then } \omega \in \mathbf{w}_2(\lambda_2^A) \bigcup \frac{\mathbf{h}_{22}}{\|\mathbf{h}_{22}\|} \bigcup \tilde{\mathcal{V}}_2^{dd}. \tag{5.97}$$

Therefore, the final candidate sets are

$$\mathcal{V}_i^{dd} = \left\{\frac{\mathbf{h}_{ii}}{\|\mathbf{h}_{ii}\|}, \tilde{\mathcal{V}}_i^{dd}, \mathbf{w}_i(\lambda_i^A)\right\}. \tag{5.98}$$

This result holds for $\mathbf{w}_1$ because the optimization problem is symmetric.

To compute the closed form λ_2^A where $\mathbf{w}_2(\lambda_2^A)$ balances channel powers, we can use the same approach as before to obtain $\lambda_2^A = \frac{\|\Pi_{\mathbf{h}_{22}}^{\perp}\mathbf{h}_{12}\|}{\|\mathbf{h}_{12}\|^2+(1+g_{11})\|\mathbf{h}_{22}\|^2-2|\mathbf{h}_{22}^H\mathbf{h}_{12}|\sqrt{1+g_{11}}}$.

5.11.6 Proof of MRT optimality conditions in the ND region

Define the following two functions in $0 \le \lambda_2 \le 1$:

- $F_1(\lambda_2)$ is a concave function in λ_2 and attains maximum at λ_2^{MRT}.
- $F_2(\lambda_2)$ is an arbitrary function in λ_2 but satisfy the following properties:
  - for any $\lambda > \lambda_2^{\text{MRT}}$, $F_2(\lambda) < F_2(\lambda_2^{\text{MRT}})$.
  - $\frac{\partial F_2(\lambda)}{\partial \lambda_2}\Big|_{\lambda_2=\lambda_2^{\text{MRT}}} < 0$.

Lemma 12. *The condition $F_2(\lambda_2^{\text{MRT}}) \ge F_1(\lambda_2^{\text{MRT}})$ is a necessary and sufficient condition for*

$$\lambda_2^{\text{MRT}} = \arg\max_{0\le\lambda_2\le 1} \min\{F_1(\lambda_2), F_2(\lambda_2)\}. \tag{5.99}$$

Proof. **"⇒":** Let $\lambda_2^* = \arg\max_{0\le\lambda_2\le 1} \min\{F_1(\lambda_2), F_2(\lambda_2)\}$. Denote a set Λ

$$\Lambda = \{\lambda_2 : F_1(\lambda_2) \le F_2(\lambda_2)\} \tag{5.100}$$

Let $\lambda_2' \in \Lambda$ and therefore $F_1(\lambda_2') \le F_1(\lambda_2^*) \le F_1(\lambda_2^{\text{MRT}})$. The second inequality is due to the fact that $F_1(\lambda_2)$ attains maximum at λ_2^{MRT}. Note that $F_1(\lambda_2^{\text{MRT}}) \le F_2(\lambda_2^{\text{MRT}})$ by assumption, thus $\lambda_2^{\text{MRT}} \in \Lambda$ and we can write

$$F_1(\lambda_2^{\text{MRT}}) \le F_1(\lambda_2^*) \le F_1(\lambda_2^{\text{MRT}}). \tag{5.101}$$

Since $F_1(\lambda_2)$ is a concave and has unique maximum at λ_2^{MRT}, we have $\lambda_2^* = \lambda_2^{\text{MRT}}$.

"⇐": We start with $\lambda_2^{\text{MRT}} = \arg\max_{\lambda_2} \min\{F_1(\lambda_2), F_2(\lambda_2)\}$ and we proceed with contradiction. Assume $F_1(\lambda_2^{\text{MRT}}) > F_2(\lambda_2^{\text{MRT}})$. Since $\frac{\partial F_2(\lambda)}{\partial \lambda_2}\Big|_{\lambda_2=\lambda_2^{\text{MRT}}} < 0$, there exist $\lambda_2^- = \lambda_2^{\text{MRT}} - \epsilon$ with arbitrary small $\epsilon > 0$, which satisfies $F_1(\lambda_2^-) \ge F_2(\lambda_2^-) \ge F_2(\lambda_2^{\text{MRT}})$ and contradicts to the assumption that $\lambda_2^{\text{MRT}} = \arg\max_{\lambda_2} \min\{F_1(\lambda_2), F_2(\lambda_2)\}$.

□

Note that the sum rate in the ND region is

$$\bar{R}^{nd} = \max_{0\leq\lambda_1,\lambda_2\leq 1} \min\{C_2(\lambda_2)+T_1(\lambda_1,\lambda_2), C_2(\lambda_2)+D_1(\lambda_1,\lambda_2)\}. \tag{5.102}$$

From Thm. 12, we can write the Pareto optimal beamforming vectors $\mathbf{w}_i$ in the ND region as a function of the real valued parameter λ_i in (5.21). Hence, we can rewrite the rate expressions in (5.3) as functions of $\lambda_i, i = 1, 2$:

$$\begin{aligned} 2^{C_2(\lambda_2)+T_1(\lambda_1,\lambda_2)} &= 1 + g_2(\lambda_2)P_{max} + \lambda_1\|\mathbf{h}_{21}\|^2 P_{max} \\ 2^{C_2(\lambda_2)+D_1(\lambda_1,\lambda_2)} &= (1+g_2(\lambda_2)P_{max})\left(1+\frac{g_1(\lambda_1)P_{max}}{1+\lambda_2\|\mathbf{h}_{12}\|^2 P_{max}}\right) \end{aligned} \tag{5.103}$$

where $g_1(\lambda_1) = \left(\sqrt{\lambda_1}\|\Pi_{21}\mathbf{h}_{11}\| + \sqrt{1-\lambda_1}\|\Pi_{21}^{\perp}\mathbf{h}_{11}\|\right)^2$ and $g_2(\lambda_2) = \left(\sqrt{\lambda_2}\|\Pi_{12}\mathbf{h}_{22}\| + \sqrt{1-\lambda_2}\|\Pi_{12}^{\perp}\mathbf{h}_{22}\|\right)^2$. Since logarithm function is monotonic, it does not change the maximization solution and from now on, we consider maximizing the minimum of the following two functions,

$$F_1(\lambda_1,\lambda_2) = 1 + g_2(\lambda_2)P_{max} + \lambda_1\|\mathbf{h}_{21}\|^2 P_{max} \tag{5.104}$$

$$F_2(\lambda_1,\lambda_2) = (1+g_2(\lambda_2)P_{max})\left(1+\frac{g_1(\lambda_1)P_{max}}{1+\lambda_2\|\mathbf{h}_{12}\|^2 P_{max}}\right). \tag{5.105}$$

Lemma 13. *It can be shown that the function $g_i(\lambda_i)$ is concave in λ_i for $i = 1, 2$. $F_1(\lambda_1, \lambda_2)$ is concave in λ_2 and attains its maximum at $\lambda_2^{\mathrm{MRT}} = \frac{\|\Pi_{21}\mathbf{h}_{11}\|^2}{\|\mathbf{h}_{21}\|^2\|\mathbf{h}_{11}\|^2}$.*

Proof. Note that the first and second derivatives of $g_i(\lambda_i)$ with respect to λ_i are $\frac{\partial}{\partial\lambda_i}g_i(\lambda_i) = \|\Pi_{ji}\mathbf{h}_{ii}\|^2 - \|\Pi_{ji}^{\perp}\mathbf{h}_{ii}\|^2 + \|\Pi_{ji}\mathbf{h}_{ii}\|\|\Pi_{ji}^{\perp}\mathbf{h}_{ii}\|\left(\frac{1-2\lambda_i}{\sqrt{\lambda_i}\sqrt{1-\lambda_i}}\right)$ and $\frac{\partial^2}{\partial\lambda_i^2}g_i(\lambda_i) = -\frac{\|\Pi_{ji}\mathbf{h}_{ii}\|\|\Pi_{ji}^{\perp}\mathbf{h}_{ii}\|}{2\lambda_i^{3/2}(1-\lambda_i)^{3/2}}$. Since λ_i is between zero and one, the second derivative of $g_i(\lambda_i)$ is always negative, for all λ_i. Set the first derivative to zero and we obtain the maximum $\lambda_2^{\mathrm{MRT}} = \frac{\|\Pi_{21}\mathbf{h}_{11}\|^2}{\|\mathbf{h}_{21}\|^2\|\mathbf{h}_{11}\|^2}$. □

Lemma 14. *$F_2(\lambda_1, \lambda_2)$ satisfies*

$$\left.\frac{\partial F_2(\lambda_1,\lambda_2)}{\partial\lambda_2}\right|_{\lambda_2=\lambda_2^{\mathrm{MRT}}} < 0.$$

Proof.

$$\begin{aligned} \left.\frac{\partial}{\partial\lambda_2}F_2(\lambda_1,\lambda_2)\right|_{\lambda_2=\lambda_2^{\mathrm{MRT}}} &= \left.\left(\frac{\partial}{\partial\lambda_2}(1+g_2(\lambda_2)P_{max})\right)\left(1+\frac{g_1(\lambda_1)P_{max}}{1+\lambda_2\|\mathbf{h}_{12}\|^2P_{max}}\right)\right|_{\lambda_2=\lambda_2^{\mathrm{MRT}}} \\ &\quad + \left.(1+g_2(\lambda_2)P_{max})\left(\frac{\partial}{\partial\lambda_2}\left(1+\frac{g_1(\lambda_1)P_{max}}{1+\lambda_2\|\mathbf{h}_{12}\|^2P_{max}}\right)\right)\right|_{\lambda_2=\lambda_2^{\mathrm{MRT}}} \\ &\overset{(a)}{=} \left.(1+g_2(\lambda_2)P_{max})\left(\frac{\partial}{\partial\lambda_2}\left(1+\frac{g_1(\lambda_1)P_{max}}{1+\lambda_2\|\mathbf{h}_{12}\|^2P_{max}}\right)\right)\right|_{\lambda_2=\lambda_2^{\mathrm{MRT}}} \\ &= -\left(1+\|\mathbf{h}_{22}\|^2P_{max}\right)\frac{g_1(\lambda_1)\|\mathbf{h}_{12}\|^2P_{max}}{(1+\lambda_2^{\mathrm{MRT}}\|\mathbf{h}_{12}\|^2P_{max})^2} \\ &< 0 \text{ for any } 0\leq\lambda_1\leq 1 \end{aligned}$$

where (a) is due to the fact that $g(\lambda_2)$ is concave and attains its maximum at λ_2^{MRT}. □

Lemma 15. *For any $\lambda > \lambda_2^{\mathrm{MRT}}$, $F_2(\lambda) < F_2(\lambda_2^{\mathrm{MRT}})$.*

Proof. For any λ, $g_2(\lambda) \leq g_2(\lambda_2^{\text{MRT}})$ because $g_2(.)$ is a concave function and attains maximum at λ_2^{MRT}. Also, for any $\lambda > \lambda_2^{\text{MRT}}$, the denominator of $F_2(\lambda_2)$ increases. Thus, for any $\lambda > \lambda_2^{\text{MRT}}$, $F_2(\lambda) < F_2(\lambda_2^{\text{MRT}})$. □

By Lemma 12, $\bar{R}^{nd}$ is maximized by λ_2^{MRT} for arbitrary fixed λ_1 if and only if $F_1(\lambda_1, \lambda_2^{\text{MRT}}) \leq F_2(\lambda_1, \lambda_2^{\text{MRT}})$ which is equivalent to the following:

$$F_1(\lambda_1, \lambda_2^{\text{MRT}}) \leq F_2(\lambda_1, \lambda_2^{\text{MRT}}) \quad \Leftrightarrow \quad \lambda_1 \|\mathbf{h}_{21}\|^2 \leq \frac{1 + \|\mathbf{h}_{22}\|^2 P_{max}}{1 + \|\mathbf{h}_{12}\|^2 \cos^2(\theta_2) P_{max}} g_1(\lambda_1) \tag{5.106}$$

Also, for arbitrary fixed λ_2, $F_1(\lambda_1, \lambda_2)$ is linearly increasing with λ_1 and $F_2(\lambda_1, \lambda_2)$ is concave in λ_1 and attains maximum at λ_1^{MRT}. Similar to the argument before, there are at most 2 intersection points between $F_1(\lambda_1, \lambda_2)$ and $F_2(\lambda_1, \lambda_2)$. We observe that

$$\begin{aligned} F_1(0, \lambda_2) &= 1 + g_2(\lambda_2) P_{max} \\ &< (1 + g_2(\lambda_2) P_{max}) \left(1 + \frac{g_1(0) P_{max}}{1 + \lambda_2 \|\mathbf{h}_{12}\|^2 P_{max}}\right) \\ &= F_2(0, \lambda_2). \end{aligned} \tag{5.107}$$

Note that $g_1(0) > 0$ except when $\mathbf{h}_{11}$ is orthogonal to $\mathbf{h}_{21}$ whose probability is zero almost surely. Since $F_1(0, \lambda_2) < F_2(0, \lambda_2)$ for any λ_2, there is at most 1 intersection point. If there is no intersection point, the curve $F_2(\lambda_1, \lambda_2)$ is above $F_1(\lambda_1, \lambda_2)$ for any λ_1 and therefore the optimal value of λ_1 which maximizes $F_1(\lambda_1, \lambda_2)$ at $\lambda_1 = 1$. If there is 1 intersection point, denote the intersection solution as $\lambda_1^{(b)}$. Graphically, it is clear to see that if and only if $\lambda_1^{(b)} < \lambda_1^{\text{MRT}}$, the optimal solution is $\lambda_1 = \lambda_1^{\text{MRT}}$. Thus, we have for arbitrary fixed λ_2,

$$\begin{aligned} \lambda_1 = 1 \quad &\text{is optimal if and only if} \quad F_1(1, \lambda_2) < F_2(1, \lambda_2) \\ \lambda_1 = \lambda_1^{\text{MRT}} \quad &\text{is optimal if and only if} \quad \lambda_1^{(b)} \leq \lambda_1^{\text{MRT}} \end{aligned}$$

where $\lambda_1^{(b)}$ is given in (5.71). Now we combine the conditions for λ_1 and λ_2 and after some manipulations, we obtain the following:

$(\lambda_1^{\text{MRT}}, \lambda_2^{\text{MRT}})$ is optimal if and only if

$$\frac{c_1 \|\Pi_{21}^{\perp} \mathbf{h}_{11}\|^2}{c_2 \|\mathbf{h}_{21}\|^2 - 2\sqrt{c_1 c_2} |\mathbf{h}_{21}^H \mathbf{h}_{11}| + c_1 \|\mathbf{h}_{11}\|^2} < \cos^2(\theta_1) \leq \frac{(1 + \|\mathbf{h}_{22}\|^2 P_{max}) \|\mathbf{h}_{11}\|^2}{(1 + \|\mathbf{h}_{12}\|^2 \cos^2(\theta_2) P_{max}) \|\mathbf{h}_{21}\|^2} \tag{5.108}$$

$(\lambda_1 = 1, \lambda_2^{\text{MRT}})$ is optimal if and only if $\|\mathbf{h}_{21}\|^2 \leq (1 + \|\mathbf{h}_{22}\|^2 P_{max}) \dfrac{\|\Pi_{21} \mathbf{h}_{11}\|^2}{1 + \|\mathbf{h}_{12}\|^2 \cos^2(\theta_2) P_{max}}$ (5.109)

where $c_1 = \frac{P_{max}}{\|\mathbf{h}_{12}\|^2 \cos^2(\theta_2) P_{max} + 1}$ and $c_2 = \frac{P_{max}}{\|\mathbf{h}_{22}\|^2 P_{max} + 1}$.

5.11.7 Proof of MRT optimality in the DD region

In this section, we provide the sum rate optimality conditions for two MRT strategies, namely: interference amplifying beamforming $\mathbf{w}_i = \frac{\mathbf{h}_{ji}}{\|\mathbf{h}_{ji}\|}$, in Section 5.11.7.1 and direct channel beamforming $\mathbf{w}_i = \frac{\mathbf{h}_{ii}}{\|\mathbf{h}_{ii}\|}$, in Section 5.11.7.2.

5.11.7.1 Optimality conditions of amplifying interference in the DD region

We aim to prove that the beamforming vector $\mathbf{w}_i = \frac{\mathbf{h}_{ji}}{\|\mathbf{h}_{ji}\|}$ is sum rate optimal in $\mathbf{R}^{dd}$ if and only if $(1+g_{jj})\|\mathbf{h}_{ii}\|^2\cos^2(\theta_i) \geq \|\mathbf{h}_{ji}\|^2$ and $\|\mathbf{h}_{ii}\|^2\cos^2(\theta_i)P_{max} \leq \frac{g_{ij}}{g_{jj}} - 1$, where $g_{km} = \|\mathbf{h}_{km}^H\mathbf{w}_m\|^2$.

Due to symmetry of the problem, the proof for $\mathbf{w}_1$ and $\mathbf{w}_2$ is similar and we only give the proof for $\mathbf{w}_2$ here. First, by the definition of Ω^{01} (5.94), we observe that $\mathbf{w}_2(\lambda_2^{\mathrm{MRT}}) = \frac{\mathbf{h}_{12}}{\|\mathbf{h}_{12}\|}$ is in the constraint set Ω^{01} if and only if the following constraints are satisfied:

$$\begin{cases} (1+g_{11})\left|\mathbf{h}_{22}^H\mathbf{w}_2(\lambda_2^{\mathrm{MRT}})\right|^2 \geq |\mathbf{h}_{12}^H\mathbf{w}_2(\lambda_2^{\mathrm{MRT}})|^2 \\ \left|\mathbf{h}_{22}^H\mathbf{w}_2(\lambda_2^{\mathrm{MRT}})\right|^2 P_{max} \leq \dfrac{g_{21}}{g_{11}} - 1 \end{cases}$$

which are equivalent to

$$\begin{cases} (1+g_{11})\|\mathbf{h}_{22}\|^2\cos^2(\theta_2) \geq \|\mathbf{h}_{12}\|^2 \\ \|\mathbf{h}_{22}\|^2\cos^2(\theta_2)P_{max} \leq \dfrac{g_{21}}{g_{11}} - 1 \end{cases}. \tag{5.110}$$

Thus, if and only if (5.110) is satisfied, the beamforming vector $\mathbf{w}_2(\lambda_2^{\mathrm{MRT}}) = \frac{\mathbf{h}_{12}}{\|\mathbf{h}_{12}\|}$ is in Ω^{01}. Now we establish that this is the sum rate optimal solution.

$\tilde{Z}_1$ is monotonically increasing with g_{22} in constraint set Ω^{11}. Note that $\mathbf{w}_2(1) = \frac{\mathbf{h}_{22}}{\|\mathbf{h}_{22}\|}$ [1] is *not* in the constraint set Ω^{11}. We see this by observing the constraint set of Ω^{11} requires:

- $|\mathbf{h}_{22}^H\mathbf{w}_2(\lambda_2)|^2 = \lambda_2\|\mathbf{h}_{22}\|^2$. Thus, we have $|\mathbf{h}_{22}^H\mathbf{w}_2(\lambda_2^{\mathrm{MRT}})|^2 \leq |\mathbf{h}_{22}^H\mathbf{w}_2(1)|^2$.
- $|\mathbf{h}_{12}^H\mathbf{w}_2(\lambda_2)|^2 = \left(\sqrt{\lambda_2}\|\Pi_{22}\mathbf{h}_{12}\| + \sqrt{1-\lambda_2}\|\Pi_{22}^{\perp}\mathbf{h}_{12}\|\right)^2$ is concave in λ_2 and attains maximum at λ_2^{MRT} where $\mathbf{w}_2(\lambda_2^{\mathrm{MRT}}) = \frac{\mathbf{h}_{12}}{\|\mathbf{h}_{12}\|}$. Thus, $|\mathbf{h}_{12}^H\mathbf{w}_2(1)|^2 \leq |\mathbf{h}_{12}^H\mathbf{w}_2(\lambda_2^{\mathrm{MRT}})|^2$.

If the conditions in (5.110) are satisfied, we have

$$(1+g_{11})|\mathbf{h}_{22}^H\mathbf{w}_2(1)|^2 \geq (1+g_{11})\|\mathbf{h}_{22}\|^2\cos^2(\theta_2) \geq \|\mathbf{h}_{12}\|^2 \geq |\mathbf{h}_{12}^H\mathbf{w}_2(1)|^2.$$

To satisfy the constraints of both Ω^{01} and Ω^{11} the sum rate optimal solution lies on the boundary between Ω^{01} and Ω^{11}, namely Ω^A.

The constraints set Ω^{10} is empty. Using the same argument as in the case of $\tilde{Z}_1$, for any λ_2 that satisfies $|\mathbf{h}_{22}^H\mathbf{w}_2(\lambda_2)|^2 \geq \frac{g_{21}}{g_{11}} - 1$ must satisfy $\lambda_2 \geq \lambda_2^{\mathrm{MRT}}$. Also, any $\lambda_2 \geq \lambda_2^{\mathrm{MRT}}$ satisfies

$$(1+g_{11})|\mathbf{h}_{22}^H\mathbf{w}_2(\lambda_2)|^2 \geq (1+g_{11})\|\mathbf{h}_{22}\|^2\cos^2(\theta_2) \geq \|\mathbf{h}_{12}\|^2 \geq |\mathbf{h}_{12}^H\mathbf{w}_2(\lambda_2)|^2. \tag{5.111}$$

Thus, for any λ_2 that satisfies $B = 0$ must have $A = 0$, whih indicates that the constraint is empty.

Similar to the argument before, $|\mathbf{h}_{22}^H\mathbf{w}_2(\lambda_2)|^2 \geq \frac{g_{21}}{g_{11}} - 1$ is a tighter constraint for $|\mathbf{h}_{22}^H\mathbf{w}_2(\lambda_2)|^2$ than $(1+g_{11})|\mathbf{h}_{22}^H\mathbf{w}_2(\lambda_2)|^2 \geq |\mathbf{h}_{12}^H\mathbf{w}_2(\lambda_2)|^2$ in Ω^{00}. As $\tilde{Z}_4$ is monotonically

[1] From now on, we write $\mathbf{w}_2(\lambda_2 = 1)$ as $\mathbf{w}_2(1)$. We must not confuse this with the first element of vector $\mathbf{w}_2$.

decreasing with $|\mathbf{h}_{22}^H\mathbf{w}_2(\lambda_2)|^2$ and increasing with $|\mathbf{h}_{12}^H\mathbf{w}_2(\lambda_2)|^2$ in Ω^{00} , the sum rate optimal solution in this case is the beamforming vector which satisfies:

$$\begin{cases} |\mathbf{h}_{22}^H\mathbf{w}_2(\lambda_2)|^2 = \dfrac{g_{21}}{g_{11}} - 1 \\ (1+g_{11})|\mathbf{h}_{22}^H\mathbf{w}_2(\lambda_2)|^2 = |\mathbf{h}_{12}^H\mathbf{w}_2(\lambda_2)|^2 \end{cases}$$

which is in Ω^B.

Now we show that $\mathbf{w}_2(\lambda_2^{\mathrm{MRT}}) = \frac{\mathbf{h}_{12}}{\|\mathbf{h}_{12}\|}$ is the optimal solution in Ω^{01}. $\tilde{Z}_2$ is monotonically increasing with g_{12}. Since we assumed that $\frac{\mathbf{h}_{12}}{\|\mathbf{h}_{12}\|}$ is in Ω^{01}, it is the optimal solution.

Finally, we notice that for any sum rate optimal solutions in Ω^A which maximizes $\tilde{Z}_1$ in Ω^{11}, it is also in the constraint set Ω^{01} and therefore achieves a smaller sum rate than $\frac{\mathbf{h}_{12}}{\|\mathbf{h}_{12}\|}$. Similarly, any solution in Ω^B that maximizes $\tilde{Z}_4$ is also in constraint set Ω^{01} and therefore achieves a smaller sum rate than $\frac{\mathbf{h}_{12}}{\|\mathbf{h}_{12}\|}$.

5.11.7.2 Optimality conditions of direct channel beamforming in the DD region

Now we prove that the beamforming vector $\mathbf{w}_i(\lambda_i) = \frac{\mathbf{h}_{ii}}{\|\mathbf{h}_{ii}\|}$ attains the maximum sum rate in the DD region, for arbitrary fixed $\mathbf{w}_j$ if $(1+g_{jj})|\mathbf{h}_{ii}^H\mathbf{w}_i(1)|^2 \leq |\mathbf{h}_{ji}^H\mathbf{w}_i(1)|^2$.

We provide the proof for $\mathbf{w}_2$ for simplicity as by reversing the role Tx 1 and Tx 2, the proof for $\mathbf{w}_1$ can be obtained. Notice that if the optimality condition is true: $(1+g_{11})|\mathbf{h}_{22}^H\mathbf{w}_2(1)|^2 \leq |\mathbf{h}_{12}^H\mathbf{w}_2(1)|^2$, then the following arguments are true.

The constraint sets Ω^{01} and Ω^{00} are empty. This is because

$$(1+g_{11})|\mathbf{h}_{22}^H\mathbf{w}_2(0)|^2 = (1+g_{11})\left|\mathbf{h}_{22}^H\frac{\Pi_{22}^{\perp}\mathbf{h}_{12}}{\|\Pi_{22}^{\perp}\mathbf{h}_{12}\|}\right|^2 = 0 \leq |\mathbf{h}_{12}^H\mathbf{w}_2(0)|^2.$$

Thus, together with the assumption above: $(1+g_{11})|\mathbf{h}_{22}^H\mathbf{w}_2(1)|^2 \leq |\mathbf{h}_{12}^H\mathbf{w}_2(1)|^2$, we have

$$\begin{cases} |\mathbf{h}_{12}^H\mathbf{w}_2(1)|^2 \geq (1+g_{11})|\mathbf{h}_{22}^H\mathbf{w}_2(1)|^2 \\ |\mathbf{h}_{12}^H\mathbf{w}_2(0)|^2 \geq (1+g_{11})|\mathbf{h}_{22}^H\mathbf{w}_2(0)|^2. \end{cases}$$

Since $|\mathbf{h}_{22}^H\mathbf{w}_2(\lambda)|^2$ is linearly increasing with λ and $|\mathbf{h}_{12}^H\mathbf{w}_2(\lambda)|^2$ is concave in λ, we draw the conclusion that for all λ, $|\mathbf{h}_{12}^H\mathbf{w}_2(\lambda)|^2 \geq (1+g_{11})|\mathbf{h}_{22}^H\mathbf{w}_2(\lambda)|^2$. Thus, for all λ, $A = 1$.

The sum rate optimal solution in Ω^{11} is either Ω^B or $\frac{\mathbf{h}_{22}}{\|\mathbf{h}_{22}\|}$. If the optimal solution is $\frac{\mathbf{h}_{22}}{\|\mathbf{h}_{22}\|}$ then we know that Ω^{10} is empty and $\frac{\mathbf{h}_{22}}{\|\mathbf{h}_{22}\|}$ is sum rate optimal. If the sum rate optimal solution in Ω^{11} is in Ω^B, then these solutions are also in constraint set Ω^{10} which achieve a smaller sum rate of $\tilde{Z}_3$ than $\frac{\mathbf{h}_{22}}{\|\mathbf{h}_{22}\|}$.

Now, we obtained the MRT optimality conditions for each transmit beamformer $\mathbf{w}_i$ given $\mathbf{w}_j$. Apply the same approach and reverse the role of Tx 1 and 2, we obtain the conditions for $\mathbf{w}_j$. Combine both inequalities to obtain the conditions as shown in Theorem 17.

Chapter 6

Conclusions and Future Work

6.1 Conclusion

In this thesis, we tackle the beamforming vectors design problem in a distributed manner in the vector Gaussian channels with single user decoding (SUD) and with interference decoding capability (IDC). We summarize the contributions in the following.

- In Chapter 3, we proposed a distributed beamforming design algorithm in the MISO-IC-SUD with little complexity that allows the users to cooperate and operate at a rate point close to the Pareto boundary. The proposed beamforming vectors are a balance of MRT (egoism) and ZF (altruism) solutions.

- In Chapter 4, we extended this notion of egoism and altruism balancing in the MIMO-IC-SUD. We proposed an iterative transceiver design algorithm which assigned carefully chosen weights on different links in the asymmetric networks and optimize the sum rate performance. These weights are functions of channel statistics, instead of the channel realizations, which decrease the amount of information exchange required as compared to the algorithms in the literature. In the high SNR regime, the proposed algorithm is shown to achieve interference alignment which guaranteed a linear scaling of sum rate performance with system SNR, if interference alignment is feasible. In the channel settings where interference alignment is infeasible, we proposed a simple binary power allocation algorithm which aimed to restore the feasibility of interference alignment. Simulations results show that with this binary power control, the proposed egoism and altruism balancing transceiver design algorithm successfully restored interference alignment feasibility and achieved better sum rate results comparing to other interference alignment based algorithms and bargaining algorithms.

- In Chapter 5, we relax the constraint of single user decoding to interference decoding capability at the receivers. We considered the 2-user MISO-IC with IDC and proposed 4 decoding structures, each Rx chose to decode-and-remove interference or treat interference as noise. We computed its overall achievable rate region and its corresponding Pareto boundary. The beamforming vectors and power allocation that attained the Pareto boundary were characterized. The Pareto optimal beamforming vectors were shown to be positive linear combinations of two channel vectors, confirming with the results in the MISO-IC-SUD [31]. As an application of the Pareto boundary characterization, we characterized the maximum sum rate

point and obtained a further reduced set of beamforming vectors that were the sum rate optimal candidates. This significantly reduced the search space of the original NP-hard maximum sum rate problem [39]. Aiming to provide a very simple transmission scheme, we investigated the conditions on channel coefficients in which the simple maximum ratio transmission strategies were sum rate optimal. Inspired by this result, we proposed a very simple transmission scheme with only a few possible choices transmit beamforming vectors. Simulation results confirmed that under some channel conditions, the proposed scheme achieve encouraging sum rate performance.

The future research directions are described briefly in the following.

- The discussion in Chapter 5 applied to a 2-user MISO-IC. The extension to K-user MISO-IC is not trivial: when there are more than 2 users in the interference channel, the number of possible decoding structure increases. For instance, in a 3-user MISO-IC, Rx 1 sees the interference signal from Tx 2 and 3. There are five possible actions:
  - N: Rx 1 treats interference as noise.
  - D_{23}: Rx 1 decodes interference by first decoding interference signal from Tx 2 while treating its own signal and interference signal from Tx 3 as noise. Remove the interference from Tx 2 and decode the interference signal from Tx 3 while treating its own signal as noise. Remove the interference from Tx 3 and finally decode its own signal with no interference.
  - Similarly, we can exchange the decoding order and obtain D_{32}.
  - D_2, Rx 1 only decodes and removes interference from Tx 2 and decodes its own signal while treating interference from Tx 3 as noise.
  - Similarly, we have D_3 if Rx 1 only decodes and removes interference from Tx 3.

  To simplify the discussion, we assume no combined decoding of Tx 2 and 3 interference signals. The increase of users in the interference channel increases the number of rate constraints significantly. Apart from the optimal decoding structure design, whether the optimal transmitter matrix is of rank one is still an open problem.

- As the general K-user MISO-IC-IDC is complicated, one can imagine the following special case, a mixed strong and very strong interference network. In a resent work [12], the authors consider a 3-user SISO-IC-IDC in which at each receiver, one interference signal is *strong* and the other one is *very strong*. Under this assumption, the capacity attaining decoding scheme is for Rx 1 to first decode the very strong interferer while treating its own signal and the other interference as noise; then remove this interference and decode the remaining signals in a MAC fashion. This is interesting to see whether the same conclusion can be drawn in the MISO case.

- Another interesting problem in the MISO-IC-IDC is to allow partial interference decoding. This transforms the problem to finding the Pareto optimal rate splitting and beamforming vectors. Here we assume successive interference removal instead of joint decoding for simplicity. The achievable rate region enabling rate splitting contains the achievable rate region we considered in Chapter 5. Let Tx 1 have two transmit symbols x_{10} and x_{11} and Tx 2 have two transmit symbols x_{20} and x_{22}.

Denote the power allocated to symbol x_{i0} by $\bar{\beta}_i P_i$ and to symbol x_{ii} by $\beta_i P_i$ and $\beta_i + \bar{\beta}_i = 1$, for $i = 1, 2$. Note that the achievable rate of user i is $R_i = R_{i0} + R_{ii}$ where R_{i0} is the rate of message x_{i0} and R_{ii} is the rate of the message x_{ii}. The received symbol at Rx i, $i = 1, 2$, is therefore

$$y_i = \mathbf{h}_{ii}^H \mathbf{w}_{i0} x_{i0} + \mathbf{h}_{ii}^H \mathbf{w}_{ii} x_{ii} + \mathbf{h}_{ij}^H \mathbf{w}_{j0} x_{j0} + \mathbf{h}_{ij}^H \mathbf{w}_{jj} x_{jj} + n_i. \tag{6.1}$$

Following the successive decoders proposed for the SISO-IC in [11], if Rx i first decodes-and-removes the message x_{i0} and then x_{j0} and finally decodes message x_{ii}, the following rates are achievable,

$$\begin{aligned}
R_{i0}(\mathbf{w}_1, \mathbf{w}_2, \beta_1, \beta_2) &= \log_2 \left(1 + \frac{|\mathbf{h}_{ii}^H \mathbf{w}_{i0}|^2 \bar{\beta}_i P_i}{|\mathbf{h}_{ii}^H \mathbf{w}_{ii}|^2 \beta_i P_i + |\mathbf{h}_{ij}^H \mathbf{w}_{j0}|^2 \bar{\beta}_j P_j + |\mathbf{h}_{ij}^H \mathbf{w}_{jj}|^2 \beta_j P_j + 1} \right) \\
R_{j0}(\mathbf{w}_1, \mathbf{w}_2, \beta_1, \beta_2) &= \log_2 \left(1 + \frac{|\mathbf{h}_{ij}^H \mathbf{w}_{j0}|^2 \bar{\beta}_j P_j}{|\mathbf{h}_{ii}^H \mathbf{w}_{ii}|^2 \beta_i P_i + |\mathbf{h}_{ij}^H \mathbf{w}_{jj}|^2 \beta_j P_j + 1} \right) \\
R_{ii}(\mathbf{w}_1, \mathbf{w}_2, \beta_1, \beta_2) &= \log_2 \left(1 + \frac{|\mathbf{h}_{ii}^H \mathbf{w}_{ii}|^2 \beta_i P_i}{|\mathbf{h}_{ij}^H \mathbf{w}_{jj}|^2 \beta_j P_j + 1} \right).
\end{aligned} \tag{6.2}$$

If Rx i reverses the decoding order of x_{i0} and x_{j0}, the following rates are achievable:

$$\begin{aligned}
R_{j0}(\mathbf{w}_1, \mathbf{w}_2, \beta_1, \beta_2) &= \log_2 \left(1 + \frac{|\mathbf{h}_{ij}^H \mathbf{w}_{j0}|^2 \bar{\beta}_j P_j}{|\mathbf{h}_{ii}^H \mathbf{w}_{i0}|^2 \bar{\beta}_i P_i + |\mathbf{h}_{ii}^H \mathbf{w}_{ii}|^2 \beta_i P_i + |\mathbf{h}_{ij}^H \mathbf{w}_{jj}|^2 \beta_j P_j + 1} \right) \\
R_{i0}(\mathbf{w}_1, \mathbf{w}_2, \beta_1, \beta_2) &= \log_2 \left(1 + \frac{|\mathbf{h}_{ii}^H \mathbf{w}_{i0}|^2 \bar{\beta}_i P_i}{|\mathbf{h}_{ii}^H \mathbf{w}_{ii}|^2 \beta_i P_i + |\mathbf{h}_{ij}^H \mathbf{w}_{jj}|^2 \beta_j P_j + 1} \right).
\end{aligned} \tag{6.3}$$

We assume here that Rx i always decode its common message before the private message, to keep the formulation simple. Hence, reversing the role of i, j in (6.2) and (6.3), we obtain for $i = 1, 2$, the following achievable rates

$$\begin{aligned}
R_{i0}(\mathbf{w}_1, \mathbf{w}_2, \beta_1, \beta_2) = \min \Bigg\{ & \log_2 \left(1 + \frac{|\mathbf{h}_{ii}^H \mathbf{w}_{i0}|^2 \bar{\beta}_i P_i}{|\mathbf{h}_{ii}^H \mathbf{w}_{ii}|^2 \beta_i P_i + |\mathbf{h}_{ij}^H \mathbf{w}_{j0}|^2 \bar{\beta}_j P_j + |\mathbf{h}_{ij}^H \mathbf{w}_{jj}|^2 \beta_j P_j + 1} \right), \\
& \log_2 \left(1 + \frac{|\mathbf{h}_{ii}^H \mathbf{w}_{i0}|^2 \bar{\beta}_i P_i}{|\mathbf{h}_{ii}^H \mathbf{w}_{ii}|^2 \beta_i P_i + |\mathbf{h}_{ij}^H \mathbf{w}_{jj}|^2 \beta_j P_j + 1} \right), \\
& \log_2 \left(1 + \frac{|\mathbf{h}_{ji}^H \mathbf{w}_{i0}|^2 \bar{\beta}_i P_i}{|\mathbf{h}_{jj}^H \mathbf{w}_{jj}|^2 \beta_j P_j + |\mathbf{h}_{ji}^H \mathbf{w}_{ii}|^2 \beta_i P_i + 1} \right), \\
& \log_2 \left(1 + \frac{|\mathbf{h}_{ji}^H \mathbf{w}_{i0}|^2 \bar{\beta}_i P_i}{|\mathbf{h}_{jj}^H \mathbf{w}_{j0}|^2 \bar{\beta}_j P_j + |\mathbf{h}_{jj}^H \mathbf{w}_{jj}|^2 \beta_j P_j + |\mathbf{h}_{ji}^H \mathbf{w}_{ii}|^2 \beta_i P_i + 1} \right) \Bigg\} \\
R_{ii}(\mathbf{w}_1, \mathbf{w}_2, \beta_1, \beta_2) = & \log_2 \left(1 + \frac{|\mathbf{h}_{ii}^H \mathbf{w}_{ii}|^2 \beta_i P_i}{|\mathbf{h}_{ij}^H \mathbf{w}_{jj}|^2 \beta_j P_j + 1} \right).
\end{aligned} \tag{6.4}$$

The Pareto optimal beamforming vectors and power allocations are therefore the

solutions to the following optimization problem, for some arbitrary $\alpha_1, \alpha_2, \bar{R}$:

$$\begin{aligned} (\mathbf{w}_1^*, \mathbf{w}_2^*, \beta_1^*, \beta_2^*) = \quad & \underset{\mathbf{w}_1, \mathbf{w}_2, \beta_1, \beta_2}{\arg\max} \ \bar{R} \\ \text{subject to} \quad & R_{10}(\mathbf{w}_1, \mathbf{w}_2, \beta_1, \beta_2) + R_{11}(\mathbf{w}_1, \mathbf{w}_2, \beta_1, \beta_2) \geq \alpha_1 \bar{R} \\ & R_{20}(\mathbf{w}_1, \mathbf{w}_2, \beta_1, \beta_2) + R_{22}(\mathbf{w}_1, \mathbf{w}_2, \beta_1, \beta_2) \geq \alpha_2 \bar{R} \end{aligned} \tag{6.5}$$

where $R_{i0}(\mathbf{w}_1, \mathbf{w}_2, \beta_1, \beta_2), R_{ii}(\mathbf{w}_1, \mathbf{w}_2, \beta_1, \beta_2)$ for $i = 1, 2$ are defined in (6.4).

Bibliography

[1] E. Z. A. Leshem, "Bargaining over the interference channel," in *IEEE International Symposium on Information Theory*, 2006.

[2] A.Leshem and E.Zehavi, "Bargaining over the interference channel," in *Proceedings of ISIT*, July 9-14 2006.

[3] V. S. Annapureddy and V. V. Veeravalli, "Sum Capacity of MIMO Interference Channels in the Low Interference Regime," *submitted to IEEE Transactions on Information Theory*, 2010.

[4] A.S.Motahari and A. Khandani, "Capacity bounds for the gaussian interference channel," *IEEE Trans. on Information Theory*, vol. 55, no. 2, February 2009.

[5] A.Vishwanath and S. Jafar, "On the capacity of vector gaussian interference channel," in *Proceedings of the Information Theory Workshop*, October 2004.

[6] B. Bandemer, A. Sezgin, and A. Paulraj, "On the Noisy Interference Regime of the MISO Gaussian Interference Channel," in *Proceedings of Asilomar CSSC 2008*, 2008.

[7] G. Bresler, A. Parekh, and D. Tse, "The approximate capacity of the many-ti-one and one-to-many gaussian interference channels," *IEEE Transactions on Information Theory*, vol. 56, no. 9, September 2010.

[8] V. Cadambe and S. Jafar, "Interference alignment via random codes and the capacity of a class of deterministic interference channels," in *Proceedings of Allerton 2009, 47th Annual Allerton Conference Allerton House, UIUC Illinois, USA*, September 30-October 2 2009.

[9] V. Cadambe, S. Jafar, and S. Shamai, "Interference alignment on the deterministic channel and application to fully connected gaussian interference networks," *IEEE Transactions on Information Theory*, vol. 55, no. 1, pp. 269–274, 2009.

[10] A. B. Carleial, "Interference Channels," *IEEE Transaction on Information Theory*, vol. IT-24, no. 1, pp. 60–70, 1978.

[11] A. Carleial, "A case where interference does not reduce capacity," *IEEE Trans. on Information Theory*, vol. IT-21, no. 5, pp. 569–570, September 1975.

[12] A. Chaaban and A. Sezgin, "The capacity region of the 3-user gaussian interference channel with mixed strong-very strong interference," in *preprint, can be obtained at http://arxiv.org/pdf/1010.4911v1*, 2010.

[13] M. Charafeddine, A. Sezgin, and A. Paulraj, "Rate Region Frontiers for n-user Interference Channel with Interference as Noise," in *Proceedings of Allerton Conference*, 2007.

[14] W. Choi and J. Andrews, "The capacity gain from intercell scheduling in multianetnna systems," in *IEEE Transactions on Wireless Communications*, Feb. 2008.

[15] N. Clemens and C. Rose, "Intelligent power allocation strategies in an unlicensed spectrum," in *IEEE DySPAN*, 2005.

[16] M. Costa, "On the gaussian interference channel," *IEEE Trans. on Information Theory*, vol. IT-31, no. 5, September 1985.

[17] R. Etkin, D. Tse, and H. Wang, "Gaussian interference channel capacity to within one bit," *IEEE Transactions on Information Theory*, vol. 54, no. 12, pp. 5534–5562, 2008.

[18] F. R. Farrokhi, K. J. R. Liu, and L. Tassiulas, "Transmit beamforming and power control for cellular wireless systems," *IEEE Journal on Selected Areas in Communications*, vol. 16, no. 8, October 1998.

[19] D. Gesbert, S. Hanly, H. Huang, S. Shamai, O. Simeone, and W. Yu, "Multi-cell MIMO cooperative networks: A new look at interference," *IEEE Journal on Selected Areas in Communications*, 2010, submitted in Jan 2010.

[20] K. S. Gomadam, V. R. Cadambe, and S. A. Jafar, "Approaching the capacity of wireless networks through distributed interference alignment," in *submitted to IEEE Transaction of Information Theory*, 2008, available at http://arxiv.org/pdf/0803.3816.

[21] T. Han and K. Kobayashi, "A new achievable rate region for the interference channel," *IEEE Trans. on Information Theory*, vol. 27, no. 1, pp. 49 – 60, January 1981.

[22] J. C. Harsanyi, "Games with incomplete information played by "bayesian" players, i-iii. part i. the basic model," *Management Science, Theory Series*, vol. 14, no. 3, November 1967.

[23] G. N. He, M. Debbah, and S. Lasaulce, "K-player bayesian waterfilling game for fading multiple access channels," in *IEEE International Workshop on Comutational Advances in Multi-Sensor Adaptive Processing*, 2009.

[24] Z. Ho and D.Gesbert, "Balancing egoism and altruism on interference channel: the MIMO case," in *Proceedings of ICC 2010, IEEE International Conference on Communications*, May 23-27 2010, pp. 1–5.

[25] Z. Ho and D. Gesbert, "Balancing egoism and altruism on the single beam MIMO interference channel," *submitted to IEEE Transaction of Signal Processing*, 2010.

[26] A. Host-Madsen and A. Nosratinia, "The multiplexing gain of wireless networks," in *Proceedings of IEEE International Symposium of Information Theory*, September 2005, pp. 2065–2069.

[27] H. Huang, V. Lau, Y. Du, and S. Liu, "Robust approximate lattice alignment design for k-pairs quasi-static MIMO interference channels with imperfect CSI," in *Proceedings of ISIT 2010*, June 13-18 2010.

[28] Z. H. J. E. Suris, L. A. DaSilva and A. B. MacKenzie, "Cooperative game theory for distributed spectrum sharing," in *ICC*, 2007.

[29] S. Jafar and S. Vishwanath, "Generalized degrees of freedom of the symmetric gaussian K user interference channel," *IEEE Transactions on Information Theory*, vol. 56, no. 7, pp. 3297–3303, 2010.

[30] A. Jafarian, J. Jose, and S. Vishwanath, "Algebaric lattice alignment for k-user interference channels," in *Proceedings of Allerton 2009, 47th Annual Allerton Conference Allerton House, UIUC Illinois, USA*, September 30-October 2 2009.

[31] E. A. Jorswieck, E. G. Larsson, and D. Danev, "Complete Characterization of the Pareto Boundary for the MISO Interference Channel," *October*, vol. 56, no. 10, pp. 5292–5296, 2008.

[32] S. G. Kiani and D. Gesbert, "Optimal and distributed scheduling for multicell capacity maximization," *IEEE Transactions on Wireless Communications*, vol. 7, no. 1, January 2008.

[33] ——, "Distributed Power Allocation for Interfering Wireless Links Based on Channel Information Partitioning," *IEEE Transactions on Wireless Communications*, vol. 8, no. 6, pp. 3004–3015, 2009.

[34] M. Y. Ku and D. W. Kim, "Tx-Rx beamforming with Multiuser MIMO Channels in MUltiple-cell systems," in *ICACT*, 2008.

[35] K. R. Kumar and F. Xue, "An iterative algorithm for joint signal and interference alignment," in *Proceedings of ISIT*, June 13-18 2010.

[36] E. G. Larsson and E. A. Jorswieck, "The MISO interference channel: Competition versus collaboration," in *Proc. Allerton Conference on Communication, Control and Computing*, September 2007.

[37] A. Laufer and A. Leshem, "Distributed coordination of spectrum and the prisoner's dilemma," in *IEEE DySPAN*, 2005.

[38] J. Lindblom, E. G. Larsson, and E. A. Jorswieck, "Parametrization of the miso ifc rate region: The case of partial channel state information," *IEEE Trans. Wireless Communications*, vol. 9, no. 2, pp. 500 – 504, Feb 2010.

[39] Y. Liu, Y. Dai, and Z. Luo, "Coordinated beamforming for MISO interference channel: Complexity Analysis and efficient algorithms," *submitted to IEEE Transaction on Signal Processing*, 2010.

[40] Z. Y. Ma and Z. Cao, "Secondary user cooperation access scheme in opportunistic cognitive radio networks," in *IEEE Military Communications Conference*, 2007.

[41] M. A. Maddah-Ali, A. S. Motahari, and A. K. Khandani, "Communication over MIMO X channels: Interference alignmnet, decomposition and performance analysis," *IEEE Transactions on Information Theory*, vol. 54, no. 8, August 2008.

[42] R. Mochaourab and E. A. Jorswieck, "Optimal Beamforming in Interference Networks with Perfect Local Channel Information," *will appear in IEEE Transaction on Signal Processing*, pp. 1–30, 2011.

[43] A. F. Molisch, *Wireless Communications*. IEEE, 2005.

[44] F. Negro, S. Shenoy, I. Ghauri, and D. Slock, "Interference alignment feasibility in constant coefficients mimo interference channels," in *SPAWC 2010, 11th IEEE International Workshop on Signal Processing Advances in Wireless Communications*, 20-23 June 2010.

[45] N. Nie and C. Comaniciu, "Adaptive channel allocation spectrum etiquette for cognitive radio networks," in *IEEE International Symposium on New Frontiers in Dynamic Spectrum Access Networks*, 2005.

[46] M. J. Osborne and A. Rubinstein, *A course in Game Theory*. The MIT Press, Cambridge, Massachusetts, 1994.

[47] A. Paulraj, R. Nabar, and D. Gore, *Introduction to space-time wireless communications*. Cambridge University Press, 2003.

[48] S. Perlaza, N. Fawaz, S. Lasaulce, and M. Debbah, "From spectrum pooling to space pooling: Opportunistic interference alignment in MIMO cognitive networks," *IEEE Transactions on Signal Processing*, vol. 58, no. 7, July 2010.

[49] S. W. Peters and R. W. Heath, "Cooperative algorithms for mimo interference channels," *submitted to IEEE Transactions on Vehicular Technology*, December 2009, available at http://arxiv.org/pdf/1002.0424v1.

[50] L. S. S. Mathur and N. B. Mandayam, "Coalitional games in gaussian interference channels," in *IEEE International Symposium on Information Theory*, 2006.

[51] H. Sato, "On the capacity region of a discrete two-user channel for strong interference," *IEEE Transactions on Information Theory*, vol. IT-24, no. 3, May 1978.

[52] ——, "The capacity of the gaussian interference channel under strong interference," *IEEE Transactions on Information Theory*, vol. IT-27, no. 6, pp. 786–788, November 1981.

[53] D. A. Schmidt, W. Utschick, and M. L. Honig, "Large system performance of interference alignment in single-beam MIMO networks," in *Proceedings of IEEE Globecom*, 2010.

[54] X. Shang, B. Chen, and H. V. Poor, "Multi-User MISO Interference Channels with Single-User Detection : Optimality of Beamforming and the Achievable Rate Region," *submitted to IEEE Transaction on Information Theory*, 2009. [Online]. Available: arXiv:0907.0505v1

[55] X. Shang, G. Kramer, and B. Chen, "A new outer bound on the noisy-interference sum-rate capacity for gaussian interference chanels," *IEEE Trans. on Information Theory*, vol. 55, no. 2, February 2009.

[56] X. Shang and B. Chen, "Achievable rate region for downlink beamforming in the presence of interference," in *Proceedings of Asilomar Conference*, November 2007.

[57] X. Shang, B. Chen, G. Kramer, and H. Poor, "Capacity regions and sum- rate capacity of vector gaussian interference channel," *submitted to Trans. Information Theory*, 2009, available at http://arxiv.org/pdf/0907.0472v1.

[58] A. Shannon, "Two-way communication channels," in *In Proceeding of 4th Berkeley Symposium of Mathematics Statistics and Probability*, vol. 1, 1961, pp. 611–644.

[59] H. Shen, B. Li, M. Tao, and X. Wang, "MSE-based transceiver designs for mimo interference channel," *IEEE Transactions on Wireless Communications*, accepted 2010.

[60] M. Shen, A.Host-Madsen, and J. Vidal, "An improved interference alignment scheme for frequency selective channels," in *Proceedings of ISIT*, July 6-11 2008.

[61] C. X. Shi, D. A. Schmidt, R. A. Berry, M. L. Honig, and W. Utschick, "Distributed interference pricing for the MIMO interference channel," in *IEEE ICC*, 2009.

[62] S. Y. Shi, M. Schubert, and H. Boche, "Rate optimization for multiuser MIMO systems with linear processing," *IEEE Transactions on Signal Processing*, vol. 56, no. 8, August 2008.

[63] S. Sridharan, A. Jafarian, S. Vishwanath, S. Jafar, and S. Shamai, "A layered lattice coding scheme for a class of three user gaussian interference channels," in *Proceedings of Allerton 2009, 47th Annual Allerton Conference Allerton House, UIUC Illinois, USA*, September 30-October 2 2009.

[64] J. Thukral and H. Boelcskei, "Interference alignment with limited feedback," in *IEEE International Symposium on Information Theory (ISIT), Seoul, Korea*, 2009, pp. 1759–1763.

[65] D. Tomecki and S. Stanczak, "On Feasible SNR region for multicast downlink channel: Two user case," in *Proceedings of IEEE International Conference on Acoustics, Speech and Signal Processing (ICASSP'10)*, 2010, pp. 3474–3477.

[66] V.R.Cadambe and S.A.Jafar, "Interference alignment and degrees of freedom of the k-user interference channel," *IEEE Transactions on Information Theory*, vol. 54, no. 8, August 2008.

[67] Y. Weng and D. Tuninetti, "On gaussian interference channels with mixed interference," in *Proceedings of International Symposium of Information Theory*, 2008.

[68] S. Ye and R. S. Blum, "Optimized signaling for MIMO interference systems with feedback," *IEEE Transactions on Signal Processing*, vol. 51, no. 11, Nov,2003.

[69] C. Yetis, T. Gou, S. Jafar, and A. Kayran, "On feasibility of interference alignment in mimo interference networks," *IEEE Transactions on Signal Processing*, vol. 58, no. 9, pp. 4771– 4782, 2010.

[70] H. Yu and Y. Sung, "Least squares approach to joint beam design for interference alignment in multiuser multi-input multi-output interference channels," *IEEE Transactions on Signal Processing*, vol. 58, no. 9, September 2010.

[71] R. Zakhour and D. Gesbert, "Coordination on the MISO interference channel using the virtual SINR framework," in *Proceedings of WSA'09, International ITG Workshop on Smart Antennas*, Feburary 2009.

[72] E. Zehavi and A. Leshem, "Alternative bargaining solutions for the interference channel," in *Proceedings of International Workshop on Computational Advances in Multi-Sensor Adaptive Processing (CAMSAP)*, 2009, pp. 9–12.

[73] R. Zhang and S. Cui, "Cooperative interference management with MISO beamforming," *IEEE Transactions on Signal Processing*, vol. 58, no. 10, pp. 5450 – 5458, 2010.